

8-2016

# Tackling Adverse Environment—Molecular Mechanism of Plant Stress Response and Biotechnology Tool Development

Ning Yuan

Clemson University, [ningy@clemson.edu](mailto:ningy@clemson.edu)

Follow this and additional works at: [https://tigerprints.clemson.edu/all\\_dissertations](https://tigerprints.clemson.edu/all_dissertations)

Part of the [Biochemistry Commons](#), and the [Genetics Commons](#)

---

## Recommended Citation

Yuan, Ning, "Tackling Adverse Environment—Molecular Mechanism of Plant Stress Response and Biotechnology Tool Development" (2016). *All Dissertations*. 2308.

[https://tigerprints.clemson.edu/all\\_dissertations/2308](https://tigerprints.clemson.edu/all_dissertations/2308)

This Dissertation is brought to you for free and open access by the Dissertations at TigerPrints. It has been accepted for inclusion in All Dissertations by an authorized administrator of TigerPrints. For more information, please contact [kokeefe@clemson.edu](mailto:kokeefe@clemson.edu).

TACKLING ADVERSE ENVIRONMENT - MOLECULAR MECHANISM OF PLANT  
STRESS RESPONSE AND BIOTECHNOLOGY TOOL DEVELOPMENT

---

A Dissertation  
Presented to  
the Graduate School of  
Clemson University

---

In Partial Fulfillment  
of the Requirements for the Degree  
Doctor of Philosophy  
Genetics and Biochemistry

---

by  
Ning Yuan  
August 2016

---

Accepted by:  
Dr. Hong Luo, Committee Chair  
Dr. James Morris  
Dr. Michael Sehorn  
Dr. Haiying Liang

## ABSTRACT

Abiotic and biotic stresses such as drought, salt, nutrition starvation, and pathogen infection are major factors threatening our agricultural production. With the rapidly increasing population and limited arable land area, genetic engineering of crops for new products with more stable and higher yield than conventional cultivars under adverse environment provides a powerful new tool for use in developing novel GMOs (Genetically Modified Organisms) to feed the large population in the immediate future. To develop novel GMOs with enhanced performance under adverse conditions, we need first to understand molecular mechanisms underlying plant stress response. To better understand how signaling transduction pathway in plants responds to stresses, we focused on a newly identified *Arabidopsis* protein kinase family *SRF* (Stress Responsive Factor). This gene family comprises of four family members (*SRF1-4*), and their expressions are strongly regulated by abiotic or biotic stress. The four SRF proteins are all localized on plasma membrane, suggesting that they may have similar functions in signaling transduction, but their different expression patterns imply that their functions are temporally and spatially distinct. By using genetic methods, we found that *SRF1* and *2* are two negative regulators of salt resistance of *Arabidopsis*, while *SRF2* positively regulates PAMPs (Pathogen-Associated Molecular Patterns)-triggered immunity of *Arabidopsis*. Results of Western analysis and Northern analysis suggest that the MAPK-mediated signaling transmission and expression of defense-related genes were enhanced in *SRF2* overexpressing plants. We also found that BAK1 is a co-receptor of *SRF2* kinase. These results suggest that SRFs

have important functions in abiotic or biotic stress resistance pathways, and the information obtained may be used to engineer crops for enhanced stress resistance.

Besides further deciphering signaling pathway in plant response to osmotic stress and biotic stress, we also investigated the role of microRNAs (miRNAs) in plant response to nutritional deficiency, specifically, the function of rice *miR395* genes responding to sulfate starvation. Our results indicated that under sulfate deficiency conditions, rice *miR395* is intensively upregulated, whereas the two predicted target genes of *miR395* are down-regulated. Overexpression of the rice *miR395h* in tobacco impairs its sulfate homeostasis. One sulfate transporter gene *NtaSULTR2* was identified to be the target of *miR395* in tobacco, which belongs to low affinity sulfate transporter group and may mediate the sulfate transportation and distribution. The critical functions of *miR395* and *NtaSULTR2* in sulfate transportation and assimilation suggest that these two genes could be utilized to improve the growth of GMOs in sulfate-limited condition.

Development of molecular tools is important in agricultural biotechnology. Tissue specific promoters are of particular interest when developing GMOs with modified traits. For example, their use can lead to reduced accumulation of undesirable heterologous proteins or final metabolites in certain organs such as fruits or seeds. We identified a novel *Arabidopsis* leaf-specific promoter *Srf3abc*. *Srf3abc* exhibits stronger activity than CaMV 35S promoter in the leaves of *Arabidopsis*. Truncation in *Srf3abc* abolishes its leaf specificity, and some truncated versions of the promoter exhibit strong constitutive activity in *Arabidopsis*. Most significantly, *Srf3abc* and its truncated versions also function across

different plant species including dicots and monocots, implying their potential wide applications in agriculture biotechnology.

## DEDICATION

I dedicate this dissertation to my parents, Ye Yuan and Hua Ning. They did their best to educate and support me. I hope this achievement will fulfill their expectations of me. This work is also dedicated to my wife Han Li, and my daughter Isabelle Yuan. Their love for me is the motivation encouraging me to move on all these years.

## ACKNOWLEDGMENTS

I would like to first express my sincere appreciation to my advisor Dr. Hong Luo for his invaluable and constructive suggestions for my research. His profound knowledge and enthusiastic encouragement have inspired me to complete my Ph.D. study and will inspire me to achieve my life goals in the future. I would like to thank my committee members Dr. James Morris, Dr. Michael Sehorn, and Dr. Haiying Liang for their patient guidance and useful critiques. My deep gratitude also goes to Dr. Zhigang Li. Without his assistance and advice, I would not have kept my research on schedule. I also would like to thank my previous and present lab members, Dr. Man Zhou, Dr. Shuangrong Yuan, and Peipei Wu for their generous help and cooperation. I would also like to extend my thanks to the following people for their great help: Dr. Liangjiang Wang and his graduate students for their help in bioinformatics analysis; Dr. Ashley Crook and Clemson Light Imaging Facility for their help in fluorescence imaging; Dr. Fumiaki Katagiri from University of Minnesota for providing various pathogen strains; all the faculty, staff, and students in the Department of Genetics and Biochemistry for their support.

## TABLE OF CONTENTS

	Page
TITLE PAGE .....	i
ABSTRACT .....	ii
DEDICATION .....	v
ACKNOWLEDGMENTS .....	vi
LIST OF FIGURES .....	ix
 CHAPTER	
ONE LITERATURE REVIEW .....	1
Osmotic stresses and plant responses .....	2
Pathogen infection and plant innate defense.....	18
SMG and SMG protein free in GMOs.....	32
References.....	41
 TWO IDENTIFICATION AND FUNCTIONAL CHARACTERIZATION OF A NEW <i>ARABIDOPSIS</i> PROTEIN KINASE GENE FAMILY INVOLVED IN STRESS RESISTANCE.....	       62
Abstract .....	63
Introduction.....	64
Results.....	66
Discussion.....	95
Materials and methods .....	105
References.....	113
 THREE HETEROLOGOUS EXPRESSION OF A RICE <i>MIR395</i> GENE IN <i>NICOTIANA TABACUM</i> IMPAIRS SULFATE HOMEOSTASIS.....	       121
Abstract .....	122
Introduction.....	123
Results.....	126
Discussion.....	143
Materials and methods .....	149



Table of Contents (Continued)

	Page
References.....	157
FOUR <i>SRF3</i> PROMOTER, A STRONG NOVEL REGULATORY ELEMENT DRIVES CONSTITUTIVE AND TISSUE SPECIFIC GENE EXPRESSION IN DIVERSE PLANT SPECIES.....	162
Abstract.....	163
Introduction.....	164
Results.....	166
Discussion.....	176
Materials and methods .....	181
References.....	185
FIVE CONCLUSIONS AND FUTURE PERSPECTIVES .....	189
APPENDICES .....	193
A: SUPPORTING MATERIAL FOR CHAPTER TWO.....	194
B: SUPPORTING MATERIAL FOR CHAPTER THREE .....	197
C: SUPPORTING MATERIAL FOR CHAPTER FOUR .....	203
D: SUPPORTING PUBLICATION FOR CHAPTER THREE .....	211
E: COPY RIGHT PERMISSION FOR CHAPTER THREE.....	225

## LIST OF FIGURES

Figure		Page
1.1	Major pathways in plant responses to osmotic stresses .....	7
1.2	Phospholipids pathway .....	10
1.3	Co-evolution of plant resistance proteins and pathogen effectors .....	21
1.4	Plant pattern-recognition receptors .....	28
2.1	Genome-wide identification of root-specific genes .....	68
2.2	Phylogenetic analysis and genomic organization of the <i>SRF</i> genes .....	69
2.3	Alignment of the SRF proteins .....	71
2.4	Expression analysis of the <i>SRF</i> genes under osmotic stresses.....	73
2.5	Expression analysis of the <i>SRF</i> genes under pathogen and elicitor treatment.....	75
2.6	Expression analysis of the <i>SRF</i> genes in different tissues of <i>Arabidopsis thaliana</i> .....	76
2.7	Activity analysis of the <i>SRF</i> gene promoters.....	78
2.8	Subcellular localization analysis of the SRF proteins.....	81
2.9	Analysis of the <i>SRF</i> T-DNA insertion mutants .....	83
2.10	Phenotypic analysis of wild type (WT), the <i>SRF2</i> T-DNA insertion mutant and the <i>SRF2</i> -overexpressing line subjected to pathogen infection through dip-inoculation.....	87
2.11	Phenotypic analysis of wild type (WT), the <i>SRF2</i> T-DNA insertion mutant and the <i>SRF2</i> -overexpressing line subjected to pathogen infection through spray-inoculation .....	88

List of Figures (Continued)

Figure	Page
2.12 Analyses of basal immunities in wild type (WT), the <i>SRF2</i> T-DNA insertion mutant and the <i>SRF2</i> -overexpressing line .....	90
2.13 Expression analysis of defense-related genes in wild type (WT), the <i>SRF2</i> T-DNA insertion mutant and the <i>SRF2</i> -overexpressing line .....	93
2.14 Phosphorylation analysis of MAPK3/6 in wild type (WT), the <i>SRF2</i> T-DNA insertion mutant and the <i>SRF2</i> -overexpressing line .....	96
2.15 Interaction of BAK1 and SRF2 under pathogen treatment.....	97
2.16 Schema of SRF2 mediated signaling pathway.....	103
3.1 Sulfate deficiency induces accumulation of <i>OsamiR395</i> in rice .....	128
3.2 Predicted target <i>OsaSULTR1</i> and <i>OsaSULTR2</i> exhibit opposite expression patterns to that of the <i>OsamiR395</i> in rice root.....	130
3.3 Expression level of pri- <i>OsamiR395h</i> and its target genes in rice leaf and root tissues at different development stages .....	132
3.4 Heterologous expression of pri- <i>OsamiR395h</i> in <i>Nicotiana tabacum</i> .....	134
3.5 Overexpression of pri- <i>OsamiR395h</i> impacts tobacco sulfate transportation and distribution .....	136
3.6 Overexpression of pri- <i>OsamiR395h</i> leads to retarded growth of transgenic tobacco .....	138
3.7 Identification of a sulfate transporter gene, <i>NtaSULTR2</i> , the target of <i>miR395</i> in tobacco .....	140
3.8 <i>NtamiR395</i> and <i>NtaSULTR2</i> exhibit opposite expression patterns in tobacco roots .....	142

List of Figures (Continued)

Figure	Page
3.9 Confirmation of <i>miR395</i> mediated cleavage of <i>NtSULTR2</i> mRNA .....	144
4.1 Structure of SRF3 protein and its expression pattern in three-week-old <i>Arabidopsis</i> .....	168
4.2 Schematic diagrams of the GUS reporter gene constructions .....	169
4.3 Histochemical GUS staining of the two-week-old <i>Arabidopsis</i> .....	170
4.4 Histochemical GUS staining of the four-week-old <i>Arabidopsis</i> .....	172
4.5 Quantitative measurement of GUS activities in transgenic <i>Arabidopsis</i> .....	173
4.6 Srf3c promoter drives foreign gene expression in transgenic <i>Arabidopsis</i> .....	174
4.7 Histochemical GUS staining of transgenic tobacco .....	175
4.8 Histochemical GUS staining of the transgenic rice and creeping bentgrass .....	177
4.9 Putative structure of the Srf3abc promoter .....	179

CHAPTER ONE

LITERATURE REVIEW

The world population in 2005 was 6.5 billion and there were nearly 1.592 billion hectares (ha) of arable land area (Alexandratos and Bruinsma, 2012). According to a United Nations report released in 2013 (<https://www.un.org/>), the world population is estimated to reach 9.6 billion by 2050, while the arable land area will only increase to 1.661 billion ha (Alexandratos and Bruinsma, 2012). The implication is that agriculture will encounter the challenge of increasing hectare yield of arable land 150% by the middle of 21st century to feed the world population.

Instead of increasing new arable land area, an alternative route is developing GMOs (Genetically Modified Organisms) with enhanced stress resistance. Developing GMOs which can survive and have high hectare yield on barren land under strike of pathogens, insects, heat, cold, salt, drought, or nutrition deficiency offers a promising way to overcome the challenges of higher population, with less arable land. To genetically engineer crops with enhanced tolerance to adverse conditions, it is essential to better understand how plants resist naturally occurring stresses. With what we know about the molecular mechanisms governing plant stress response, we can identify valuable genes, which have critical functions in the resistance mechanisms and utilize them for crop genetic improvement to increase plant resistance to adverse environments.

## **OSMOTIC STRESSES AND PLANT RESPONSES**

Agricultural production now is consuming about 70% of the freshwater withdrawals (Alexandratos and Bruinsma, 2012). Though it does not exceed available water resources, agricultural production still brings big water pressure to water renewing

and recycling. Because of precipitation, hot climate, and water reclamation technique imbalances between different countries and areas, osmotic stresses are the most common threats to agricultural production, especially in water-stressed developing countries and areas such as sub-Saharan Africa and Northwest China. Understanding how plants tailor to the osmotic stresses can help us to develop GMOs with enhanced tolerance to water-limited conditions.

In the broadest definition, osmotic stresses encompass drought stress and salt stress. Both of them cause dehydration in plants. Signal transduction plays a pivotal role in resistance pathways against osmotic stresses. When plants are subjected to osmotic stresses, they need to relay environmental signals into cells via signaling transduction, starting up appropriate responses. Several resistance pathways have been well studied in plants, including SOS (Salt Overly Sensitive) pathway, ABA (Abscisic Acid)-dependent pathway, ABA-independent pathway, and microRNA pathway. Modification of resistance pathways has been used as a powerful approach to elevate osmotic stress tolerance of transgenic crops (Kovtun et al., 2000; Yamaguchi-Shinozaki and Shinozaki, 2001; Umezawa et al., 2004).

### **SOS mediated salt resistance**

SOS is the first identified pathway mediating salt resistance. SOS pathway comprises of a plasma membrane anchored  $\text{Na}^+/\text{H}^+$  antiporter SOS1, a SnRK3 (SNF1-Related Protein Kinase 3) protein SOS2, and an EF-hand-type calcium-binding protein SOS3 (Zhu, 2000). The SOS pathway helps *Arabidopsis* to maintain its sodium

homeostasis under salt stress. Overexpression of SOS genes has been proven to be an efficient way to increase salt tolerance of *Arabidopsis* (Yang et al., 2009).

As shown in Figure 1.1, in *Arabidopsis thaliana*,  $\text{Ca}^{2+}$  stream elicited by salt stress activates SOS3 by binding with its three EF-hands (Ishitani et al., 2000). Activated SOS3 then interacts with and activates protein kinase SOS2 (Halfter et al., 2000; Liu et al., 2000). SOS2-SOS3 complex then upregulates the expression of *SOS1* gene, leading to the efflux of  $\text{Na}^+$  (Shi et al., 2000). Besides SOS2, SOS3 also interacts with other protein kinases to regulate the biosynthesis of ABA under osmotic stresses (Zhu, 2000).

AtHKT1 is a membrane-anchored  $\text{Na}^+$  transporter involved in the  $\text{Na}^+$  transportation in xylem (Sunarpi et al., 2005). The phenotype of lost-of-function mutant in SOS3 could be rescued by repressing the expression of *AtHKT1* gene, implying that SOS2-SOS3 complex also represses the function of AtHKT1 when *Arabidopsis* is subjected to salt treatment (Rus et al., 2001).

Previous research suggested that the SOS3 have very low expression level in shoots, while SOS1 and SOS2 are strong expressed in both root and shoot tissues (Ji et al., 2013). This fact raises a question: how does SOS pathway work in *Arabidopsis* shoots? Later experiments indicated that there is another protein named SCaBP8 (SOS3-like Calcium Binding Protein 8) that can interact with and activate SOS2 in shoots (Quan et al., 2007). SCaBP8-SOS2 complex, similar to SOS3-SOS2 complex, positively regulates the expression of SOS1, and thus helps shoot cells to exclude  $\text{Na}^+$  and keep sodium homeostasis (Lin et al., 2009).

Although SOS pathway has critical function in *Arabidopsis* to exclude  $\text{Na}^+$  out of



cell cytoplasm in roots, it is not sufficient when the plant is in high salt environment (Ji et al., 2013). Under high salt condition,  $\text{Na}^+$  will overcome the exclusion function of SOS pathway and enter cortex, endodermis, and xylem. In such a situation,  $\text{Na}^+$  ions are loaded in xylem by SOS1 and eventually transported into shoots (Shi et al., 2002). Besides long-distance transportation of  $\text{Na}^+$ , SOS pathway can also compartmentalize excess  $\text{Na}^+$  ions into vacuole of root cells probably with the help of endomembrane anchored  $\text{Na}^+/\text{H}^+$  antiporter NHK and  $\text{H}^+$  transporter  $\text{H}^+$ -ATPase, relieving the dehydration damage caused by high salt stress (Zhu, 2002; Oh et al., 2010).

Later research suggests that SOS1 is also a target of PLD (Phospholipase D) resistance pathway (Yu et al., 2010). When *Arabidopsis* is stricken with high salt stress, lipid second messenger PA (Phosphatidic Acid) rapidly accumulates with the increasing activity of PLD $\alpha$ 1 (Phospholipase D  $\alpha$ 1), followed by the activation of MPK6, which in turn phosphorylates SOS1 and induces the efflux of  $\text{Na}^+$ . This fact suggests that the different resistance pathways can integrate together for responding to osmotic stresses rather than standalone.

Furthermore, more experiments implied that SOS pathway may also help plant to avoid salt stress by regulating the postembryonic development of root tissue, repressing the root growth, and changing the root tropism (Sun et al., 2008; Wang et al., 2008)

### **ABA-dependent osmotic stress resistance**

Phytohormone ABA plays an essential role in plant resistance to water deficiency. Osmotic stresses up-regulate the expressions of several genes which have critical functions

in the biosynthesis of ABA, such as *ZEP*, *NCED*, *ABA2* and *LOS5/ABA3/AAO*, causing the over-accumulation of ABA in plants. Excess ABA is then bound by cytoplasm-localized ABA receptor PYR1 (Pyrabactin Resistance1)/RCAR (Regulatory Components of ABA Receptors), and ABA-PYR1/RCAR complex interacts with protein ABI (ABA-Insensitive)/PP2C (Protein Phosphatase 2c) (Nishimura et al., 2010; Gonzalez-Guzman et al., 2012). ABI/PP2C is a negative regulator of ABA signaling pathway. It blocks the ABA-induced signaling transduction by repressing the activities of OST1 (Open Stomata 1) and SnRK2Cs (SNF1-Related Protein Kinase 2C). The interaction between ABA-PYR1/RCAR complex and ABI/PP2C can repress the activity of the latter protein, leading to the activation of OST1 and SnRK2C proteins. Activated OST1 and SnRK2Cs initiate ABA mediated signaling pathway in two major directions: (a) stomata closure caused by anion efflux, and (b) expression of osmotic resistance genes, such as LEA (Late Embryogenesis Abundant) and HSP (Heat Shock Protein), helping plants to increase their tolerance to osmotic stresses (Figure 1.1)

OST1 is a critical regulator functioning in anion efflux of guard cells. When OST1 is activated by ABA in the guard cells, on the one hand, it blocks the ion influx by repressing the potassium channel KAT1 localized on the plasma membrane; on the other hand, OST1 induces the activity of plasma membrane anchored ion channel SLAC1 which is responsible for the ion efflux. These above-mentioned reactions cause the closure of stomata under osmotic stresses.

SnRK2Cs target transcription factors involved in the ABA signaling pathway. Genes responding to ABA could be classified to two groups: early response genes and

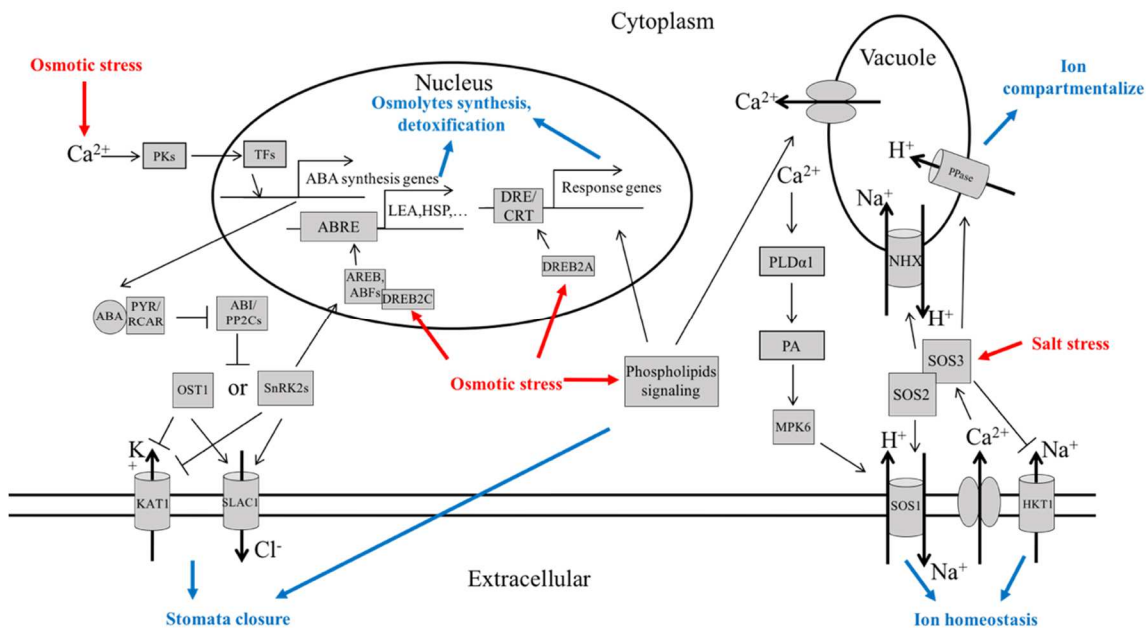


**Figure 1.1. Major pathways in plant responses to osmotic stresses.** Osmotic stresses initiate calcium signal, which enhances the ABA synthesis. ABA forms complex with PYR/RCAR, which induces anion efflux and causes leaf closure by suppressing the activity of ABI/PP2Cs. ABA-PYR/RCAR complex can also induce expression of downstream genes, such as *LEA* and *HSP*. Osmotic stresses can also stimulate phospholipids signaling transduction and activate CBF/DREB transcription factors, which mediate the expression of stress protein genes and initiate the calcium signal. Salt stress and calcium signal initiate formation of SOS3-SOS2 complex, which in turn stimulates SOS1 responsible for the  $\text{Na}^+/\text{H}^+$  exchange. SOS3-SOS2 complex may also stimulate vacuolar  $\text{H}^+$  transporter Ppase and  $\text{Na}^+$  transporter NHX, and suppress the plasma membrane  $\text{K}^+$  and  $\text{Na}^+$  transporters, balancing ion homeostasis under salt stress. Stresses are highlighted with red color. Plant responses are indicated with blue color. PK: protein kinase; TF: transcription factor; PYR1: pyrabactin resistance; RCAR: regulatory components of ABA receptor; ABI: ABA-insensitive; PP2C: protein phosphatase 2c; OST1: open stomata 1; SnRK2: SNF1-related protein kinase 2; KAT1: potassium transporter1; SLAC1: S-type anion channel; AREBs: ABA responsive element binding proteins; ABFs: ABRE binding factors; ABRE: ABA-responsive element; LEA: Late embryogenesis abundant; HSP: heat shock protein; DREB: drought responsive element binding factor; DRE: drought responsive element; CRT: C-repeat; HKT1: high-affinity  $\text{K}^+$  transporter1; NHX: vacuolar  $\text{Na}^+/\text{H}^+$  exchanger; Ppase:  $\text{H}^+$ -ATPases; PLD: phospholipase D  $\alpha$ 1; PA: phosphatidic acid; MPK6: mitogen-activated protein kinase6. Figure summarized from (Zhu, 2002)

delayed response genes (Zhu, 2002). Most of the early response genes encode TFs (Transcription Factors), such as AREBs (ABA Responsive Element Binding Proteins) and

ABFs (ABRE Binding Factors), while most delayed response genes are osmolyte biosynthesis genes, heat shock proteins, and late embryogenesis abundant proteins. Expression of early response genes is quick and transient under osmotic stresses and ABA treatment. In ABA signaling, SnRK2Cs activate AREBs/ABFs via direct phosphorylation (Kulik et al., 2011). By recognizing and binding to the corresponding *cis*-regulatory elements ABRE (ABA-Responsive Element) in the promoter regions of the delayed response genes, phosphorylated AREBs/ABFs induce the expression of delayed response genes.

Recent research suggested that there are three groups of SnRK2Cs (Kulik et al., 2011). The above-mentioned SnRK2Cs belong to group II. SnRK2C-III proteins are also activated by ABA via the same pathway as SnRK2C-II. But unlike the second group which targets TFs, SnRK2C-III proteins phosphorylate and regulate ion channels (KAT1 and SLAC1) localized on the plasma membrane, leading to stomata closure under osmotic stresses (Kulik et al., 2011). SnRK2C-III proteins repress KAT1 and activate SLAC1, exhibiting a similar function to OST1.

## **ABA-independent osmotic stress resistance**

### ***Phospholipid signaling pathway***

Phospholipids comprise the plasma membrane of plant cells, offering the cell a stable and orderly protoplasm environment that is isolated from external conditions. In the meantime, phospholipids also participate in the defense pathways by serving as second messengers under osmotic stresses (Figure 1.2).

Based on the early studies, when *Arabidopsis* is subjected to osmotic stresses, the expression of genes encoding two key proteins, PIP5K (phosphatidylinositol-4-phosphate 5-kinase) and PLC (phospholipase C), involved in the phospholipids signaling pathway, are induced. PIP5K phosphorylates PI(4)P (phosphatidylinositol-4-phosphate) to PI(4,5)P<sub>2</sub> (phosphatidylinositol-4,5-diphosphate), followed by the PLC-catalyzed cleavage of PI(4,5)P<sub>2</sub> to produce DAG (diacylglycerol) and Ins(1,4,5)P<sub>3</sub> (inositol-1,4,5-trisphosphate) (Zhu, 2002).

In mammals, Ins(1,4,5)P<sub>3</sub> is an important second messenger mediating the signal transduction under stresses. It induces the release of Ca<sup>2+</sup> in mammal cells via ligand-gated calcium channels localized on the endomembrane, which in turn promotes the expression of defense-related genes.

This PIP(4,5)P<sub>2</sub> – Ins(1,4,5)P<sub>3</sub> – Ca<sup>2+</sup> – defense-related genes route seems straight forward and promising in plants (Munnik et al., 1998). But recent research showed that there are very low amount of PIP(4,5)P<sub>2</sub> in plant cells (Vermeer et al., 2006; van Leeuwen et al., 2007; Vermeer et al., 2009). And more importantly, no ligand-gated calcium channels have been identified on the endomembrane of plant cells, implying that Ins(1,4,5)P<sub>3</sub> may not mediate the release of Ca<sup>2+</sup> in plants under osmotic stresses.

On the contrary, the quantity of PI(4)P is much higher than PIP(4,5)P<sub>2</sub> in plant cells. PI(4)P is also a perfect substrate of PLC, which catalyzes PI(4)P to Ins(1,4)P<sub>2</sub>. Two novel IPKs (Inositol Dual-specificity Polyphosphate Multikinases) have been identified in *Arabidopsis* (Stevenson-Paulik et al., 2005). These two kinases catalyze Ins(1,4)P<sub>2</sub> to InsP<sub>6</sub> (Inositol hexakisphosphate), which is also an important second messenger in plant cells.

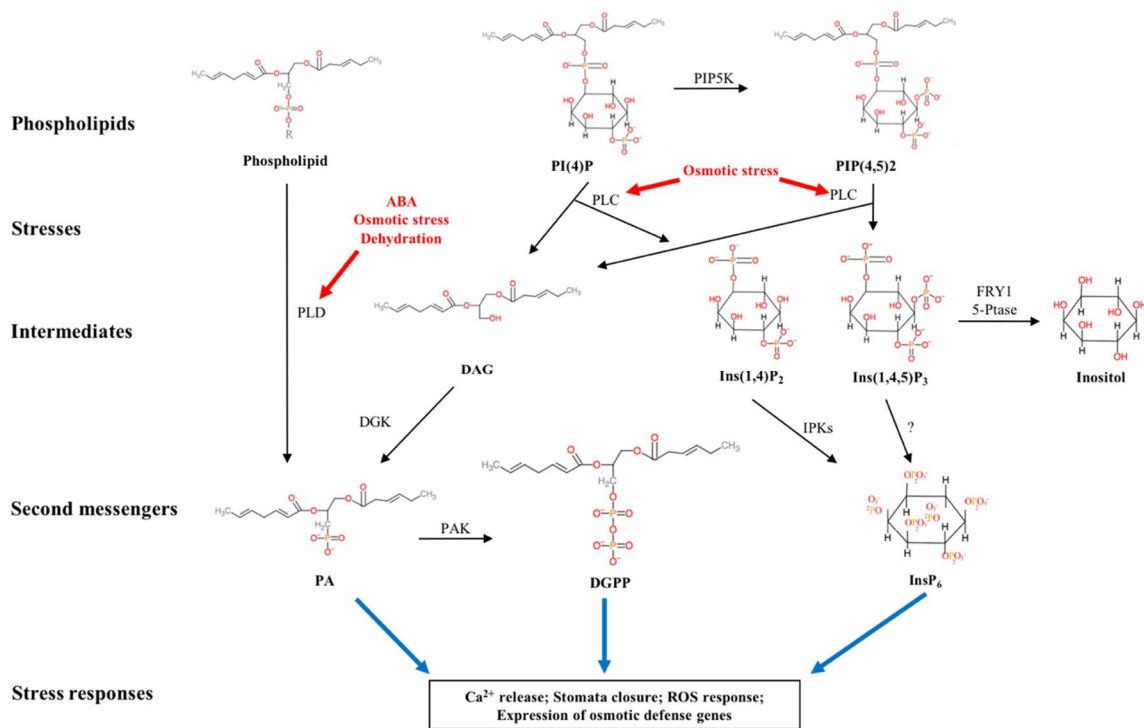


**Figure 1.2. Phospholipids pathway.** Each black arrow represents a reaction in the phospholipids pathway with the associated enzyme beside it. Stresses are highlighted with red color. Plant responses are indicated with blue color. PIP5K: Phosphatidylinositol-4-phosphate 5-Kinase; PI(4)P: Phosphatidylinositol-4-phosphate; PI(4,5)P<sub>2</sub>: Phosphatidylinositol-4,5-diphosphate; PLC: Phospholipase C; DAG: Diacylglycerol; Ins(1,4,5)P<sub>3</sub>: Inositol-1,4,5-trisphosphate; Ins(1,4)P<sub>3</sub>: Inositol-1,4-diphosphate; IPKs: Inositol dual-specificity polyphosphate multikinases; FRY1: phosphoinositide 1-phosphatase; 5-Ptase: phosphoinositide 5-phosphatase; PA: Phosphatidic acid; DGK: DG kinase; PLD: Phospholipase D; DGPP: Diacylglycerolpyrophosphate; PAK: PA kinase. InsP<sub>6</sub>: Inositol hexakisphosphate. Figure summarized from (Zhu, 2002)

Based on the above facts, a PI(4)P involved signaling pathway could be drawn as follows: under osmotic stresses, PI(4)P is cleaved by PLC to produce DAG and Ins(1,4)P<sub>2</sub>, and the latter intermediate is phosphorylated to produce InsP<sub>6</sub> by IPKs. Instead of Ins(1,4,5)P<sub>3</sub>, InsP<sub>6</sub> triggers the release of Ca<sup>2+</sup> and promotes plant responses to osmotic

stresses. As for the  $\text{Ins}(1,4,5)\text{P}_3$  derived from  $\text{PIP}(4,5)\text{P}_2$ , it may be converted to  $\text{InsP}_6$ , which participates in the lipid mediated stress-resistance pathway (Munnik et al., 1998).

FRY1 (phosphoinositide 1-phosphatase) and 5-Ptase (phosphoinositide 5-phosphatase) are two negative regulators of the  $\text{Ins}(1,4,5)\text{P}_3$ -mediated signaling pathway. They are responsible for the turnover of  $\text{Ins}(1,4,5)\text{P}_3$ . Previous research showed that the accumulation of  $\text{Ins}(1,4,5)\text{P}_3$  is increased in FRY1 knockout mutant *fry1*, but this mutant is even more sensitive to salt, drought and cold stress. This experiment suggested that the phospholipids-mediated pathway is an elaborate signaling network and that, any interruption in the phospholipids homeostasis could bring negative consequences and make plants more susceptible to osmotic stresses (Xiong et al., 2001).

Another product of PLC-catalyzed  $\text{PI}(4,5)\text{P}_2$  hydrolysis is DAG, which is rapidly phosphorylated to PA (phosphatidic acid) under the catalysis of DGK (DG kinase) (Munnik, 2001; Testerink and Munnik, 2005; Wang et al., 2006).

In addition to the  $\text{PI}(4,5)\text{P}_2$  – DAG – PA route, PA can also be generated from membrane phospholipids including PC (phosphatidylcholine) and PE (phosphatidylethanolamine). Under dehydration stress, PLD (phospholipase D) catalyzes the hydrolysis of PC and PE, producing PA and free head groups.

PA is another essential second messenger in the phospholipids signaling pathway. It induces stomata closure in the guard cells, exhibiting a similar function to ABA. Studies in *Arabidopsis* and rice indicated that there are 12 and 17 PLDs, respectively (Wang, 2005; Bargmann and Munnik, 2006; Li et al., 2007a). Among the 12 PLDs in *Arabidopsis*,  $\text{AtPLD}\alpha$ ,  $\text{AtPLD}\delta$ , and  $\text{AtPLD}\epsilon$  have been proven to be involved in ABA, salt and osmotic

responses (Zhang et al., 2004; Devaiah et al., 2007; Hong et al., 2008; Bargmann et al., 2009; Hong et al., 2009). A recent study indicated that PA could be phosphorylated to DGPP (diacylglycerolpyrophosphate) by PAK (PA Kinase). DGPP is also a signaling molecule triggering plant response under stresses (Wang et al., 2006).

### ***Transcription factors-mediated osmotic resistance***

CBFs (C-repeat Binding Factor)/DREBs (Drought Responsive Element Binding factor) are specific transcription factors that recognize and bind *cis*-regulatory elements named CRT (C-repeat)/ DRE (Drought Responsive Element) localized in the promoter regions of many cold or salt and drought responding genes (Figure 1.1).

Although two subgroups of CBF/DREB1 have been identified in plants, they are involved in different stress response pathways. The first subgroup (CBF/DREB1) induces gene expression under low temperatures (Hua, 2009), while the second subgroup (DREB2) functions in the signaling pathways responding to osmotic or/and heat stresses. Osmotic stresses, such as high salt and drought, can intensively induce the expression of DREB2A, which in turn binds DRE region in the promoters of osmotic resistance genes and induces their expression, initiating plant response to osmotic stresses (Sakuma et al., 2006). A large amount of the downstream genes regulated by DREB2A mediate the production of osmolytes which help plant to keep high osmotic pressure under salt and drought stress, reducing water loss from plants.

Two rice NAC (NAM, ATAF1/2 and CUC1) transcription factors – OsNAC5 and OsNAC6 – have been proven to be positive regulators of plant resistance against osmotic



stresses. The expression of OsNAC5 and OsNAC6 is upregulated under high salt environment or ABA treatment. Transgenic rice plants overexpressing OsNAC5 or OsNAC6 exhibited enhanced tolerance to salt and drought stresses (Nakashima et al., 2007; Takasaki et al., 2010). Later experiments suggest that overexpression of other two NAC proteins, SNAC1 and SNAC2, can also enhance salt and drought tolerance in transgenic rice (Hu et al., 2006; Hu et al., 2008).

These results show that TFs have critical roles in regulating osmotic resistance in plants through ABA-independent pathway. Nevertheless, DREB and NAC proteins can also mediate the cooperation of ABA-independent pathway and ABA-dependent pathway by physically interacting with the transcription factors involved in the ABA-dependent pathway.

DREB2C is a member of the DREB2 subgroup identified in *Arabidopsis*. By interacting with ABA inducible transcription factor ABF, this protein can bind to the ABA responsive bind elements and induce the expression of ABA responsive genes (Lee et al., 2010). Transgenic *Arabidopsis* overexpressing DREB2C exhibits increased tolerance to cold and heat stresses, but is more sensitive to osmotic stresses than wild type plants (Lee et al., 2010). *Arabidopsis*-derived NAC protein ANAC096 is an important transcription factor involved in the dehydration and osmotic stress responses. By interacting with ABF, ANAC096 regulates ABA-induced stomata closure. Loss-of-function mutant *anac096* exhibits impaired stomata closure and increased water loss under osmotic stresses (Xu et al., 2013).

### ***The roles of other phytohormones in osmotic stresses resistance***

Abundant evidence has shown that in addition to ABA, other phytohormones, such as gibberellin, cytokinin, auxin and ethylene, are also involved in osmotic stress responses. When plants are under salt or drought treatment, the levels of these phytohormones decline, which is usually accompanied with the increase of ABA level in plants. These changes in phytohormone levels cause retarded plant growth, reduced photosynthesis, stomata closure, and leaf senescence and abscission, resulting in remarkably reduced water and energy usage, and thus these conserved resources are used to ensure plant survival and accelerate seed development (He et al., 2005; Achard et al., 2006; Rivero et al., 2009; Kohli et al., 2013). More studies are needed to understand how the levels of these phytohormones are regulated under osmotic stresses. A recent research on CBF1 gene shed light on this question. Transgenic *Arabidopsis* with overexpressed CBF1 shows slow growth, but enhanced freezing tolerance. Further research indicates that CBF1 stimulates the expression of a key enzyme named GA-2 oxidase involved in the degradation of gibberellin. As a consequence of CBF1 overexpression in transgenic *Arabidopsis*, the level of gibberellin decreases and the growth-repressing DELLA proteins accumulate, leading to retarded growth and enhanced freezing tolerance (Achard et al., 2008).

### **MicroRNA mediated abiotic stress resistance**

#### ***Biogenesis of microRNA in plants***

In plants, microRNA (miRNA) genes are first transcribed by Pol II into long pri-miRNAs. DCL1(Dicer-like1)-HYL1(Hyponastic leaves1)-SE(Serrate) complex in D-

bodies cleaves pri-miRNAs to yield pre-miRNAs with stem-loop structure (Kurihara et al., 2006; Liu et al., 2009; Voinnet, 2009; Axtell et al., 2011). Recent research indicated TOUGH protein and two cap-binding proteins CAP80 and CBP20 also help with the cleavage of pri-miRNAs (Laubinger et al., 2008; Ren et al., 2012). Pre-miRNAs are sliced again by DCL1-HYL1-SE complex to yield miRNAs/anti-miRNA duplexes, which are then methylated by HEN1 (HUA enhancer1), followed by degradation of anti-miRNA in the duplex (Park et al., 2002). The remaining 21nt single strand mature miRNAs are translocated into cytoplasm through HST1 (HASTY1), forming RISC (RNA-Induced Silencing Complex) with cytoplasm cellular protein AGO1 (Argonaute1) (Fagard et al., 2000; Park et al., 2005). In RISC, mature miRNAs recruit and form near-perfect pairs with mRNAs of their target genes, followed by cleavage of the base-pairing region and degradation of the transcripts, leading to the expression repression of their targets (Bartel, 2004). Mature miRNAs can also repress the expressions of their target genes by inhibiting mRNA translation (Li et al., 2013).

### ***Functions of plant miRNAs in abiotic stress***

Since the discovery of the first plant miRNA in *Arabidopsis*, more than 8000 miRNAs have been identified in plants. The targets of miRNAs are found to encode various proteins from transcription factors to functional enzymes, implying that miRNAs have essential roles in many important metabolisms, including axial meristem initiation, leaf development, flower development, leaf morphogenesis, oxidative stress resistance, nutrition starvation response, drought and salt resistance (Rhoades et al., 2002; Palatnik et

al., 2003; Sunkar et al., 2006; Lin et al., 2008; Kawashima et al., 2009; Wu et al., 2009; Zhao et al., 2009; Zhou et al., 2013; Yuan et al., 2015).

*MiR159* is found to be involved in the ABA-dependent osmotic resistance, targeting several MYB transcription factors which positively regulate ABA response. Under ABA or drought treatment, *miR159* transcripts accumulate in *Arabidopsis*, repressing expressions of its putative target genes including *MYB33* and *MYB101* (Reyes and Chua, 2007). *Arabidopsis* overexpressing *miR159* is ABA hyposensitive. On the contrary, transcript levels of two MYB encoding genes - *MYB33* and *MYB56* - increase in *miR159ab* double mutant, and this double mutant exhibits constitutive drought responses as curled leaves, small siliques and small seeds (Allen et al., 2007; Reyes and Chua, 2007). Similar to *miR159*, *miR160* plays an important role in ABA-dependent osmotic resistance. The target gene of *miR160* encodes an ARF (Auxin Response Factor) protein. *Arabidopsis* plants overexpressing *miR160* are ABA hyposensitive, but *Arabidopsis* expressing *mARF10*, a *miR160* resistant *ARF10* gene, is ABA hypersensitive (Liu et al., 2007). These results indicate that miRNA negatively regulate ABA responses under osmotic stresses.

miRNAs also mediate ABA-independent osmotic stress resistance. As one of the most conserved miRNA family in plants, *miR319* responds to salt, cold and dehydration intensively across different plant species, including *Arabidopsis*, sugarcane, and rice (Axtell and Bowman, 2008; Liu et al., 2008; Lv et al., 2010; Thiebaut et al., 2012). The target gene of *miR319* encodes TCP (Teosinte branched/Cycloidea/Pcf) transcription factors, which regulate leaf morphogenesis and control cell proliferation (Ori et al., 2007; Liu et al., 2008; Nag et al., 2009). One well-known defense and stress responsive element

TC-rich repeat is identified in the promoter region of *miR319*, indicating its role in the stress resistance mechanisms (Liu et al., 2008). Zhou and her colleagues found that overexpression of rice *miR319* in creeping bentgrass confers the transgenic plants with enhanced salt and drought tolerance (Zhou et al., 2013). Furthermore, morphology change was also observed in the *miR319* overexpression creeping bentgrass, and four PCF (Proliferating Cell Factors) transcription factors were proven to be the targets of *miR319* and down-regulated in the transgenic plants (Zhou et al., 2013). These facts reveal that *miR319* functions in both abiotic stress resistance and plant development. Similarly, salinity stress resistance of transgenic creeping bentgrass with overexpression of rice *miR528* is enhanced (Yuan et al., 2015). One of the potential target genes of *miR528* in creeping bentgrass encodes AAO (Ascorbic Acid Oxidase). Ascorbic acid eliminates ROS when plant is subjected to stresses. In transgenic creeping bentgrass, high level of *miR528* represses expression of AAO and thus, the accumulation of ascorbic acid is upregulated, which, in turn, scavenges ROS, leading to the enhanced growth of transgenic plant under salt stress (Yuan et al., 2015). Deep-sequencing and microarray analyses indicate that *miR528* responds to multiple stresses, including salt, drought, cold and nitrate starvation, implying that *miR528* is an essential positive regulator of abiotic stress resistance in monocot plants (Zhang et al., 2008; An et al., 2011; Xu et al., 2011; Ferreira et al., 2012; Nischal et al., 2012; Sharma et al., 2015).

Based on previous works, miRNAs also participate in nutrition starvation responses. *MiR399* responds to phosphorus starvation stress by targeting UBC24 (Ubiquitin-Conjugating E2) in *Arabidopsis*, which represses the phosphate transporter

PHT1 (Chiou et al., 2006). Overexpression of miR399 represses UBC24 and thus induces accumulation of phosphate (Fujii et al., 2005). Another well-studied miRNA family responding to nutrition starvation is *miR395* family, which is intensively upregulated under sulfate starvation (Kawashima et al., 2009). The targets of miR395 in *Arabidopsis* are low-affinity SULTRs (Sulphate Transporters) mediating sulfate distribution between leaves of different ages, and ATPS (ATP Sulfurylases) mediating assimilation of sulfate (Lunn et al., 1990; Klonus et al., 1994; Rotte and Leustek, 2000; Takahashi et al., 2000; Patron et al., 2008). Upon sulfate starvation, accumulation of *miR395* in plants strongly suppresses low-affinity SULTRs and ATPS, which facilitate accumulation of sulfate in shoot under sulfate starvation (Liang et al., 2010). A recent study showed that transgenic creeping bentgrass overexpressing *miR528* exhibits enhanced resistance to nitrate starvation, implying its role in plant response to nutrient deficiency maintaining nitrate homeostasis (Yuan et al., 2015).

## **PATHOGEN INFECTION AND PLANT INNATE DEFENSE**

### **Pathogen-plant interaction: from antagonism to coevolution**

In the wild environment, microbial pathogens can infect plants via air, water, soil and physical contact between healthy and infected plants. To successfully establish infection and multiply in the apoplasmic spaces, pathogens need to penetrate the surface of plant leaves and roots. There are many natural channels on the surface of plants that pathogens can utilize to penetrate the interior, such as stomata, pores and wounds. Once

successfully breaching the cell wall, microbes can obtain nutrition from plant cells and cause sickness to plants.

To resist the attack of pathogens, plants adopt two layers of defense: innate immunity and adaptive immunity (Dodds and Rathjen, 2010). Innate immunity is carried out by the interaction between pathogen specific molecules and plant PRRs (Pattern Recognition Receptors) localized on the plasma membrane of plant cells (Antolin-Llovera et al., 2012). The interactions between PRRs and pathogen specific molecules cause conformational change in the kinase domain of PRRs, which promotes PRRs to phosphorylate down-stream MAPK modules (Sun et al., 2013). Activated MAPK modules then phosphorylate transcription factors, which in turn induce the expressions of defense-related genes and spur the plant defenses against microbial pathogens. Because the whole immunity process is based on the recognition of pathogen specific molecules named PAMPs (Pathogen Associated Molecular Patterns) by plant PRRs, this innate immunity is termed PTI (PAMP Triggered Immunity).

Virulence pathogens can repress the innate immunity by interfering with the recognition of PAMPs by PRRs or injecting effector proteins into the plant cytoplasm through pathogen type-III secretion system (Dodds and Rathjen, 2010). Specifically, these effectors can interact with and inactivate key components of the PTI pathway, causing the PTI to break out and facilitating the pathogen invasion (Dodds and Rathjen, 2010). But plants have developed an adaptive immunity system termed ETI (Effector Triggered Immunity) to defend themselves. In ETI pathway, a group of NB-LRR (Nucleotide-Binding Leucine-Rich-Repeats) receptor proteins can directly or indirectly interact with

specific effectors and trigger extensive plant defenses. Nevertheless, virulence pathogens, in turn, will secrete another group of effectors to target and inactivate the NB-LRRs and overcome the ETI pathway.

The above facts indicate that the defense mechanisms of plants are heavily dependent on the recognition of pathogen specific molecules by PRRs and NB-LRRs. These plant receptors (PRRs and NB-LRRs) responsible for the recognition are called resistance (R) proteins. Pathogens carrying molecules (especially effector proteins) that could be recognized by the R proteins will fail to infect these plants; thus they are called avirulent pathogens, and these molecules are called avirulence (Avr) molecules. Under some circumstances, avirulent pathogens are also pathogens that have mutations in their type-III secretion systems, and therefore resulting in the loss of their abilities to inject effectors into the plants for repressing the PTI pathway. If a plant fails to recognize the pathogen Avr molecule(s), due to absence of the Avr gene(s) in the pathogen and/or absence of the corresponding R gene(s) in the plant, this plant will be a susceptible host of the pathogen. This phenomenon is firstly described by Flor as gene to gene relationship (Flor, 1971).

Most of the pathogen molecules recognized by PRRs are indispensable components for the growth and development of pathogens, such as lipopolysaccharide, flagellin, and EF-Tu (Elongation Factor Thermo Unstable). Any change in these components may result in seriously negative impacts to the survival of pathogens. So the best choice, if not the only, for virulence pathogens is to evolve novel effector (E) genes and therefore can circumvent or repress the plant ETI pathway. As for the plants, under the pressure of



virulence pathogen infection, they must be able to evolve R genes to recognize the corresponding novel E genes. Thus the pathogen and plant apply selective pressures on each other and use their evolutionary mechanisms to overcome the pressures brought by the other side, making them are locked in an antagonistic coevolution (Figure 1.3).

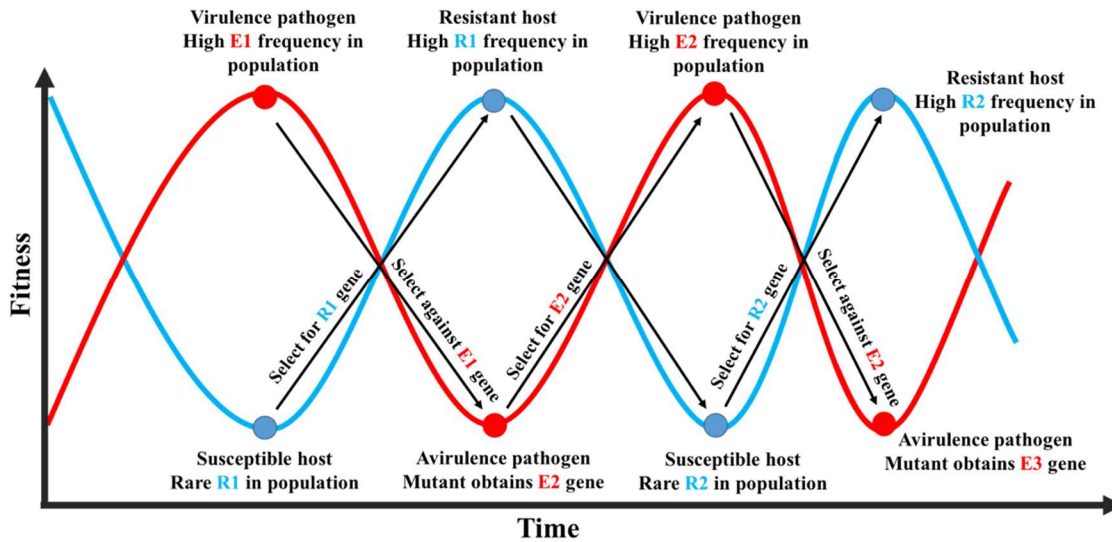


**Figure 1.3. Co-evolution of plant resistance proteins and pathogen effectors.** Virulence pathogen carries a prevalent effector gene (E1), which is recognized by a rare resistance protein (R1) in susceptible host plant, resulting in selection for host individuals with R1 and selection against pathogen individuals with E1. Thus, the fitness of the virulence pathogen reduces, and it becomes avirulence pathogen to the host plant; on the contrary, the fitness of the host plant increases, and it becomes resistant host to the pathogen. Then, effector mutates in some pathogen individuals, producing novel effector genes including E2. Pathogen individuals carrying E2 become virulence pathogen, which can grow on resistant host. This will lead to increase of pathogen fitness and decrease of host plant fitness, and thus the frequency of E2 increases in pathogen population. The pathogen again becomes virulent to the host plant, while the host plant is susceptible to this virulence pathogen. Nevertheless, few individuals in the host population carry resistance protein R2, which either is the result of mutation or has been existing in host population but at low frequency for a long time. Thus, this cycle is continuously turning and occurs at various R and E loci, pushing the evolutions of the pathogen and the host plant.

---

### PRRs-mediated PAMPs recognition

For innate immunities of both animals and plants, PRRs localized on plasma membrane confer the ability to detect the presence of microbial pathogens through PAMPs recognition (Medzhitov, 2001; Gomez-Gomez and Boller, 2002). PAMPs are ideal targets of receptors of PTI pathway. First, PAMPs are unique pathogen molecules which are not present in hosts, so their presences allow the host PRRs to distinguish non-self microbe components from self host components. Second, most of PAMPs, such as lipopolysaccharide, flagellin and EF-Tu of Gram-negative bacteria, peptidoglycans and glucans of Gram-positive bacteria, and chitins of fungus, are essential components for pathogen to survive (Zipfel and Felix, 2005; Jones and Dangl, 2006). Pathogens cannot tolerant even small amount of mutations in their PAMPs, which may either reduce their fitness or be lethal. This feature makes PAMPs highly conserved across different pathogen strains. So a limited number of PRRs is enough for hosts to detect a larger number of microbial pathogens. For example, FLS2 (Flagellin Sensing 2) can detect nearly all flagellated pathogens.

### ***LRR-RLKs receptors***

In animals, Toll-like receptors represent the most important PRRs. A classic Toll protein comprises a signal peptide for subcellular localization, an extracellular LRRs (Leucine Rich Repeats) domain for ligands recognition, a membrane-spanning region, and an intercellular Toll/IL(Interleukin)-1R(TIR) tyrosine kinase domain for signaling transduction (Medzhitov, 2001). LRR-RLKs, on the other hand, are the most important PRRs in plants. LRR-RLKs are composed of signal peptide, extracellular LRRs domain,

membrane-spanning region and an intercellular serine-threonine kinase domain, sharing similar structures to Toll proteins in animals (Torii, 2004).

Although previous research showed that the expressions of 49 out of 235 identified LRR-RLKs are upregulated more than two folds upon pathogen treatment in *Arabidopsis*, only two LRR-RLKs - FLS2 and EFR (EF-tu Receptor) - have been proven to directly recognize and interact with PAMPs (Figure 1.4) (Kemmerling et al., 2011).

As the first identified PRR in *Arabidopsis*, the function of FLS2 has been well studied. FLS2 is responsible for the recognition of flagellin protein comprising microbe flagella (Gomez-Gomez and Boller, 2000). *Arabidopsis* plants with mutations in FLS2 exhibit reduced flagellin responses, and are more susceptible to *Pst* DC3000 (*Pseudomonas syringae* pathovar *tomato* strain, DC3000) when they are surface inoculated with *Pst* DC3000 (Gomez-Gomez and Boller, 2000; Zipfel et al., 2004). FLS2 contains 28 LRR domains in its extracellular structure, in which 14 LRR domains (from LRR3 to LRR16) comprise the flagellin binding site. Upon pathogen infection, flagellin binds the 14 LRR domains, triggering the formation of FLS-BAK1 complex (Sun et al., 2013).

BAK1 is a multiple functional LRR-RLK in *A. thaliana*. Besides its critical role in the perception of brassinosteroid, BAK1 is also an important co-receptor in *Arabidopsis* PTI pathway. Previous study showed that after FLS2 bind flagellin, C-terminus of BAK1 LRR domains immediately form a sandwich structure with C-terminus of flagellin and FLS2 LRR domains (Li et al., 2002; Sun et al., 2013). Conformational changes caused by this BAK1-flagellin-FLS2 sandwich structure promote BAK1 to autophosphorylate its own kinase domain and transphosphorylate kinase domain of FLS2, and then the activated

FLS2 and/or BAK1 recruit and activate downstream signaling cascades (Schwessinger et al., 2011). Mutations in critical amino acid residues of the BAK1 LRR domains attenuate both interaction between FLS2 and BAK1 and phosphorylation of this heterodimer, and mutation in the BAK1 kinase domain negatively impact its phosphorylation ability (Schwessinger et al., 2011; Sun et al., 2013).

Just like flagellin protein, EF-Tu protein also broadly exists in over thousands of bacterial species and is essential for their survival. As a classic LRR-RLK which contains 21 LRR domains, EFR is another important PRR in the *Arabidopsis* PTI pathway. EFR can recognize and interact with EF-Tu protein, followed by the formation of EFR-BAK1 heterodimer (Zipfel et al., 2006; Roux et al., 2011). *Arabidopsis* expressing loss-of-function EFR is susceptible to *Agrobacterium* infection (Zipfel et al., 2006).

Both EFR and FLS2 are non-RD (Non-Arginine-Aspartate) kinases, indicating that they have very weak kinase activity. To transfer the signal to downstream MAPK modules, EFR and FLS2 are dependent on the phosphorylation activity of their co-receptor BAK1. Aspartate residue in its sub kinase domain VIb confers BAK1 both autophosphorylation ability and transphosphorylation ability (Schwessinger et al., 2011). After the formation of EFR-BAK1 and FLS2-BAK1 heterodimer, BAK1 transphosphorylates the kinase domain of EFR and FLS2 (Schwessinger et al., 2011). The phosphorylated kinase domain confers EFR and FLS2 ability to transmit signals into cells by recruiting and phosphorylating downstream MAPK modules.

PEPR1 and PEPR2 are another two LRR-RLKs triggering innate immunity upon pathogen infection (Figure 1.4). Instead of interacting with PAMPs, PEPR1/2 interacts

with plant endogenous peptides Pep1 to Pep6 to induce basal immunities against pathogens (Yamaguchi et al., 2006; Yamaguchi et al., 2010; Yamaguchi and Huffaker, 2011). Pep1 to Pep6, termed DAMPs (Damage Associated Molecular Patterns), are host endogenous molecules. They are released into extracellular space by plant cells upon wounding or pathogen infection. BAK1 has been proved to be co-receptor of PEPR1/2 during the signal transduction upon pathogen invasion (Li et al., 2002; Chinchilla et al., 2007; Postel et al., 2010; Schulze et al., 2010).

Similar to LRR-RLKs, plasma membrane anchored proteins LRR-RLPs (Leucine Rich Repeats Receptor Like Proteins) also contain LRR domains in their extracellular structure responsible for PAMPs binding, but lack kinase domain in their intracellular structure. In tomato, LeEiX1 and LeEiX2 are two LRR-RLPs found to mediate the perception of fungal derived elicitor EiX (Ethylene Inducing Xylanase) (Figure 1.4). Though both LeEiX proteins can bind EiX elicitor, only LeEiX2 has the ability to transmit signals into cytoplasm (Ron and Avni, 2004). Because LeEiX2 is only a receptor like protein without kinase domain, it must work with protein kinase(s) for signal transduction. But no co-receptor of LeEiX2 has been identified so far.

### ***LysM receptors***

LRR-RL receptors bind peptides and proteins, while LysM (Lysin Motif) receptors bind N-acetylchitooligosaccharides and N-acetylglucosamine, basic unit of fungal chitin and bacterial PGN (Peptidoglycan).

In plants, LysM receptors could be divided into two groups: LYKs (LysM Receptor Like Protein Kinases) and LYPs (LysM Receptor Like Proteins). LYKs contain extracellular LysM domain (with 1 to 3 LysMs), transmembrane domain and intracellular kinase domain, so they can mediate both PAMPs recognition and signaling transduction. The structure of LYPs is similar to LYKs, except that the kinase domain is absent in their intracellular structure. LYPs need to form complex with LYKs for signaling transmission after they bind PAMPs.

OsCEBiP (*Oryza sativa* Chitin Elicitor-Binding Protein) is a classic LYP in rice. OsCEBiP is localized on plasma membrane and contains two LysMs domains in its extracellular structure (Kaku et al., 2006). The binding of CEBiP with chitin oligosaccharide elicitor derived from fungal cell wall is essential for activating chitin induced innate immunities. But because OsCEBiP has no kinase domain, a receptor-like protein kinase is required to act as co-receptor of OsCEBiP for signaling through chitin recognition to downstream MAPK modules. LYP OsCERK1 (*Oryza sativa* Chitin Elicitor Receptor Kinase 1) has been proven to be the essential co-receptor of OsCEBiP in rice (Shimizu et al., 2010). OsCERK1 contains one extracellular LysM domain and an intercellular serine-threonine kinase domain. Upon pathogen infection, the presence of chitin induces the formation of OsCEBiP-OsCERK1 heterodimer, in which OsCERK1 functions as a signal transducer phosphorylating downstream MAPK modules for signaling transduction (Figure 1.4) (Shimizu et al., 2010).

*Arabidopsis* utilizes a similar protein to perceive chitin signaling (Figure 1.4). AtCERK1, the counterpart of rice OsCERK1 in *Arabidopsis*, is a plasma membrane

anchored LYK which contains three LysMs in its extracellular domain. Knockout of AtCERK1 in *Arabidopsis* compromises its innate defense against fungal pathogen (Miya et al., 2007). Homologs of OsCEBiP were identified in *Arabidopsis*, named LYM1, LYM2, and LYM3. But research on LYMs knockout mutants suggests that LMYs are not required in chitin perception, though LYM2 indeed bind chitin (Shinya et al., 2012). AtCERK1 alone is enough for chitin perception and signaling transduction in *Arabidopsis*, while both OsCERK1 and OsCEBiP are indispensable in rice, implying that different mechanisms are adopted in chitin signaling transduction in these two model plants (Shinya et al., 2012). LYM1, LYM3, and AtCERK1 are also involved in bacterial PGN perception. In LYM1-LYM3-AtCERK1 complex, LYM1 and LYM3 interact with PGN physically, and AtCERK1 is responsible for signaling transmission through plasma membrane to cytoplasm. Knocking out of any components in the LYM1-LYM3-AtCERK1 complex will make *Arabidopsis* susceptible to bacterial pathogen (Willmann et al., 2011).

### **MAPK modules and transcription factors**

MAPK modules are located downstream of PRRs. After plasma membrane-anchored PRRs recognize PAMPs, the signal will be transmitted into cell through MAPK signal cascade. MAPK cascade is composed of three layers of protein kinases, including MAPKKK/MEKKs (Mitogen-Activated Protein Kinase Kinase Kinases), MAPKK/MKKs (Mitogen-Activated Protein Kinase Kinases), and MAPK/MPKs (Mitogen-Activated Protein Kinases) (Pitzschke et al., 2009). MAPK-mediated signaling transduction is a cascade reaction. After MEKK receives signals from PRRs when plant is

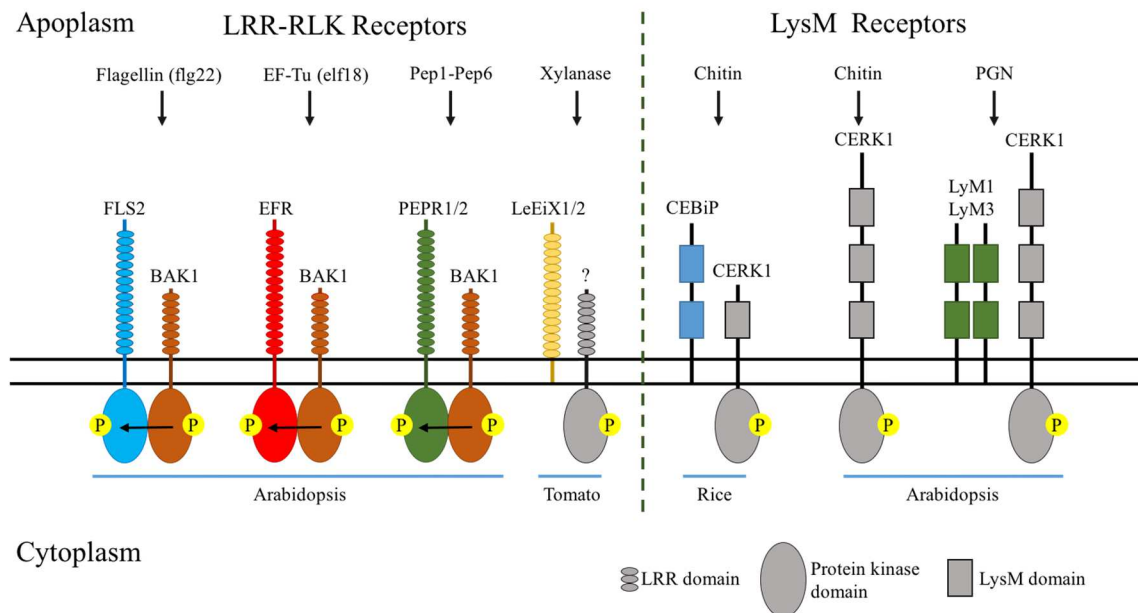


**Figure 1.4. Plant pattern-recognition receptors.** LRR-RLK receptors are responsible for recognition of pathogen or host proteins. Pathogen proteins flagellin/flg22, EF-Tu/elf18 and xylanase are recognized by FLS2, EFR and LeEiX1/2, respectively. Plant endogenous peptides Pep1-Pep6 released by plant under damage or pathogen infection are recognized by PEPR1/2. BAK1 has been identified as co-receptor of FLS2, EFR and PEPR1/2. To transmit signal into cell, the RD kinase domain of BAK1 is auto-phosphorylated and then transphosphorylates non-RD kinase domain of its con-receptor. The co-receptor of LeEiX1/2 has not been identified yet. LysM receptors recognize basic units of pathogen cell wall. In rice, LysM receptor like protein CEBiP contains chitin binding site, and its co-receptor - LysM receptor like protein kinase CERK1 - is responsible for signaling transduction. Orthologue of rice CERK1 has been identified in *Arabidopsis*. *Arabidopsis* CERK1 can bind chitin and transmits signal into cell alone. *Arabidopsis* CERK1 can also form complex with two LysM receptor like proteins LyM1 and LyM3, which recognizes PGN. Figure summarized from (Zipfel, 2008)

subjected to pathogen or PAMPs challenge, it will phosphorylate its downstream MKKs.

Phosphorylated MKKs will, in turn, activate MPKs that function at the third layer of the MAKP modules.

MAPK module, MEKK-MKK4/5-MPK3/6, is implied to play a positive role in plant defenses against pathogens (Vidhyasekaran, 2014). Previous research indicated



pathogen infection and PAMP elicitors, such as flg22 and elf18, induce strong MPK3/6 phosphorylation, which positively regulates the downstream basal responses (Takahashi et al., 2007; Beckers et al., 2009; Pitzschke et al., 2009; Meng et al., 2013). The function of MPK3 and MPK6 overlap each other in *Arabidopsis* innate defenses, but this overlapping is not complete. Galletti and her colleagues found that *Arabidopsis* with loss-of-function *mpk3* exhibited compromised basal defenses against fungal pathogen *Botrytis cinerea*, while MPK6-knocked out *Arabidopsis* exhibited reduced flg22 and OGs (Oligogalacturonides) induced resistance to *Botrytis cinerea* (Galletti et al., 2011).

Another MAPK module, MEKK1-MKK1/2-MPK4, also mediates PAMP elicitor induced PTI response in *A. thaliana* (Meszaros et al., 2006). Both *Arabidopsis* *mkk1-mkk2* double mutant and *mekk1-mpk4* double mutant exhibited spontaneous cell death and constitutive defense responses, indicating that MEKK1-MKK1/2-MPK4 module negatively regulates *Arabidopsis* innate immunity (Gao et al., 2008). *Arabidopsis* constitutively overexpressing activated MPK4 shows no morphological phenotype under normal condition, but it's more susceptible to bacterial pathogen *Pst* DC3000 than wild type, providing another piece of evidence supporting that MPK4 plays a negative role in pathogen resistance (Colcombet et al., 2013).

Activated MPKs induce the expressions of defense-related genes through activating transcription factors (Gomez-Gomez and Boller, 2002; Pitzschke et al., 2009). WRKY transcription factors are DNA-binding proteins which can recognize and bind to the *cis*-regulatory elements in the promoter region of functional genes, regulating their expressions on transcriptional level. Under pathogen infection or SA treatment, 49 out of 72 WRKY

mRNA levels are altered, indicating that they are important components involved in the pathogen defense mechanisms (Dong et al., 2003). Many WRKY proteins (e.g. WRKY22 and WRKY29) have been identified as direct targets of MAPKs in the pathogen defense signaling transmission, and activated WRKY proteins then activate transcriptions of R genes, such as PR-1 (Pathogenesis Related 1) and PR-5 (Gomez-Gomez et al., 1999; Asai et al., 2002; Takahashi et al., 2007).

WRKY53 is identified as both a positive and negative regulator of basal responses, and it can target at least seven other WRKY proteins including WRKY22 and WRKY29, suggesting that it's a centerpiece of the plant defense signaling transduction (Miao et al., 2004; Zentgraf et al., 2010). Previous studies indicated that WRKY53 is not the direct substrate of activated MPK3/6 (Pitzschke et al., 2009), but suggested that WRKY22 may be directly regulated by MPK3/6 when *Arabidopsis* is under the treatment of flg22 (Asai et al., 2002).

W-boxes are found in the promoter region of many WRKY proteins, suggesting that WRKYs super gene family is a self-regulation gene family (Dong et al., 2003; Miao et al., 2004; Zentgraf et al., 2010). A recent study showed that the WRKY22 T-DNA insertion mutant has low transcripts level of WRKY53 in submergence-treated *Arabidopsis*, indicating that WRKY53 may be regulated by WRKY22 (Hsu et al., 2013). In addition, WRKY53 is proved to target many other WRKY proteins including WRKY22 and WRKY29 (Miao et al., 2004).

### **Defense-related genes and basal defenses**

Basal defenses associated with PTI pathway include three major responses: production of reactive-oxygen species (ROS), cell wall reinforcement, and stomata closure. ROS burst and ROS accumulation are essential basal responses during the pathogen invasion. ROS not only can repress the expansion of pathogen, but also regulate other PAMPs-triggered basal defenses such as callose deposition and peroxidase-dependent gene expression (Daudi et al., 2012). Heterotrimeric G proteins, composed of  $\alpha$ ,  $\beta$ , and  $\gamma$  subunits, are able to transmit outside signals into cytoplasm by cooperating with GPCR (G Protein Coupled Receptor) proteins, initiating ROS burst during pathogen infection.  $\alpha$  subunit encoding gene *XLG2* and  $\beta$  subunit encoding gene *AGB1* are found to be intensively upregulated upon elicitor treatment and pathogen infection. Both *xlg2* and *agb1* mutants exhibit compromised elicitor response and pathogen resistance, such as impaired ROS burst (Ishikawa, 2009; Zhu et al., 2009). A recent research suggested that under normal condition, the three G protein subunits function together to degrade BIK1 (Receptor-Like Cytoplasmic Kinase), a positive regulator of FLS2-BAK1 induced signal transduction. When *Arabidopsis* is treated with flg22,  $\alpha$  subunit XLG2 dissociates from  $\beta$  subunit AGB1, and the N terminus of XLG2 is phosphorylated by BIK1. The activated XLG will then promote ROS burst, allowing plants to fight against pathogen infection (Liang et al., 2016).

Cell wall reinforcement is achieved as callose deposition in cell wall. After PTI is activated, callose will be synthesized and form matrix in the apoplast, facilitating the deposition of antimicrobial compounds that can repress the growth of pathogen (Luna et al., 2011). GLS5 (Glucan Synthase-Like 5) is a key callose synthase in *Arabidopsis*. When

the expression of GLS5 is repressed, the wound callose and papillary callose syntheses are impaired under pathogen infection (Jacobs et al., 2003). Further studies suggest that the growth of avirulence pathogen - *Pst DC3000 hrcC* or *P. syringae* pv *phaseolicola* - is enhanced in *gls5* single mutant or *gls5 pad4* double mutant (Kim et al., 2005; Ham et al., 2007). These results indicate that pathogen-induced callose deposition in *Arabidopsis* partly depends on GLS5-mediated callose synthesis, implying that *GLS5* is an important downstream gene in PTI pathway, but how GLS5 is regulated remains unknown.

Within the first hour of pathogen infection, stomata will be actively closed to avoid the entry of pathogen. Previous research indicated that stomatal closure during pathogen infection depends on ABA mediated ion efflux from guard cells through OST1 and potassium channel GORK1 (Hosy et al., 2003; Melotto et al., 2006). Another phytohormone SA mediates the stomatal closure in plants (Joon-Sang, 1998; Hao et al., 2011). Melotto and her colleagues found that PAMPs-induced stomatal closure is impaired in two SA-deficient *Arabidopsis* mutants *nahG* and *eds16* (Melotto et al., 2006).

### **SMG AND SMG PROTEIN FREE IN GMOs**

In the past 30 years, knowledge advancement and technological revolution in the biology field have had a significant impact on the agricultural industry. GMOs (Genetically Modified Organisms) are one of the benefits brought by rapidly developing molecular biological and genetic approaches. In the past, scientists needed to crossbreed related plants and screen the candidates from countless descendants to obtain plants with desirable traits. This is a labor-intensive and time-consuming work, and the results were not always desired

because of random recombinations of parental traits. Thanks to the development of recombinant DNA and transgenic technology, scientists have an easier and more precise option to breed plants with expected characters than traditional plant breeding. By inserting gene expression cassette between T-DNA boundaries of a binary vector and using *Agrobacterium* mediated plant transformation, the T-DNA region which contains exogenous genes can become integrated into the plant genome and express the desired traits (An, 1985; Valvekens et al., 1988; Hiei et al., 1994; Ishida et al., 1996; Hiei et al., 1997).

After the breeding of a GMO, a selectable marker gene is generally superfluous. However, the presence of the useless selectable marker gene in a GMO makes the approval of transgenic crop release and commercialization very difficult. Several molecular strategies can be adopted to specifically remove the SMG (Selectable Marker Gene) from a GMO but keep trait gene intact or prevent the accumulations of SMG and its product from edible parts of a GMO.

### **Site-specific recombination**

Site-specific recombination systems used in SMG removal include the *Cre/loxP* system derived from Bacteriophage P1, the *FLP/FRT* System derived from *Saccharomyces cerevisiae*, the *R/RS* system derived from *Zygosaccharomyces rouxii*, and the *Gin* system derived from phage Mu (Araki et al., 1985; Dale and Ow, 1990; Maeser and Kahmann, 1991; Onouchi et al., 1991; Lyznik et al., 1993). Additional systems have also recently been developed (Kittiwongwattana et al., 2007; Moon et al., 2010).

The Bacteriophage P1 derived *Cre/loxP* system is one of the best studied recombination systems. *Cre/loxP* is comprised of a recombinase *Cre* and a 34 bp specific DNA sequence *loxP*. DNA recombination between two *loxP* sites occurs with the help of the *Cre* protein. Although it can be used for both site-specific DNA integration and excision, the *Cre/loxP* system is mainly a genetic tool used for SMG excision in GMO (Gilbertson, 2003).

*Cre/loxP* was first examined in tobacco cells. Transiently expressed *Cre* recombinase in tobacco protoplast cells can enter the nucleus and recognize a pair of adjacent *loxP* repeats that were introduced previously, followed by a crossover of this pair of *loxP* repeats and excision of the DNA sequence flanked by them (Dale and Ow, 1990). After this site-specific recombination system was proven to be functional in tobacco protoplast cells, it has since been broadly utilized to delete SMGs across different species, such as tobacco, *Arabidopsis*, maize, rice, potato, wheat and soybean (Odell et al., 1990; Dale and Ow, 1991; Russell et al., 1992; Hoa et al., 2002; Zhang et al., 2003; Cuellar et al., 2006; Li et al., 2007b; Mészáros et al., 2014).

Delivery of the *Cre* protein into transgenic plants carrying *loxP* sites can be achieved through different strategies. In the earliest method, in order to deliver the *Cre*, one transgenic plant line harboring a trait gene and a *loxP* repeats-flanked SMG is crossed with another transgenic plant line harboring the *Cre* gene. In the F1 plant, crossover will occur between the two directly repeated *loxP* sites followed by removal of the SMG. In the next generation (F2), a trait gene and *Cre* localized in different genomic loci will segregate independently and a marker-free transgenic line harboring only trait gene will be obtained

(Gilbertson, 2003). This early strategy to remove SMGs from GMOs is time consuming and only suitable for seed-propagated plants.

A more efficient strategy was later developed to overcome these disadvantages. In this strategy, *Cre*, the trait gene and the SMG are all constructed in a same T-DNA region and a single pair of directly repeated *loxP* is constructed to flank both the *Cre* gene, which is driven by an inducible promoter, and the SMG. After the transgenic plant harboring this T-DNA region is established, the inducible promoter will be active under specific conditions and induce the expression of *Cre*, causing the removal of the SMG, *Cre* and all other DNA sequences between the two *loxP* repeats. The greatest advantage of this strategy is efficiency in that a GMO harboring only the trait gene can be obtained in the R<sub>0</sub> generation (Gilbertson, 2003). Many inducible promoters can be used to control the expression of *Cre*, such as heat shock promoter, chemically inducible promoter, cold-inducible promoter and floral specific promoter (Zuo et al., 2001; Gilbertson, 2003; Zhang et al., 2003; Wang et al., 2005; Cuellar et al., 2006; Bai et al., 2008; Khattri et al., 2011; Petri et al., 2012; Garcia-Almodovar et al., 2014; Mészáros et al., 2014). Specifically, the cold-inducible promoter and the floral specific promoter can be activated during the natural processes of vernalization and florescence respectively. This activation induces the excision of *loxP*-flanked DNA sequences, which can greatly reduce workload (Bai et al., 2008; Mészáros et al., 2014).

Another commonly used site-specific recombination system is the *FLP/FRT* system, which is originally from the 2- $\mu$ m plasmid of the eukaryotic organism *Saccharomyces cerevisiae* and is related to *Cre/loxP* system mechanistically (Chow et al.,

1995). As a recombinase, FLP can induce the recombination between two *FRT* repeats. The first paper that confirmed that the FLP/*FRT* system could function in plant protoplasts was published in 1993 (Lyznik et al., 1993). Then, evidence from later experiments showed that the FLP/*FRT* recombination system could also work well in tobacco, *Arabidopsis*, rice and other plant species, indicating that this recombination system can be utilized to delete SMGs in GMOs (Lloyd and Davis, 1994; Kilby et al., 1995; Sonti et al., 1995; Luo et al., 2000; Hu et al, 2008). Zhang *et al.* eliminated the SMG *als* flanked with directly repeated *FRT* sites in transgenic maize harboring Na<sup>+</sup>/H<sup>+</sup> antiporter genes by crossing it with FLP expression transgenic maize (Li et al., 2010). In tobacco, Woo et al. (2009) constructed a stress inducible promoter driven auto-excision vector by using FLP/*FRT* system, in which T-DNA region carried two *FRT* sites flanking an *hpt* gene driven by the CaMV 35S promoter and a *FLP* gene driven by the hydrogen peroxide inducible promoter, Ppod. They confirmed that *hpt* and *FLP* genes were excised in the transgenic tobacco when the transgenic plants were subjected to a hydrogen peroxide environment (Woo et al., 2009).

### **Homologous recombination**

HR (Homologous Recombination) is a native spontaneous event occurring in plants. HR allows plant cells to accurately repair DNA double strand breaks by DNA exchange and duplication between identical DNA sequences. HR can also allow plants to delete DNA sequence flanked by two short identical DNA repeats. Compared to site-specific recombination, HR does not require a recombinase to induce SMG removal so it is a simpler strategy and has been implemented to delete SMG in GMO.



For example, a vector that carries the trait gene, *uidA*, and the two SMGs, *aadA* and *bar*, with the SMGs being flanked by three 418 bp direct repeats, was constructed. Particle bombardment was performed to deliver this vector into tobacco leaves followed by the selection of plastid transformants. In response to the high rate spontaneous homologous recombination, SMG-free transplastomic plants harboring only *uidA* genes were obtained (Day et al., 2005). To obtain a high rate of homologous recombination events to remove marker gene from the final GMO product, the number and sizes of direct repeats should be increased (Day et al., 2005). Another factor that impacts the rate of homologous recombination is the sequence of the repeats. In a previously described experiment, 418 bp direct repeats were generated with the 3' *NtpsbA* regulatory element (Iamtham and Day, 2000; Day et al., 2005). In another study, Zubko *et al.* (2000) used a 352 bp *attP* (attachment P) region of bacteriophage  $\lambda$  as flanking repeats. During tobacco transformation, two SMGs and the *GPF* gene flanked by pairs of *attP* repeats in the T-DNA region were eliminated by homologous recombination (Zubko et al., 2000). They went on to construct a TBS (Transformation Booster Sequence) in the adjacent upstream of the *attP*, which could enhance the rate of homologous and illegitimate recombination (Zubko et al., 2000).

### **Co-transformation**

Co-transformation is an easy way to exclude marker genes from final GMO products. The principle of co-transformation is that a trait gene and a SMG are inserted in two different T-DNA regions. During *Agrobacterium*-mediated transformation with both

T-DNA regions, there is a high probability they will be inserted at two independent plant genomic loci in a single meristem cell. A  $T_0$  plant regenerated from this single meristem cell will self-cross to produce  $T_1$  plants. If the two genes do not link with each other closely, by the law of segregation  $T_1$  plants only harboring the trait gene will be obtained (Miki and McHugh, 2004). Two different methods have been developed to conduct co-transformation of the two T-DNA regions. In the first method, two different vectors are used. One carries the target gene and the other one carries the SMG. The two vectors can be transformed into a single *Agrobacterium* strain or into two different *Agrobacterium* strains (Depicker et al., 1985; Deframond et al., 1986; McKnight et al., 1987; Deblock and Debrouwer, 1991; DeNeve et al., 1997; Daley et al., 1998; Matthews et al., 2001; McCormac et al., 2001; Sripriya et al., 2008). In the second method, a single vector containing two independent T-DNA regions is constructed. The trait gene is inserted in one T-DNA region, and the SMG is inserted in the other (Komari et al., 1996; Xing et al., 2000; McCormac et al., 2001; Miller et al., 2002).

These co-transformation methods are conventional, easy to implement and have been explored in 10 different species (Goldstein et al., 2005; Tuteja et al., 2012). The disadvantages of this strategy are also evident. These methods are time-consuming and exhibit poor transformation efficiency. These methods are also limited to flowering plants, which limits their commercial applications.

### **Inducible and tissue specific promoters**

In order to efficiently express a foreign gene in GMOs, many constitutive promoters

such as CaMV 35S and maize *Ubi-1* promoters have been identified and utilized, (Odell et al., 1985; Benfey and Chua, 1990; Toki et al., 1992; Christensen and Quail, 1996). However, constitutive promoters induce massive accumulation of heterologous proteins or final metabolites which may cause many adverse consequences: (1) interrupt the metabolic homeostasis of transgenic plants, which may repress their growth and development; (2) induce plant defense mechanism to minimize the adverse effect brought by excess transcripts of foreign genes, leading to a phenomenon called transgene silencing or co-suppression ; (3) makes the approval of transgenic crop release and commercialization very difficult (Kumpatla et al., 1998; Kooter et al., 1999; Dietz-Pfeilstetter, 2010). To avoid these adversities, many inducible and tissue specific promoters have been developed, such as rice original light inducible promoter *rbcS* which is specifically expressed in leaf and stem, soybean heat inducible promoter *Gmhsp17*, rice light inducible and green tissue specific promoter *Cab1R*, *Arabidopsis* root and seedling specific promoter *Pyk10*, tomato fruit specific promoter *E-8*, and *Brassica napus* seed specific promoter *napin* (Schoffl et al., 1989; Luan and Bogorad, 1992; Ellerstrom et al., 1996; Nomura et al., 2000; Krasnyanski et al., 2001; Nitz et al., 2001). The greatest strength of inducible and tissue specific promoters is that they are active only under certain conditions or in specific tissues and thus reduce the accumulation of heterologous proteins or final metabolites in transgenic plants. The leaf specific promoter is one of the most useful tissue specific promoters in agriculture industry, because it can reduce accumulation of heterologous proteins or final metabolites in the fruits or seeds of GMOs. So far only one promoter *Gh-rbcS* identified in cotton has been reported to show predominant leaf specificity (Song et

al., 2000).

### **Scope of the dissertation research**

The SOS pathway, key enzymes in ABA biosynthesis, transcription factors, and microRNAs have all been utilized to develop GMOs with enhanced osmotic stress tolerance (Yamaguchi-Shinozaki and Shinozaki, 2001; Yang et al., 2009; Yue et al., 2012; Yuan et al., 2015). Furthermore, overexpression of PRRs and modification of pathogen response pathways can also help produce transgenic crops highly resistant to disease (Goddard et al., 2014; Jones et al., 2014; Schwessinger et al., 2015). The success in crop genetic engineering for new cultivars with enhanced performance under adverse environmental conditions largely hinges on a better understanding of molecular mechanisms underlying plant responses to biotic and abiotic stresses. The available molecular tools for use in plant biotechnology are also the key in producing GMOs with the most desirable traits. To maximize the potential of biotechnology approaches in crop trait modification for enhanced tolerance to environmental stress, we have explored novel mechanisms controlling plant response to pathogen infection and nutrition starvation, and development of new molecular tools for plant biotechnology. In this dissertation, I first present data reporting the cloning and characterization of a novel LRR-RLK gene family, *SRF* and molecular mechanisms of *SRF* involvement in plant response to biotic stress. I then report the study of a rice microRNA involved in plant sulfate starvation. I also report research on the identification and characterization of a new leaf specific promoter and discuss its potential use in agricultural biotechnology.

## REFERENCES

- Achard, P., Gong, F., Cheminant, S., Alioua, M., Hedden, P., and Genschik, P.** (2008). The cold-inducible CBF1 factor-dependent signaling pathway modulates the accumulation of the growth-repressing DELLA proteins via its effect on gibberellin metabolism. *Plant Cell* **20**, 2117-2129.
- Achard, P., Cheng, H., De Grauwe, L., Decat, J., Schoutteten, H., Moritz, T., Van Der Straeten, D., Peng, J., and Harberd, N.P.** (2006). Integration of plant responses to environmentally activated phytohormonal signals. *Science* **311**, 91-94.
- Alexandratos, N., and Bruinsma, J.** (2012). World agriculture towards 2030/2050: the 2012 revision (ESA Working paper Rome, FAO).
- Allen, R.S., Li, J., Stahle, M.I., Dubroue, A., Gubler, F., and Millar, A.A.** (2007). Genetic analysis reveals functional redundancy and the major target genes of the Arabidopsis miR159 family. *Proc Natl Acad Sci USA* **104**, 16371-16376.
- An, F.M., Hsiao, S.R., and Chan, M.T.** (2011). Sequencing-based approaches reveal low ambient temperature-responsive and tissue-specific microRNAs in phalaenopsis orchid. *Plos One* **6**, e18937.
- An, G.** (1985). High efficiency transformation of cultured tobacco cells. *Plant Physiology* **79**, 568-570.
- Antolin-Llovera, M., Ried, M.K., Binder, A., and Parniske, M.** (2012). Receptor Kinase Signaling Pathways in Plant-Microbe Interactions. *Annual Review of Phytopathology* **50**, 451-473.
- Araki, H., Jearnpipatkul, A., Tatsumi, H., Sakurai, T., Ushio, K., Muta, T., and Oshima, Y.** (1985). Molecular and functional organization of yeast plasmid pSR1. *Journal of molecular biology* **182**, 191-203.
- Asai, T., Tena, G., Plotnikova, J., Willmann, M.R., Chiu, W.L., Gomez-Gomez, L., Boller, T., Ausubel, F.M., and Sheen, J.** (2002). MAP kinase signalling cascade in Arabidopsis innate immunity. *Nature* **415**, 977-983.
- Axtell, M.J., and Bowman, J.L.** (2008). Evolution of plant microRNAs and their targets. *Trends Plant Sci* **13**, 343-349.
- Axtell, M.J., Westholm, J.O., and Lai, E.C.** (2011). Vive la difference: biogenesis and evolution of microRNAs in plants and animals. *Genome Biol* **12**, 221.

- Bai, X.Q., Wang, Q.Y., and Chu, C.C.** (2008). Excision of a selective marker in transgenic rice using a novel Cre/loxP system controlled by a floral specific promoter. *Transgenic Research* **17**, 1035-1043.
- Bargmann, B.O., and Munnik, T.** (2006). The role of phospholipase D in plant stress responses. *Current Opinion in Plant Biology* **9**, 515-522.
- Bargmann, B.O., Laxalt, A.M., ter Riet, B., van Schooten, B., Merquiol, E., Testerink, C., Haring, M.A., Bartels, D., and Munnik, T.** (2009). Multiple PLDs required for high salinity and water deficit tolerance in plants. *Plant Cell Physiology* **50**, 78-89.
- Bartel, D.P.** (2004). MicroRNAs: genomics, biogenesis, mechanism, and function. *Cell* **116**, 281-297.
- Beckers, G.J., Jaskiewicz, M., Liu, Y., Underwood, W.R., He, S.Y., Zhang, S., and Conrath, U.** (2009). Mitogen-activated protein kinases 3 and 6 are required for full priming of stress responses in *Arabidopsis thaliana*. *Plant Cell* **21**, 944-953.
- Benfey, P.N., and Chua, N.H.** (1990). The Cauliflower Mosaic Virus 35S Promoter: Combinatorial Regulation of Transcription in Plants. *Science* **250**, 959-966.
- Chinchilla, D., Zipfel, C., Robatzek, S., Kemmerling, B., Nurnberger, T., Jones, J.D., Felix, G., and Boller, T.** (2007). A flagellin-induced complex of the receptor FLS2 and BAK1 initiates plant defense. *Nature* **448**, 497-500.
- Chiou, T.J., Aung, K., Lin, S.I., Wu, C.C., Chiang, S.F., and Su, C.L.** (2006). Regulation of phosphate homeostasis by MicroRNA in *Arabidopsis*. *Plant Cell* **18**, 412-421.
- Chow, W.Y., Wang, C.K., Lee, W.L., Kung, S.S., and Wu, Y.M.** (1995). Molecular characterization of a deletion-prone region of plasmid pAE1 of *Alcaligenes eutrophus* H1. *J Bacteriol* **177**, 4157-4161.
- Christensen, A.H., and Quail, P.H.** (1996). Ubiquitin promoter-based vectors for high-level expression of selectable and/or screenable marker genes in monocotyledonous plants. *Transgenic Research* **5**, 213-218.
- Colcombet, J., Berriri, S., and Hirt, H.** (2013). Constitutively active MPK4 helps to clarify its role in plant immunity. *Plant Signal Behav* **8**, e22991.
- Cuellar, W., Gaudin, A., Solorzano, D., Casas, A., Nopo, L., Chudalayandi, P., Medrano, G., Kreuze, J., and Ghislain, M.** (2006). Self-excision of the antibiotic

- resistance gene nptII using a heat inducible Cre-loxP system from transgenic potato. *Plant Molecular Biology* **62**, 71-82.
- Dale, E.C., and Ow, D.W.** (1990). Intra- and intermolecular site-specific recombination in plant cells mediated by bacteriophage P1 recombinase. *Gene* **91**, 79-85.
- Dale, E.C., and Ow, D.W.** (1991). Gene transfer with subsequent removal of the selection gene from the host genome. *Proc Natl Acad Sci USA* **88**, 10558-10562.
- Daley, M., Knauf, V.C., Summerfelt, K.R., and Turner, J.C.** (1998). Co-transformation with one *Agrobacterium tumefaciens* strain containing two binary plasmids as a method for producing marker-free transgenic plants. *Plant Cell Rep* **17**, 489-496.
- Daudi, A., Cheng, Z.Y., O'Brien, J.A., Mammarella, N., Khan, S., Ausubel, F.M., and Bolwell, G.P.** (2012). The Apoplastic Oxidative Burst Peroxidase in *Arabidopsis* Is a Major Component of Pattern-Triggered Immunity. *Plant Cell* **24**, 275-287.
- Day, A., Kode, V., Madesis, P., and Iamtham, S.** (2005). Simple and efficient removal of marker genes from plastids by homologous recombination. *Methods in Molecular Biology* **286**, 255-270.
- Deblock, M., and Debrouwer, D.** (1991). 2 T-Dnas Co-Transformed into Brassica-Napus by a Double *Agrobacterium-Tumefaciens* Infection Are Mainly Integrated at the Same Locus. *Theoretical and Applied Genetics* **82**, 257-263.
- Deframond, A.J., Back, E.W., Chilton, W.S., Kayes, L., and Chilton, M.D.** (1986). 2 Unlinked T-Dnas Can Transform the Same Tobacco Plant-Cell and Segregate in the F1 Generation. *Molecular & General Genetics* **202**, 125-131.
- DeNeve, M., DeBuck, S., Jacobs, A., VanMontagu, M., and Depicker, A.** (1997). T-DNA integration patterns in co-transformed plant cells suggest that T-DNA repeats originate from co-integration of separate T-DNAs. *Plant J* **11**, 15-29.
- Depicker, A., Herman, L., Jacobs, A., Schell, J., and Vanmontagu, M.** (1985). Frequencies of Simultaneous Transformation with Different T-Dnas and Their Relevance to the *Agrobacterium* Plant-Cell Interaction. *Molecular & General Genetics* **201**, 477-484.
- Devaiah, S.P., Pan, X., Hong, Y., Roth, M., Welti, R., and Wang, X.** (2007). Enhancing seed quality and viability by suppressing phospholipase D in *Arabidopsis*. *Plant J* **50**, 950-957.
- Dietz-Pfeilstetter, A.** (2010). Stability of transgene expression as a challenge for genetic engineering. *Plant Science* **179**, 164-167.

- Dodds, P.N., and Rathjen, J.P.** (2010). Plant immunity: towards an integrated view of plant-pathogen interactions. *Nat Rev Genet* **11**, 539-548.
- Dong, J., Chen, C., and Chen, Z.** (2003). Expression profiles of the Arabidopsis WRKY gene superfamily during plant defense response. *Plant Molecular Biology* **51**, 21-37.
- Ellerstrom, M., Stalberg, K., Ezcurra, I., and Rask, L.** (1996). Functional dissection of a napin gene promoter: identification of promoter elements required for embryo and endosperm-specific transcription. *Plant Molecular Biology* **32**, 1019-1027.
- Fagard, M., Boutet, S., Morel, J.B., Bellini, C., and Vaucheret, H.** (2000). AGO1, QDE-2, and RDE-1 are related proteins required for post-transcriptional gene silencing in plants, quelling in fungi, and RNA interference in animals. *Proc Natl Acad Sci USA* **97**, 11650-11654.
- Ferreira, T.H., Gentile, A., Vilela, R.D., Costa, G.G., Dias, L.I., Endres, L., and Menossi, M.** (2012). microRNAs associated with drought response in the bioenergy crop sugarcane (*Saccharum* spp.). *Plos One* **7**, e46703.
- Flor, H.H.** (1971). Current status of the gene-for-gene concept. *Annual Review of Phytopathology* **9**, 275-296.
- Fujii, H., Chiou, T.J., Lin, S.I., Aung, K., and Zhu, J.K.** (2005). A miRNA involved in phosphate-starvation response in Arabidopsis. *Current Biology* **15**, 2038-2043.
- Galletti, R., Ferrari, S., and De Lorenzo, G.** (2011). Arabidopsis MPK3 and MPK6 play different roles in basal and oligogalacturonide- or flagellin-induced resistance against *Botrytis cinerea*. *Plant Physiology* **157**, 804-814.
- Gao, M., Liu, J., Bi, D., Zhang, Z., Cheng, F., Chen, S., and Zhang, Y.** (2008). MEKK1, MKK1/MKK2 and MPK4 function together in a mitogen-activated protein kinase cascade to regulate innate immunity in plants. *Cell Res* **18**, 1190-1198.
- Garcia-Almodovar, R.C., Petri, C., Padilla, I.M.G., and Burgos, L.** (2014). Combination of site-specific recombination and a conditional selective marker gene allows for the production of marker-free tobacco plants. *Plant Cell Tiss Org* **116**, 205-215.
- Gilbertson, L.** (2003). Cre-lox recombination: Creative tools for plant biotechnology. *TRENDS in Biotechnology* **21**, 550-555.
- Goddard, R., Peraldi, A., Ridout, C., and Nicholson, P.** (2014). Enhanced Disease Resistance Caused by BRI1 Mutation Is Conserved Between *Brachypodium*



- distachyon and Barley (*Hordeum vulgare*). *Molecular Plant-Microbe Interactions* **27**, 1095-1106.
- Goldstein, D.A., Tinland, B., Gilbertson, L.A., Staub, J.M., Bannon, G.A., Goodman, R.E., McCoy, R.L., and Silvanovich, A.** (2005). Human safety and genetically modified plants: a review of antibiotic resistance markers and future transformation selection technologies. *Journal of Applied Microbiology* **99**, 7-23.
- Gomez-Gomez, L., and Boller, T.** (2000). FLS2: an LRR receptor-like kinase involved in the perception of the bacterial elicitor flagellin in *Arabidopsis*. *Mol Cell* **5**, 1003-1011.
- Gomez-Gomez, L., and Boller, T.** (2002). Flagellin perception: a paradigm for innate immunity. *Trends Plant Sci* **7**, 251-256.
- Gomez-Gomez, L., Felix, G., and Boller, T.** (1999). A single locus determines sensitivity to bacterial flagellin in *Arabidopsis thaliana*. *Plant J* **18**, 277-284.
- Gonzalez-Guzman, M., Pizzio, G.A., Antoni, R., Vera-Sirera, F., Merilo, E., Bassel, G.W., Fernandez, M.A., Holdsworth, M.J., Perez-Amador, M.A., Kollist, H., and Rodriguez, P.L.** (2012). *Arabidopsis* PYR/PYL/RCAR receptors play a major role in quantitative regulation of stomatal aperture and transcriptional response to abscisic acid. *Plant Cell* **24**, 2483-2496.
- Halfter, U., Ishitani, M., and Zhu, J.K.** (2000). The *Arabidopsis* SOS2 protein kinase physically interacts with and is activated by the calcium-binding protein SOS3. *Proc Natl Acad Sci USA* **97**, 3735-3740.
- Ham, J.H., Kim, M.G., Lee, S.Y., and Mackey, D.** (2007). Layered basal defenses underlie non-host resistance of *Arabidopsis* to *Pseudomonas syringae* pv. *phaseolicola*. *Plant J* **51**, 604-616.
- Hao, J.H., Wang, X.L., Dong, C.J., Zhang, Z.G., and Shang, Q.M.** (2011). Salicylic acid induces stomatal closure by modulating endogenous hormone levels in cucumber cotyledons. *Russ J Plant Physiology* **58**, 906-913.
- He, X.J., Mu, R.L., Cao, W.H., Zhang, Z.G., Zhang, J.S., and Chen, S.Y.** (2005). AtNAC2, a transcription factor downstream of ethylene and auxin signaling pathways, is involved in salt stress response and lateral root development. *Plant J* **44**, 903-916.
- Hiei, Y., Komari, T., and Kubo, T.** (1997). Transformation of rice mediated by *Agrobacterium tumefaciens*. *Plant Molecular Biology* **35**, 205-218.

- Hiei, Y., Ohta, S., Komari, T., and Kumashiro, T.** (1994). Efficient transformation of rice (*Oryza sativa* L.) mediated by *Agrobacterium* and sequence analysis of the boundaries of the T-DNA. *Plant J* **6**, 271-282.
- Hoang, T.T., Bong, B.B., Huq, E., and Hodges, T.K.** (2002). Cre/ lox site-specific recombination controls the excision of a transgene from the rice genome. *Theor Appl Genet* **104**, 518-525.
- Hong, Y., Devaiah, S.P., Bahn, S.C., Thamasandra, B.N., Li, M., Welti, R., and Wang, X.** (2009). Phospholipase D epsilon and phosphatidic acid enhance Arabidopsis nitrogen signaling and growth. *Plant J* **58**, 376-387.
- Hong, Y.Y., Pan, X.Q., Welti, R., and Wang, X.M.** (2008). Phospholipase D alpha 3 is involved in the hyperosmotic response in Arabidopsis. *Plant Cell* **20**, 803-816.
- Hosy, E., Vavasseur, A., Mouline, K., Dreyer, I., Gaymard, F., Poree, F., Boucherez, J., Lebaudy, A., Bouchez, D., Very, A.A., Simonneau, T., Thibaud, J.B., and Sentenac, H.** (2003). The Arabidopsis outward K<sup>+</sup> channel GORK is involved in regulation of stomatal movements and plant transpiration (vol 100, pg 5549, 2003). *Proc Natl Acad Sci USA* **100**, 7418-7418.
- Hsu, F.C., Chou, M.Y., Chou, S.J., Li, Y.R., Peng, H.P., and Shih, M.C.** (2013). Submergence confers immunity mediated by the WRKY22 transcription factor in Arabidopsis. *Plant Cell* **25**, 2699-2713.
- Hu, H., You, J., Fang, Y., Zhu, X., Qi, Z., and Xiong, L.** (2008). Characterization of transcription factor gene SNAC2 conferring cold and salt tolerance in rice. *Plant Molecular Biology* **67**, 169-181.
- Hu, H., Dai, M., Yao, J., Xiao, B., Li, X., Zhang, Q., and Xiong, L.** (2006). Overexpressing a NAM, ATAF, and CUC (NAC) transcription factor enhances drought resistance and salt tolerance in rice. *Proc Natl Acad Sci USA* **103**, 12987-12992.
- Hu, Q., Kononowicz-Hodges, H., Nelson-Vasilchik, K., Viola, D., Zeng, P., Liu, H., Kausch, A.P., Chandless, J.M., Hodges, T.K., and Luo, H.** (2008). FLP recombinase-mediated site-specific recombination in rice. *Plant Biotechnol J* **6**, 176-188
- Hua, J.** (2009). From freezing to scorching, transcriptional responses to temperature variations in plants. *Current Opinion in Plant Biology* **12**, 568-573.
- Iamtham, S., and Day, A.** (2000). Removal of antibiotic resistance genes from transgenic tobacco plastids. *Nature Biotechnology* **18**, 1172-1176.

- Ishida, Y., Saito, H., Ohta, S., Hiei, Y., Komari, T., and Kumashiro, T.** (1996). High efficiency transformation of maize (*Zea mays* L.) mediated by *Agrobacterium tumefaciens*. *Nature Biotechnology* **14**, 745-750.
- Ishikawa, A.** (2009). The Arabidopsis G-Protein beta-Subunit Is Required for Defense Response against *Agrobacterium tumefaciens*. *Biosci Biotech Bioch* **73**, 47-52.
- Ishitani, M., Liu, J., Halfter, U., Kim, C.S., Shi, W., and Zhu, J.K.** (2000). SOS3 function in plant salt tolerance requires N-myristoylation and calcium binding. *Plant Cell* **12**, 1667-1678.
- Jacobs, A.K., Lipka, V., Burton, R.A., Panstruga, R., Strizhov, N., Schulze-Lefert, P., and Fincher, G.B.** (2003). An Arabidopsis callose synthase, *GSL5*, is required for wound and papillary callose formation. *Plant Cell* **15**, 2503-2513.
- Ji, H., Pardo, J.M., Batelli, G., Van Oosten, M.J., Bressan, R.A., and Li, X.** (2013). The Salt Overly Sensitive (SOS) pathway: established and emerging roles. *Mol Plant* **6**, 275-286.
- Jones, J.D., and Dangl, J.L.** (2006). The plant immune system. *Nature* **444**, 323-329.
- Jones, J.D.G., Witek, K., Verweij, W., Jupe, F., Cooke, D., Dorling, S., Tomlinson, L., Smoker, M., Perkins, S., and Foster, S.** (2014). Elevating crop disease resistance with cloned genes. *Philos T R Soc B* **369**.
- Joon-Sang, L.** (1998). The mechanism of stomatal closing by salicylic acid in *Commelina communis* L. *Journal of Plant Biology* **41**, 97-102.
- Kaku, H., Nishizawa, Y., Ishii-Minami, N., Akimoto-Tomiyama, C., Dohmae, N., Takio, K., Minami, E., and Shibuya, N.** (2006). Plant cells recognize chitin fragments for defense signaling through a plasma membrane receptor. *Proc Natl Acad Sci USA* **103**, 11086-11091.
- Kawashima, C.G., Yoshimoto, N., Maruyama-Nakashita, A., Tsuchiya, Y.N., Saito, K., Takahashi, H., and Dalmay, T.** (2009). Sulphur starvation induces the expression of microRNA-395 and one of its target genes but in different cell types. *Plant J* **57**, 313-321.
- Kemmerling, B., Halter, T., Mazzotta, S., Mosher, S., and Nurnberger, T.** (2011). A genome-wide survey for Arabidopsis leucine-rich repeat receptor kinases implicated in plant immunity. *Front Plant Sci* **2**, 88.
- Khattari, A., Nandy, S., and Srivastava, V.** (2011). Heat-inducible Cre-lox system for marker excision in transgenic rice. *Journal of Biosciences* **36**, 37-42.

- Kilby, N.J., Davies, G.J., and Snaith, M.R.** (1995). FLP recombinase in transgenic plants: constitutive activity in stably transformed tobacco and generation of marked cell clones in Arabidopsis. *Plant J* **8**, 637-652.
- Kim, M.G., da Cunha, L., McFall, A.J., Belkhadir, Y., DebRoy, S., Dangl, J.L., and Mackey, D.** (2005). Two *Pseudomonas syringae* type III effectors inhibit RIN4-regulated basal defense in Arabidopsis. *Cell* **121**, 749-759.
- Kittiwongwattana, C., Lutz, K., Clark, M., and Maliga, P.** (2007). Plastid marker gene excision by the phiC31 phage site-specific recombinase. *Plant Molecular Biology* **64**, 137-143.
- Klonus, D., Hofgen, R., Willmitzer, L., and Riesmeier, J.W.** (1994). Isolation and characterization of two cDNA clones encoding ATP-sulfurylases from potato by complementation of a yeast mutant. *Plant J* **6**, 105-112.
- Kohli, A., Sreenivasulu, N., Lakshmanan, P., and Kumar, P.P.** (2013). The phytohormone crosstalk paradigm takes center stage in understanding how plants respond to abiotic stresses. *Plant Cell Rep* **32**, 945-957.
- Komari, T., Hiei, Y., Saito, Y., Murai, N., and Kumashiro, T.** (1996). Vectors carrying two separate T-DNAs for co-transformation of higher plants mediated by *Agrobacterium tumefaciens* and segregation of transformants free from selection markers. *Plant J* **10**, 165-174.
- Kooter, J.M., Matzke, M.A., and Meyer, P.** (1999). Listening to the silent genes: transgene silencing, gene regulation and pathogen control. *Trends Plant Sci* **4**, 340-347.
- Kovtun, Y., Chiu, W.L., Tena, G., and Sheen, J.** (2000). Functional analysis of oxidative stress-activated mitogen-activated protein kinase cascade in plants. *Proc Natl Acad Sci USA* **97**, 2940-2945.
- Krasnyanski, S.F., Sandhu, J., Domier, L.L., Buetow, D.E., and Korban, S.S.** (2001). Effect of an enhanced CaMV 35S promoter and a fruit-specific promoter on UIDA gene expression in transgenic tomato plants. *In Vitro Cell Dev-Pl* **37**, 427-433.
- Kulik, A., Wawer, I., Krzywinska, E., Bucholc, M., and Dobrowolska, G.** (2011). SnRK2 protein kinases--key regulators of plant response to abiotic stresses. *OMICS* **15**, 859-872.
- Kumpatla, S.P., Chandrasekharan, M.B., Iyer, L.M., Guofu, L., and Hall, T.C.** (1998). Genome intruder scanning and modulation systems and transgene silencing. *Trends in Plant Science* **3**, 97-104.

- Kurihara, Y., Takashi, Y., and Watanabe, Y.** (2006). The interaction between DCL1 and HYL1 is important for efficient and precise processing of pri-miRNA in plant microRNA biogenesis. *RNA* **12**, 206-212.
- Laubinger, S., Sachsenberg, T., Zeller, G., Busch, W., Lohmann, J.U., Ratsch, G., and Weigel, D.** (2008). Dual roles of the nuclear cap-binding complex and SERRATE in pre-mRNA splicing and microRNA processing in *Arabidopsis thaliana*. *Proc Natl Acad Sci USA* **105**, 8795-8800.
- Lee, S.J., Kang, J.Y., Park, H.J., Kim, M.D., Bae, M.S., Choi, H.I., and Kim, S.Y.** (2010). DREB2C interacts with ABF2, a bZIP protein regulating abscisic acid-responsive gene expression, and its overexpression affects abscisic acid sensitivity. *Plant Physiology* **153**, 716-727.
- Li, B., Li, N., Duan, X., Wei, A., Yang, A., and Zhang, J.** (2010). Generation of marker-free transgenic maize with improved salt tolerance using the FLP/FRT recombination system. *Journal of Biotechnology* **145**, 206-213.
- Li, G., Lin, F., and Xue, H.W.** (2007a). Genome-wide analysis of the phospholipase D family in *Oryza sativa* and functional characterization of PLD beta 1 in seed germination. *Cell Res* **17**, 881-894.
- Li, J., Wen, J., Lease, K.A., Doke, J.T., Tax, F.E., and Walker, J.C.** (2002). BAK1, an *Arabidopsis* LRR receptor-like protein kinase, interacts with BRI1 and modulates brassinosteroid signaling. *Cell* **110**, 213-222.
- Li, S., Liu, L., Zhuang, X., Yu, Y., Liu, X., Cui, X., Ji, L., Pan, Z., Cao, X., Mo, B., Zhang, F., Raikhel, N., Jiang, L., and Chen, X.** (2013). MicroRNAs inhibit the translation of target mRNAs on the endoplasmic reticulum in *Arabidopsis*. *Cell* **153**, 562-574.
- Li, Z., Xing, A., Moon, B.P., Burgoyne, S.A., Guida, A.D., Liang, H., Lee, C., Caster, C.S., Barton, J.E., Klein, T.M., and Falco, S.C.** (2007b). A Cre/loxP-mediated self-activating gene excision system to produce marker gene free transgenic soybean plants. *Plant Molecular Biology* **65**, 329-341.
- Liang, G., Yang, F., and Yu, D.** (2010). MicroRNA395 mediates regulation of sulfate accumulation and allocation in *Arabidopsis thaliana*. *Plant J* **62**, 1046-1057.
- Liang, X.X., Ding, P.T., Liang, K.H., Wang, J.L., Ma, M.M., Li, L., Li, L., Li, M., Zhang, X.J., Chen, S., Zhang, Y.L., and Zhou, J.M.** (2016). *Arabidopsis* heterotrimeric G proteins regulate immunity by directly coupling to the FLS2 receptor. *Elife* **5**: e13568

- Lin, H., Yang, Y., Quan, R., Mendoza, I., Wu, Y., Du, W., Zhao, S., Schumaker, K.S., Pardo, J.M., and Guo, Y.** (2009). Phosphorylation of SOS3-LIKE CALCIUM BINDING PROTEIN8 by SOS2 protein kinase stabilizes their protein complex and regulates salt tolerance in Arabidopsis. *Plant Cell* **21**, 1607-1619.
- Lin, S.I., Chiang, S.F., Lin, W.Y., Chen, J.W., Tseng, C.Y., Wu, P.C., and Chiou, T.J.** (2008). Regulatory network of microRNA399 and PHO2 by systemic signaling. *Plant Physiology* **147**, 732-746.
- Liu, H.H., Tian, X., Li, Y.J., Wu, C.A., and Zheng, C.C.** (2008). Microarray-based analysis of stress-regulated microRNAs in Arabidopsis thaliana. *RNA* **14**, 836-843.
- Liu, J., Ishitani, M., Halfter, U., Kim, C.S., and Zhu, J.K.** (2000). The Arabidopsis thaliana SOS2 gene encodes a protein kinase that is required for salt tolerance. *Proc Natl Acad Sci USA* **97**, 3730-3734.
- Liu, P.P., Montgomery, T.A., Fahlgren, N., Kasschau, K.D., Nonogaki, H., and Carrington, J.C.** (2007). Repression of AUXIN RESPONSE FACTOR10 by microRNA160 is critical for seed germination and post-germination stages. *Plant J* **52**, 133-146.
- Liu, Q., Feng, Y., and Zhu, Z.** (2009). Dicer-like (DCL) proteins in plants. *Functional & Integrative Genomics* **9**, 277-286.
- Lloyd, A.M., and Davis, R.W.** (1994). Functional expression of the yeast FLP/FRT site-specific recombination system in Nicotiana tabacum. *Molecular & General Genetics* : MGG **242**, 653-657.
- Luan, S., and Bogorad, L.** (1992). A rice cab gene promoter contains separate cis-acting elements that regulate expression in dicot and monocot plants. *Plant Cell* **4**, 971-981.
- Luna, E., Pastor, V., Robert, J., Flors, V., Mauch-Mani, B., and Ton, J.** (2011). Callose deposition: a multifaceted plant defense response. *Molecular Plant-Microbe Interactions* : MPMI **24**, 183-193.
- Lunn, J.E., Droux, M., Martin, J., and Douce, R.** (1990). Localization of ATP sulfurylase and O-acetylserine (thiol) lyase in spinach leaves. *Plant Physiology* **94**, 1345-1352.
- Luo, H., Lyznik, L.A., Gidoni, D., and Hodges, T.K.** (2000). FLP-mediated recombination for use in hybrid plant production. *Plant J* **23**, 423-430.

- Lv, D.K., Bai, X., Li, Y., Ding, X.D., Ge, Y., Cai, H., Ji, W., Wu, N., and Zhu, Y.M.** (2010). Profiling of cold-stress-responsive miRNAs in rice by microarrays. *Gene* **459**, 39-47.
- Lyznik, L.A., Mitchell, J.C., Hirayama, L., and Hodges, T.K.** (1993). Activity of yeast FLP recombinase in maize and rice protoplasts. *Nucleic Acids Res* **21**, 969-975.
- Maeser, S., and Kahmann, R.** (1991). The Gin Recombinase of Phage Mu Can Catalyze Site-Specific Recombination in Plant-Protoplasts. *Molecular & General Genetics* **230**, 170-176.
- Matthews, P.R., Wang, M.B., Waterhouse, P.M., Thornton, S., Fieg, S.J., Gubler, F., and Jacobsen, J.V.** (2001). Marker gene elimination from transgenic barley, using co-transformation with adjacent 'twin T-DNAs' on a standard *Agrobacterium* transformation vector. *Molecular Breeding* **7**, 195-202.
- McCormac, A.C., Fowler, M.R., Chen, D.F., and Elliott, M.C.** (2001). Efficient co-transformation of *Nicotiana tabacum* by two independent T-DNAs, the effect of T-DNA size and implications for genetic separation. *Transgenic Research* **10**, 143-155.
- McKnight, T.D., Lillis, M.T., and Simpson, R.B.** (1987). Segregation of genes transferred to one plant cell from two separate *Agrobacterium* strains. *Plant Molecular Biology* **8**, 439-445.
- Medzhitov, R.** (2001). Toll-like receptors and innate immunity. *Nat Rev Immunol* **1**, 135-145.
- Melotto, M., Underwood, W., Koczan, J., Nomura, K., and He, S.Y.** (2006). Plant stomata function in innate immunity against bacterial invasion. *Cell* **126**, 969-980.
- Meng, X., Xu, J., He, Y., Yang, K.Y., Mordorski, B., Liu, Y., and Zhang, S.** (2013). Phosphorylation of an ERF transcription factor by *Arabidopsis* MPK3/MPK6 regulates plant defense gene induction and fungal resistance. *Plant Cell* **25**, 1126-1142.
- Mészáros, K., Éva, C., Kiss, T., Bányai, J., Kiss, E., Téglás, F., Láng, L., Karsai, I., and Tamás, L.** (2014). Generating Marker-Free Transgenic Wheat Using Minimal Gene Cassette and Cold-Inducible Cre/Lox System. *Plant Molecular Biology Reporter*, 1-11.
- Meszaros, T., Helfer, A., Hatzimasoura, E., Magyar, Z., Serazetdinova, L., Rios, G., Bardoczy, V., Teige, M., Koncz, C., Peck, S., and Bogre, L.** (2006). The

- Arabidopsis MAP kinase kinase MKK1 participates in defense responses to the bacterial elicitor flagellin. *Plant J* **48**, 485-498.
- Miao, Y., Laun, T., Zimmermann, P., and Zentgraf, U.** (2004). Targets of the WRKY53 transcription factor and its role during leaf senescence in Arabidopsis. *Plant Molecular Biology* **55**, 853-867.
- Miki, B., and McHugh, S.** (2004). Selectable marker genes in transgenic plants: applications, alternatives and biosafety. *Journal of Biotechnology* **107**, 193-232.
- Miller, M., Tagliani, L., Wang, N., Berka, B., Bidney, D., and Zhao, Z.Y.** (2002). High efficiency transgene segregation in co-transformed maize plants using an *Agrobacterium tumefaciens* 2 T-DNA binary system. *Transgenic Research* **11**, 381-396.
- Miya, A., Albert, P., Shinya, T., Desaki, Y., Ichimura, K., Shirasu, K., Narusaka, Y., Kawakami, N., Kaku, H., and Shibuya, N.** (2007). CERK1, a LysM receptor kinase, is essential for chitin elicitor signaling in Arabidopsis. *Proc Natl Acad Sci USA* **104**, 19613-19618.
- Moon, H.S., Li, Y., and Stewart, C.N.** (2010). Keeping the genie in the bottle: transgene biocontainment by excision in pollen. *Trends in Biotechnology* **28**, 3-8.
- Munnik, T.** (2001). Phosphatidic acid: an emerging plant lipid second messenger. *Trends Plant Sci* **6**, 227-233.
- Munnik, T., Irvine, R.F., and Musgrave, A.** (1998). Phospholipid signalling in plants. *Biochim Biophys Acta* **1389**, 222-272.
- Nag, A., King, S., and Jack, T.** (2009). miR319a targeting of TCP4 is critical for petal growth and development in Arabidopsis. *Proc Natl Acad Sci USA* **106**, 22534-22539.
- Nakashima, K., Tran, L.S., Van Nguyen, D., Fujita, M., Maruyama, K., Todaka, D., Ito, Y., Hayashi, N., Shinozaki, K., and Yamaguchi-Shinozaki, K.** (2007). Functional analysis of a NAC-type transcription factor OsNAC6 involved in abiotic and biotic stress-responsive gene expression in rice. *Plant J* **51**, 617-630.
- Nischal, L., Mohsin, M., Khan, I., Kardam, H., Wadhwa, A., Abrol, Y.P., Iqbal, M., and Ahmad, A.** (2012). Identification and comparative analysis of microRNAs associated with low-N tolerance in rice genotypes. *Plos One* **7**, e50261.
- Nishimura, N., Sarkeshik, A., Nito, K., Park, S.Y., Wang, A., Carvalho, P.C., Lee, S., Caddell, D.F., Cutler, S.R., Chory, J., Yates, J.R., and Schroeder, J.I.** (2010).



- PYR/PYL/RCAR family members are major in-vivo ABI1 protein phosphatase 2C-interacting proteins in Arabidopsis. *Plant J* **61**, 290-299.
- Nitz, I., Berkefeld, H., Puzio, P.S., and Grundle, F.M.W.** (2001). Pyk10, a seedling and root specific gene and promoter from Arabidopsis thaliana. *Plant Science* **161**, 337-346.
- Nomura, M., Katayama, K., Nishimura, A., Ishida, Y., Ohta, S., Komari, T., Miyao-Tokutomi, M., Tajima, S., and Matsuoka, M.** (2000). The promoter of *rbcS* in a C3 plant (rice) directs organ-specific, light-dependent expression in a C4 plant (maize), but does not confer bundle sheath cell-specific expression. *Plant Molecular Biology* **44**, 99-106.
- Odell, J., Caimi, P., Sauer, B., and Russell, S.** (1990). Site-directed recombination in the genome of transgenic tobacco. *Molecular & General Genetics : MGG* **223**, 369-378.
- Odell, J.T., Nagy, F., and Chua, N.H.** (1985). Identification of DNA sequences required for activity of the cauliflower mosaic virus 35S promoter. *Nature* **313**, 810-812.
- Oh, D.H., Lee, S.Y., Bressan, R.A., Yun, D.J., and Bohnert, H.J.** (2010). Intracellular consequences of SOS1 deficiency during salt stress. *J Exp Bot* **61**, 1205-1213.
- Oliver, M.J., Quisenberry, J.E., Trolinder, N.L.G., and Keim, D.L.** (1998). Control of plant gene expression (Google Patents).
- Onouchi, H., Yokoi, K., Machida, C., Matsuzaki, H., Oshima, Y., Matsuoka, K., Nakamura, K., and Machida, Y.** (1991). Operation of an efficient site-specific recombination system of *Zygosaccharomyces rouxii* in tobacco cells. *Nucleic Acids Res* **19**, 6373-6378.
- Ori, N., Cohen, A.R., Etzioni, A., Brand, A., Yanai, O., Shleizer, S., Menda, N., Amsellem, Z., Efroni, I., Pekker, I., Alvarez, J.P., Blum, E., Zamir, D., and Eshed, Y.** (2007). Regulation of LANCEOLATE by miR319 is required for compound-leaf development in tomato. *Nat Genet* **39**, 787-791.
- Palatnik, J.F., Allen, E., Wu, X., Schommer, C., Schwab, R., Carrington, J.C., and Weigel, D.** (2003). Control of leaf morphogenesis by microRNAs. *Nature* **425**, 257-263.
- Park, M.Y., Wu, G., Gonzalez-Sulser, A., Vaucheret, H., and Poethig, R.S.** (2005). Nuclear processing and export of microRNAs in Arabidopsis. *Proc Natl Acad Sci USA* **102**, 3691-3696.

- Park, W., Li, J., Song, R., Messing, J., and Chen, X.** (2002). CARPEL FACTORY, a Dicer homolog, and HEN1, a novel protein, act in microRNA metabolism in *Arabidopsis thaliana*. *Curr Biol* **12**, 1484-1495.
- Patron, N.J., Durnford, D.G., and Kopriva, S.** (2008). Sulfate assimilation in eukaryotes: fusions, relocations and lateral transfers. *BMC Evol Biol* **8**, 39.
- Petri, C., Lopez-Noguera, S., Wang, H., Garcia-Almodovar, C., Albuquerque, N., and Burgos, L.** (2012). A chemical-inducible Cre-LoxP system allows for elimination of selection marker genes in transgenic apricot. *Plant Cell Tiss Org* **110**, 337-346.
- Pitzschke, A., Schikora, A., and Hirt, H.** (2009). MAPK cascade signalling networks in plant defense. *Current Opinion in Plant Biology* **12**, 421-426.
- Postel, S., Kufner, I., Beuter, C., Mazzotta, S., Schwedt, A., Borlotti, A., Halter, T., Kemmerling, B., and Nurnberger, T.** (2010). The multifunctional leucine-rich repeat receptor kinase BAK1 is implicated in *Arabidopsis* development and immunity. *Eur J Cell Biol* **89**, 169-174.
- Quan, R., Lin, H., Mendoza, I., Zhang, Y., Cao, W., Yang, Y., Shang, M., Chen, S., Pardo, J.M., and Guo, Y.** (2007). SCABP8/CBL10, a putative calcium sensor, interacts with the protein kinase SOS2 to protect *Arabidopsis* shoots from salt stress. *Plant Cell* **19**, 1415-1431.
- Ren, G., Xie, M., Dou, Y., Zhang, S., Zhang, C., and Yu, B.** (2012). Regulation of miRNA abundance by RNA binding protein TOUGH in *Arabidopsis*. *Proc Natl Acad Sci USA* **109**, 12817-12821.
- Reyes, J.L., and Chua, N.H.** (2007). ABA induction of miR159 controls transcript levels of two MYB factors during *Arabidopsis* seed germination. *Plant J* **49**, 592-606.
- Rhoades, M.W., Reinhart, B.J., Lim, L.P., Burge, C.B., Bartel, B., and Bartel, D.P.** (2002). Prediction of plant microRNA targets. *Cell* **110**, 513-520.
- Rivero, R.M., Shulaev, V., and Blumwald, E.** (2009). Cytokinin-dependent photorespiration and the protection of photosynthesis during water deficit. *Plant Physiology* **150**, 1530-1540.
- Ron, M., and Avni, A.** (2004). The receptor for the fungal elicitor ethylene-inducing xylanase is a member of a resistance-like gene family in tomato. *Plant Cell* **16**, 1604-1615.

- Rotte, C., and Leustek, T.** (2000). Differential subcellular localization and expression of ATP sulfurylase and 5'-adenylylsulfate reductase during ontogenesis of arabidopsis leaves indicates that cytosolic and plastid forms of ATP sulfurylase may have specialized functions. *Plant Physiology* **124**, 715-724.
- Roux, M., Schwessinger, B., Albrecht, C., Chinchilla, D., Jones, A., Holton, N., Malinovsky, F.G., Tor, M., de Vries, S., and Zipfel, C.** (2011). The Arabidopsis leucine-rich repeat receptor-like kinases BAK1/SERK3 and BKK1/SERK4 are required for innate immunity to hemibiotrophic and biotrophic pathogens. *Plant Cell* **23**, 2440-2455.
- Rus, A., Yokoi, S., Sharkhuu, A., Reddy, M., Lee, B.H., Matsumoto, T.K., Koiwa, H., Zhu, J.K., Bressan, R.A., and Hasegawa, P.M.** (2001). AtHKT1 is a salt tolerance determinant that controls Na<sup>+</sup> entry into plant roots. *Proc Natl Acad Sci USA* **98**, 14150-14155.
- Russell, S.H., Hoopes, J.L., and Odell, J.T.** (1992). Directed excision of a transgene from the plant genome. *Molecular & General Genetics : MGG* **234**, 49-59.
- Sakuma, Y., Maruyama, K., Osakabe, Y., Qin, F., Seki, M., Shinozaki, K., and Yamaguchi-Shinozaki, K.** (2006). Functional analysis of an Arabidopsis transcription factor, DREB2A, involved in drought-responsive gene expression. *Plant Cell* **18**, 1292-1309.
- Schoffl, F., Rieping, M., Baumann, G., Bevan, M., and Angermuller, S.** (1989). The function of plant heat shock promoter elements in the regulated expression of chimaeric genes in transgenic tobacco. *Molecular & General Genetics : MGG* **217**, 246-253.
- Schulze, B., Mentzel, T., Jehle, A.K., Mueller, K., Beeler, S., Boller, T., Felix, G., and Chinchilla, D.** (2010). Rapid Heteromerization and Phosphorylation of Ligand-activated Plant Transmembrane Receptors and Their Associated Kinase BAK1. *J Biol Chem* **285**, 9444-9451.
- Schwessinger, B., Bahar, O., Thomas, N., Holton, N., Nekrasov, V., Ruan, D., Canlas, P.E., Daudi, A., Petzold, C.J., Singan, V.R., Kuo, R., Chovatia, M., Daum, C., Heazlewood, J.L., Zipfel, C., and Ronald, P.C.** (2015). Transgenic expression of the dicotyledonous pattern recognition receptor EFR in rice leads to ligand-dependent activation of defense responses. *Plos Pathog* **11**, e1004809.
- Schwessinger, B., Roux, M., Kadota, Y., Ntoukakis, V., Sklenar, J., Jones, A., and Zipfel, C.** (2011). Phosphorylation-dependent differential regulation of plant growth, cell death, and innate immunity by the regulatory receptor-like kinase BAK1. *PLoS Genet* **7**, e1002046.

- Sharma, D., Tiwari, M., Lakhwani, D., Tripathi, R.D., and Trivedi, P.K.** (2015). Differential expression of microRNAs by arsenate and arsenite stress in natural accessions of rice. *Metallomics* **7**, 174-187.
- Shi, H., Ishitani, M., Kim, C., and Zhu, J.K.** (2000). The *Arabidopsis thaliana* salt tolerance gene *SOS1* encodes a putative Na<sup>+</sup>/H<sup>+</sup> antiporter. *Proc Natl Acad Sci USA* **97**, 6896-6901.
- Shi, H., Quintero, F.J., Pardo, J.M., and Zhu, J.K.** (2002). The putative plasma membrane Na<sup>(+)</sup>/H<sup>(+)</sup> antiporter *SOS1* controls long-distance Na<sup>(+)</sup> transport in plants. *Plant Cell* **14**, 465-477.
- Shimizu, T., Nakano, T., Takamizawa, D., Desaki, Y., Ishii-Minami, N., Nishizawa, Y., Minami, E., Okada, K., Yamane, H., Kaku, H., and Shibuya, N.** (2010). Two LysM receptor molecules, CEBiP and OsCERK1, cooperatively regulate chitin elicitor signaling in rice. *Plant J* **64**, 204-214.
- Shinya, T., Motoyama, N., Ikeda, A., Wada, M., Kamiya, K., Hayafune, M., Kaku, H., and Shibuya, N.** (2012). Functional characterization of CEBiP and CERK1 homologs in *Arabidopsis* and rice reveals the presence of different chitin receptor systems in plants. *Plant Cell Physiology* **53**, 1696-1706.
- Song, P., Heinen, J.L., Burns, T.H., and Allen, R.D.** (2000). Expression of two tissue-specific promoters in transgenic cotton plants. *The Journal of Cotton Science* **4**, 217-223.
- Sonti, R.V., Tissier, A.F., Wong, D., Viret, J.F., and Signer, E.R.** (1995). Activity of the yeast FLP recombinase in *Arabidopsis*. *Plant Molecular Biology* **28**, 1127-1132.
- Sripriya, R., Raghupathy, V., and Veluthambi, K.** (2008). Generation of selectable marker-free sheath blight resistant transgenic rice plants by efficient co-transformation of a cointegrate vector T-DNA and a binary vector T-DNA in one *Agrobacterium tumefaciens* strain. *Plant Cell Rep* **27**, 1635-1644.
- Stevenson-Paulik, J., Bastidas, R.J., Chiou, S.T., Frye, R.A., and York, J.D.** (2005). Generation of phytate-free seeds in *Arabidopsis* through disruption of inositol polyphosphate kinases. *Proc Natl Acad Sci USA* **102**, 12612-12617.
- Sun, F., Zhang, W., Hu, H., Li, B., Wang, Y., Zhao, Y., Li, K., Liu, M., and Li, X.** (2008). Salt modulates gravity signaling pathway to regulate growth direction of primary roots in *Arabidopsis*. *Plant Physiology* **146**, 178-188.

- Sun, Y., Li, L., Macho, A.P., Han, Z., Hu, Z., Zipfel, C., Zhou, J.M., and Chai, J.** (2013). Structural basis for flg22-induced activation of the Arabidopsis FLS2-BAK1 immune complex. *Science* **342**, 624-628.
- Sunarpi, Horie, T., Motoda, J., Kubo, M., Yang, H., Yoda, K., Horie, R., Chan, W.Y., Leung, H.Y., Hattori, K., Konomi, M., Osumi, M., Yamagami, M., Schroeder, J.I., and Uozumi, N.** (2005). Enhanced salt tolerance mediated by AtHKT1 transporter-induced Na unloading from xylem vessels to xylem parenchyma cells. *Plant J* **44**, 928-938.
- Sunkar, R., Kapoor, A., and Zhu, J.K.** (2006). Posttranscriptional induction of two Cu/Zn superoxide dismutase genes in Arabidopsis is mediated by downregulation of miR398 and important for oxidative stress tolerance. (vol 18, pg 2051, 2006). *Plant Cell* **18**, 2415-2415.
- Takahashi, F., Yoshida, R., Ichimura, K., Mizoguchi, T., Seo, S., Yonezawa, M., Maruyama, K., Yamaguchi-Shinozaki, K., and Shinozaki, K.** (2007). The mitogen-activated protein kinase cascade MKK3-MPK6 is an important part of the jasmonate signal transduction pathway in Arabidopsis. *Plant Cell* **19**, 805-818.
- Takahashi, H., Watanabe-Takahashi, A., Smith, F.W., Blake-Kalff, M., Hawkesford, M.J., and Saito, K.** (2000). The roles of three functional sulphate transporters involved in uptake and translocation of sulphate in Arabidopsis thaliana. *Plant J* **23**, 171-182.
- Takasaki, H., Maruyama, K., Kidokoro, S., Ito, Y., Fujita, Y., Shinozaki, K., Yamaguchi-Shinozaki, K., and Nakashima, K.** (2010). The abiotic stress-responsive NAC-type transcription factor OsNAC5 regulates stress-inducible genes and stress tolerance in rice. *Mol Genet Genomics* **284**, 173-183.
- Testerink, C., and Munnik, T.** (2005). Phosphatidic acid: a multifunctional stress signaling lipid in plants. *Trends Plant Sci* **10**, 368-375.
- Thiebaut, F., Rojas, C.A., Almeida, K.L., Grativol, C., Domiciano, G.C., Lamb, C.R., Engler Jde, A., Hemerly, A.S., and Ferreira, P.C.** (2012). Regulation of miR319 during cold stress in sugarcane. *Plant Cell Environ* **35**, 502-512.
- Toki, S., Takamatsu, S., Nojiri, C., Ooba, S., Anzai, H., Iwata, M., Christensen, A.H., Quail, P.H., and Uchimiya, H.** (1992). Expression of a Maize Ubiquitin Gene Promoter-bar Chimeric Gene in Transgenic Rice Plants. *Plant Physiology* **100**, 1503-1507.
- Torii, K.U.** (2004). Leucine-rich repeat receptor kinases in plants: Structure, function, and signal transduction pathways. *Int Rev Cytol* **234**, 1-+.

- Tuteja, N., Verma, S., Sahoo, R.K., Raveendar, S., and Reddy, I.N.** (2012). Recent advances in development of marker-free transgenic plants: regulation and biosafety concern. *Journal of Biosciences* **37**, 167-197.
- Umezawa, T., Yoshida, R., Maruyama, K., Yamaguchi-Shinozaki, K., and Shinozaki, K.** (2004). SRK2C, a SNF1-related protein kinase 2, improves drought tolerance by controlling stress-responsive gene expression in *Arabidopsis thaliana*. *Proc Natl Acad Sci USA* **101**, 17306-17311.
- Valvekens, D., Vanmontagu, M., and Vanlijsebettens, M.** (1988). *Agrobacterium-Tumefaciens-Mediated Transformation of Arabidopsis-Thaliana Root Explants by Using Kanamycin Selection.* *Proc Natl Acad Sci USA* **85**, 5536-5540.
- van Leeuwen, W., Vermeer, J.E., Gadella, T.W., Jr., and Munnik, T.** (2007). Visualization of phosphatidylinositol 4,5-bisphosphate in the plasma membrane of suspension-cultured tobacco BY-2 cells and whole *Arabidopsis* seedlings. *Plant J* **52**, 1014-1026.
- Vermeer, J.E., Thole, J.M., Goedhart, J., Nielsen, E., Munnik, T., and Gadella, T.W., Jr.** (2009). Imaging phosphatidylinositol 4-phosphate dynamics in living plant cells. *Plant J* **57**, 356-372.
- Vermeer, J.E., van Leeuwen, W., Tobena-Santamaria, R., Laxalt, A.M., Jones, D.R., Divecha, N., Gadella, T.W., Jr., and Munnik, T.** (2006). Visualization of PtdIns3P dynamics in living plant cells. *Plant J* **47**, 687-700.
- Vidhyasekaran, P.** (2014). Mitogen-activated protein kinase cascades in plant innate immunity. In *PAMP Signals in Plant Innate Immunity* (Springer), pp. 331-374.
- Voinnet, O.** (2009). Origin, biogenesis, and activity of plant microRNAs. *Cell* **136**, 669-687.
- Wang, X.** (2005). Regulatory functions of phospholipase D and phosphatidic acid in plant growth, development, and stress responses. *Plant Physiology* **139**, 566-573.
- Wang, X., Devaiah, S.P., Zhang, W., and Welti, R.** (2006). Signaling functions of phosphatidic acid. *Prog Lipid Res* **45**, 250-278.
- Wang, Y., Chen, B., Hu, Y., Li, J., and Lin, Z.** (2005). Inducible excision of selectable marker gene from transgenic plants by the cre/lox site-specific recombination system. *Transgenic Research* **14**, 605-614.

- Wang, Y.N., Zhang, W.S., Li, K.X., Sun, F.F., Han, C.K., Wang, Y., and Li, X.** (2008). Salt-induced plasticity of root hair development is caused by ion disequilibrium in *Arabidopsis thaliana*. *Journal of Plant Research* **121**, 87-96.
- Willmann, R., Lajunen, H.M., Erbs, G., Newman, M.A., Kolb, D., Tsuda, K., Katagiri, F., Fliegmann, J., Bono, J.J., Cullimore, J.V., Jehle, A.K., Gotz, F., Kulik, A., Molinaro, A., Lipka, V., Gust, A.A., and Nurnberger, T.** (2011). *Arabidopsis* lysin-motif proteins LYM1 LYM3 CERK1 mediate bacterial peptidoglycan sensing and immunity to bacterial infection. *Proc Natl Acad Sci USA* **108**, 19824-19829.
- Woo, H.J., Cho, H.S., Lim, S.H., Shin, K.S., Lee, S.M., Lee, K.J., Kim, D.H., and Cho, Y.G.** (2009). Auto-excision of selectable marker genes from transgenic tobacco via a stress inducible FLP/FRT site-specific recombination system. *Transgenic Research* **18**, 455-465.
- Wu, G., Park, M.Y., Conway, S.R., Wang, J.W., Weigel, D., and Poethig, R.S.** (2009). The sequential action of miR156 and miR172 regulates developmental timing in *Arabidopsis*. *Cell* **138**, 750-759.
- Xing, A.Q., Zhang, Z.Y., Sato, S., Staswick, P., and Clemente, T.** (2000). The use of the two T-DNA binary system to derive marker-free transgenic soybeans. *In Vitro Cell Dev-Pl* **36**, 456-463.
- Xiong, L., Lee, B., Ishitani, M., Lee, H., Zhang, C., and Zhu, J.K.** (2001). FIERY1 encoding an inositol polyphosphate 1-phosphatase is a negative regulator of abscisic acid and stress signaling in *Arabidopsis*. *Genes Dev* **15**, 1971-1984.
- Xu, Z., Zhong, S., Li, X., Li, W., Rothstein, S.J., Zhang, S., Bi, Y., and Xie, C.** (2011). Genome-wide identification of microRNAs in response to low nitrate availability in maize leaves and roots. *Plos One* **6**, e28009.
- Xu, Z.Y., Kim, S.Y., Hyeon do, Y., Kim, D.H., Dong, T., Park, Y., Jin, J.B., Joo, S.H., Kim, S.K., Hong, J.C., Hwang, D., and Hwang, I.** (2013). The *Arabidopsis* NAC transcription factor ANAC096 cooperates with bZIP-type transcription factors in dehydration and osmotic stress responses. *Plant Cell* **25**, 4708-4724.
- Yamaguchi, Y., and Huffaker, A.** (2011). Endogenous peptide elicitors in higher plants. *Current Opinion in Plant Biology* **14**, 351-357.
- Yamaguchi, Y., Pearce, G., and Ryan, C.A.** (2006). The cell surface leucine-rich repeat receptor for AtPep1, an endogenous peptide elicitor in *Arabidopsis*, is functional in transgenic tobacco cells. *Proc Natl Acad Sci USA* **103**, 10104-10109.

- Yamaguchi, Y., Huffaker, A., Bryan, A.C., Tax, F.E., and Ryan, C.A.** (2010). PEPR2 is a second receptor for the Pep1 and Pep2 peptides and contributes to defense responses in Arabidopsis. *Plant Cell* **22**, 508-522.
- Yamaguchi-Shinozaki, K., and Shinozaki, K.** (2001). Improving plant drought, salt and freezing tolerance by gene transfer of a single stress-inducible transcription factor. *Novartis Found Symp* **236**, 176-186; discussion 186-179.
- Yang, Q., Chen, Z.Z., Zhou, X.F., Yin, H.B., Li, X., Xin, X.F., Hong, X.H., Zhu, J.K., and Gong, Z.** (2009). Overexpression of SOS (Salt Overly Sensitive) genes increases salt tolerance in transgenic Arabidopsis. *Mol Plant* **2**, 22-31.
- Yu, L., Nie, J., Cao, C., Jin, Y., Yan, M., Wang, F., Liu, J., Xiao, Y., Liang, Y., and Zhang, W.** (2010). Phosphatidic acid mediates salt stress response by regulation of MPK6 in Arabidopsis thaliana. *New Phytol* **188**, 762-773.
- Yuan, S., Li, Z., Li, D., Yuan, N., Hu, Q., and Luo, H.** (2015). Constitutive Expression of Rice MicroRNA528 Alters Plant Development and Enhances Tolerance to Salinity Stress and Nitrogen Starvation in Creeping Bentgrass. *Plant physiology* **169**, 576-593.
- Yue, Y., Zhang, M., Zhang, J., Tian, X., Duan, L., and Li, Z.** (2012). Overexpression of the AtLOS5 gene increased abscisic acid level and drought tolerance in transgenic cotton. *J Exp Bot* **63**, 3741-3748.
- Zentgraf, U., Laun, T., and Miao, Y.** (2010). The complex regulation of WRKY53 during leaf senescence of Arabidopsis thaliana. *Eur J Cell Biol* **89**, 133-137.
- Zhang, W., Qin, C., Zhao, J., and Wang, X.** (2004). Phospholipase D alpha 1-derived phosphatidic acid interacts with ABI1 phosphatase 2C and regulates abscisic acid signaling. *Proc Natl Acad Sci USA* **101**, 9508-9513.
- Zhang, W., Subbarao, S., Addae, P., Shen, A., Armstrong, C., Peschke, V., and Gilbertson, L.** (2003). Cre/lox-mediated marker gene excision in transgenic maize (*Zea mays* L.) plants. *Theor Appl Genet* **107**, 1157-1168.
- Zhang, Z., Wei, L., Zou, X., Tao, Y., Liu, Z., and Zheng, Y.** (2008). Submergence-responsive MicroRNAs are potentially involved in the regulation of morphological and metabolic adaptations in maize root cells. *Ann Bot* **102**, 509-519.
- Zhao, B., Ge, L., Liang, R., Li, W., Ruan, K., Lin, H., and Jin, Y.** (2009). Members of miR-169 family are induced by high salinity and transiently inhibit the NF-YA transcription factor. *BMC Mol Biol* **10**, 29.



- Zhou, M., Li, D., Li, Z., Hu, Q., Yang, C., Zhu, L., and Luo, H.** (2013). Constitutive expression of a miR319 gene alters plant development and enhances salt and drought tolerance in transgenic creeping bentgrass (*Agrostis stolonifera* L.). *Plant Physiology* **161**, 1375-1391.
- Zhu, H., Li, G.-J., Ding, L., Cui, X., Berg, H., Assmann, S.M., and Xia, Y.** (2009). Arabidopsis extra large G-protein 2 (XLG2) interacts with the G $\beta$  subunit of heterotrimeric G protein and functions in disease resistance. *Mol Plant* **2**, 513-525.
- Zhu, J.K.** (2000). Genetic analysis of plant salt tolerance using Arabidopsis. *Plant Physiology* **124**, 941-948.
- Zhu, J.K.** (2002). Salt and drought stress signal transduction in plants. *Annual Review of Plant Biology* **53**, 247-273.
- Zipfel, C.** (2008). Pattern-recognition receptors in plant innate immunity. *Current opinion in immunology* **20**, 10-16.
- Zipfel, C., and Felix, G.** (2005). Plants and animals: a different taste for microbes? *Current Opinion in Plant Biology* **8**, 353-360.
- Zipfel, C., Robatzek, S., Navarro, L., Oakeley, E.J., Jones, J.D.G., Felix, G., and Boller, T.** (2004). Bacterial disease resistance in Arabidopsis through flagellin perception. *Nature* **428**, 764-767.
- Zipfel, C., Kunze, G., Chinchilla, D., Caniard, A., Jones, J.D., Boller, T., and Felix, G.** (2006). Perception of the bacterial PAMP EF-Tu by the receptor EFR restricts *Agrobacterium*-mediated transformation. *Cell* **125**, 749-760.
- Zubko, E., Scutt, C., and Meyer, P.** (2000). Intrachromosomal recombination between attP regions as a tool to remove selectable marker genes from tobacco transgenes. *Nature Biotechnology* **18**, 442-445.
- Zuo, J., Niu, Q.W., Moller, S.G., and Chua, N.H.** (2001). Chemical-regulated, site-specific DNA excision in transgenic plants. *Nature Biotechnology* **19**, 157-161

CHAPTER TWO

IDENTIFICATION AND FUNCTIONAL CHARACTERIZATION OF A NEW  
*ARABIDOPSIS* PROTEIN KINASE GENE FAMILY INVOLVED IN STRESS  
RESISTANCE

## ABSTRACT

Environmental stress is an important factor that significantly impacts plant development. Broad understanding of molecular mechanisms underlying plant stress response allows development of novel molecular strategies in genetically engineering crop species for enhanced performance under adverse conditions. We have identified a new *Arabidopsis* protein kinase family SRF (Stress Responsive Factor) comprising of four members (SRF1-4) whose expressions are strongly regulated by biotic or abiotic stresses. These four genes are highly conserved and clustered in the same chromosome region. Subcellular localization using GFP reporter system revealed SRF proteins are all localized on plasma membrane, indicating they may function similarly in plant stress response signaling. Gene expression analyses using real-time PCR and GUS reporter system revealed different expression patterns of the four genes, suggesting their similar, but temporally and spatially distinct functions in plants. Simultaneous knockout of *SRF1* and *2* using RNA interference enhanced plant abiotic stress tolerance. Furthermore, overexpression of *SRF2* significantly increases pathogen resistance in *Arabidopsis* by enhancing the PTI triggered basal defenses. Northern analysis result showed that the expression level of *WRKY53* and *FRK1* was upregulated in plants that overexpress *SRF2*. The result of Western analysis suggests MPK3/6 phosphorylation was enhanced in *SRF2* overexpressing plant upon pathogen and elicitor treatment. The result of bimolecular fluorescence complementation indicates that the BAK1 protein is a co-receptor of SRF2 kinase in the signal transduction pathway during the pathogen invasion.

**Key words:** LRR-RLK, Stress resistance, signal transduction, PTI, salt resistance

## **INTRODUCTION**

Environmental stress is one of the most important factors impacting agriculture production. Many stresses, such as salt stress and pathogen infection, can limit plant growth and development. Understanding molecular mechanisms underlying plant response to adverse environmental conditions will provide us basic but critical knowledge to develop molecular strategies for genetic improvement of crop species.

To reduce damage caused by osmotic stress, plants adopt different mechanisms and strategies. Before severe water deficit symptoms occur, plants can escape stress by accelerating their life cycle and fruiting early. Plants can also adopt avoidance and tolerance strategies during drought or salinity stress: stomata are closed to prevent plants from losing water, osmolytes such as proline are synthesized for keeping a high osmotic pressure in cell, expression of transporter genes is regulated to help plants exclude or compartmentalize harmful ions such as sodium, and growth of root is greatly promoted to maximize water uptaking (Chaves et al., 2003; Shkolnik-Inbar et al., 2012).

Biotic stress caused by pathogens also could cause severe damage to plants. To fight against pathogen infection, plants adopt two layers of innate immunity (Glazebrook, 2005). PTI (PAMP-Triggered Immunity) pathway that offers plants ability to recognize PAMPs (Pathogen-Associated Molecular Patterns), such as flagellin or elongation factor Tu, constitutes the first layer of plant immunity system. If PTI is repressed by type-III effectors injected into plant cells by pathogens, ETI (Effector-Triggered Immunity) that

constitutes the second layer of plant immunity system will be initiated in plants to resist pathogen through suppressing the effectors (Jones and Dangl, 2006).

Plasma membrane offers plant cells a stable and orderly protoplasm environment that is isolated from external environment (Serrano, 1984; Laude and Prior, 2004). On the other hand, to fight against stress and survive adverse environment, cells need to receive and transduce extracellular stress signal into the intracellular environment through the plasma membrane barrier. Many membrane-anchored proteins, such as receptor like protein kinases, act as sensors and receptors mediating the signaling transduction. LRR-RLKs (Leucine-Rich Repeat Receptor Like Protein Kinases) compose the largest subfamily of transmembrane receptor like protein kinases in *Arabidopsis* (Torii, 2004). Over the course of the past 20 years, plant LRR-RLKs were found to play fundamental roles in cell proliferation, photomorphogenesis, biotic and abiotic stress responses (Deeken and Kaldenhoff, 1997; Li and Chory, 1997; Fletcher et al., 1999; Xiang et al., 2006; de Lorenzo et al., 2009; Antolin-Llovera et al., 2012). A *Medicago truncatula* LRR-RLK gene SRLK were proven to be a possible receptor which functions in plant resistance against salt stress (de Lorenzo et al., 2009). RPK1, an *Arabidopsis* LRR-RLK, is intensively upregulated under abiotic stress and ABA treatment (Hong et al., 1997). *Arabidopsis* line overexpressing RPK1 exhibits enhanced salt tolerance, indicating the important function of RPK1 in abiotic stress resistance (Osakabe et al., 2010). So far, only a few LRR-RLKs, such as FLS2 (Flagellin Sensitive2), EFR (EF-Tu Receptor), PEPR1 (PEP Receptor1), and BAK1 (BRI1-Associated Receptor Kinase 1) have been identified to function in signal transduction upon pathogen invasion (Chinchilla et al., 2007; Postel et al., 2010; Schulze

et al., 2010). These LRR-RLKs act as receptors in PTI pathway, recognizing external PAMP elicitors and triggering internal signaling transduction.

We have identified a novel LRR-RLK family, SRF (Stress Responsive Factor) gene family using bioinformatics analysis with *Arabidopsis* cDNA microarray data. Here, we demonstrate that the four SRF family members may participate in different stress-resistance signaling transduction pathways in *Arabidopsis*, though their highly conserved sequences indicate they may have similar functions. Using a *SRF2* T-DNA insertion mutant and *SRF2*-overexpressing line, we determined that *SRF2* is a critical element in the PTI pathway. *SRF2* positively regulates plant basal defenses against pathogens. Evidence from our research indicates that *SRF2* interacts with BAK1 upon pathogen infection to recruit and activate downstream MAPK cascade, inducing the expression of WRKY53 and FRK1 and triggering basal defense responses. Furthermore, our result also suggests that *SRF1* and *SRF2* negatively regulate salt resistance. Our research sheds light on understanding of the functions of *SRF* gene family and how different family members contribute to different stress resistance pathways.

## **RESULTS**

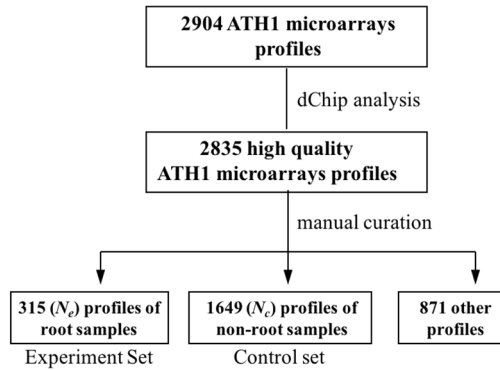
### **Identification of the *Arabidopsis thaliana* SRF gene family**

As the first affected tissue under osmotic stress, root plays an important role for the plant to sense and respond to osmotic stress. The first step of our research was to identify genes specifically or predominately expressed in *Arabidopsis* root tissues (Figure 2.1). We started with 2904 publicly available *Arabidopsis* gene expression profiles conducted on

ATH1 microarray (Craigon et al., 2004). After data quality control was performed using dChip analysis, 2835 high quality profiles were used for further analysis (Li and Wong, 2007). After manual curation of samples/tissue types, these profiles were grouped to two sets: (1) 315 profiles of root samples (experiment set); (2) 1649 profiles of non-root samples (control set) (Figure 2.1 a). The remaining 871 profiles were not used in this analysis. Using the experiment and control data sets to search for root specific/predominate genes with our algorithm, we finally identified 324 root-specific gene targets prioritized by the priority score (Figure 2.1 b) (Wang et al., 2010).

Among these 321 genes, we focused on LRR-RLKs which function as important receptors in signal transduction pathways. Based on our preliminary experiments, SRF1 attracted our attention. *SRF1* is a classic LRR-RLK gene predominately expressed in root tissue, and it is intensively regulated by salt stress. According to the preliminary data, we hypothesized that *SRF1* may have crucial function in plant salt stress response. In order to understand evolution details of SRF1, protein sequences of 343 LRR-RLKs in *Arabidopsis* and other plant species, including a number of well-studied LRR-RLKs, such as TMK1 (Chang et al., 1992), BR1I (Zhou et al., 2004), CLAVATA1 (Clark et al., 1997), RLK5 (Stone et al., 1994), were obtained from NCBI (National Center for Biotechnology Information) (<http://www.ncbi.nlm.nih.gov>) database and used for phylogeny analysis with SRF1 protein (Figure 2.2). The phylogeny analysis indicates that SRF1 has a close evolutionary relationship with three other *Arabidopsis* LRR-RLKs. Their coding sequences are all localized on the *Arabidopsis* chromosome I closely (Figure 2.2), forming a gene cluster.

(a)



(b)

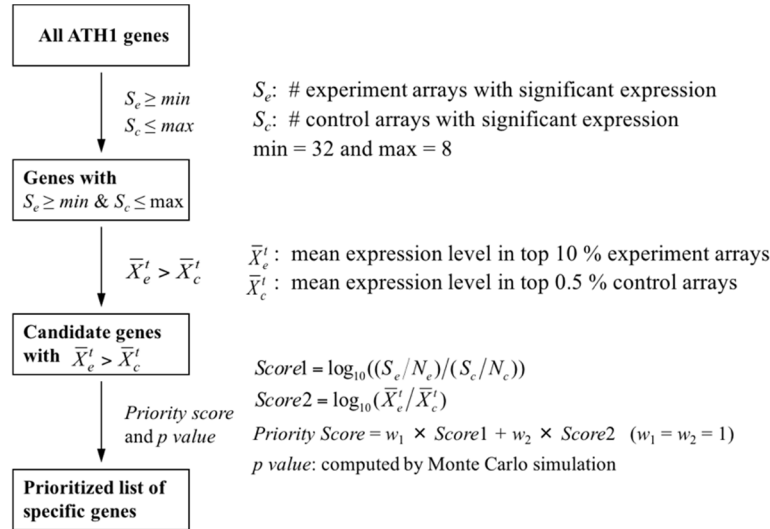
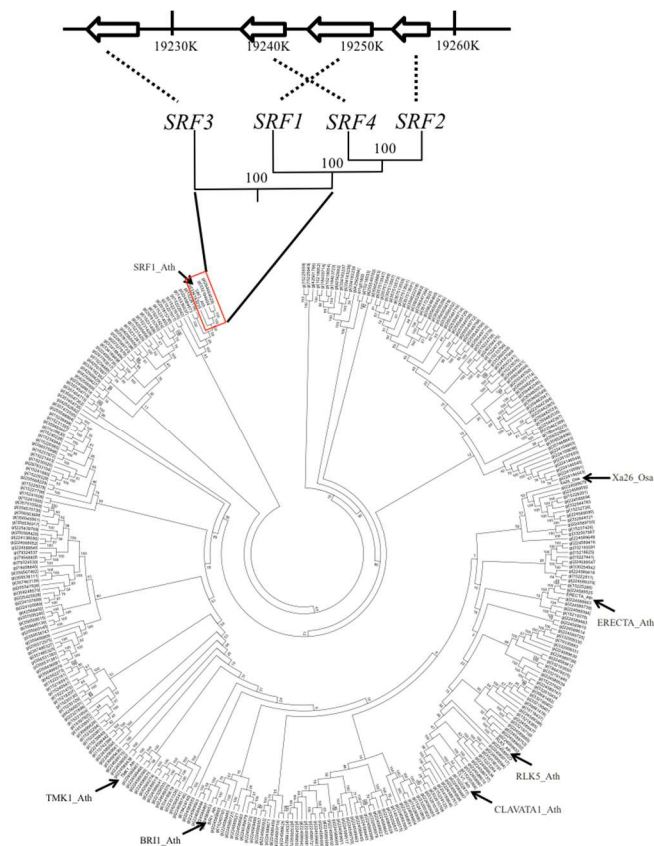


**Figure 2.1. Genome-wide identification of root-specific genes.** (a) Flowchart for bioinformatics analysis. 2904 ATH1 microarray profiles were downloaded from public database (<http://affymetrix.arabidopsis.info>). After dChip analysis and manual curation, 2835 high quality profiles were assigned to three groups (sets). Experiment set and control set were used in further analysis. (b) Flowchart for screening root specific genes using experiment set and control set. ATH1 microarray contains 22,746 probe sets. Priority score of each probe (represents one gene) was calculated following the indicated algorithm (Wang et al., 2010). Gene with higher priority score is more root-specific.



**Figure 2.2. Phylogenetic analysis and genomic organization of the *SRF* genes.**

The analysis involved 338 amino acid sequences, including sequences of four SRF proteins. The evolutionary history was inferred using the Neighbor-Joining method. The bootstrap consensus tree inferred from 100 replicates is taken to represent the evolutionary history of the taxa analyzed. Branches corresponding to partitions reproduced in less than 50% bootstrap replicates are collapsed. The evolutionary distances were computed using the p-distance method and are in the units of the number of amino acid differences per site. All ambiguous positions were removed for each sequence pair. There were a total of 3410 positions in the final dataset. Evolutionary analyses were conducted in MEGA5. The four *SRF* genes are all located closely on *Arabidopsis* chromosome 1, forming a gene cluster. ‘K’ indicates Kb.



According to a previous sequence analysis of *Arabidopsis* LRR-RLKs conducted by Gou et al., these four proteins were all grouped to LRR subfamily LRR I-2 in *Arabidopsis* (Gou et al., 2010). Based on these results, we group these four proteins into a gene family named SRF.

As the largest protein kinase subfamily, the structures of LRR-RLK proteins have been well studied. Generally, a classic LRR-RLK contains several different domains, including an N-terminal signal peptide, an extracellular LRR domain (usually from 1 to 32 LRRs), a transmembrane domain, and a cytoplasmic protein kinase domain (Torii, 2004). Specifically, LRR which shares a highly conserved sequence as L-L-L-L-L-N-L-G-IP-- (where the ‘-’ stands for non-conserved amino acid residues, the ‘L’ represents Val, Leu or

Ile, the 'N' represents Asn, Thr, Ser, or Cys, and the 'C' represents Cys or Ser) between different plant species has a crucial function for plants to percept extracellular ligands or signals (Jones and Jones, 1997; Enkhbayar et al., 2004). SRFs are classic LRR-RLK proteins, as each SRF protein contains an N-terminal signal peptide with a length of 21 (SRF2, SRF2 and SRF4) or 28 (SRF1) amino acid residues, an extracellular LRR domain contains two LRRs, a transmembrane domain, and a serine/threonine protein kinase domain (Figure 2.3). The SRF proteins have high sequence similarity with each other from 73% to 86%.

### ***SRFs* respond to abiotic stress and biotic stress**

Our preliminary data indicate that *SRF1* responds to abiotic stresses (data not shown). Given that *SRF1* is one of the four members of the *SRF* gene family and the sequences of all four members are highly conserved, we assume that the four genes have similar function and will respond to the same stresses. To prove our hypothesis, we conducted real-time PCR to investigate the expression of the *SRFs* under abiotic stresses.

As predicted, the four genes all responded to salt stress (200 mM NaCl treatment), but exhibited different expression patterns. In the leaf tissue, *SRF2* was down regulated in the first two hours and then upregulated at four hours after salt treatment, while the expression levels of *SRF3* and *SRF4* increased in the first half hour and then declined (Figure 2.4 a). Transcripts of *SRF1* were not detected probably because of its root specificity. In the root tissue, *SRF1*, *SRF3* and *SRF4* were all dramatically up-regulated, while the expression level of *SRF2* progressively went down.

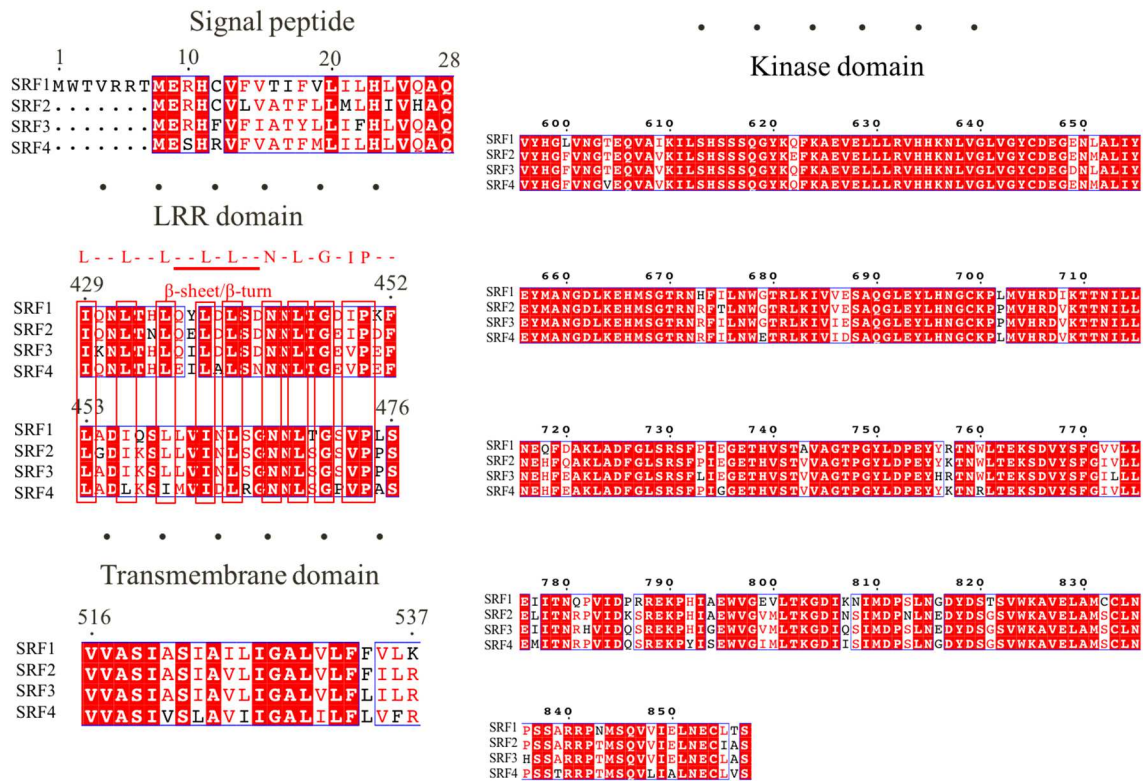


**Figure 2.3. Alignment of the SRF proteins.** Protein alignment was conducted with an online analysis tool ‘Multalin’ (<http://multalin.toulouse.inra.fr/multalin/multalin.html>). In the alignment, white letters in red background represent amino acid residues conserved across all four proteins, red letters in white background represent amino acid residues conserved across three family members, black letters in white background represent non-conserved amino acid residues. Ellipses represent amino acid sequences between the four main domains. The numbers indicate the positions of amino acid residues. The LRR motif is highlighted with red boxes as L--L--L--L-L--N-L-G-IP--, and the predicted  $\beta$ -strand/ $\beta$ -turn structure is underlined as --L-L--, where the ‘-’ stands for non-conserved amino acid residues, the ‘L’ represents Leu or Ile, and the ‘I’ represents Val or Ile.

When *Arabidopsis* was subjected to drought stress, the four genes again responded differently (Figure 2.4 b). In leaf tissue, *SRF2* and *SRF3* exhibited opposite expression patterns. The drought stress induced the accumulation of the *SRF2* transcripts, while repressed the expression of *SRF3*. Specifically, the transcripts of the *SRF3* were undetectable at four hours after drought treatment. In the root tissue, *SRF1* and *SRF2* were

both down regulated upon drought treatment, but *SRF4* was upregulated in the first half hour and then down regulated. The expression pattern of the *SRF3* in root tissue was different from that in leaf tissue, as it was slightly upregulated in the root under drought stress.

Previous studies indicated that the transcripts of *SRF2* and *SRF4* accumulate in leaf tissue after *Arabidopsis* are infected with biotrophic pathogen *Hyaloperonospora arabidopsidis* and *Pst* DC3000 (*Pseudomonas syringae* pathovar *tomato* strain, DC3000) (Hok et al., 2011; Czarnecka et al., 2012). To find out whether or not *SRFs* are involved in the pathogen resistance pathway, we first investigated the expression levels of the three leaf-expressing *SRFs* in leaves infiltrated with *Pst* DC3000. We also used a mutant strain of *Pst* DC3000 named *Pst* DC3000 *hrcC*<sup>-</sup> which is deficient in type-III secretion system, and two PAMP elicitors - flg22 and elf18 - for leaf treatment to test the *SRF* responses.

Under mock treatment, all three leaf-expressing *SRFs* exhibited the highest expression at one hour (Figure 2.5 a). But under pathogen or PAMPs treatment, *SRF2*, as well as *SRF4*, exhibited different expression patterns from mock treatment. The transcript levels of the two *SRFs* reached the peak at two hours after infiltrate-inoculation of leaves with pathogens or PAMPs (Figure 2.5 b-e). Specifically, the expression level of *SRF2* increased thousands of times upon *Pst* DC3000 *hrcC*<sup>-</sup> or elf18 treatment (Figure 2.5 c, e), or hundreds of times upon *Pst* DC3000 or flg22 treatment (Figure 2.5 b, d). Compared with *SRF2*, the expression level of *SRF4* exhibited a lower but still significant ( $P < 0.05$ ) increase

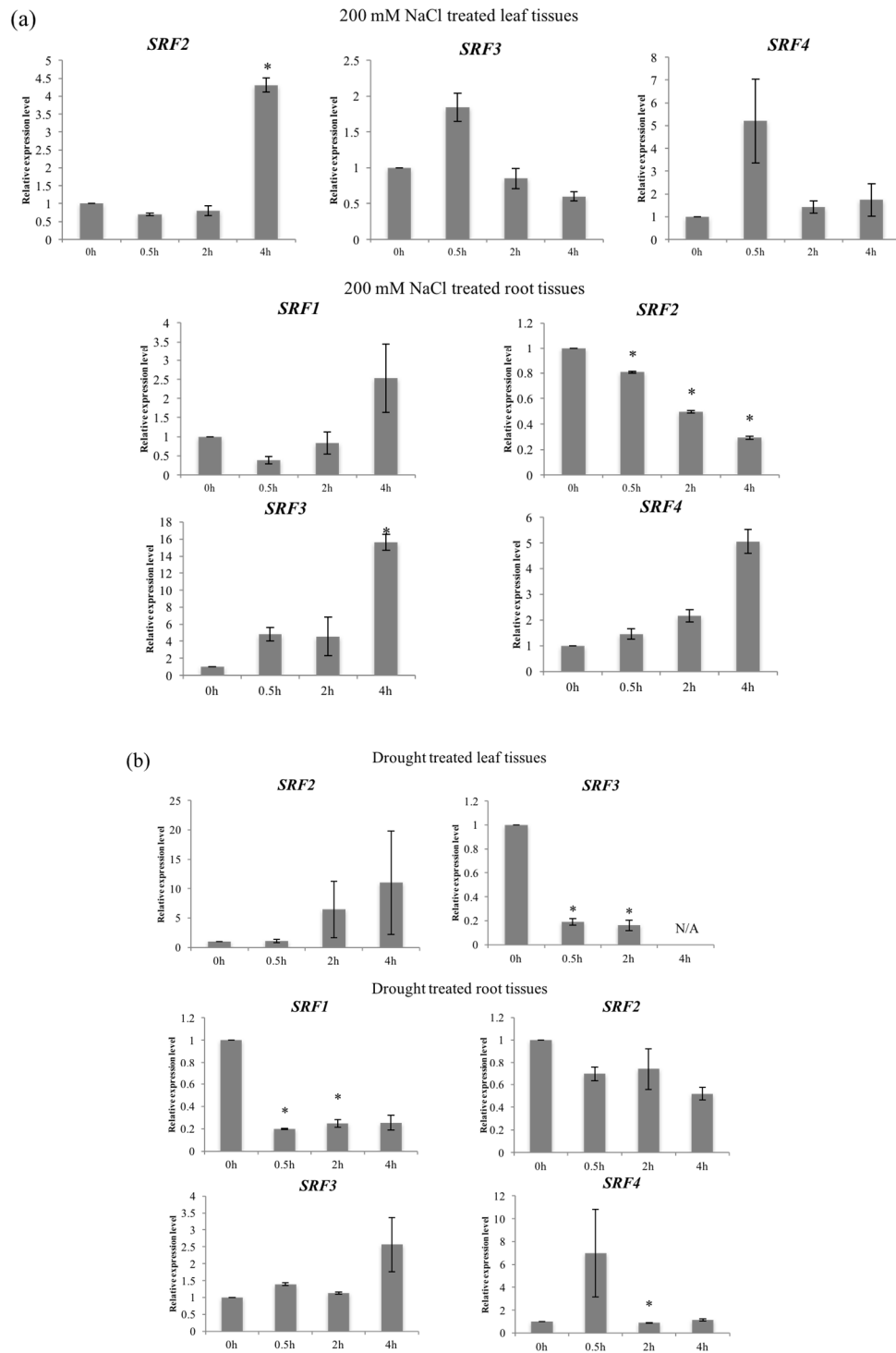


Figure 2.4

**Figure 2.4. Expression analysis of the *SRF* genes under osmotic stresses.** Two-week-old seedlings grown in hydroponic system were treated with (a) 200 mM NaCl or (b) drought. Leaf or root samples were collected at indicated time points and used in real-time PCR analysis. *Actin2* was used as the reference gene. Data shown are an average of three technical replicates for two independent biological replicates. Error bars represent S.D. (n=6). Asterisks indicate the significant differences between 0 hour and other times points. P < 0.05 was marked as \*. P < 0.01 was marked as \*\*.

---

upon *Pst* DC3000, *Pst* DC3000 *hrcC* or elf18 treatment. *SRF4* had a higher expression level than *SRF2* under flg22 treatment (Figure 2.5 d). Unlike *SRF2* and *SRF4*, *SRF3* exhibited similar expression patterns upon mock, pathogens and PAMPs treatments. These results indicate that *SRF2* and *SRF4* respond to pathogens and PAMPs intensely, suggesting their potentially important functions for *Arabidopsis* to defense against pathogen.

Taken together, these results imply that *SRF* gene family may have multiple functions and be involved in both abiotic and biotic stress resistance pathways.

### ***SRFs* exhibited spatial and temporal specificity**

To further understand the function of the *SRF* gene family, we investigated the expression levels of the four *SRFs* in different tissues of two-week-old or four-week-old *Arabidopsis*. According to the real-time PCR results (Figure 2.6 a), *SRF1* was only expressed in root tissue of two-week-old plants, *SRF3* and *SRF4* were only expressed in leaf tissue, whereas *SRF2* was expressed in both root and leaf tissues.

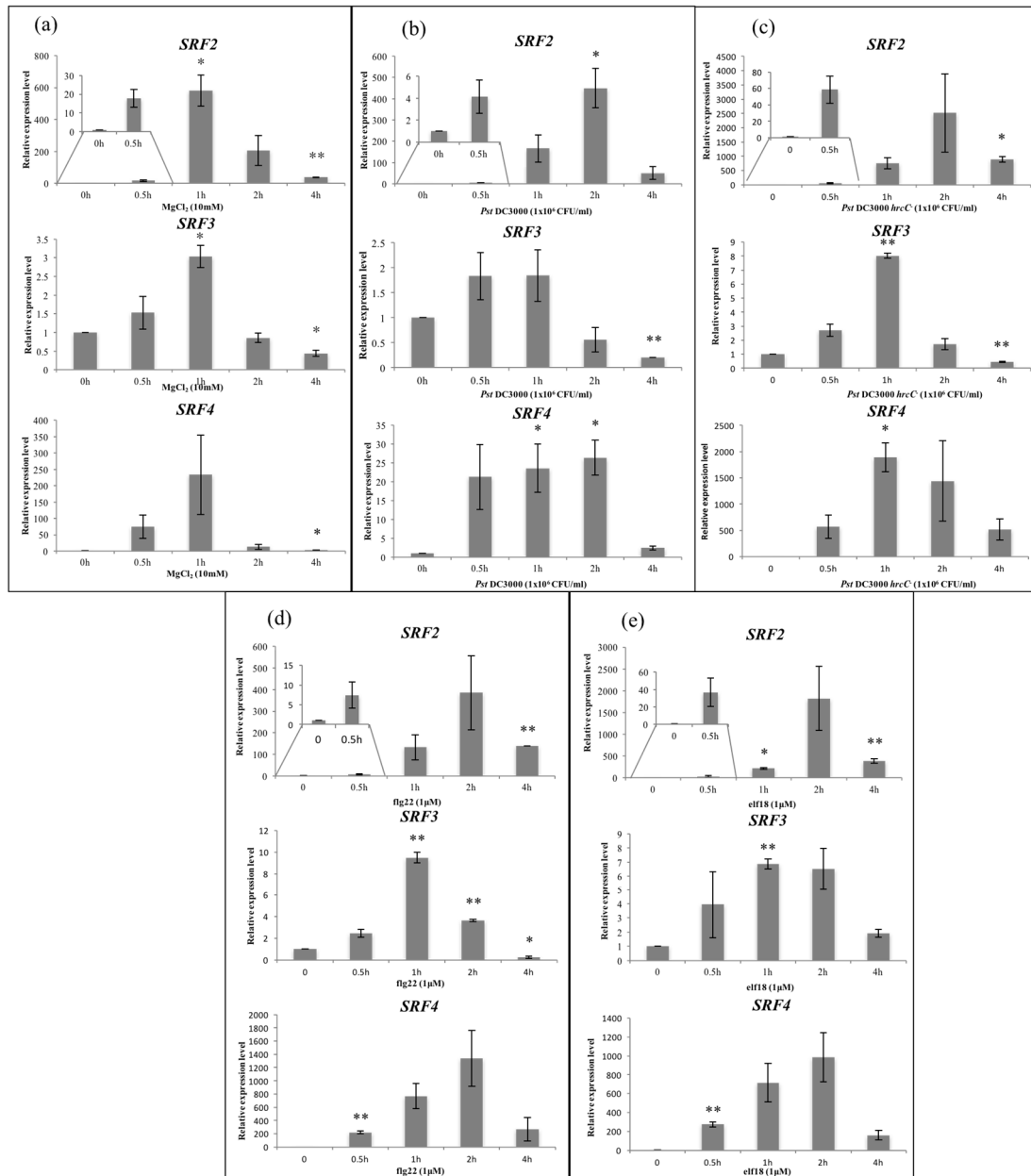


**Figure 2.5. Expression analysis of the *SRF* genes under pathogen and elicitor treatment.** Leaves of two-week-old wild type *Arabidopsis thaliana* plants were infiltrated with (a) 10 mM MgCl<sub>2</sub> as mock control, (b) Pst DC3000 (1x10<sup>6</sup> CFU/ml), (c) Pst DC3000 hrcC<sup>-</sup> (1x10<sup>6</sup> CFU/ml), (d) 1 µM flg22, or (e) 1 µM elf18. Leaf samples were collected at indicated time points and used in real-time PCR analysis. Actin2 was used as the reference gene. Data shown are an average of three technical replicates for two independent biological replicates. Error bars represent S.D. (n=6). Asterisks indicate the significant differences between 0 hour and other times points. P < 0.05 was marked as \*. P < 0.01 was marked as \*\*.

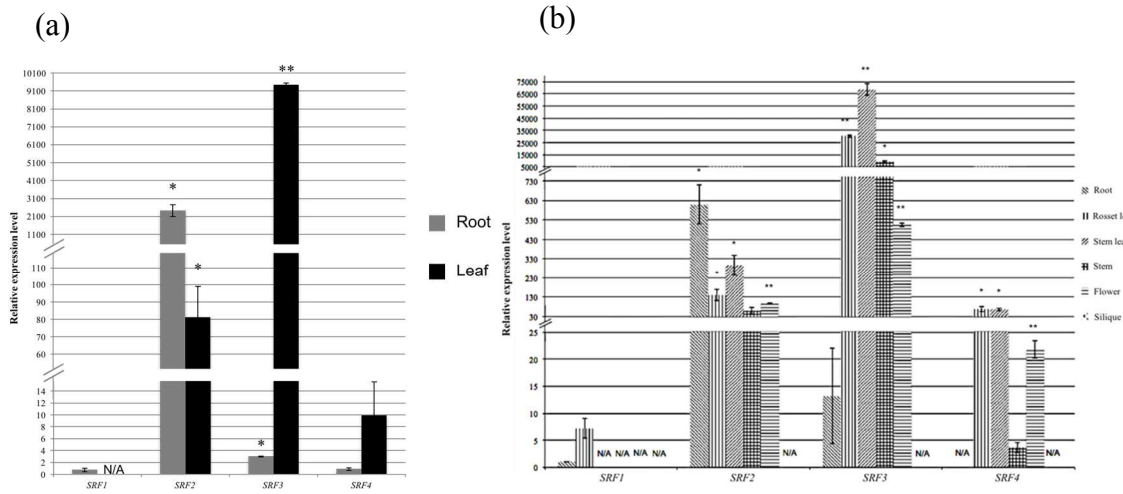


**Figure 2.6. Expression analysis of the *SRF* genes in different tissues of *Arabidopsis thaliana*.** (a) Root and leaf samples from two-week-old wild type plants and (b) root, rosset leaf, stem leaf, stem, flower, and silique samples from four-week-old wild type plants were collected and used in real-time PCR analysis. *Actin2* was used as the reference gene. Data shown are an average of three technical replicates for two independent biological replicates. Error bars represent S.D. (n=6). Asterisks indicate the significant differences between expression levels of the *SRF1* in root tissue and the indicated genes in the indicated tissues. P < 0.05 was marked as \*. P < 0.01 was marked as \*\*.

According to the real-time PCR results, the expression patterns of the four genes change over time with the development of *Arabidopsis* (Figure 2.6 b). The expression level of the *SRF1* in four-week-old *Arabidopsis* was quite low, and could only be detected in root and rosset leaf. Different from *SRF1*, *SRF2* exhibited a universal expression in four-week-old plants, and its transcription level was higher in root than that in rosset leaf, stem leaf, stem and flower. *SRF3* exhibited a similar expression pattern to *SRF2*, but its expression level was much higher. It exhibited the highest expression in leaves, stem and flowers among the four family members, but a significantly lower expression than *SRF2*



and *SRF4* in root tissue. *SRF4* was expressed in rosette leaf, stem leaf, stem and flower, but exhibited lower expression than *SRF2* and *SRF3* in all tissues.

Promoter regions (named *SRF1<sub>pro</sub>*, *SRF2<sub>pro</sub>*, *SRF3<sub>pro</sub>* and *SRF4<sub>pro</sub>*) of the four genes were cloned and fused to *GUS* gene to construct *GUS* reporter systems, resulting in *SRF1<sub>pro</sub>/GUS*, *SRF2<sub>pro</sub>/GUS*, *SRF3<sub>pro</sub>/GUS* and *SRF4<sub>pro</sub>/GUS*, respectively (Jefferson et al., 1987). Two-week-old and four-week-old transgenic *Arabidopsis* plants harboring one of the four constructs were harvested, and histochemical GUS staining was performed to analyze the promoter activity.

Blue stain indicating promoter activity was observed predominately in root tissue only, both root and leaf tissues, or leaf tissue only in two-week-old transgenic *Arabidopsis* harboring *SRF1<sub>pro</sub>/GUS*, *SRF2<sub>pro</sub>/GUS* or *SRF3<sub>pro</sub>/GUS*, respectively (Figure 2.7 a). These results are consistent with the real-time PCR result (Figure 2.6 a). Blue staining in *SRF4<sub>pro</sub>/GUS Arabidopsis* was observed in both root and leaf tissues (Figure 2.7 a), while real-time PCR results show that *SRF4* was only expressed in leaf tissue of two-week-old *Arabidopsis* plants (Figure 2.6 a), indicating that *SRF4* gene may be differentially regulated in different *Arabidopsis* tissues at the post-transcriptional level.

In four-week-old *Arabidopsis* (Figure 2.7 b), histochemical staining results suggest that *SRF2<sub>pro</sub>* was active in roots and leaves, but weak in sepals, and it did not exhibit any activity in siliques, seeds and other parts of flower. The spectrum of *SRF4<sub>pro</sub>* activity is similar to *SRF2<sub>pro</sub>*. Obvious blue staining in *SRF3<sub>pro</sub>/GUS Arabidopsis* could be observed in leaves and sepals, but root, silique and stylus were only very slightly colored in blue. These results are consistent with the real-time PCR data (Figure 2.6 b). Unexpectedly, the

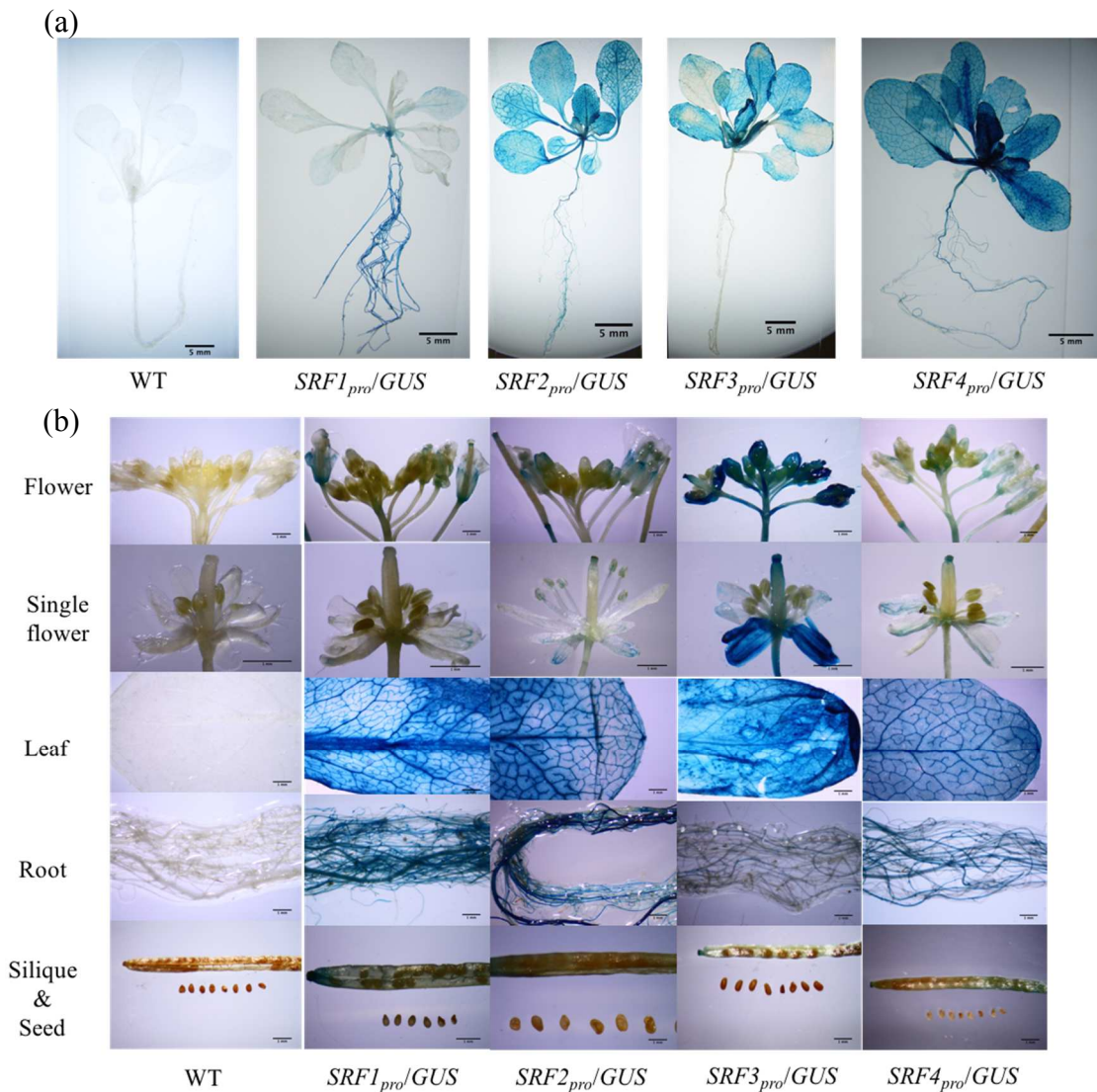


**Figure 2.7. Activity analysis of the *SRF* gene promoters.** Histochemical GUS-staining of (a) two-week-old and (b) four-week-old transgenic *Arabidopsis thaliana* plants harboring noted *GUS* reporter systems. For each transgenic plant line, at least two plants from two independent transformation events were stained. Pictures were taken under an optical microscope. One representative was exhibited.

activity of *SRF1<sub>pro</sub>* in four-week-old *Arabidopsis* was very strong in leaf and root tissues, but it exhibited weak activity in sepals and siliques. These *SRF1<sub>pro</sub>* GUS-staining results are different from those of *SRF1* expression analysis using real-time PCR analysis,

indicating that *SRF1* gene may also be strictly regulated at post-transcriptional level in four-week-old *Arabidopsis*.

### **SRF are plasma membrane-anchored proteins**

Protein kinases with different functions are localized in different subcellular structures (Nigg et al., 1985; Torii et al., 1996; Wang et al., 1996; Depege et al., 2003). As receptors in signaling transduction, LRR-RLKs are usually localized on plasma membrane (Torii, 2004). Because the four SRF proteins belong to the LRR-RLKs protein family, and all of them contain a transmembrane domain and a signal peptide with 21 or 28 amino acid residues in their N-terminals (Figure 2.3), we hypothesized that the four SRFs may be localized on plasma membrane. To verify our hypothesis, we investigated the subcellular localization of the four SRF proteins by using GFP reporter system (Chiu et al., 1996). For SRF2, SRF3 and SRF4, GFP was fused to the downstream of their C-terminals. Because full length SRF1 cannot be transiently expressed in tobacco leaf, GFP was fused to the C-terminal of the first 200 amino acid residues of its N-terminus, which contains signal peptides (Figure 2.8 a). Besides constructing the SRF-GFP fusion proteins, we also obtained another fusion protein, PIP2A-mCherry that emits red fluorescence. Because PIP2A is a membrane-anchored protein, PIP2A-mCherry was used as a plasma membrane marker to indicate the location of the SRF-GFP proteins in cell (Figure 2.8 b).

SRF-GFP fusion protein and PIP2A-mCherry fusion protein were co-expressed in tobacco (*Nicotiana benthamiana*) leaves. Under confocal laser scanning microscope, we observed that green fluorescence and red fluorescence emerged on the same region and

perfectly overlay with each other to emit yellow fluorescence, indicating that the four fusion proteins are all localized on the plasma membrane (Figure 2.8 c).

### ***SRFs* play crucial roles in abiotic and biotic stress resistance pathways**

In order to further understand the function of *SRFs*, we evaluated the growth of WT (Wild Type) *Arabidopsis*, *SRF* OE (Over-Expression) lines, and *SRF* T-DNA insertion mutants under different stresses.

To obtain *SRF* OE lines, we firstly cloned the full-length cDNA of *SRF1* and *SRF2* genes by using RACE (Rapid Amplification of cDNA Ends) method. We cloned the full-length cDNA of *SRF3* and *SRF4* based on the information of on-line database TAIR (<http://www.arabidopsis.org/index.jsp>). All the primers for the RACE assay and for the cloning of the *SRF3* and *SRF4* cDNAs were designed based on the sequence information collected from the on-line database mentioned above. Four chimeric gene constructs in which the full-length cDNA of the *SRF1*, *SRF2*, *SRF3* or *SRF4* driven by CaMV 35S (Cauliflower Mosaic Virus 35S) promoter were then generated and introduced into *Arabidopsis thaliana* by using floral dip assay (Clough and Bent, 1998). RT-PCR analyses indicate that the four *SRFs* were successfully overexpressed in transgenic *Arabidopsis* (Appendix Figure A-1).

T-DNA insertion mutants of *SRFs* were obtained from ABRC (Arabidopsis Biological Resource Center) (Alonso et al., 2003). According to the insertion flanking sequence information given by the ABRC, the T-DNA was inserted in the seventh intron of the *SRF1* gene in the *SRF1* T-DNA insertion mutant. In the *SRF2* T-DNA insertion

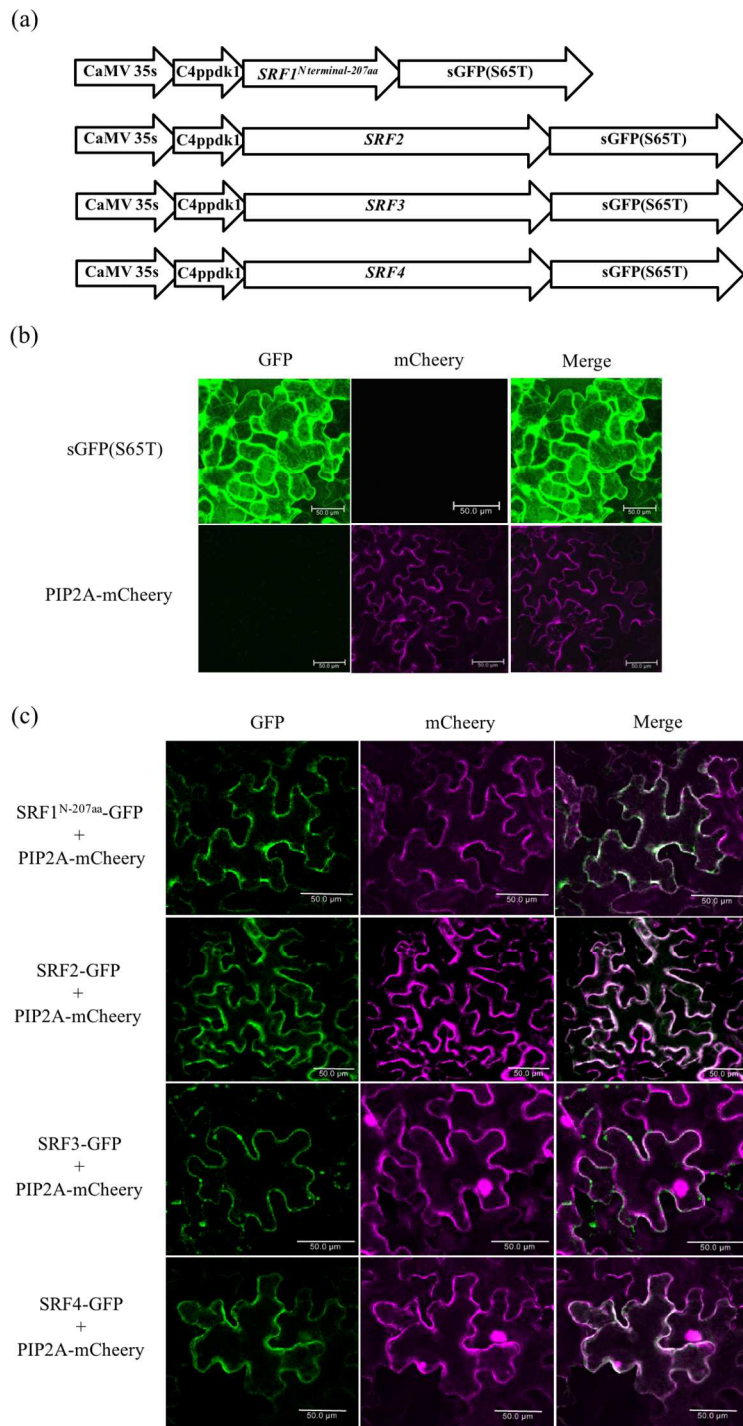


**Figure 2.8. Subcellular localization analysis of the SRF Proteins.** (a) The Schematic diagram of the constructs used for subcellular localization of the four SRF proteins. The DNA sequence encodes the first 207 amino acid residues in the N-terminal of the SRF1, the full length SRF2, SRF3 or SRF4 protein was fused with the coding sequence of the GFP(S65T) protein and under the control of CaMV 35S promoter. (b) GFP and plasma membrane marker PIP2A-mCherry were transiently expressed in tobacco leaves as positive controls. (c) SRF-GFP(S65T) was transiently co-expressed with PIP2A-mCherry in tobacco leaves. Leaf samples were examined under Leica SPE confocal microscope. Fluorescence of the SRF-GFP(S65T) was depicted in green, and fluorescence of PIP2A-mCherry was depicted in red.

mutant, the T-DNA was inserted in the second exon of the *SRF2* gene. In the T-DNA insertion line *srf3* and *srf4*, T-DNA was inserted in the third exon of the *SRF3* and *SRF4*, respectively (Figure 2.9 a). T-DNA positions in these T-DNA insertion lines were confirmed by using three primers. Two primers (LP and RP) were located on the *Arabidopsis* genomic DNA flanking the T-DNA, and the third one (BP) was located on the left border within the T-DNA (Figure 2.9 a). When PCR is conducted with genomic DNA extracted from WT plants, the amplicon will be the DNA sequence between LP and BP. But for the homozygous T-DNA insertion lines, the amplicon should be the DNA sequence between RP to the insertion site plus 110 bases of the T-DNA left border sequence. For heterozygous T-DNA insertion plants, both amplicons will be obtained in PCR. According to the PCR results, all four *SRFs* T-DNA insertion lines are homozygous (Figure 2.9 b). RT-PCR results indicate that the expression levels of the *SRFs* are significantly repressed in their T-DNA insertion lines (Figure 2.9 c).

Because *SRFs* are highly conserved in sequences, and some *SRFs* exhibit similar responses under abiotic or biotic stress (Figure 2.4), suggesting that *SRFs* may be functionally redundant. To further understand the functions of *SRFs*, it is necessary to repress multiple *SRF* genes simultaneously in a single *Arabidopsis* line. However, the four tandemly arrayed *SRFs* genes make it extremely difficult to obtain double, triple, or quadruple mutant by crossing *SRF* T-DNA insertion mutants. The alternative approach we adopted was to make a RNAi (RNA interference) construct which targets a sequence that is highly conserved across the whole SRF gene family (Appendix Figure A-2A). RT-PCR was performed to investigate the expression levels of SRFs in RNAi line. The result

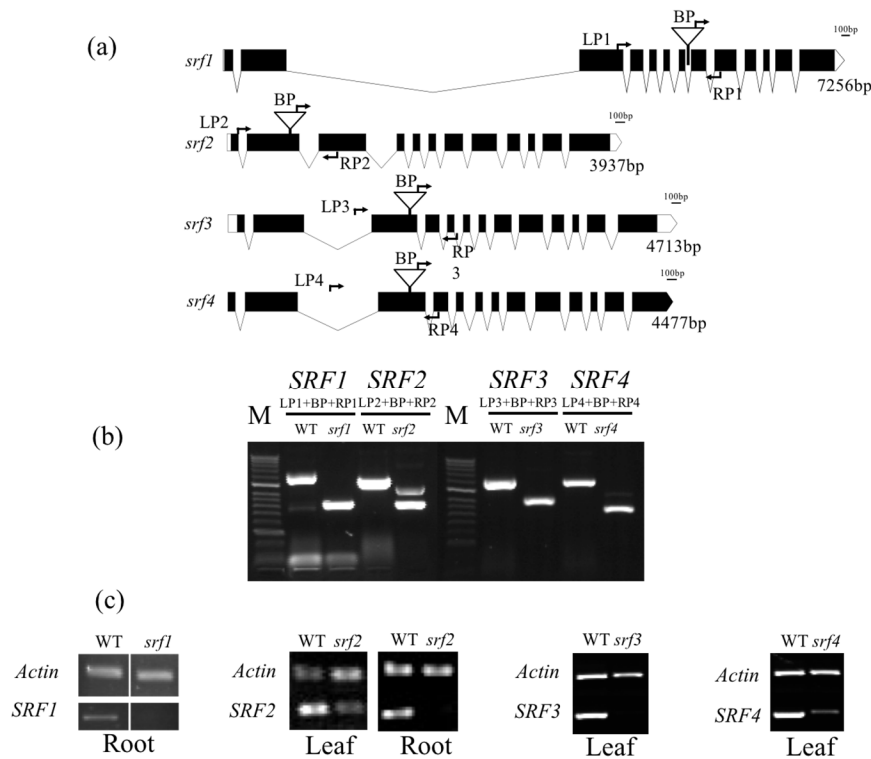


**Figure 2.9. Analysis of the *SRF* T-DNA insertion mutants.** (a) Positions of the T-DNA insertions within the *SRF1*, *SRF2*, *SRF3*, and *SRF4* genes in *srf1*, *srf2*, *srf3*, and *srf4* T-DNA insertion mutants. (b) PCR analysis of the positions of the T-DNA insertions in the four T-DNA insertion mutants. Genomic DNA was extracted from WT (wild type), *srf1*, *srf2*, *srf3*, and *srf4* T-DNA insertion mutants and used for the PCR analysis. LP and RP: primers on the *Arabidopsis* genomic DNA flanking the T-DNA sequence. BP: primer on the left border within the T-DNA sequence. (c) RT-PCR analysis of the *SRFs* expression in the mutants. Root and leaf tissues of two-week-old WT and T-DNA insertion mutant plants were collected for extracting RNA used for RT-PCR analysis. *Actin2* was used as reference gene.

indicates that only *SRF1* and *SRF2* were partially down-regulated in the three events of RNAi line (Appendix Figure A-2B).

We first investigated the growth of WT, RNAi line, OE lines (*SRF1* OE – *SRF4* OE) and T-DNA insertion lines (*srf1-srf4*) under the treatment of virulent pathogen *Pst* DC3000. Leaves of four-week-old *Arabidopsis* were infiltrated with *Pst* DC3000 ( $1 \times 10^5$

cfu/ml). 10 mM MgCl<sub>2</sub> was used as mock treatment. Three days later, *SRF2* OE line exhibited a slighter symptom than WT plants and other *Arabidopsis* lines, as reduced necrosis and chlorosis symptom were observed on its leaves. On the contrary, the pathogen infection symptoms on *srf2* leaves were more severe than WT, indicating that *srf2* is more susceptible to pathogen than WT and *SRF2* OE lines (Appendix Figure A-3A). For other *SRFs*, no significant growth difference was observed between their OE lines and T-DNA insertion lines (Appendix Figure A-3A).

To confirm this result, we spray-inoculated *Pst* DC3000 ( $5 \times 10^6$  cfu/ml) onto leaves of four-week-old *Arabidopsis* plants and similar results were obtained. Three days after inoculation, only a slight symptom was observed on the leaves of *SRF2* OE line, which exhibited the strongest resistance to pathogen than any other *Arabidopsis* lines. The *srf2* again exhibited increased susceptibility to pathogen (Appendix Figure A-3B). These results indicate that overexpression of *SRF2* facilitates plant resistance to pathogen *Pst* DC3000. On the contrary, repression of *SRF2* compromises pathogen resistance in *Arabidopsis*. These data suggest that *SRF2* may be involved in plant biotic resistance pathway and play a positive role *Arabidopsis* resistance to pathogen infection.

Besides biotic stress, we also compared the growth of different *Arabidopsis* lines under salt stress. Since only *SRF1* and *SRF2* respond to salt treatment intensely, we conducted the salt treatment experiment by using only WT, RNAi line, *SRF1* OE, and *SRF2* OE lines. Two-week-old *Arabidopsis* plants were treated with 200 mM of NaCl for five days, and then recovered with watering for three weeks. As observed in Appendix Figure A-4A, compared to WT and OE lines, RNAi line survived and recovered from the high salt



treatment. In another salt treatment experiment, we compared WT, RNAi line, and two T-DNA insertion lines, *srf1* and *srf2*. Two-week-old *Arabidopsis* plants were treated with 175 mM of NaCl for three days, followed by recovery with watering for 10 days. In this experiment, all *Arabidopsis* lines recovered from salt treatment. However, RNAi line exhibited the best growth, whereas the growth of the WT plants was the worst (Appendix Figure A-4B). These results indicate the *SRF1* and *SRF2* may also be involved in the salt resistance pathway of *Arabidopsis* as negative regulators.

### **Overexpression of *SRF2* enhances pathogen resistance**

Our results so far strongly suggest that *SRF2* may have a crucial function in pathogen defense mechanism. Overexpression of *SRF2* in *Arabidopsis* leads to enhanced pathogen resistance, whereas repression of *SRF2* makes *Arabidopsis* plants more vulnerable to pathogen infection. To further confirm our observation, we conducted more experiments to test the plant response to pathogen infection by including the avirulence pathogen, *Pst* DC3000 *hrcC*<sup>-</sup> in addition to the virulence pathogen, *Pst* DC3000.

We dip-inoculated five-week-old *Arabidopsis* plants with  $5 \times 10^8$  cfu/ml *Pst* DC3000 or *Pst* DC3000 *hrcC*<sup>-</sup> and evaluated the pathogen development in plant leaves. At three days and five days after the *Pst* DC3000 inoculation, a slighter chlorosis developed on the leaves of the *SRF2* OE line than that on WT and *srf2* leaves, (Figure 2.10 a). Similar phenotype was observed on the *Pst* DC3000 *hrcC*<sup>-</sup> inoculated plants (Figure 2.10 b). The results of bacterial titer analysis correlated with the phenotype observed, as less pathogen developed in the leaves of the two *SRF2* OE plants (Figure 2.10 c, d), indicating that

overexpression of SRF2 can repress the growth of pathogen. Furthermore, we observed that the growth of *Pst* DC3000 and *Pst* DC3000 *hrcC*<sup>-</sup> increased in *srf2* leaves, indicating the increased susceptibility of the *srf2* to pathogen (Figure 2.10 c, d). *Pst* DC3000 *hrcC*<sup>-</sup> is deficient in type-III secretion system, which means that only PTI will be triggered in *Pst* DC3000 *hrcC*<sup>-</sup> infected plants. The growth of *Pst* DC3000 *hrcC*<sup>-</sup> was repressed in the *SRF2* OE plants but increased in the *srf2* plants, suggesting the PTI response was enhanced in the *SRF2* OE lines but repressed in the *srf2* plants.

Spray-inoculation of *Arabidopsis* plants with  $2.5 \times 10^8$  cfu/ml *Pst* DC3000 or  $2.5 \times 10^8$  cfu/ml *Pst* DC3000 *hrcC*<sup>-</sup> gave rise to similar results. As shown in Figure 2.11, at three days after inoculation, while much more severe symptoms developed on the leaves of the *srf2* plants than that on WT leaves, less chlorosis and necrosis were formed on the leaves of the *SRF2* OE lines than both WT and *srf2* mutant plants (Figure 2.11 a). Bacterial titer results also suggest that compared to WT controls, pathogen growth was enhanced in the *srf2* mutants, but significantly repressed in the *SRF2* OE lines (Figure 2.11 b).

Together, these results further confirm that *SRF2* plays a positive role in the pathogen resistance pathway, and may participate in the PTI response.

### ***SRF2* regulates PAMPs triggered basal immunities**

Once pathogen contacts the surface of plant, PRR (Pattern Recognition Receptors) localized on the plant plasma membrane will recognize PAMPs of the pathogen and triggered the first layer of the plant immunity PTI to repress the development and

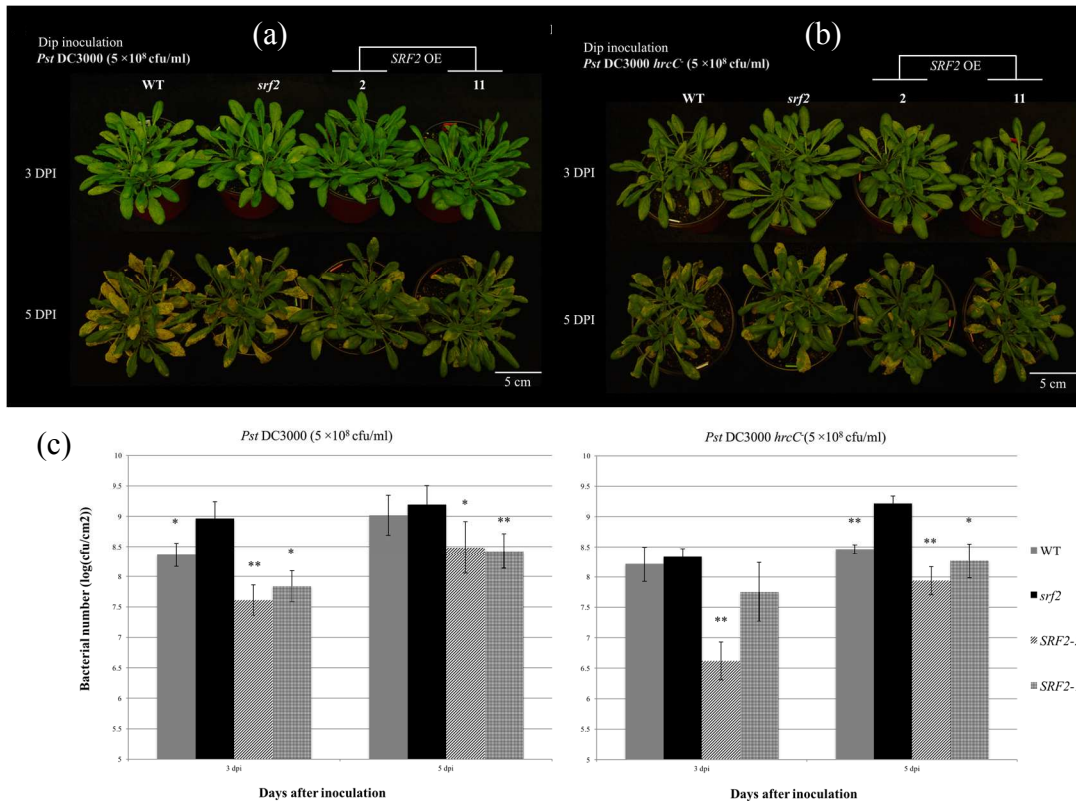


**Figure 2.10. Phenotypic analysis of wild type (WT), the *SRF2* T-DNA insertion mutant and the *SRF2*-overexpressing lines subjected to pathogen infection through dip-inoculation.** Five-week-old plants grown in soil under short day condition (8 h/16 h day/night) were dip-inoculated with (a) pathogen, *Pst* DC3000 or (b) *Pst* DC3000 *hrcC*. Plants were photographed three days and five days after inoculation. DPI: day post inoculation. (c) Bacterial number in dip-inoculated *Arabidopsis* leaves. Leaves exhibiting symptom were collected from *Arabidopsis* plants three days and five days after pathogen inoculation and used for determination of bacterial titer. Data shown are an average of four independent biological replicates. Error bars represent S.D. (n=4). Asterisks indicate the significant differences between *srf1* and other *Arabidopsis* lines. P < 0.05 was marked as \*. P < 0.01 was marked as \*\*.

expansion of the pathogen (Jones and Dangl, 2006). Several basal responses will be activated in the PTI pathway, including callose deposition, stomatal closure, accumulation of the reactive oxygen species, expression of defense-related genes, and MAPK activation (Zipfel, 2008; Pitzschke et al., 2009; Luna et al., 2011; Daudi et al., 2012). Our results

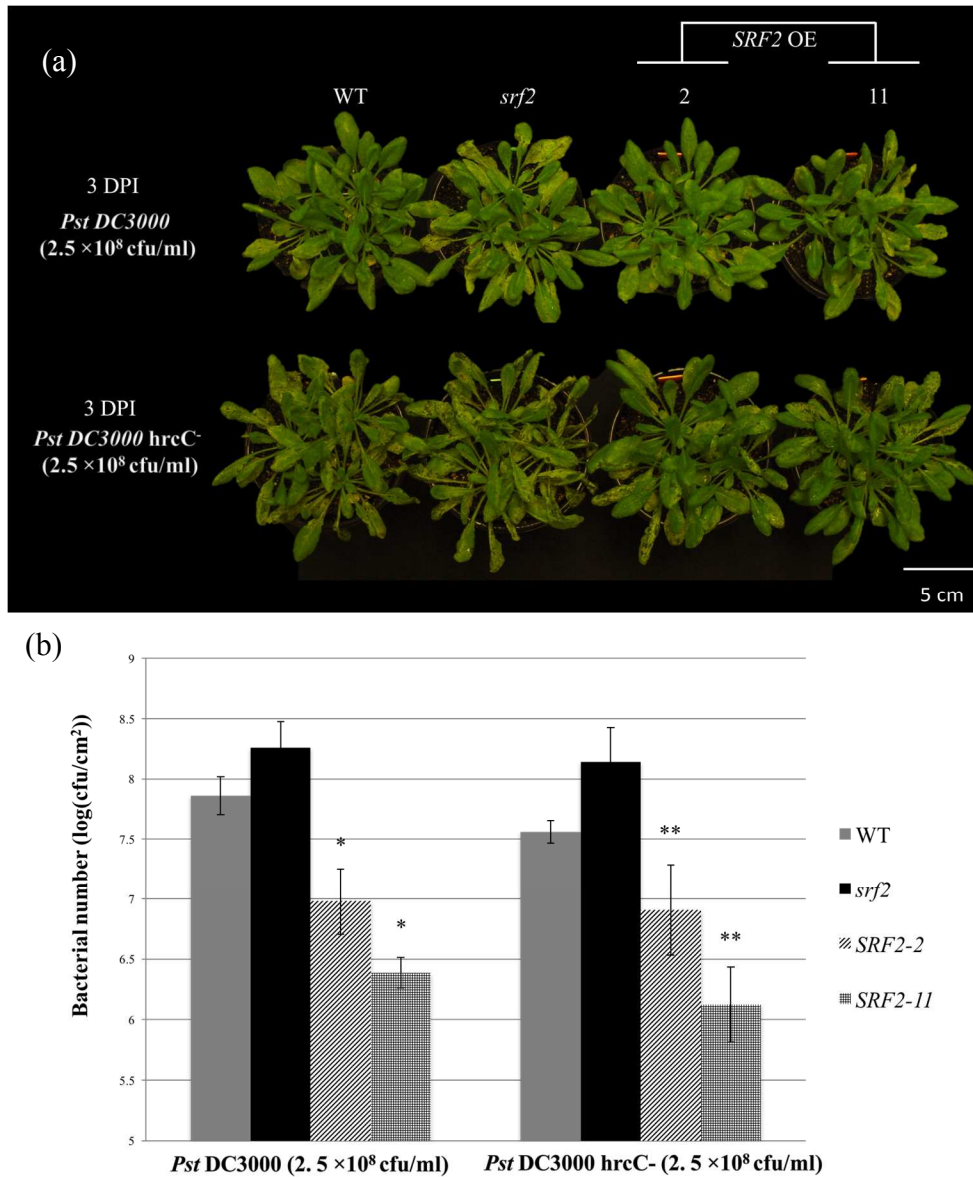


**Figure 2.11. Phenotypic analysis of the wild type (WT), the *SRF2* T-DNA insertion mutant and the *SRF2*-overexpressing lines subjected to pathogen infection through spray-inoculation.** (a) Five-week-old plants grown in soil under short day condition (8 h/16 h day/night) were spray-inoculated with pathogen *Pst DC3000* or *Pst DC3000 hrcC-*. Plants were photographed three days after inoculation. DPI: day post inoculation. (b) Bacterial number in spray-inoculated *Arabidopsis* leaves. Leaves exhibiting symptom were collected from *Arabidopsis* plants three days after pathogen inoculation and used for determination of bacterial titer. Data shown are an average of four independent biological replicates. Error bars represent S.D. (n=4). Asterisks indicate the significant differences between *srf1* and other *Arabidopsis* lines. P < 0.05 was marked as \*. P < 0.01 was marked as \*\*.

analyzing *SRF2*-mediated plant response to pathogen obtained so far led us to hypothesize that *SRF2* is involved in the PTI pathway. Since *SRF2* is a receptor like protein kinase localized on the plasma membrane, it may act as a PRR, which recognizes PAMPs and triggers the downstream basal responses. To verify this hypothesis, we tested whether or not overexpression of *SRF2* enhances plant basal responses.

The first basal response we tested was callose deposition. Upon PTI activation, callose will be synthesized and form matrix in the apoplast, facilitating the deposition of antimicrobial compounds which can repress the growth of pathogen (Luna et al., 2011). As shown in Figure 2.12 a, no callose deposition was observed in any *Arabidopsis* lines six hours after mock treatment (Figure 2.12 a, upper panel). Upon *Pst* DC3000 ( $1 \times 10^8$  cfu/ml) treatment, callose deposition was observed in all the plants. However, the deposition was significantly more in the *SRF2* OE lines, but less in the *srf2* mutants than in WT controls (Figure 2.12 a, middle panel). A similar phenomenon was also observed upon *Pst* DC3000 *hrcC*<sup>-</sup> ( $1 \times 10^8$  cfu/ml) treatment, as callose was deposited more in the *SRF2* OE plants, but less in the *srf2* mutants than WT controls (Figure 2.12 a, lower panel). These results indicate that *SRF2* regulates callose deposition.

Stomatal closure is another important defense mechanism triggered by PTI. Within the first hour of pathogen infection, stomata will be actively closed to avoid the entry of pathogen (Melotto et al., 2008). To overcome the stomata-based defense and successfully invade the plants, virulence pathogen like *Pst* DC3000 will inject a virulence factor named coronatine to interrupt the SA/ABA promoted stomatal closure and reopen the stomata (Melotto et al., 2008; Lee et al., 2013). Since we presume that *SRF2*- mediated PAMP

recognition triggers basal immunities through PTI pathway, we measured the stomatal aperture of *Arabidopsis* under pathogen treatment to test whether or not *SRF2* regulates

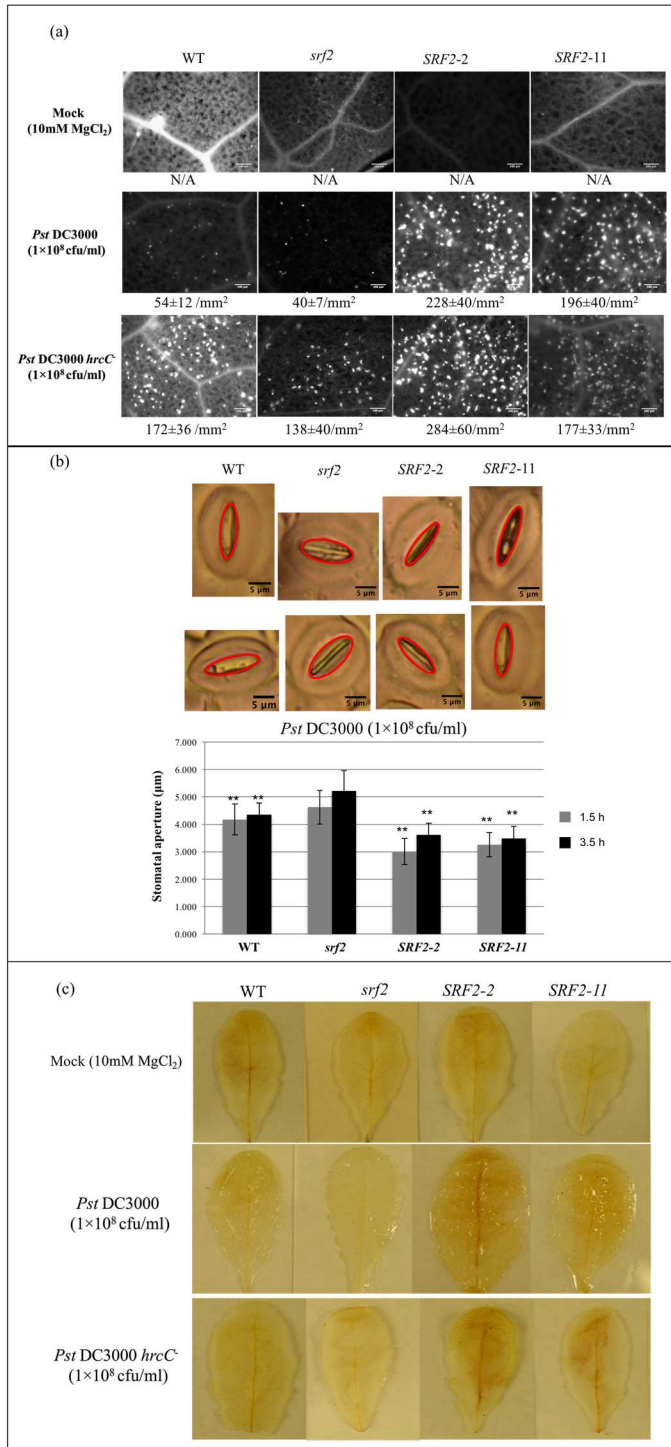


**Figure 2.12. Analyses of basal immunities in wild type (WT), the *SRF2* T-DNA insertion mutant and the *SRF2*-overexpressing line.** (a) Callose deposition in *Arabidopsis* leaves under pathogen treatment. The leaves of five-week-old *Arabidopsis* were infiltrated with MgCl<sub>2</sub>, *Pst* DC3000, or *Pst* DC3000 *hrcC* with the indicated concentrations. Six hours later, leaves were aniline blue stained and observed under a UV length light. Data shown are an average of nine independent biological replicates, and two leaves were analyzed for each biological replicates. Error represents S.D. (n=18). Scale bar: 100 μm. (b) Stomatal apertures of *Arabidopsis* leaves under *Pst* DC3000 treatment. The leaves of five-week-old *Arabidopsis* plants were immersed in *Pst* DC3000 (1×10<sup>8</sup> cfu/ml). At 1.5 and 3.5 h after treatment, stomata in the randomly chosen regions in the leaf epidermal of four fully expanded leaves from four plants (four leaves in total) were photographed under optical microscope. The width of the stomatal aperture was measured using the ‘measure’ function of ImageJ. Data shown are an average of four independent biological replicates each consisting of 15 stomatal apertures. Error represents S.D. (n=60). Asterisks indicate the significant differences between the *srf2* and other *Arabidopsis* lines. P < 0.05 was marked as \*. P < 0.01 was marked as \*\*. Scale bar: 5 μm. (c) ROS accumulation in *Arabidopsis* leaves under pathogen treatment. The leaves of five-week-old *Arabidopsis* plants were infiltrated with MgCl<sub>2</sub>, *Pst* DC3000, or *Pst* DC3000 *hrcC* with the indicated concentrations. One and half an hours later, three leaves from three plants (nine leaves in total) were assayed for DAB staining.

stomata-based defense. Upon *Pst* DC3000 treatment, larger stomatal aperture was observed on leaves of the *srf2* mutant than WT controls, whereas stomata closure was significantly enhanced in *SRF2* OE plants (Figure 2.12 b). A similar result was obtained when *Arabidopsis* plants were treated with *Pst* DC3000 *hrcC*<sup>-</sup> (Appendix Figure A-5). Compared to WT controls, the stomatal closure was reduced in the *srf2* plants, but enhanced in *SRF2* plants. These facts suggest that SRF2 also regulates stomatal aperture to help *Arabidopsis* plants resist against pathogen invasion.

ROS accumulation is an essential basal response to pathogen invasion. This basal response not only represses the expansion of pathogen, but also regulates other PAMPs-triggered basal resistances such as callose deposition and peroxidase-dependent gene expression (Daudi et al., 2012). Under the *Pst* DC3000 treatment, diminished DAB staining was observed on the leaves of *srf2*, indicating reduced ROS accumulation in the T-DNA insertion mutant line caused by reduced H<sub>2</sub>O<sub>2</sub>-dependent polymerization reaction (Thordal-Christensen et al., 1997). On the contrary, the ROS accumulation was strongly enhanced in *SRF2* plants compared with WT controls as strong DAB staining was observed. When plants were inoculated with avirulence pathogen *Pst* DC3000 *hrcC*<sup>-</sup>, the *srf2* mutants again exhibited reduced ROS accumulation, whereas the *SRF2* plants had enhanced ROS accumulation. These results indicate that *SRF2* regulates ROS accumulation (Figure 2.12 c).

Put together, these results confirmed that *SRF2* indeed has an essential function in regulating basal immunities triggered by pathogen PAMPs.

### ***SRF2* regulates expressions of pathogen responding genes**

WRKY transcription factors regulate the expression of a large number of stress responding genes in plants under stresses. To test whether the altered pathogen resistance in *srf2* and *SRF2* OE plants is attributable to the *SRF2*-regulated defense-related genes, we investigated the expression levels of *WRKY53* together with another innate immunity maker gene *FRK1* (Flagellin-induced Receptor-like Kinase 1) upon pathogen infection.

Northern analysis results show that the transcripts of *WRKY53* were undetectable under normal conditions, but significantly accumulated half an hour after pathogen inoculation (Figure 2.13). *WRKY53* in WT, *srf2* and *SRF2* OE plants shared this expression pattern upon treatment of both pathogen strains. In the early time point of infection (0-30 min), the expression of *WRKY53* was only slightly different from each other among various *Arabidopsis* lines. Unexpectedly, the transcript level of *WRKY53* was higher in *srf2* than in WT plant. At one hour after inoculation of *Pst* DC3000 or *Pst* DC3000 *hrcC*<sup>-</sup>, the transcript level of *WRKY53* rapidly declined in WT and *srf2* plants, but maintained at a high level in *SRF2* OE lines (Figure 2.13).

The transcripts of *FRK1* were detected two hours after pathogen inoculation. Compared with WT plants, a higher *FRK1* transcription in the *SRF2* OE plants, but a lower *FRK1* transcription in the *srf2* mutants than in WT controls was observed under the *Pst* DC3000 treatment. On the contrary, under the *Pst* DC3000 *hrcC*<sup>-</sup> treatment, no significant difference in *FRK1* expression was observed between various *Arabidopsis* lines (Figure 2.13).



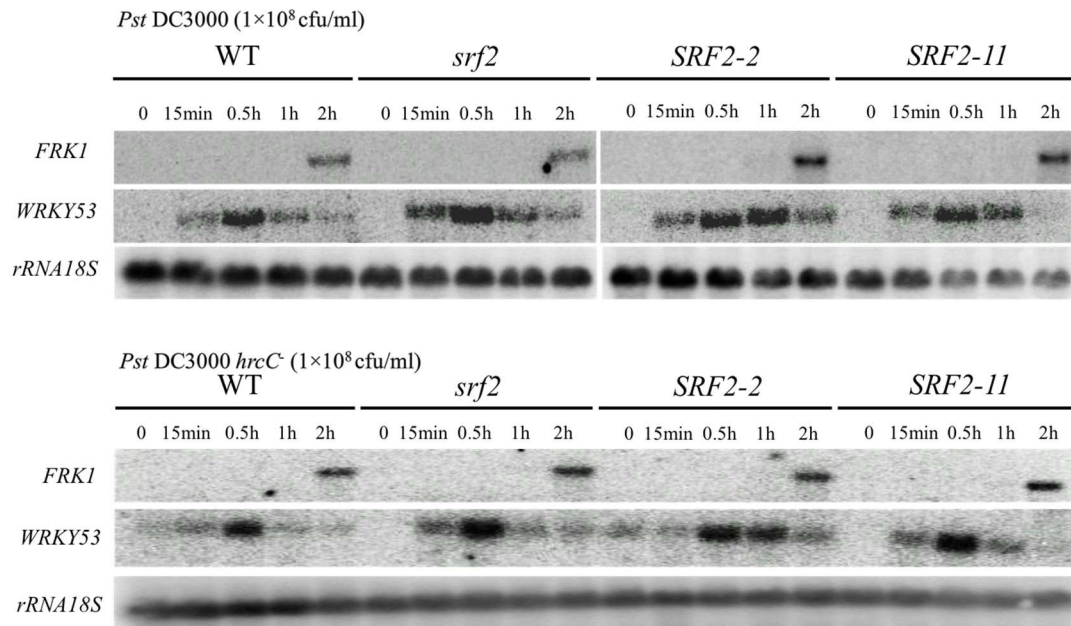


**Figure 2.13. Expression analysis of defense-related genes in the wild type (WT), the *SRF2* T-DNA insertion mutant and the *SRF2*-overexpressing line.** The leaves of five-week-old *Arabidopsis* plants were infiltrated with *Pst* DC3000 or *Pst* DC3000 *hrcC*<sup>-</sup> with the indicated concentration. Samples were harvested at the indicated time points and used for Northern blot analysis to detect the transcript levels of *FRK1* and *WRKY53*. *rRNA 18s* was used as reference gene to show approximately equal loading. Experiment was repeated twice and the result of one representative was shown.

### ***SRF2* regulates the phosphorylation level of mitogen-activated protein kinases**

In the PTI pathway, MAPK (Mitogen-Activated Protein Kinase) kinase modules mediate signaling transduction from perception of PAMPs to expression of defense-related genes (Pitzschke et al., 2009). In order to investigate whether or not *SRF2* regulates basal immunities and gene expression through MAPK module, we investigated the phosphorylation level of MPK3 and MPK6, which positively regulate pathogen resistance.

At 15 minutes after *Pst* DC3000 infiltration, the phosphorylation level of MPK3/6 was slightly higher in the *SRF2* OE lines than in the WT and *srf2* plants (Figure 2.14).

Surprisingly, the MPK3/6 exhibited stronger activity in the *srf2* plants than in WT plants, implying a complex regulation process in which SRF2 activates MAPK cascade. There was no significant difference observed between various *Arabidopsis* lines upon the *Pst* DC3000 *hrcC* treatment.

When the leaf tissue was infiltrated with PAMP elicitor flg22 or elf18, a third band representing MPK4 was observed (Figure 2.14). Unlike MPK3 and MPK6, MPK4 is a negative regulator of the SA-mediated plant immunity response, but may also positively regulate the JA-mediated plant defense (Gao et al., 2008; Berriri et al., 2012; Vidhyasekaran, 2014). Compared with WT and *srf2* plants, all three MPKs exhibited much enhanced phosphorylation level in *SRF2* OE plants upon treatment with flg22 or elf18.

### **SRF2 interacts with BAK1 under pathogen treatment**

Plasma membrane-anchored LRR-RLK BAK1 has multiple functions in *Arabidopsis thaliana*. BAK1 can interact with another LRR-RLK BRI1 (Brassinosteroid-Insensitive1) forming heterodimer involved in the perception of brassinosteroid (Li et al., 2002). Besides regulation of plant growth and development, BAK1 also participates in signal transduction during pathogen invasion as a co-receptor by forming heterodimer with other plasma membrane-localized LRR-RLKs (Postel et al., 2010; Roux et al., 2011; Schwessinger et al., 2011). We are curious about whether or not SRF2 interacts with BAK1 to initiate the subsequent signal transduction after it recognizes the extracellular elicitors during pathogen infection.

BIFC (Bimolecular Fluorescence Complementation) assay was performed to test

the interaction between SRF2 and BAK1 under pathogen treatment. SRF2, BAK1 or CERK1 were fused to the C-terminal (VYCE) or N-terminal (VYNE) of Venus protein, separately (Figure 2.15 a). CERK1-VYCE and CERK1-VYNE proteins were used as positive control to assess the efficiency of this BIFC system. The results show that with or without *Pst* DC3000 treatment, strong YFP fluorescence was always detected on the plasma membrane of the tobacco leaves co-expressing CERK1-VYCE and CERK1-VYNE proteins (Figure 2.15 b). On the other hand, YFP fluorescence was only detected on the plasma membrane of tobacco leaves co-expressing SRF2-VYCE and BAK1-VYNE or BAK1-VYCE and SRF2-VYNE after the infiltration of *Pst* DC3000 (Figure 2.15 c), suggesting that SRF2 and BAK1 interact with each other only under pathogen infection.

## **DISCUSSION**

With more than 600 family members, *Arabidopsis* RLKs compose the largest protein kinase subfamily. RLKs play important roles in various plant mechanisms, including signal transduction, plant development and stress response (Shiu et al., 2004). As classical receptor like kinases, *Arabidopsis* LRR-RLKs share several signature domains, including an N-terminal signal peptide, 1 to 32 LRR domain(s), a membrane-spanning region, and a protein kinase domain (Torii, 2004). Specifically, LRR domain can identify and interact with extracellular signaling ligand, and transduce signals into cells to initial cellular response. This important function of LRR domain confers the LRR-RLKs the ability to perceive the signal of pathogen invasion by detecting pathogen-specific molecular patterns when pathogen cells attach to the surface of plant leaves. Previous

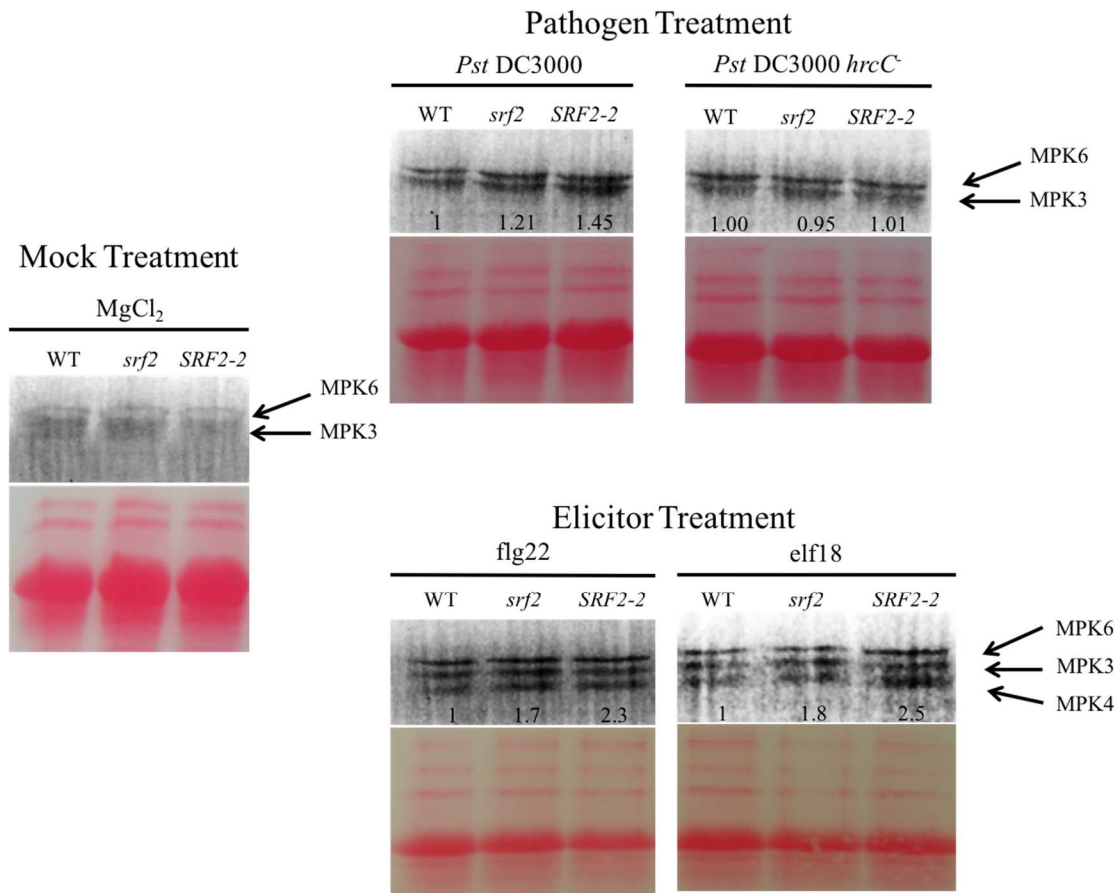


**Figure 2.14. Phosphorylation analysis of MAPK3/6 in wild type (WT), the *SRF2* T-DNA insertion mutant and the *SRF2*-overexpressing line.** The leaves of five-week-old *Arabidopsis* plants were infiltrated with *Pst* DC3000, *Pst* DC3000 *hrcC*<sup>-</sup>, flg22 or elf18 in indicated concentration. At 15 min after infiltration, 100mg leaf sample was harvested and used for protein Western blot analysis to detect the phosphorylation levels of MAPK3, MAPK6 and MAPK4. Total protein on the PVDF membrane was stained with Ponceau S dye to show approximately equal loading. Experiment was repeated twice and the results of one representative were shown. The level of MAPKs is quantified using Ponceau S image as reference and shown below each lane. The WT sample is arbitrarily set as 1.

---

research showed that the expression levels of 49 out of 235 identified LRR-RLKs in *Arabidopsis* are upregulated more than two fold upon one or more pathogen treatments (Kemmerling et al., 2011). FLS2 is a well-studied LRR-RLK family member that is

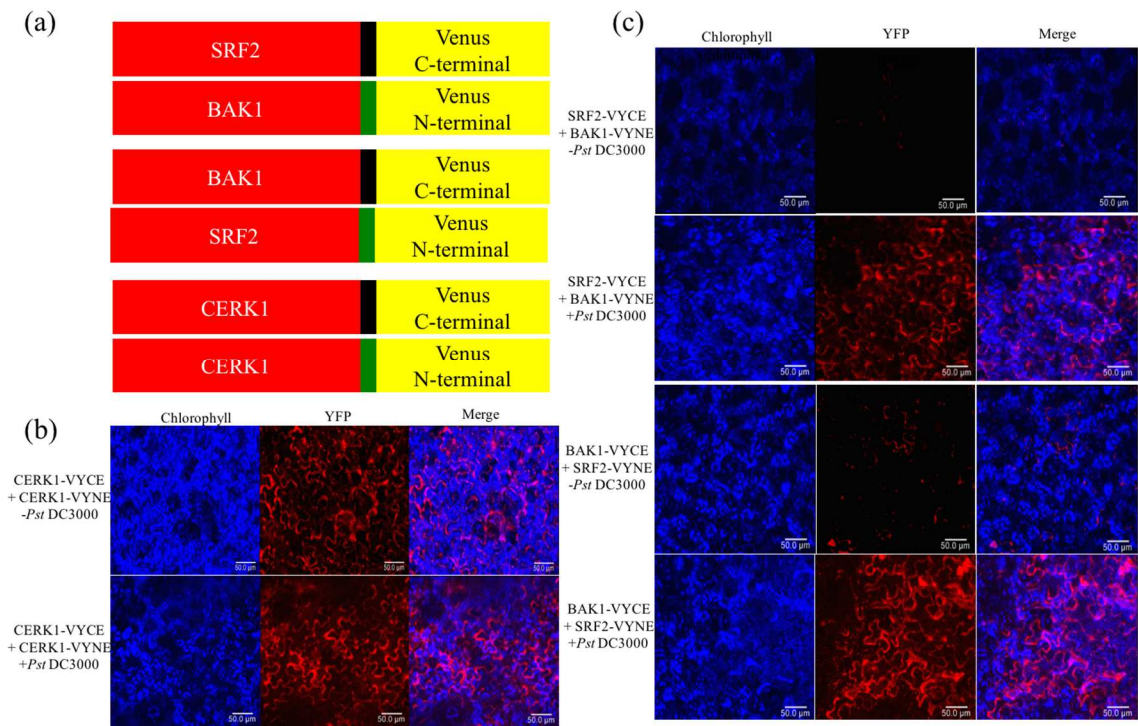


**Figure 2.15. Interaction of BAK1 and SRF2 under pathogen treatment.** (a) The Schematic diagram of the constructs used for BiFC (Bimolecular fluorescence complementation). (b) CERK1-VYCE and CERK1-VYNE were transiently co-expressed in tobacco leaves as positive control. (c) SRF2-VYCE and BAK1-VYNE or BAK1-VYCE and SRF2-VYNE were transiently co-expressed in tobacco leaves. Leaf samples infiltrated with or without DC3000. Thirty minutes after infiltration, leaves were examined under Leica SPE confocal microscope. Fluorescence of Venus was depicted in red. Chlorophyll autofluorescence is depicted in blue. Scale bar: 50 μm.

important for *Arabidopsis* to resist pathogen infection. Upon pathogen invasion, flagellin binds to 14 LRR domains (from LRR3 to LRR16) of FLS2, triggering the formation of FLS-BAK1 complex (Sun et al., 2013). The FLS-BAK1 complex then initiates the downstream basal immunities (Chinchilla et al., 2007). EFR is another important PRR involved in the *Arabidopsis* PTI pathway. After binding pathogen elongation factor EF-Tu, EFR will form heterodimer with BAK1 and trigger PTI response (Zipfel et al., 2006; Roux et al., 2011). Different from FLS2 and EFR that recognize PAMPs, PEPR1 and

PEPR2 bind plant endogenous peptides Pep1 to Pep6 and induce basal immunities against pathogens (Yamaguchi et al., 2006; Yamaguchi et al., 2010; Yamaguchi and Huffaker, 2011). Recently, another LRR-RLK IOS1 (Impaired Oomycete Susceptibility1) was identified to mediate BABA-triggered PTI response (Chen et al., 2014). Only a few LRR-RLKs have been identified to be involved in the PTI response in *Arabidopsis* so far. In our work, SRF2 was demonstrated to play an important role to prime PTI response upon pathogen infection. Our data show that the constitutive expression of SRF2 help *Arabidopsis* against pathogen invasion, but the T-DNA insertion mutant *srf2* is more susceptible to pathogen (Figure 2.10 and 2.11). The enhanced resistance in *SRF2* overexpressing line is due to the enhanced basal immunities, including callose deposition, stomata closure, and ROS accumulation (Figure 2.12 a-c). These enhanced basal immunities block the entry of pathogen through the stomata and repress the development of pathogen in the leaf tissue.

BAK1 is a multiple-function LRR-RLK in *Arabidopsis thaliana*. Besides its critical role in the perception of brassinosteroid, previous studies showed that BAK1 also mediates PAMPs perception in PTI by forming heterodimer with FLS2, EFR, or PEPR1/2 (Li et al., 2002; Chinchilla et al., 2007; Postel et al., 2010; Schulze et al., 2010; Schwessinger et al., 2011; Sun et al., 2013). Furthermore, BAK1-FLS/EFR heterodimer also needs to interact with SERK family member SERK4/BKK1 (BAK-LIKE1) to trigger innate plant immunity (Roux et al., 2011). An *Arabidopsis* plant with mutations in both BAK1 and BKK1 is hypersusceptible to *P. syringae* and *Hyaloperonospora arabidopsidis* (Roux et al., 2011). All the above studies indicate that BAK1 is an indispensable element in the signaling

transduction. All known LRR-RLK PRRs need to form complex with BAK1 to prime PTI response. Based on our BiFC results, we find that SRF2 also needs to interact with BAK1 forming heterodimer (Figure 2.15 c). This interaction between SRF2 and BAK1 depends on pathogen infection, indicating that this interaction follows the BAK1-flagellin-FLS2 model that requires a PAMP to act as glue to make the BAK1-FLS2 stable.

After plasma membrane-anchored PRRs recognize PAMPs, the signal will be interpreted into cell through MAPKs signal modules. MEKK1-MKK4/5-MPK3/6 is implicated to play a positive role in regulating plant defense mechanism (Vidhyasekaran, 2014). MPK3 or MPK6 knockout mutant exhibited compromised ability to resist pathogen infection (Galletti et al., 2011). In this study, we observed that the phosphorylation level of MPK3/6 in *SRF2* OE plants was higher than that in WT and *srf2* plants upon pathogen or elicitor treatment, suggesting that SRF2 utilizes MPK3/MPK6 signaling pathway to regulate plant defense (Figure 2.14). Overexpression of *SRF2* enhances the MPK3/MPK6-mediated signaling transduction, causing more intensive basal immunities in OE plants. We also noticed that MPK3/6 activity was stronger in *srf2* than in WT under *Pst* DC3000 and elicitor treatment (Figure 2.14). This phenomenon implies that *SRF2* may negatively regulate the signaling transduction in the early stage of pathogen infection, making our hypothetical SRF2-MEKK1-MKK4/5-MPK3/6-Resistant genes model more complex. Strongly activated MPK4 was also observed in *flg22* or *elf18* infiltrated *Arabidopsis* plants (Figure 2.14). This result is compatible with previous study that MEKK1-MKK1/2-MPK4 mediates PAMP elicitor-induced PTI response in *Arabidopsis thaliana* (Meszaros et al., 2006).

In this study, we found that among different *Arabidopsis* lines, the SRF2-2 OE line had the highest expression level of *WRKY53* one hour after pathogen treatment (Figure 2.13), and this line exhibited the strongest basal defenses (Figure 2.12 a-c). This fact demonstrates that overexpression of *SRF2* enhances the expression of *WRKY53* at a later time point of pathogen infection, which then directly (induction of cell senescence) or indirectly (through other *WRKY* protein networks) induces strong basal defenses against pathogen. Miao et al. show that *MEKK1* can directly interact with *WRKY53* and induce its expression, implying that *SRF2* may also be involved in the plant defense through *SRF2*-*MEKK1*-*WRKY53*-Resistant genes signaling pathway (Miao et al., 2007).

Similar to MAPK Western analysis, we noticed that there were more *WRKY53* transcripts accumulating in *srf2* plants than in WT on the early stage of pathogen infection (0-30 min) in the Northern analysis (Figure 2.13). How to explain this result is one of our important tasks in the future. We hypothesize that this is because of the competition between *SRF2* and other PRRs (e.g. *FLS2* and *EFR*) in the signaling transduction process. According to the real-time PCR result, the expression level of *SRF2* was upregulated only four times half an hour after *Pst* DC3000 treatment and 60 times half an hour after *Pst* DC3000 hrcC<sup>-</sup> treatment. But at one hour after *Pst* DC3000 or *Pst* DC3000 hrcC<sup>-</sup> treatment, the expression level of *SRF2* was rapidly up-regulated 132 times or 219 times (Figure 2.5 d-e). This fact implies that *SRF2* may play a critical role in plant defense at a later time point of pathogen infection (after one hour), but *SRF2* protein expressed at basal level under normal condition still forms heterodimer with *BAK1* in the early time point of pathogen infection (the first 30 mins). Knocking-down of *SRF2* results in more *BAK1*



protein available on the plasma membrane, facilitating the interaction between other PRRs and BAK1 in the early time point of pathogen infection. Consequently, more MAPK cascades are activated and the expression of WRKY proteins is upregulated more intensively. Further study needs to be conducted to prove this hypothesis. The Northern analysis also suggests that the regulation of *FRK1* was affected by the altered expression of *SRF2* upon *Pst* DC3000 infection (Figure 2.13). *FRK1* expression was largely repressed in the *srf2*, while it was strongly enhanced in *SRF2* OE lines. This result again suggests that *SRF2* plays an important role in PTI.

Taken all the results together, we can draw a hypothetic pathway showing how SRF2 is involved in the signaling pathway. As shown in figure 2.16, when the pathogen cells attach to the surface of *Arabidopsis* leaves, SRF2 recognizes and binds to PAMP elicitor, priming the formation of SRF2-elicitor-BAK1 sandwich structure. Upon possible occurrence of intensive transphosphorylation and autophosphorylation, the activated kinase domain of BAK1 and/or SRF2 activate(s) MEKK1 protein. The following process may proceed in two possible routes. The first route is a short cut, in which the MEKK1 directly interacts with and activates WRKY53, which then induces strong basal immunities by regulating other WRKY protein and/or defense-related genes. In another route, the classic MEKK1-MKK4/5-MPK3/6 cascade is activated, followed by the activation of its downstream WRKY proteins, which, in turn, enhance the expression of pathogen resistance genes and induce the basal immunities. Furthermore, W-boxes are found in the promoter region of many *WRKY* genes, suggesting that *WRKYs* super gene family is a self-regulation gene family (Dong et al., 2003; Miao et al., 2004; Zentgraf et al., 2010). This

fact implies that the both routes may exit and have crosstalk in our signaling transduction model.

In this rough map, many questions remain to be answered. The first question is what the specific PAMP elicitor is recognized by SRF2? Unlike the most PRRs such as FLS2 and EFR that are non-RD (arginine-aspartate) RLKs, SRF2 is a RD RLK. This means that SRF2 should be able to transphosphorylate BAK1 and autophosphorylate itself, so the second question is how the SRF2-BAK1 complex works needs to be addressed? Our present research also suggests that the phosphorylation level of MPK3/6 and expression level of WRKY53 are both enhanced in *SRF2* OE plants. However, according to previous studies, WRKY53 is not the direct substrate of activated MPK3/6 (Pitzschke et al., 2009). So the third question is how the signal is transduced through MAPK cascade to WRKY53 protein? Previous study suggested that WRKY22 is directly regulated by MPK3/6 when *Arabidopsis* is under the treatment of flg22 (Asai et al., 2002). A recent research showed that the WRKY22 T-DNA insertion mutant has low transcripts level of *WRKY53* in submergence-treated *Arabidopsis*, indicating that WRKY53 may be regulated by WRKY22 (Hsu et al., 2013). In addition, WRKY53 was proven to target many other WRKY proteins including WRKY22 and WRKY29 (Miao et al., 2004). These studies suggested that MPK3/6 may regulate WRKY53 protein by activating WRKY22, and then activated WRKY53 and WRKY22 regulate each other to amplify the signal.

### ***Versatile functions of SRF gene family***

In *Arabidopsis*, BAK1 belongs to multiple-function kinase family SERK (Somatic

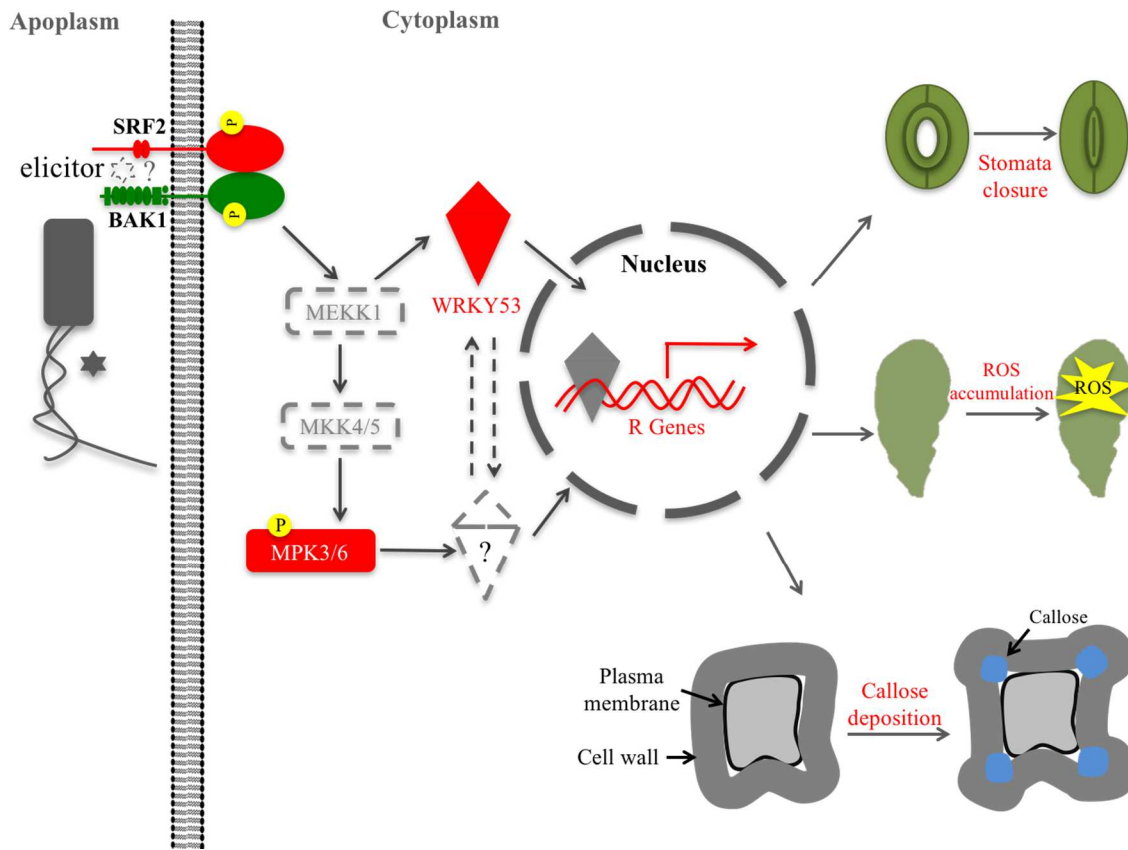


**Figure 2.16. Schema of SRF2-mediated signaling pathway.** Upon pathogen infection, SRF2 binds PAMP elicitor, causing the formation of SRF2-elicitor-BAK1 complex. MEKK1 is phosphorylated by activated kinase domain of BAK1 and/or SRF2, leading to the activation MKK4/5 and finally MPK3/6. Active MPK3/6 then interacts with downstream WRKY protein(s), which positively regulate(s) WRKY53. Phosphorylated MEKK1 may also interact with WRKY53 directly. WRKY53 and other possibly involved WRKY proteins then induce the expression of resistance genes, ultimately leading to the activation of basal immunities including callose deposition, ROS accumulation, and stomata closure. Verified steps and elements in this schema are highlighted in red color.

Embryogenesis Receptor Kinase), which is comprised of five LRR-RLKs, including SERK1, SERK2, SERK3/BAK1, SERK4/BKK1, and SERK5 (Hecht et al., 2001; Albrecht et al., 2008). The five SERK family members are involved in different signaling pathways. SERK1-4 are important positive regulators of brassinosteroid perception signaling

pathway (Albrecht et al., 2008; Gou et al., 2012). Besides the perception of BR, SERK3/BAK1 together with SERK4/BKK1 also mediate the signaling transduction of plant defense triggered by FLS2 or EFR (Roux et al., 2011).

SRF gene family, like SERK kinase family, may play multiple roles in different *Arabidopsis* resistance mechanisms. Though all four SRF proteins are plasma membrane anchored proteins and have similar structures (Figure 2.3 and Figure 2.8), their expression patterns are distinct from each other (Figure 2.6). Additionally, SRF1 - SRF4 are regulated differently under abiotic stresses and biotic stresses (Figure 2.4 and 2.5). In later experiments, we found that SRF1 and SRF2 are negative regulators of salt resistance (Appendix Figure A-4), and SRF2 is also a critical positive regulator in the pathogen defense mechanism. All these results suggest that SRF gene family is a versatile-function kinase family. Locating on the plasma membrane of *Arabidopsis* cells, SRFs have similar functions: interpret extracellular signals to intracellular signals. But these sensors recognize different ligands and elicitors, causing their involvement in different resistance mechanisms responding to different stresses. In the future, we first need to verify the functions of SRF1 and SRF2 in the salt response. Second, we want to understand the roles of SRF3 and SRF4. These two genes are strongly expressed in green tissues (Figure 2.6), especially in leaf tissue, suggestion their important functions in aerial part of *Arabidopsis*. Based on machine learning technique, a large-scale data analysis showed that *SRF4* was intensively regulated under salt, drought and wound stresses (Ma et al., 2014). Both our work and pervious study showed that *SRF4* was strongly upregulated when *Arabidopsis*

was treated with *Pst* DC3000 (Figure 2.5) (Hok et al., 2011). These data give clues of the SRF4 function.

## **MATERIALS AND METHODS**

### **growth conditions of plant and bacterium**

For abiotic stress experiments, *Arabidopsis thaliana* were grown in soil under a 16 h-day/8 h-night photoperiod at 22 °C-day /20 °C-night in growth chamber. For quantitatively analysis of gene expression under abiotic stresses, *Arabidopsis thaliana* plants were grown in hydroponic system under a 16 h-day/8 h-night photoperiod at 22 °C-day /20 °C-night in growth chamber (Huttner and Bar-Zvi, 2003). For biotic stress experiments and quantitatively analysis of gene expression under biotic stresses, *Arabidopsis thaliana* plants were grown in soil under an 8 h-day/16 h-night photoperiod at 22 °C-day /20 °C-night in growth chamber.

For biotic experiment, *Pst* DC3000 and *Pst* DC3000 *hrcC*<sup>-</sup> were grown in KB (King's medium B) liquid medium with rifampin for 24 h at 28°C (King et al., 1954). Then pathogen culture was centrifuged, and pathogen cells were resuspended in 10mM MgCl<sub>2</sub> to desired densities.

### **DNA isolation, RNA isolation, and cDNA synthesis**

Plant genomic DNA was isolated following previously described method (Zhou et al., 2013).

Plant Total RNA was isolated with Trizol reagent (Ambion, USA) from 100 mg plant samples according to the manufacturer's instructions.

For synthesis of the first strand cDNA, RNA was treated with RNase-free DNase I (Invitrogen, USA) to remove genomic DNA, and two µg total DNA-free RNA was used to synthesize first strand cDNA with SuperScript III Reverse Transcriptase (Invitrogen, USA) according to the manufacturer's instructions.

### **Rapid Amplification of cDNA Ends**

To obtain 5'end and 3'end cDNA fragments of *SRF1* and *SRF2*, total RNA was extracted from root tissue (for cloning of *SRF1*) and leaf tissue (for cloning of *SRF2*) of three-week-old WT *Arabidopsis* and treated with RNase-free DNase I (Invitrogen, USA) to remove genomic DNA. One µg total RNA was then used to amplify 5'end and 3'end cDNA fragments of *SRF1* and *SRF2* with SMARTer RACE 5'/3' commercial kit (Clontech, USA) following the manufacturer's instruction. Then, the 5'end and 3'end cDNA fragments were sequenced, and the sequence information was used to design primers for cloning of full-length cDNA.

Primers used for the amplification of cDNA ends were all showing in Appendix Table A-1

### **Quantitatively analysis of gene expression**

For Northern analysis, 15 µg total RNA denatured at 95 °C was separated in 1% agarose formaldehyde gel and transferred to Hybond-N+ nylon membrane (Amersham,

UK) using capillary method. To prepare the radiolabeled probes, 300 bp-400 bp DNA fragments of target genes were synthesized by using PCR method and labeled with  $\alpha$ -[ $^{32}\text{P}$ ]-CTP by using Ridiprimer DNA labeling system (Amersham, UK), followed by purification of labeled probes with G-50 micro column. RNA membrane was then hybridized with radiolabeled probes, and autoradiography signals were detected on a phosphorimaging screen.

For real-time PCR, first-strand cDNA samples were diluted with water to 0.025 to 0.005 times based on the concentration of the first-strand cDNA samples. Real-time PCR was performed with SYBR Green Supermix (Bio-Rad, USA) according to the manufacturer's instructions, and the iQ5 real-time detection system (Bio-Rad) was used to detect and analyze the real-time PCR result. Real-time PCR results were determined by using  $\Delta\Delta\text{Ct}$  method (Yuan et al., 2016).

Primers used for PCR and Northern analysis were all showing in Appendix Table A-1

### **Protein extraction and Western analysis**

To analyze the phosphorylation level of MPK3/6 in *Arabidopsis thaliana* plants under pathogen or elicitor treatment, plant samples were grounded to fine powder in liquid nitrogen and resuspended in protein extraction buffer [150 mM NaCl, 1% (V/V) NP-40, 0.1% SDS, 50 mM pH 8.0 Tris-HCl, 1 mM PMFS, 1% (V/V)  $\beta$ -mercaptoethanol, protease and phosphatase inhibitor mini tablet (Thermo Scientific, USA)], followed by centrifuge at 16,000 g for 2 min at 8 °C. Supernatant was transfer to a new 1.5 ml Eppendorf tube,

and protein concentration of the extract was determined following the Bradford's method (Bradford, 1976). Then, 30 µg – 50 µg of extract was mixed with 2 × loading buffer [4% (W/V) SDS, 20% (V/V) glycerol, 10% (V/V) β-mercaptoethanol, 0.004% bromophenol blue, 125 mM pH 6.8 Tris-HCl] and heated at 70 °C for 10 mins. Denatured mixture was separated in 12.5% SDS-PAGE gel till the bromophenol blue reached the bottom of the gel and transferred to PVDF membrane (Merck Millipore, USA). Western analysis was performed using Phospho-p44/42 MAPK (Erk1/2) (Thr202/Tyr204) Rabbit mAb (Cell Signaling Technology, USA) as primary antibody at a dilution of 1:600 in 5% (W/V) BSA TBST (Tris-Buffered Saline-Tween) and Dylight 633 conjugated goat anti-rabbit IgG (H+L) (Thermo Scientific, USA) as secondary antibody at a dilution of 1:5000 in TBST. Signal was detected using Typhoon FLA 7000 laser scanner (GE Healthcare Life Sciences, USA) at 650 nm.

### **Plasmid construction, bacterial strains and plant transformation**

For histochemical GUS staining experiment, the predicted 2078 bp *SRF1* promoter region, the predicted 828 bp *SRF2* promoter region, the predicted 1524 bp *SRF3* promoter region, and the predicted 1141 bp *SRF4* promoter region were amplified from *Arabidopsis thaliana* genomic DNA with iProof high-fidelity DNA polymerase and subcloned into binary vector pSBbar#5-GUS-nos in the upstream of *GUS* gene, resulting p35s/*bar*/nos-*SRF1*<sub>pro</sub>/*GUS*/nos, p35s/*bar*/nos-*SRF2*<sub>pro</sub>/*GUS*/nos, p35s/*bar*/nos-*SRF3*<sub>pro</sub>/*GUS*/nos, and p35s/*bar*/nos-*SRF4*<sub>pro</sub>/*GUS*/nos.



To investigate the sublocalization of SRFs in plant cell, the cDNA encoding the first 207 amino acid residues of the SRF1 N-terminal, the full length *SRF2* cDNA without stop codon, the full length *SRF3* cDNA without stop codon, and the full length *SRF4* cDNA without stop codon were cloned from first strand cDNA pool with iProof high-fidelity DNA polymerase and subcloned into the binary vector pCambiahptII-sGFP(S65T)/nos before the sGFP(S65T) separately, resulting p35s/C4ppdk1/*SRF1*<sup>N-207aa</sup>-sGFP(S65T)/nos-p35s/*hptII*/nos, p35s/C4ppdk1/*SRF2*-sGFP(S65T)/nos-p35s/*hptII*/nos, p35s/C4ppdk1/*SRF3*-sGFP(S65T)/nos-p35s/*hptII*/nos, and p35s/C4ppdk1/*SRF4*-sGFP(S65T)/nos-p35s/*hptII*/nos. The expression of fusion proteins was under the control of CaMV 35s and enhanced by the enhancer C4ppdk1 cloned from *Zea mays*.

The two plasmids p35s/C4ppdk1/*SRF3*-sGFP(S65T)/nos-p35s/*hptII*/nos and p35s/C4ppdk1/*SRF4*-sGFP(S65T)/nos-p35s/*hptII*/nos were also used to overexpress *SRF3* and *SRF4* in *Arabidopsis thaliana*. For the overexpression of *SRF1* and *SRF2*, the full length cDNA of *SRF1* and *SRF2* were cloned from first strand cDNA pool with iProof high-fidelity DNA polymerase and subcloned into the binary vector pCambiahptII-nos under the control of CaMV 35s promoter separately, resulting p35s/*SRF1*/nos-p35s/*hptII*/nos and p35s/*SRF2*/nos-p35s/*hptII*/nos.

For the construction of plasmid used for RNA interference, a 320 bp DNA fragment highly conserved across the whole SRF gene family was cloned from first strand cDNA pool with iProof high-fidelity DNA polymerase. Then this DNA fragment was subcloned into the binary vector forming rice Ubi promoter/SRF homology (anti)/3'GUS/ SRF homology -p35s/*hptII*/nos. Primers used for plasmid construction were all listed in

Appendix Table A-1. The *Escherichia coli* strain used in this experiment is DH5 $\alpha$ . The chimeric expression cassettes were then mobilized into *Agrobacterium tumefaciens* strain LBA4404 or 3101 by electroporation for plant transformation. *Arabidopsis thaliana* transformation was conducted according to the previous described method (Clough and Bent, 1998).

### **Histochemical GUS staining**

GUS activity was assayed by histochemical staining with 1 mM X-Gluc (Biosynth AG, Switzerland). Plant sample immersed in 100  $\mu$ l to 10 mL reaction buffer containing X-Gluc were vacuum infiltrated for 10mins twice, followed by incubation at 37  $^{\circ}$ C overnight. Prior to photography, plant samples were destained in 70% ethanol.

### **Measurement of callose deposition**

Callose was counted following previously described method (Singh et al., 2012). Briefly, *Arabidopsis* leaf samples were collected and destained in 100% ethanol for at least 24 hours. Then, transparent leaves were stained in 0.07 M phosphate buffer (pH 9.0) with 0.01% aniline blue for at least one hour and observed under Zeiss Axiovert 200M microscope with UV filter. Callose was quantified by using the “analyze particles” function of ImageJ software.

### **Detective of reactive oxidative species accumulation**

Leaf samples were collected and vacuum-infiltrated with 1 mg/ml DAB solution (pH 3.8), followed by incubation in dark for 14 hours at room temperature. Then, samples were destained in 90% ethanol at 70 °C until chlorophyll was removed completely and stored in 70% ethanol.

### **Measurement of stomata aperture**

Stomata aperture was measured following previously described method (Tsai et al., 2011) with modification. Briefly, *Arabidopsis* plants were exposed to light for 3 hours in order to open stomata. Fully expanded leaves were collected and immersed in pathogen for 1.5 or 3 hours. The lower epidermis of leaves was imprinted with clear nail varnish and observed under optical microscope. Stomata from random regions were photographed. The width of the stomatal aperture was measured using the measure function of ImageJ.

### **Bacterial titer**

Leaves used for determination of bacterial titer were harvested and washed in H<sub>2</sub>O for 30 s. Two leaf disks with a diameter of 0.5 cm excised from one leaf sample were homogenized with 1 ml 10 mM MgCl<sub>2</sub> and diluted with H<sub>2</sub>O to various dilutions. Then, 10 µl samples from dilutions were plated on KB plates and incubated at 28 °C. Colonies were counted 3 days later. The data are presented as common logarithm of the colony number per cm<sup>2</sup> leaf disk.

### **Subcellular localization and bimolecular fluorescence complementation**

Subcellular localization and bimolecular fluorescence complementation were performed according to previous methods (Sparkes et al., 2006) (Gehl et al., 2009). Generally, *Agrobacterium* strain harboring the desired binary vector was cultivated overnight at 28 °C in liquid L.B. medium. The bacterial culture was centrifuged and then the bacterial cells were resuspended and washed with 1ml infiltration buffer [100 mM MgCl<sub>2</sub>, 100 μM Acetosyringone] for 3 times. Then, the resuspended bacterial cells were incubated in 1ml infiltration buffer at room temperature for 2 hours, and then diluted to OD<sub>600</sub> of 0.4 with H<sub>2</sub>O. For co-expression of proteins, different *Agrobacterium* strains were diluted to OD<sub>600</sub> of 0.4 and mixed together. The leaves of four-week-old *Nicotiana benthamiana* were syringe-infiltrated with diluted bacterial culture, and the infiltrated plants were grown under a 16 h-day/8 h-night photoperiod at 23 °C for 3-5 days. The infiltrated leaves were then examined and photographed using Leica TCS SPE confocal microscope.

Primers used for the BiFC were all showing in Appendix Table A-1.

### **Accession numbers**

Sequence data from this article can be found in the *Arabidopsis* Genome Initiative database and European Molecular Biology Laboratory under the following accession numbers:

*SRF1* (AT1G51840 and AT1G51830), *SRF2* (AT1G51850), *SRF3* (AT1G51805), *SRF4* (AT1G51820), *Actin2* (AT3G18780), *FRK1* (AT2G19190), *WRKY53* (AT4G23810), *rRNA 18s* (X16077), *MPK3* (AT3G4564), *MPK6* (AT2G4379).

## REFERENCES

- Albrecht, C., Russinova, E., Kemmerling, B., Kwaaitaal, M., and de Vries, S.C.** (2008). Arabidopsis SOMATIC EMBRYOGENESIS RECEPTOR KINASE proteins serve brassinosteroid-dependent and -independent signaling pathways. *Plant Physiology* **148**, 611-619.
- Alonso, J.M., Stepanova, A.N., Leisse, T.J., Kim, C.J., Chen, H., Shinn, P., Stevenson, D.K., Zimmerman, J., Barajas, P., Cheuk, R., Gadrinab, C., Heller, C., Jeske, A., Koesema, E., Meyers, C.C., Parker, H., Prednis, L., Ansari, Y., Choy, N., Deen, H., Geralt, M., Hazari, N., Hom, E., Karnes, M., Mulholland, C., Ndubaku, R., Schmidt, I., Guzman, P., Aguilar-Henonin, L., Schmid, M., Weigel, D., Carter, D.E., Marchand, T., Risseuw, E., Brogden, D., Zeko, A., Crosby, W.L., Berry, C.C., and Ecker, J.R.** (2003). Genome-wide insertional mutagenesis of Arabidopsis thaliana. *Science* **301**, 653-657.
- Antolin-Llovera, M., Ried, M.K., Binder, A., and Parniske, M.** (2012). Receptor Kinase Signaling Pathways in Plant-Microbe Interactions. *Annual Review of Phytopathology* **50**, 451-473.
- Asai, T., Tena, G., Plotnikova, J., Willmann, M.R., Chiu, W.L., Gomez-Gomez, L., Boller, T., Ausubel, F.M., and Sheen, J.** (2002). MAP kinase signalling cascade in Arabidopsis innate immunity. *Nature* **415**, 977-983.
- Berriri, S., Garcia, A.V., Frei dit Frey, N., Rozhon, W., Pateyron, S., Leonhardt, N., Montillet, J.L., Leung, J., Hirt, H., and Colcombet, J.** (2012). Constitutively active mitogen-activated protein kinase versions reveal functions of Arabidopsis MPK4 in pathogen defense signaling. *Plant Cell* **24**, 4281-4293.
- Bradford, M.M.** (1976). A rapid and sensitive method for the quantitation of microgram quantities of protein utilizing the principle of protein-dye binding. *Anal Biochem* **72**, 248-254.
- Chang, C., Schaller, G.E., Patterson, S.E., Kwok, S.F., Meyerowitz, E.M., and Bleecker, A.B.** (1992). The TMK1 gene from Arabidopsis codes for a protein with structural and biochemical characteristics of a receptor protein kinase. *Plant Cell* **4**, 1263-1271.
- Chaves, M.M., Maroco, J.P., and Pereira, J.S.** (2003). Understanding plant responses to drought - from genes to the whole plant. *Funct Plant Biol* **30**, 239-264.
- Chen, C.W., Panzeri, D., Yeh, Y.H., Kadota, Y., Huang, P.Y., Tao, C.N., Roux, M., Chien, S.C., Chin, T.C., Chu, P.W., Zipfel, C., and Zimmerli, L.** (2014). The Arabidopsis Malectin-Like Leucine-Rich Repeat Receptor-Like Kinase IOS1

- Associates with the Pattern Recognition Receptors FLS2 and EFR and Is Critical for Priming of Pattern-Triggered Immunity. *Plant Cell* **26**, 3201-3219.
- Chinchilla, D., Zipfel, C., Robatzek, S., Kemmerling, B., Nurnberger, T., Jones, J.D., Felix, G., and Boller, T.** (2007). A flagellin-induced complex of the receptor FLS2 and BAK1 initiates plant defense. *Nature* **448**, 497-500.
- Chiu, W.-I., Niwa, Y., Zeng, W., Hirano, T., Kobayashi, H., and Sheen, J.** (1996). Engineered GFP as a vital reporter in plants. *Current Biology* **6**, 325-330.
- Clark, S.E., Williams, R.W., and Meyerowitz, E.M.** (1997). The CLAVATA1 gene encodes a putative receptor kinase that controls shoot and floral meristem size in *Arabidopsis*. *Cell* **89**, 575-585.
- Clough, S.J., and Bent, A.F.** (1998). Floral dip: a simplified method for *Agrobacterium*-mediated transformation of *Arabidopsis thaliana*. *Plant J* **16**, 735-743.
- Craigon, D.J., James, N., Okyere, J., Higgins, J., Jotham, J., and May, S.** (2004). NASCArrays: a repository for microarray data generated by NASC's transcriptomics service. *Nucleic Acids Res* **32**, D575-577.
- Czarnecka, E., Verner, F.L., and Gurley, W.B.** (2012). A strategy for building an amplified transcriptional switch to detect bacterial contamination of plants. *Plant Molecular Biology* **78**, 59-75.
- Daudi, A., Cheng, Z.Y., O'Brien, J.A., Mammarella, N., Khan, S., Ausubel, F.M., and Bolwell, G.P.** (2012). The Apoplastic Oxidative Burst Peroxidase in *Arabidopsis* Is a Major Component of Pattern-Triggered Immunity. *Plant Cell* **24**, 275-287.
- De Lorenzo, L., Merchan, F., Laporte, P., Thompson, R., Clarke, J., Sousa, C., and Crespi, M.** (2009). A novel plant leucine-rich repeat receptor kinase regulates the response of *Medicago truncatula* roots to salt stress. *Plant Cell* **21**, 668-680.
- Deeken, R., and Kaldenhoff, R.** (1997). Light-repressible receptor protein kinase: a novel photo-regulated gene from *Arabidopsis thaliana*. *Planta* **202**, 479-486.
- Depege, N., Bellafiore, S., and Rochaix, J.-D.** (2003). Role of chloroplast protein kinase Stt7 in LHCII phosphorylation and state transition in *Chlamydomonas*. *Science Signalling* **299**, 1572.
- Dong, J., Chen, C., and Chen, Z.** (2003). Expression profiles of the *Arabidopsis* WRKY gene superfamily during plant defense response. *Plant Molecular Biology* **51**, 21-37.

- Enkhbayar, P., Kamiya, M., Osaki, M., Matsumoto, T., and Matsushima, N.** (2004). Structural principles of leucine-rich repeat (LRR) proteins. *Proteins* **54**, 394-403.
- Fletcher, J.C., Brand, U., Running, M.P., Simon, R., and Meyerowitz, E.M.** (1999). Signaling of cell fate decisions by CLAVATA3 in Arabidopsis shoot meristems. *Science* **283**, 1911-1914.
- Galletti, R., Ferrari, S., and De Lorenzo, G.** (2011). Arabidopsis MPK3 and MPK6 play different roles in basal and oligogalacturonide- or flagellin-induced resistance against *Botrytis cinerea*. *Plant Physiology* **157**, 804-814.
- Gao, M., Liu, J., Bi, D., Zhang, Z., Cheng, F., Chen, S., and Zhang, Y.** (2008). MEKK1, MKK1/MKK2 and MPK4 function together in a mitogen-activated protein kinase cascade to regulate innate immunity in plants. *Cell Res* **18**, 1190-1198.
- Gehl, C., Waadt, R., Kudla, J., Mendel, R.R., and Hansch, R.** (2009). New GATEWAY vectors for High Throughput Analyses of Protein-Protein Interactions by Bimolecular Fluorescence Complementation. *Mol Plant* **2**, 1051-1058.
- Glazebrook, J.** (2005). Contrasting mechanisms of defense against biotrophic and necrotrophic pathogens. *Annual Review of Phytopathology* **43**, 205-227.
- Gou, X., He, K., Yang, H., Yuan, T., Lin, H., Clouse, S.D., and Li, J.** (2010). Genome-wide cloning and sequence analysis of leucine-rich repeat receptor-like protein kinase genes in *Arabidopsis thaliana*. *BMC Genomics* **11**, 19.
- Gou, X., Yin, H., He, K., Du, J., Yi, J., Xu, S., Lin, H., Clouse, S.D., and Li, J.** (2012). Genetic evidence for an indispensable role of somatic embryogenesis receptor kinases in brassinosteroid signaling. *PLoS Genet* **8**, e1002452.
- Hecht, V., Vielle-Calzada, J.P., Hartog, M.V., Schmidt, E.D.L., Boutilier, K., Grossniklaus, U., and de Vries, S.C.** (2001). The Arabidopsis SOMATIC EMBRYOGENESIS RECEPTOR KINASE 1 gene is expressed in developing ovules and embryos and enhances embryogenic competence in culture. *Plant Physiology* **127**, 803-816.
- Hok, S., Danchin, E.G., Allasia, V., Panabieres, F., Attard, A., and Keller, H.** (2011). An Arabidopsis (malectin-like) leucine-rich repeat receptor-like kinase contributes to downy mildew disease. *Plant Cell Environ* **34**, 1944-1957.
- Hong, S.W., Jon, J.H., Kwak, J.M., and Nam, H.G.** (1997). Identification of a receptor-like protein kinase gene rapidly induced by abscisic acid, dehydration, high salt, and cold treatments in *Arabidopsis thaliana*. *Plant Physiology* **113**, 1203-1212.

- Hsu, F.C., Chou, M.Y., Chou, S.J., Li, Y.R., Peng, H.P., and Shih, M.C.** (2013). Submergence confers immunity mediated by the WRKY22 transcription factor in *Arabidopsis*. *Plant Cell* **25**, 2699-2713.
- Huttner, D., and Bar-Zvi, D.** (2003). An improved, simple, hydroponic method for growing *Arabidopsis thaliana*. *Plant Molecular Biology Reporter* **21**, 59-63.
- Jefferson, R.A., Kavanagh, T.A., and Bevan, M.W.** (1987). GUS fusions: beta-glucuronidase as a sensitive and versatile gene fusion marker in higher plants. *Embo J* **6**, 3901-3907.
- Jones, D.A., and Jones, J.** (1997). The role of leucine-rich repeat proteins in plant defenses. *Advances in Botanical Research* **24**, 89-167.
- Jones, J.D., and Dangl, J.L.** (2006). The plant immune system. *Nature* **444**, 323-329.
- Kemmerling, B., Halter, T., Mazzotta, S., Mosher, S., and Nurnberger, T.** (2011). A genome-wide survey for *Arabidopsis* leucine-rich repeat receptor kinases implicated in plant immunity. *Front Plant Sci* **2**, 88.
- King, E.O., Ward, M.K., and Raney, D.E.** (1954). Two simple media for the demonstration of pyocyanin and fluorescein. *J Lab Clin Med* **44**, 301-307.
- Laude, A.J., and Prior, I.A.** (2004). Plasma membrane microdomains: Organization, function and trafficking (Review). *Molecular Membrane Biology* **21**, 193-205.
- Lee, S., Ishiga, Y., Clermont, K., and Mysore, K.S.** (2013). Coronatine inhibits stomatal closure and delays hypersensitive response cell death induced by nonhost bacterial pathogens. *PeerJ* **1**, e34.
- Li, C., and Wong, W.** (2007). dChip Software: Analysis and visualization of gene expression and SNP microarrays. URL <http://biosun1.harvard.edu/complab/dchip>.
- Li, J., and Chory, J.** (1997). A putative leucine-rich repeat receptor kinase involved in brassinosteroid signal transduction. *Cell* **90**, 929-938.
- Li, J., Wen, J., Lease, K.A., Doke, J.T., Tax, F.E., and Walker, J.C.** (2002). BAK1, an *Arabidopsis* LRR receptor-like protein kinase, interacts with BRI1 and modulates brassinosteroid signaling. *Cell* **110**, 213-222.
- Luna, E., Pastor, V., Robert, J., Flors, V., Mauch-Mani, B., and Ton, J.** (2011). Callose deposition: a multifaceted plant defense response. *Molecular Plant-Microbe Interactions : MPMI* **24**, 183-193.



- Ma, C., Xin, M., Feldmann, K.A., and Wang, X.** (2014). Machine Learning-Based Differential Network Analysis: A Study of Stress-Responsive Transcriptomes in Arabidopsis. *Plant Cell* **26**, 520-537.
- Melotto, M., Underwood, W., and He, S.Y.** (2008). Role of stomata in plant innate immunity and foliar bacterial diseases. *Annual Review of Phytopathology* **46**, 101-122.
- Meszaros, T., Helfer, A., Hatzimasoura, E., Magyar, Z., Serazetdinova, L., Rios, G., Bardoczy, V., Teige, M., Koncz, C., Peck, S., and Bogre, L.** (2006). The Arabidopsis MAP kinase kinase MKK1 participates in defense responses to the bacterial elicitor flagellin. *Plant J* **48**, 485-498.
- Miao, Y., Laun, T.M., Smykowski, A., and Zentgraf, U.** (2007). Arabidopsis MEKK1 can take a short cut: it can directly interact with senescence-related WRKY53 transcription factor on the protein level and can bind to its promoter. *Plant Molecular Biology* **65**, 63-76
- Miao, Y., Laun, T., Zimmermann, P., and Zentgraf, U.** (2004). Targets of the WRKY53 transcription factor and its role during leaf senescence in Arabidopsis. *Plant Molecular Biology* **55**, 853-867.
- Nigg, E., Schafer, G., Hilz, H., and Eppenberger, H.** (1985). Cyclic-AMP-dependent protein kinase type II is associated with the Golgi complex and with centrosomes. *Cell* **41**, 1039.
- Osakabe, Y., Mizuno, S., Tanaka, H., Maruyama, K., Osakabe, K., Todaka, D., Fujita, Y., Kobayashi, M., Shinozaki, K., and Yamaguchi-Shinozaki, K.** (2010). Overproduction of the Membrane-bound Receptor-like Protein Kinase 1, RPK1, Enhances Abiotic Stress Tolerance in Arabidopsis. *J Biol Chem* **285**, 9190-9201.
- Pitzschke, A., Schikora, A., and Hirt, H.** (2009). MAPK cascade signalling networks in plant defense. *Current Opinion in Plant Biology* **12**, 421-426.
- Postel, S., Kufner, I., Beuter, C., Mazzotta, S., Schwedt, A., Borlotti, A., Halter, T., Kemmerling, B., and Nurnberger, T.** (2010). The multifunctional leucine-rich repeat receptor kinase BAK1 is implicated in Arabidopsis development and immunity. *Eur J Cell Biol* **89**, 169-174.
- Roux, M., Schwessinger, B., Albrecht, C., Chinchilla, D., Jones, A., Holton, N., Malinovsky, F.G., Tor, M., de Vries, S., and Zipfel, C.** (2011). The Arabidopsis leucine-rich repeat receptor-like kinases BAK1/SERK3 and BKK1/SERK4 are

- required for innate immunity to hemibiotrophic and biotrophic pathogens. *Plant Cell* **23**, 2440-2455.
- Schulze, B., Mentzel, T., Jehle, A.K., Mueller, K., Beeler, S., Boller, T., Felix, G., and Chinchilla, D.** (2010). Rapid Heteromerization and Phosphorylation of Ligand-activated Plant Transmembrane Receptors and Their Associated Kinase BAK1. *J Biol Chem* **285**, 9444-9451.
- Schwessinger, B., Roux, M., Kadota, Y., Ntoukakis, V., Sklenar, J., Jones, A., and Zipfel, C.** (2011). Phosphorylation-dependent differential regulation of plant growth, cell death, and innate immunity by the regulatory receptor-like kinase BAK1. *PLoS Genet* **7**, e1002046.
- Serrano, R.** (1984). Plasma-Membrane Atpase of Fungi and Plants as a Novel Type of Proton Pump. *Curr Top Cell Regul* **23**, 87-126.
- Shiu, S.H., Karlowski, W.M., Pan, R., Tzeng, Y.H., Mayer, K.F., and Li, W.H.** (2004). Comparative analysis of the receptor-like kinase family in Arabidopsis and rice. *Plant Cell* **16**, 1220-1234.
- Shkolnik-Inbar, D., Adler, G., and Bar-Zvi, D.** (2012). ABI4 downregulates expression of the sodium transporter HKT1;1 in Arabidopsis roots and affects salt tolerance. *Plant J* **73**, 993-1005
- Singh, P., Kuo, Y.C., Mishra, S., Tsai, C.H., Chien, C.C., Chen, C.W., Desclos-Theveniau, M., Chu, P.W., Schulze, B., Chinchilla, D., Boller, T., and Zimmerli, L.** (2012). The Lectin Receptor Kinase-VI.2 Is Required for Priming and Positively Regulates Arabidopsis Pattern-Triggered Immunity. *Plant Cell* **24**, 1256-1270.
- Sparkes, I.A., Runions, J., Kearns, A., and Hawes, C.** (2006). Rapid, transient expression of fluorescent fusion proteins in tobacco plants and generation of stably transformed plants. *Nat Protoc* **1**, 2019-2025.
- Stone, J.M., Collinge, M.A., Smith, R.D., Horn, M.A., and Walker, J.C.** (1994). Interaction of a protein phosphatase with an Arabidopsis serine-threonine receptor kinase. *Science* **266**, 793-795.
- Sun, Y., Li, L., Macho, A.P., Han, Z., Hu, Z., Zipfel, C., Zhou, J.M., and Chai, J.** (2013). Structural basis for flg22-induced activation of the Arabidopsis FLS2-BAK1 immune complex. *Science* **342**, 624-628.

- Thordal-Christensen, H., Zhang, Z., Wei, Y., and Collinge, D.B.** (1997). Subcellular localization of H<sub>2</sub>O<sub>2</sub> in plants. H<sub>2</sub>O<sub>2</sub> accumulation in papillae and hypersensitive response during the barley—powdery mildew interaction. *Plant J* **11**, 1187-1194.
- Torii, K.U.** (2004). Leucine-rich repeat receptor kinases in plants: Structure, function, and signal transduction pathways. *Int Rev Cytol* **234**, 1-+.
- Torii, K.U., Mitsukawa, N., Oosumi, T., Matsuura, Y., Yokoyama, R., Whittier, R.F., and Komeda, Y.** (1996). The Arabidopsis ERECTA gene encodes a putative receptor protein kinase with extracellular leucine-rich repeats. *The Plant Cell Online* **8**, 735-746.
- Tsai, C.H., Singh, P., Chen, C.W., Thomas, J., Weber, J., Mauch-Mani, B., and Zimmerli, L.** (2011). Priming for enhanced defense responses by specific inhibition of the Arabidopsis response to coronatine. *Plant J* **65**, 469-479.
- Vidhyasekaran, P.** (2014). Mitogen-activated protein kinase cascades in plant innate immunity. In *PAMP Signals in Plant Innate Immunity* (Springer), pp. 331-374.
- Wang, H.-G., Rapp, U.R., and Reed, J.C.** (1996). Bcl-2 targets the protein kinase Raf-1 to mitochondria. *Cell* **87**, 629.
- Wang, L., Srivastava, A.K., and Schwartz, C.E.** (2010). Microarray data integration for genome-wide analysis of human tissue-selective gene expression. *BMC Genomics* **11 Suppl 2**, S15.
- Xiang, Y., Cao, Y., Xu, C., Li, X., and Wang, S.** (2006). Xa3, conferring resistance for rice bacterial blight and encoding a receptor kinase-like protein, is the same as Xa26. *Theor Appl Genet* **113**, 1347-1355.
- Yamaguchi, Y., and Huffaker, A.** (2011). Endogenous peptide elicitors in higher plants. *Current Opinion in Plant Biology* **14**, 351-357.
- Yamaguchi, Y., Pearce, G., and Ryan, C.A.** (2006). The cell surface leucine-rich repeat receptor for AtPep1, an endogenous peptide elicitor in Arabidopsis, is functional in transgenic tobacco cells. *Proc Natl Acad Sci USA* **103**, 10104-10109.
- Yamaguchi, Y., Huffaker, A., Bryan, A.C., Tax, F.E., and Ryan, C.A.** (2010). PEPR2 is a second receptor for the Pep1 and Pep2 peptides and contributes to defense responses in Arabidopsis. *Plant Cell* **22**, 508-522.
- Yuan, N., Yuan, S., Li, Z., Li, D., Hu, Q., and Luo, H.** (2016). Heterologous expression of a rice miR395 gene in *Nicotiana tabacum* impairs sulfate homeostasis. *Sci Rep* **6**, 28791.

- Zentgraf, U., Laun, T., and Miao, Y.** (2010). The complex regulation of WRKY53 during leaf senescence of *Arabidopsis thaliana*. *Eur J Cell Biol* **89**, 133-137.
- Zhou, A., Wang, H.C., Walker, J.C., and Li, J.** (2004). BRL1, a leucine-rich repeat receptor-like protein kinase, is functionally redundant with BRI1 in regulating *Arabidopsis* brassinosteroid signaling. *Plant J* **40**, 399-409.
- Zhou, M., Li, D., Li, Z., Hu, Q., Yang, C., Zhu, L., and Luo, H.** (2013). Constitutive expression of a miR319 gene alters plant development and enhances salt and drought tolerance in transgenic creeping bentgrass (*Agrostis stolonifera* L.). *Plant Physiology* **161**, 1375-1391.
- Zipfel, C.** (2008). Pattern-recognition receptors in plant innate immunity. *Current Opinion in Immunology* **20**, 10-16.
- Zipfel, C., Kunze, G., Chinchilla, D., Caniard, A., Jones, J.D., Boller, T., and Felix, G.** (2006). Perception of the bacterial PAMP EF-Tu by the receptor EFR restricts *Agrobacterium*-mediated transformation. *Cell* **125**, 749-760.

CHAPTER THREE

HETEROLOGOUS EXPRESSION OF A RICE *MIR395* GENE IN *NICOTIANA*  
*TABACUM* IMPAIRS SULFATE HOMEOSTASIS

## ABSTRACT

Sulfur participates in many important mechanisms and pathways of plant development. The most common source of sulfur in soil -  $\text{SO}_4^{2-}$  - is absorbed into root tissue and distributed into aerial part through vasculature system, where it is reduced into sulfite and finally sulfide within the subcellular organs such as chloroplasts and mitochondria and used for cysteine and methionine biosynthesis. MicroRNAs are involved in many regulation pathways by repressing the expression of their target genes. *MiR395* family in *Arabidopsis thaliana* has been reported to be an important regulator involved in sulfate transport and assimilation, and a high-affinity sulphate transporter and three ATP sulfurylases were the target genes of *AthmiR395* (*Arabidopsis thaliana miR395*). Our results indicated that in rice, transcript level of *OsamiR395* (*Oryza sativa miR395*) increased under sulfate deficiency conditions, and the two predicted target genes of *miR395* were down-regulated under the same conditions. Overexpression of *OsamiR395h* in tobacco impaired its sulfate homeostasis, and sulfate distribution was also slightly impacted among leaves of different ages. One sulfate transporter gene *NtaSULTR2* was identified to be the target of *miR395* in *Nicotiana tabacum*, which belongs to low affinity sulfate transporter group. Both *miR395* and *NtaSULTR2* respond to sulfate starvation in tobacco.

**Key words:** Heterologous expression, miR395, sulfate homeostasis

## INTRODUCTION

As a rudimental and essential element, sulfur is one of the six macronutrients required for plant growth and participates in many important physiological and biochemical processes. In nature, sulfur exists in both inorganic and organic forms, and sulfate ( $\text{SO}_4^{2-}$ ) is the most common inorganic source of sulfur plants acquire from soil.

The sulfate absorption and assimilation pathway in plants is a complex system. In the very beginning, sulfate is absorbed into root tissue. Except for a small amount of sulfate stored in vacuole of root cells, the majority of them are distributed into aerial part through vasculature system. Upon transfer into subcellular organelles such as chloroplasts and mitochondria in cells of aerial part, the sulfate is reduced into sulfite, then sulfide used for the synthesis of cysteine and methionine, two amino acids that play a pivotal role in sulfate assimilation pathway (Takahashi et al., 2011), and essential for supporting many important redox reactions in plants. The reduced form of the cysteine could function as an electron donor and its oxidized form could act as an electron acceptor.

Given the important role sulfur plays in plant growth and development, its deficiency (-S) would cause severe problems to plants, resulting in decreased plant yields and quality (Hawkesford, 2000). To genetically improve plant sulfate uptake and utilization under -S conditions, it is essential to fully understand the functions of the genes encoding sulfate transporters and other important components involved in sulfate assimilation pathways (Hawkesford, 2000),.

Over the course of the past 20 years, essential genes involved in sulfate uptake, distribution and assimilation pathways have been identified and well-studied in different

plant species. *Shst 1*, *Shst 2* and *Shst 3* were the first sulfate transporter genes cloned from *Stylosanthes hamate* responsible for initial sulfate uptake and internal transport (Smith et al., 1995). In *Arabidopsis*, since the cloning of the first sulfate transporters, AST56 and AST68 two decades ago (Takahashi et al., 1997), at least 12 *Arabidopsis* sulfate transporters belonging to five different groups have been identified (Kopriva, 2006). These include two high-affinity sulfate transporters SULTR1;1 and SULTR1;2 responsible for uptake of sulfate from soil (Takahashi et al., 2000; Shibagaki et al., 2002) low-affinity sulfate transporters SULTR2;1 and SULTR2;2 responsible for internal transport of sulfate from root to shoot (Takahashi et al., 2000), SULTR3;5, the function partner of the SULTR2;1 that facilitates the influx of sulfate (Kataoka et al., 2004a), and SULTR4;1 and SULTR4;2 involved in distribution of sulfate between *Arabidopsis* vacuoles and symplastic (Kataoka et al., 2004b). The *ORYsa;Sultr1;1* and *ORYsa;Sultr4;1* are the first two sulfate transporters cloned from rice in early 2000s (Godwin et al., 2003), followed by the identification of additional 12 sulfate transporters (Kumar et al., 2011).

Synthesis of the essential metabolic intermediate, ATPS catalyzes the adenosine 5'-phosphosulfate (APS), and this step is the branch point of the sulfate assimilation pathway followed by the synthesis subpathways of either cysteine or other sulfated compounds. ATPS has been extensively studied for the past decade because of its important role in the sulfate assimilation pathway (Lunn et al., 1990; Klonus et al., 1994; Rotte and Leustek, 2000; Patron et al., 2008). *SULTR* or *ATPS* gene families would be the ideal targets for genetic modification to increase the efficiency of plant sulfate uptake and



assimilation under -S conditions. It is therefore important to understand how they are regulated in plants.

MicroRNAs are short non-coding RNAs with only 20-24 nt, regulating many metabolisms in the post-transcriptional level by repressing translation of their target genes. In plants, with the help of RISC (RNA inducing silence complex), mature miRNA could form near-perfect pairs with its complementary sequences of the mRNA target, followed by cleavage of the base-pairing region and degradation of the transcripts (Bartel, 2004). Among thousands of identified *miRNAs*, *miR395* family in *Arabidopsis* was previously reported to be an important regulator involved in sulfate transport and assimilation (Jones-Rhoades et al., 2006; Kawashima et al., 2009; Liang et al., 2010). The targets of *AthmiR395* (*Arabidopsis thaliana miR395*) are sulfate transporter genes and *ATPS*, such as high-affinity sulfate transporter gene, *AthSULTR2:1* and ATP sulfurylase genes, *AthATPS1,3*, and 4 (Bonnet et al., 2004; Adai et al., 2005; Liang et al., 2010; Jagadeeswaran et al., 2014).

The divergence of monocot and dicot plants occurred at 200 million years ago (Wolfe et al., 1989), but the miRNA-mediated gene regulation mechanism has an even longer history, which is more than 425 million years (Zhang et al., 2006a). These facts suggest that monocot and dicot plants should have a similar miRNA-mediated gene regulation mechanism and conserved miRNA families sharing the same gene ancestors and regulating the same biological events. Research for the past two decades has led to the identification of 21 miRNA families including many well-studied ones such as miR156 and miR399 that seem to be highly conserved between monocots and dicots (Cuperus et al., 2011). *MiR395* is also on the list, but experimental support is still lacking.

Sequences of mature *miR395* are highly conserved between model plant, *Arabidopsis* and crop species. Understanding the role *miR395* plays in important food crops would allow development of novel biotechnology approaches to genetically engineer these plants for ameliorated nutrient uptake and utilization, improving plant growth, yield and agricultural productivity. We have cloned pri-*OsamiR395h* (*Oryza sativa miR395*) from rice (*Oryza sativa*) and studied its function in plant nutritional response. Our results showed that transcript level of *OsamiR395* increased under -S condition accompanied with down regulation of its two predicted target genes. Overexpression of pri-*OsamiR395h* in tobacco (*Nicotiana tabacum*) impaired its sulfate homeostasis. Sulfate distribution was also slightly impacted between leaves of different ages in transgenic plants. One potential target gene of *miR395* named *NtaSULTR2* was identified in tobacco (*Nicotiana tabacum*), which encodes a sulfate transporter. The expression of both endogenous *NtamiR395* (*Nicotiana tabacum miR395*) and *NtaSULTR2* was significantly induced under low sulfate conditions in tobacco leaf tissues, but the expression level of *NtaSULTR2* was inversely correlated to that of *NtamiR395* under different sulfate conditions in root tissues. All these results indicate that *OsamiR395* responds to -S by inducing degradation of two target genes, and pri-*OsamiR395h* can function in dicot plant tobacco and impact its sulfate transportation and distribution. As the first target gene of *miR395* identified in tobacco, *NtaSULTR2* encodes a sulfate transporter belonging to the low-affinity group.

## RESULTS

### Sulfate regulates the expression of *OsamiR395* and its target genes

According to previous research and miRNA database (<http://mirbase.org>), 24 family members belonging to four clusters comprise *OsamiR395* family (Guddeti et al., 2005). The sequence of mature *OsamiR395* is highly conserved while the pre-microRNA sequences are divergent. It has previously been demonstrated in *Arabidopsis* that mature *AthmiR395* transcript accumulates under sulfur-limited conditions (Jones-Rhoades and Bartel, 2004; Kawashima et al., 2009; Liang et al., 2010) To investigate whether *OsamiR395* also responds to low sulfate conditions as its counterpart in *Arabidopsis*, transcript level of *OsamiR395* in two-week-old rice plants grown in N6 solid medium supplemented with different concentrations of sulfate was analyzed. Both Northern analysis and stem-loop RT-PCR results showed that the transcripts of mature *OsamiR395* accumulated under low sulfate conditions (0 and 20  $\mu\text{M SO}_4^{2-}$ ), but declined significantly under sulfate-adequate conditions (1500 and 2000  $\mu\text{M SO}_4^{2-}$ , Figure 3.1 a and b).

In a plant nucleus, *miRNA* gene is first transcribed into a long *pri-miRNA*, which is then processed into *pre-miRNA* and finally mature *miRNA* that is later translocated by HASTY into cytoplasm and induces the degradation of its target gene(s). To further understand whether *OsamiR395* is regulated at the transcription level or post-transcription level, real-time PCR experiment was conducted to investigate the transcript level of *pri-OsamiR395h* in two-week-old rice plants grown in N6 solid medium supplemented with 0, 20, 1500 or 2000  $\mu\text{M SO}_4^{2-}$ . Real-time PCR results showed that excess sulfate could repress the accumulation of *pri-OsamiR395h* transcript (Figure 3.1 c). Conversely, the

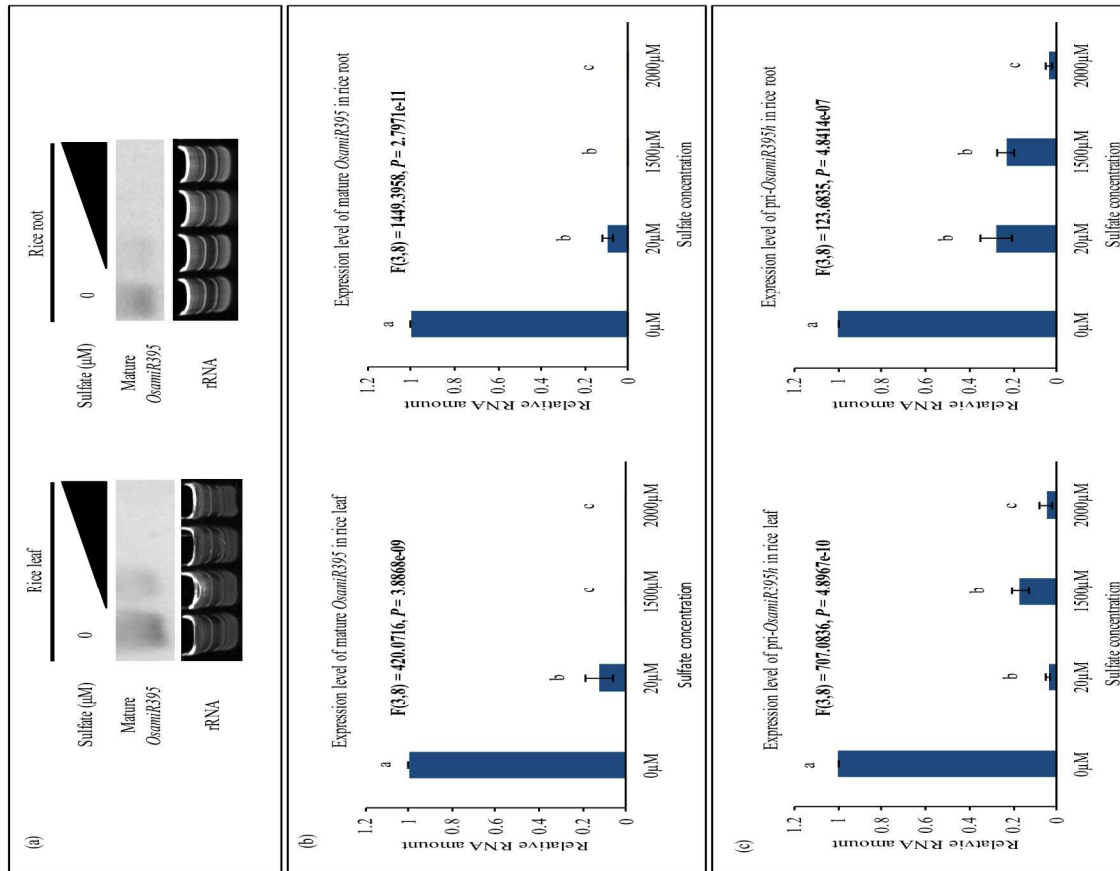


**Figure 3.1. Sulfate deficiency induces accumulation of *OsamiR395* in rice.** (a) Small RNA Northern analysis analysis of mature *OsamiR395* under different sulfate concentrations. Total RNA samples were prepared from leaf and root tissues of two-week-old rice grown in N6 medium with 0, 20, 1500 or 2000  $\mu\text{M}$   $(\text{NH}_4^+)_2\text{SO}_4$  and used for small RNA Northern analysis analysis. Antisense oligonucleotides of *OsamiR395* was labeled with  $\gamma$ - $[^{32}\text{P}]$  ATP and used as probe to detect the transcript level of mature *OsamiR395*. rRNA was used as a loading control. (b) Stem-loop real-time PCR analysis of mature *OsamiR395* under different sulfate concentrations. Total RNA samples were prepared as in (a) and used for stem-loop real-time PCR analysis. *OsaSIZ1* was used as a reference gene. Data are presented as means of three technique replicates, error bars represent SD (n = 3). (c) Real-time PCR analysis of rice pri-*OsamiR395h* under different sulfate concentrations. Total RNA samples were prepared as in (a) and used for real-time PCR analysis. *OsaSIZ1* was used as a reference gene. Data are presented as means of three technique replicates, error bars represent SD (n = 3). The statistically significant difference between groups was determined by one-way ANOVA ( $F(\text{df}_{\text{between}}, \text{df}_{\text{within}}) = F$  ratio,  $p = p$ -value, where  $\text{df} = \text{degrees of freedom}$ ). Means not sharing the same letter are statistically significantly different ( $P < 0.05$ ).

transcription level of pri-*OsamiR395h* increased significantly under sulfate deficient conditions (0 and 20  $\mu\text{M}$   $\text{SO}_4^{2-}$ , Figure 3.1 c). Transcript levels of pri- and mature *OsamiR395* exhibit the same trend under sulfate starvation stress, indicating that *OsamiR395* expression is transcriptionally regulated by sulfate. Sulfate starvation stress induces the expression of pri-*OsamiR395h*, leading to the production of more mature *OsamiR395* transcripts.

Computational analysis of the rice genome sequences leads to the identification of four putative targets of *OsamiR395*, including one *ATPS* and three sulfate transporter genes, *OsaSULTR2;1*, *OsaSULTR2* and *OsaSULTR3;4* (Figure 3.2 a) (Jones-Rhoades and Bartel, 2004; Jones-Rhoades et al., 2006). RT-PCR results indicated that *OsaATPS* did not exhibit any responses in both roots and leaves under -S stress. *OsaSULTR3;4* did not respond to sulfate treatment in leaves either, but was down-regulated in roots with the increasing sulfate concentrations, exhibiting similar expression pattern as *OsamiR395* (Figure 3.2 b). *OsaSULTR2;1* and *OsaSULTR2* genes were both down-regulated in leaves with the increasing sulfate concentrations (Figure 3.2 b), similar to the expression pattern of *OsamiR395* in response to sulfate treatment (Figure 3.1). On the contrary, they were both up-regulated in roots in response to increasing sulfate concentrations (Figure 3.2 b). It should be noted that *OsaSULTR2* exhibited the highest induction under 20  $\mu\text{M}$  sulfate, suggesting that other regulation machineries may also participate in the regulation of the *OsaSULTR2* gene under this particular condition. These results support the hypothesis that *OsaSULTR2;1* and *OsaSULTR2* are the putative target genes of, and regulated by *OsamiR395* in rice roots. In rice leaves, however, *OsamiR395*-mediated transcript cleavage

of the *OsaSULTR2;1* and *OsaSULTR2* genes may not be able to take place due to their non-overlapping tissue-specific expression. Instead, there may exist some other

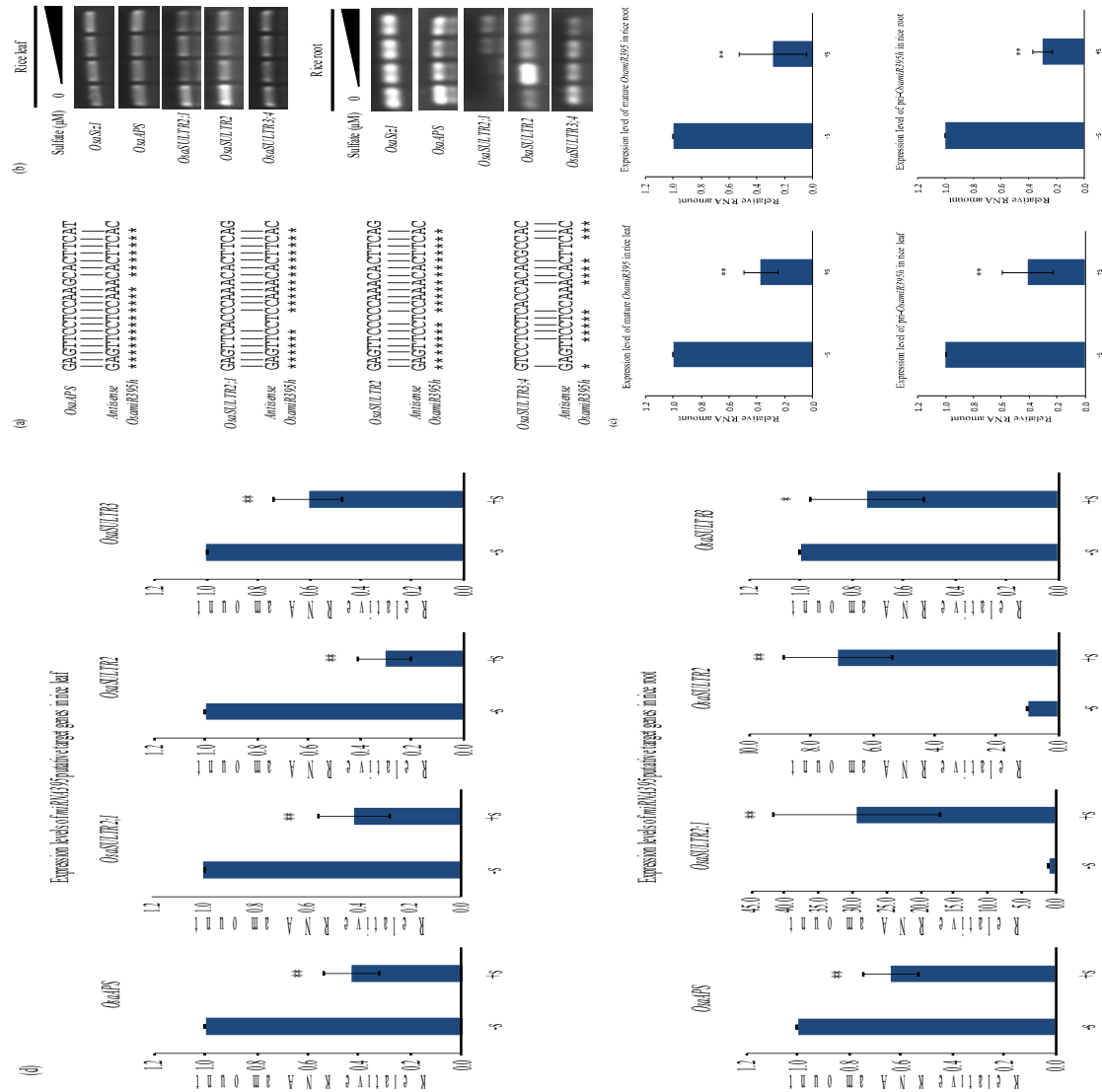


**Figure 3.2. Predicted target *OsaSULTR1* and *OsaSULTR2* exhibit opposite expression patterns to that of the *OsamiR395* in rice root.** (a) Target sites of the four putative *OsamiR395* target genes in rice. The target sites were compared with the complementary sequence of mature *OsamiR395h*. Asterisks indicate the identical sequences. (b) RT-PCR analysis of expression levels of the *OsamiR395* putative targets. Total RNA samples used for RT-PCR were extracted from leaf and root tissues of two-week-old rice grown in N6 medium with 0, 20, 1500 or 2000  $\mu\text{M}$   $(\text{NH}_4^+)_2\text{SO}_4$  and used for RT-PCR analysis. *OsaSIZ1* was used as a reference gene. Experiment was repeated three times. (c) Stem-loop real-time PCR analysis of mature *OsamiR395* and real-time PCR analysis of *pri-OsamiR395h*. Total RNA samples were prepared from leaf and root tissues of two-week-old rice grown in regular N6 medium in regular N6 medium with  $\text{SO}_4^{+}$  (+S) or N6 medium without  $\text{SO}_4^{+}$  (-S) and used for PCR analysis. *OsaSIZ1* was used as a reference gene.

(Figure 3.2 continued) (d) Real-time PCR analysis was also conducted to determine the expression levels of the *OsamiR395* putative targets in rice leaves and roots. Total RNA samples were prepared as in (c) and used for real-time PCR analysis. *OsaSIZ1* was used as a reference gene. For (c) and (d), data are presented as means of two independent biological replicates and three technical replicates, error bars represent SD (n=6). Asterisks indicate the significant differences between expression levels under -S and +S conditions. P < 0.05 is marked as \*. P < 0.01 is marked as \*\*.

---

mechanisms regulating the expression of *OsaSULTR2;1* and *OsaSULTR2*. This is also likely the case for *OsaSULTR3;4* in roots. Similar phenomena was previously observed in *Arabidopsis* (Kawashima et al., 2009; Liang et al., 2010) It should be noted that there are multiple mismatches in the *OsamiR395* target sequence of the *OsaSULTR3;4* (Figure 3.2 a). This raises the question of whether or not *OsaSULTR3;4* is indeed the true target of *OsamiR395*.

To confirm the results of semi-quantitative RT-PCR, real-time PCR was conducted to determine the expression levels of *OsamiR395* and its putative targets in rice under -S condition (N6 medium without sulfate) and +S condition (regular N6 medium). Real-time results consist with the semi-quantitative RT-PCR. In both leaves and roots, pri- and mature *OsamiR395* were up-regulated under -S condition (Figure 3.2 c). But among the four putative target genes, only *OsaSULTR2;1* and *OsaSULTR2* were significantly down-regulated in rice roots under -S condition, exhibiting opposite trend to *OsamiR395* (Figure 3.2 d). According to the real-time results, the hypothesis that *OsaSULTR2;1* and *OsaSULTR2* are the putative targets of *OsamiR395* in rice roots is confirmed.

### **Expression of the *OsamiR395* and its target genes is spatiotemporally regulated**

Besides the response of *OsamiR395* and its targets to sulfate starvation stress, we also investigated the expression patterns of *OsamiR395* and its target genes in different

developmental stages and tissues. To this end, we particularly focused on the primary miRNA level for one of the rice *OsamiR395* genes, *OsamiR395h* and the expression of its putative target genes in both roots and leaves at different developmental stages under normal growth conditions. The RT-PCR results showed that the expression of pri-*OsamiR395h* was strongly induced only in the roots of the four-week-old plants, but otherwise remained very low in both roots and leaves in any other developmental stages (Fig. 3.3).

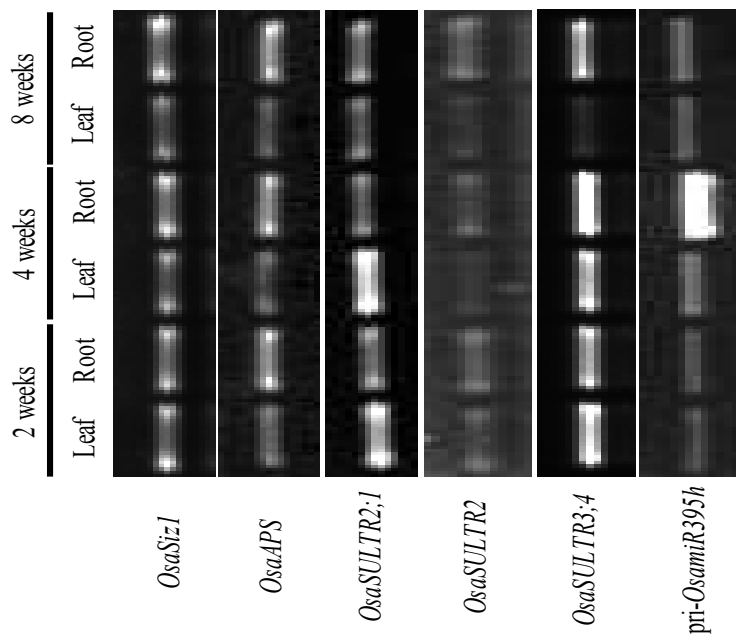


**Figure 3.3. Expression level of pri-*OsamiR395h* and its target genes in rice leaf and root tissues at different developmental stages.** Total RNA samples were prepared from leaf and root tissues of rice harvested at indicated time points and used for RT-PCR analysis. *OsaSIZ1* was used as a reference gene. Experiment was repeated three times.

---

The expression of the *ATPS* again was quite stable in both tissues throughout the rice development, but an elevated expression level in roots was observed compared to that



in leaves (Fig. 3). The expression levels of the three sulfate transporter genes were variable, but none of them was inversely correlated with that of the *OsamiR395h* (Fig. 3).

### **Heterologous expression of pri-*OsamiR395h* in *Nicotiana tabacum***

To further study the role *OsamiR395* plays in sulfate transportation and distribution, we generated a chimeric DNA construct containing the pri-*OsamiR395h* sequence driven by the CaMV35S promoter (Figure 3.4 a). This construct was then introduced into tobacco (*Nicotiana tabacum*) to produce a total of 10 independent transgenic events. RT-PCR analysis suggested rice pri-*OsamiR395h* was successfully expressed in tobacco (Figure 3.4 b), and small RNA Northern analysis result suggested rice pri-*OsamiR395h* was successfully processed into mature *miRNA* (Figure 3.4 c). The detection of tobacco endogenous mature *NtamiR395* in Northern analysis indicated that mature *NtamiR395* shares a highly conserved sequence with its rice homolog. Three independent transgenic events were selected for further analysis.

### **Overexpression of the rice pri-*OsamiR395h* impairs sulfate homeostasis and leads to retarded plant growth in transgenic tobacco**

It has previously been shown that overexpression of *AthmiR395* in *Arabidopsis* impairs its sulfate distribution and assimilation (Liang et al., 2010). To evaluate the impact of the *OsamiR395* in tobacco sulfate metabolism and plant development, we first measured the total sulfur contents in transgenic tobacco plants and wild type (WT) controls. Not surprisingly, the total leaf sulfur content of all the transgenic lines was 2.16 to 2.50 times

higher than that in WT controls. On the contrary, the root sulfur content in transgenic lines was 32% to 42% less than that in WT controls (Figure 3.5 a).

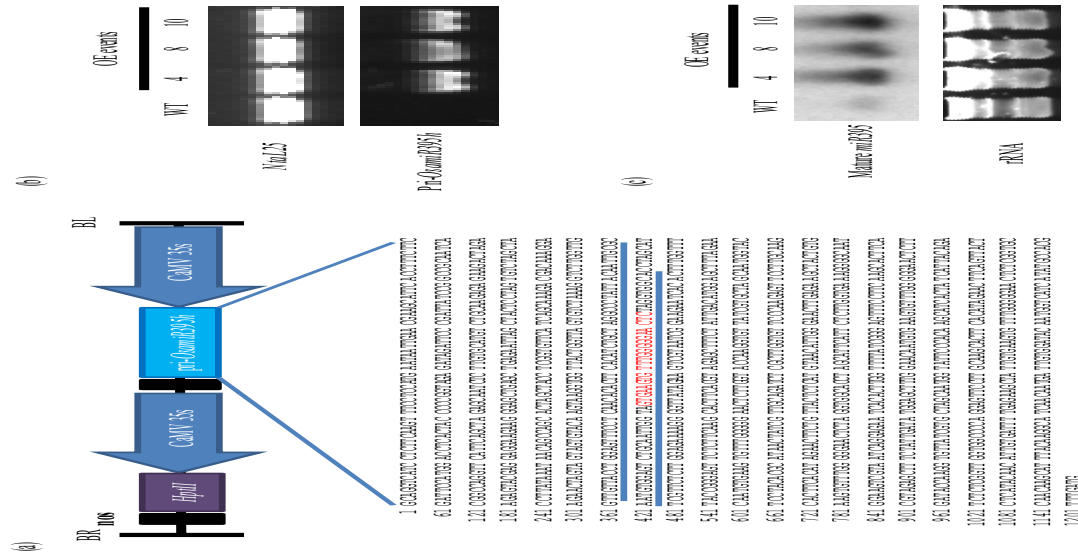


**Figure 3.4. Heterologous expression of pri-*OsamiR395h* in *Nicotiana tabacum*.** (a) The Schematic diagram of rice pri-*OsamiR395h* overexpression construct. Rice pri-*OsamiR395h* sequence containing stem-loop structure of *OsamiR395h* was cloned from rice genomic DNA and put under the control of the CaMV35S promoter. The *hptII* gene driven by CaMV35S promoter was used as selectable maker. The pre-*OsamiR395h* sequence was underlined. Sequence emphasized with red color indicates the mature *miR395h*. LB, Left border; RB, right border. (b) RT-PCR analysis of pri-*OsamiR395h* expression in wild type and three transgenic tobacco lines. Total RNA samples were prepared from two-week-old wild type and transgenic tobacco plants grown in MS medium. *NtaL25* was used as reference gene. (c) Small RNA Northern analysis analysis of mature *miR395* transcripts in wild type and three transgenic tobacco lines. Total RNA samples were prepared from two-week-old wild type and transgenic tobacco plants grown in MS medium. rRNA was used as loading control. WT: wild type plant. OE: overexpression line.

Next, we determined the sulfate-S (sulfate-sulfur) concentration in WT and transgenic plants. Again, the difference in sulfate-S concentrations between transgenics and WT controls was similar to that of the total sulfur contents. In transgenic leaf tissues, the sulfate-S concentration was 1.35 to 1.96 times higher than that in WT leaves, whereas

in roots, transgenics had 38% to 57% less sulfate than WT controls (Figure 3.5 b). This result indicated that the high-level of *miR395* accumulation in transgenic plants impacts the uptake and transportation of sulfur and sulfate.

Similar to a previous report in *Arabidopsis* that overexpression of *AthmiR395* represses the expression of sulfate transporter gene *AthSULTR2;1* and causes impaired sulfate distributions between leaves of different ages (Liang et al., 2010), we also observed that leaf sulfate distribution patterns are different between transgenic tobacco plants and WT controls (Figure 3.5 c). Because sulfate or sulfur compounds could be transported from old to young leaves under normal or sulfate-adequate conditions (Takahashi, 2010), sulfate accumulation in young leaves should be higher than that in old ones as observed in WT control plants (Figure 3.5 c). Contrary to this, transgenic tobacco plants accumulate fewer sulfates in younger leaves than in older ones (Figure 3.5 c), indicating that sulfate delivery pathway is impaired in transgenics, which is most likely one of the consequences caused by repressed expression of sulfate transporter genes. Furthermore, compared with WT controls, transgenic tobacco exhibited retarded growth (Figure 3.6 a and d). As shown in Figure 3.6 b and c, one-month-old transgenic plants displayed shorter root and less fresh weight than wild type controls, a similar phenotype observed in transgenic *Arabidopsis* overexpressing *AthmiR395* (Liang et al., 2010). The slow-growth phenotype of transgenic plants suggests that the expression of *ATPS* may also have been strongly repressed in transgenics, resulting in interrupted sulfate assimilation pathway and consequently retardation in plant growth because of the shortage of cysteine and other sulfate metabolic products.

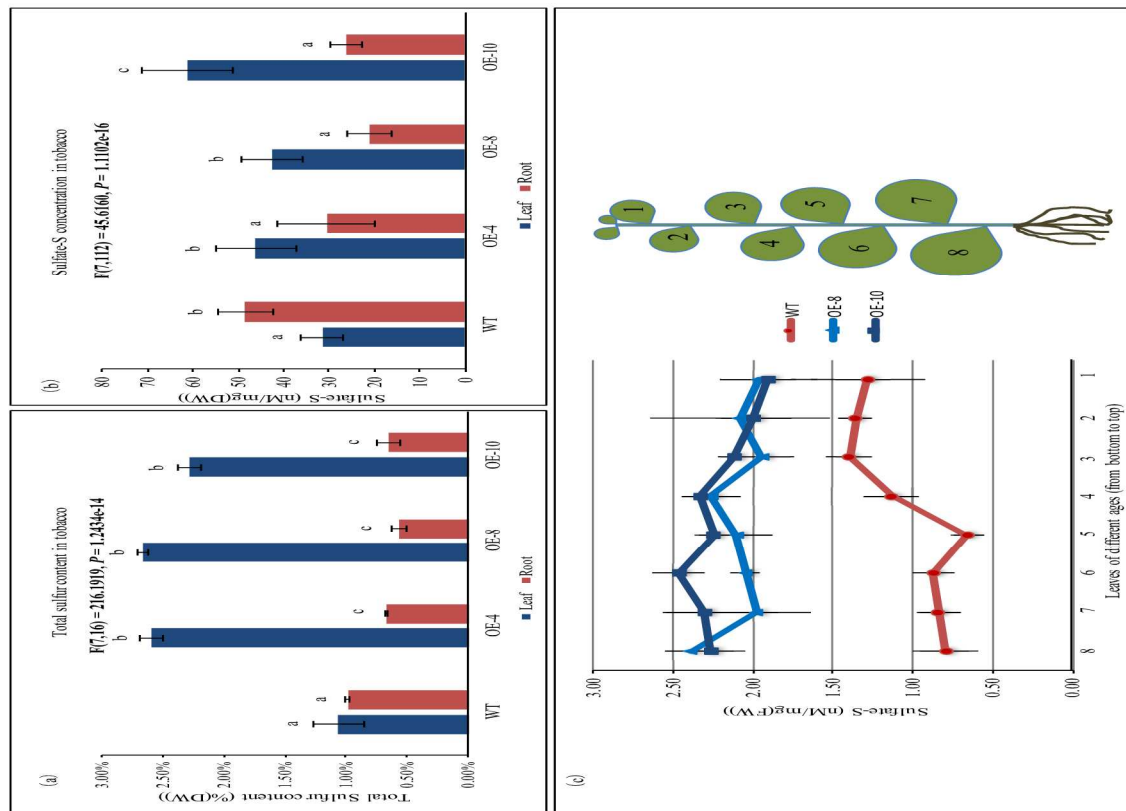


**Figure 3.5. Overexpression of *pri-OsamiR395h* impacts tobacco sulfate transportation and distribution.** (a) Statistical analysis of total sulfur in leaf and root tissues. Samples were harvested from four-week-old wild type and three transgenic tobacco lines. Data are presented as means of three biological replicates contains mixed samples from five biological replications, error bars represent SD (n=3). (b) Statistical analysis of sulfate-S concentrations in leaf and root tissues. Samples were harvested from four-week-old wild type plants and three transgenic tobacco lines. Data are presented as means of fifteen biological replicates, error bars represent SD (n=15). The statistically significant difference between groups was determined by one-way ANOVA ( $F(df_{\text{between}}, df_{\text{within}}) = F \text{ ratio}, p = p\text{-value}$ , where  $df = \text{degrees of freedom}$ ). Means not sharing the same letter are statistically significantly different ( $P < 0.05$ ). (c) Statistical analysis of sulfate concentration in tobacco leaves of different ages. Leaves of 12-week-old wild type and three transgenic tobacco lines were harvested in the positions as indicated in the figure. Data shown are an average of three biological replicates, error bars represent SD (n=3). DW: dry weight. FW: fresh weight. WT: wild type.

## Identification of *miR395* target gene in tobacco

To understand how the excess *miR395* impacts tobacco sulfate homeostasis at the molecular level, we sought to identify putative new target genes of *miR395* using two approaches (Frazier et al., 2010). We first used the DNA sequences of the *Arabidopsis* *SULTR2;1* and *ATPS* genes to blastn against the *Nicotiana tabacum* EST sequences. All the DNA sequences with high similarity (identity of more than 70%) were used to do alignment with complementary sequence of the mature *OsamiR395h*. The following criteria were used to determine the predicted target sequences with minor modifications: (1) No more than four mismatches between *OsamiR395h* and its predicted target genes; (2) No more than two constitutive mismatches between *OsamiR395h* and its predicted target genes; (3) No mismatches between position 10 and 11; (4) No gaps between *OsamiR395h* and its predicted target genes (Frazier et al., 2010). Besides, we also designed primers based on the *AthmiR395* target genes (*AthSULTR2;1* and *AthATPS1*, 3, 4) to amplify and identify the putative homologous genes in tobacco.

Using these approaches, we identified a novel gene named *NtaSUTLR2* to be a putative target of *OsamiR395h* (Figure 3.7). Semi-quantitative RT-PCR analysis revealed that *NtaSULTR2* was significantly down-regulated in transgenic tobacco (Figure 3.7 a). We cloned the full-length cDNA sequence of *NtaSULTR2* using the RACE (Rapid Amplification of cDNA Ends) method, and identified the target site of *miR395* that is located between 135bp and 156bp of its coding region. There are four mismatches and three mismatches between *NtaSULTR2* target sequence and mature *OsamiR395* and *NtamiR395*, separately (Figure 3.7 b), indicating that *NtaSUTLR2* should be efficiently regulated by *miR395* because of their near perfect complementary sequence.

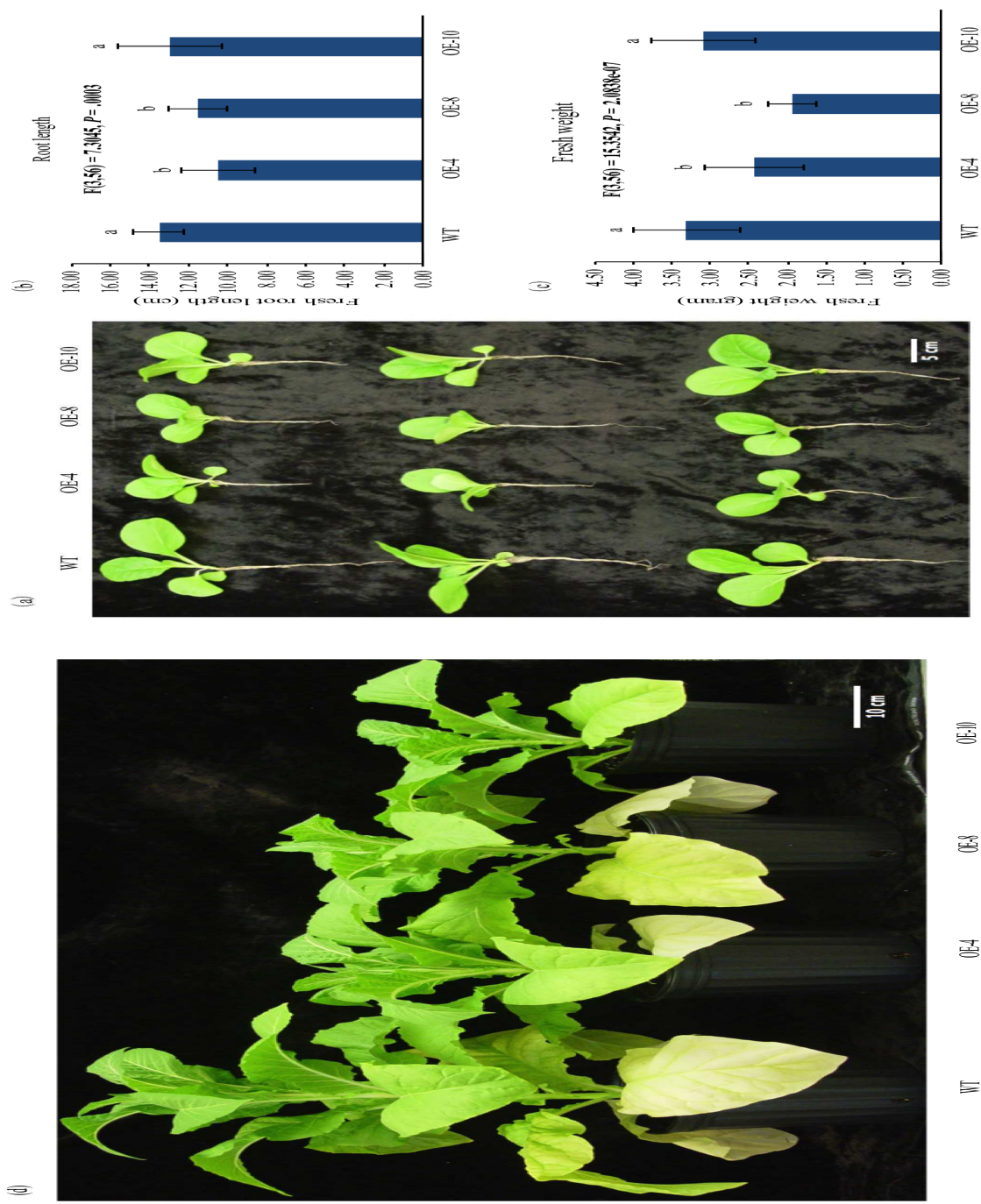


**Figure 3.6**

**Figure 3.6. Overexpression of pri-*OsamiR395h* leads to retarded growth of transgenic tobacco.** Wild type and transgenic tobacco were grown in soil under 16h light/8h dark in greenhouse. Photos were taken (a) four weeks and (d) seven weeks after seed germination. Representative plants were shown. (b) Root length and (c) fresh weight of wild type and transgenic tobacco were measured. Data are presented as means of fifteen biological replicates, error bars represent SD (n=15). The statistically significant difference between groups was determined by one-way ANOVA ( $F(df_{\text{between}}, df_{\text{within}}) = F \text{ ration}, p = p\text{-value}$ , where  $df = \text{degrees of freedom}$ ). Means not sharing the same letter are statistically significantly different ( $P < 0.05$ ). WT: wild type plant. OE: overexpression line.

---

We further characterized *NtaSULTR2* by generating a phylogenetic tree using protein sequence of *NtaSULTR2* and other sixteen well-studied sulfate transporters from rice and *Arabidopsis* using MEGA6. In this phylogenetic tree, *NtaSULTR2* protein is classified into the second group of sulfate transporter subfamily together with *AthSULTR2;1*, *AthSULTR2;2* and *OsaSULTR2;1* proteins (Figure 3.7 c). The three sulfate transporters from *Arabidopsis* and rice are low-affinity sulfate transporters and involved in the inter-organ delivery of sulfate in vascular to transport sulfate from root to leaf, and distribution of sulfate between leaves (Takahashi et al., 1997; Takahashi et al., 2000; Kataoka et al., 2004a).

Taken together, our results indicate that overexpression of *OsamiR395h* in tobacco represses sulfate transporter *NtaSULTR2*, which may play an important role in sulfate transportation and distribution, thus interrupting sulfate homeostasis and distribution in transgenics.

### **Sulfate regulates tobacco *NtamiR395* and *NtaSULTR2***

To confirm that *NtaSULTR2* is the target of *miR395* in tobacco, we investigated the expression level of both *NtaSULTR2* and mature *NtamiR395* under different sulfate concentrations.

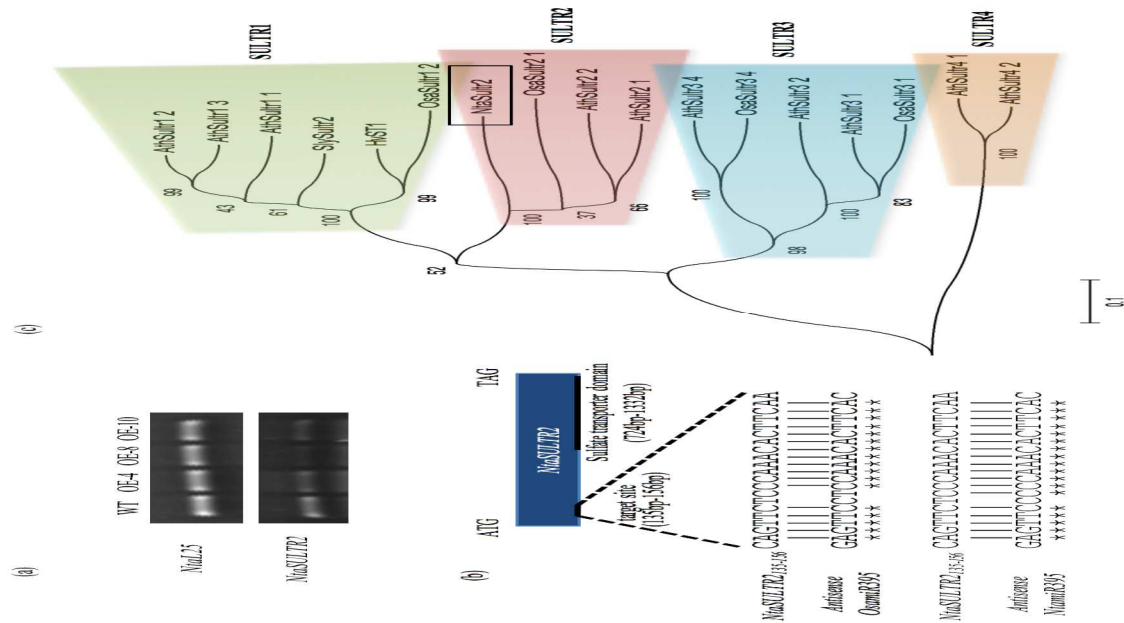


**Figure 3.7. Identification of a sulfate transporter gene, *NtaSULTR2*, the target of *miR395* in tobacco.** (a) RT-PCR analysis of *NtaSULTR2* expression in tobacco. Total RNA samples were prepared from two-week-old wild type and transgenic tobacco and used for RT-PCR analysis. *NtaL25* was used as a reference gene. Experiment was repeated three times. (b) General structure of tobacco gene *NtSULTR2*. *NtaSULTR2* with a length of 1335 bp contains a sulfate transporter domain between 724 bp to 1332 bp, and a *miR395* target site between 135 bp to 156 bp. The target site was compared with the complementary sequence of mature *OsamIR395h* and *NtamiR395*. Asterisks indicate the identical sequences. (c) phylogenetic analysis of *NtaSULTR2* protein. Protein sequences of *NtaSULTR2* and 16 sulfate transporters of rice and *Arabidopsis* were used to establish phylogenetic tree with MEGA6. In this phylogenetic tree, *NtaSULTR2* protein is classified into the second group of sulfate transporter subfamily together with *AthSULTR2*;1, *AthSULTR2*;2 and *OsaSULTR2*;1.

In leaf tissues, the transcription of the mature *NtamiR395* was gradually up-regulated, contrary to the gradually reduced sulfate concentration. However, *NtaSULTR2*



did not exhibit an opposite, but a similar expression pattern to *NtamiR395* with its lowest transcript level being under 1500  $\mu\text{M}$ , but not 2000  $\mu\text{M}$   $(\text{NH}^{4+})_2\text{SO}_4$  (Figure 3.8 a).

In root tissues, the situation was different. The transcript level of the mature *NtamiR395* increased in response to sulfate depletion, similar to that observed in leaves, whereas *NtaSULTR2* exhibited a roughly opposite, but more complex expression pattern (Figure 3.8 b). Compared to sulfate depletion conditions with 0  $\mu\text{M}$   $(\text{NH}^{4+})_2\text{SO}_4$  supply, *NtaSULTR2* was up-regulated under both 20  $\mu\text{M}$  and 2000  $\mu\text{M}$   $(\text{NH}^{4+})_2\text{SO}_4$ , but down-regulated under 1500  $\mu\text{M}$   $(\text{NH}^{4+})_2\text{SO}_4$ . The results indicate that *NtaSULTR2* might be regulated by *NtamiR395* in roots but not in leaf tissues. These results correspond to the previous studies in *Arabidopsis* and rice showed that the expression level of *AthSULTR2* is opposite to that of *AthmiR395* in some, but not all plant tissues most likely due to the fact that the spatial expression pattern of *AthmiR395* does not overlap with that of *AthSULTR2;1* (Kawashima et al., 2009; Liang et al., 2010; Jeong et al., 2011), which could probably also explain the similar observation in tobacco from this study.

### ***MiR395* mediates the cleavage of *NtaSULTR2* miRNA**

To further confirm that *NtaSULTR2* is the true target of *miR395*, we conducted RLM-RACE (T4 RNA Ligase Mediated Rapid Amplification of cDNA Ends) using transgenic tobacco to verify that *NtaSULTR2* transcripts are cleaved by *miR395*. Transgenic tobacco was used because overexpression of mature *miRNA395* induces continuous cleavage of *NtaSULTR2* mRNA, which makes the detection of cleaved *NtaSULTR2* mRNA easier.

We used forward ASP (Adapter Specific Primer) and reverse GSP (Gene Specific Primer) to conduct the first round PCR after the adapter-linked first strand cDNA ends were generated. The RNA adapter has a length of 44 bp, and the reverse GSP is localized

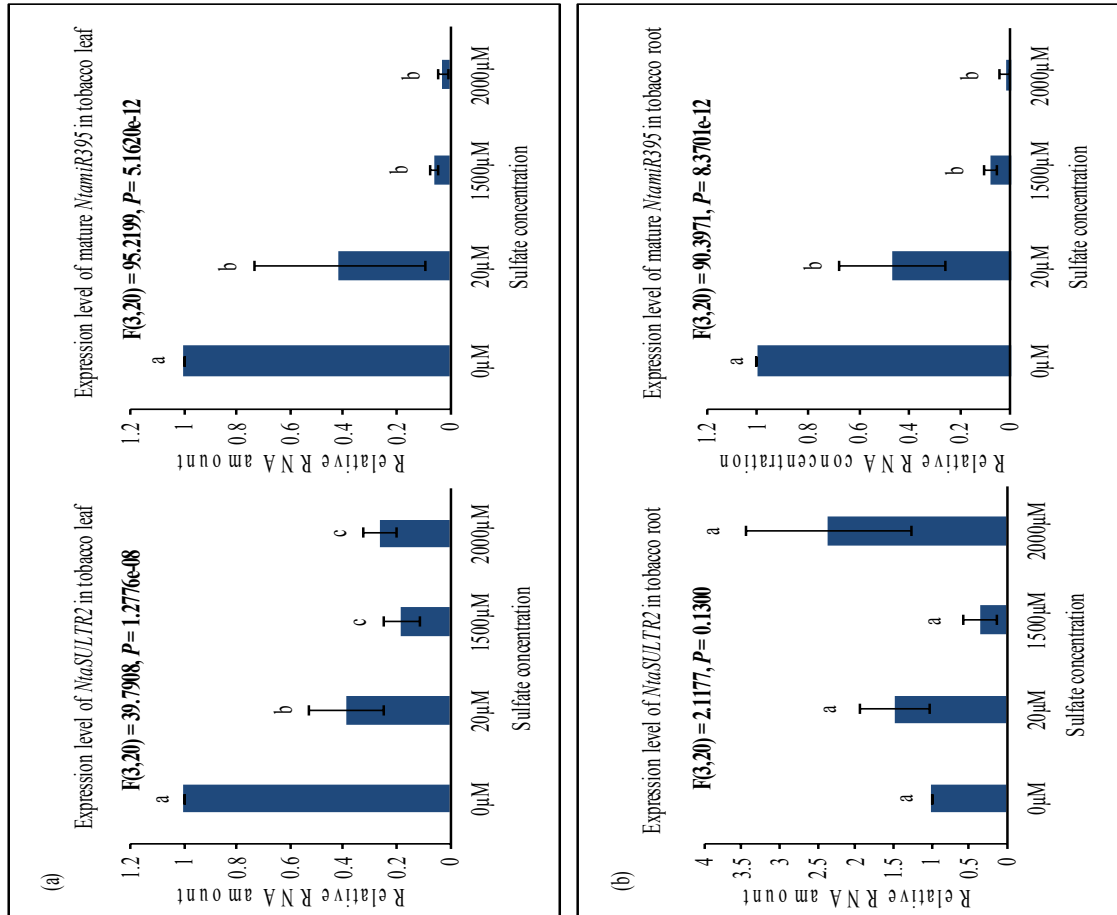


**Figure 3.8. *NtamiR395* and *NtaSULTR2* exhibit opposite expression patterns in tobacco roots.** Real-time PCR analysis of expressions of *NtaSULTR2* and mature *NtamiR395* under different sulfate concentrations. Total RNA samples were prepared from (a) leaf tissue and (b) root tissue of four-week-old tobacco grown in MS medium with 0, 20, 1500 or 2000  $\mu\text{M}$   $(\text{NH}_4^+)_2\text{SO}_4$ . *NtaL25* was used as a reference gene. Data are presented as means of three technical replicates and two biological replicates, error bars represent SD (n=6). The statistically significant difference between groups was determined by one-way ANOVA ( $F(\text{df}_{\text{between}}, \text{df}_{\text{within}}) = F$  ratio,  $p = p$ -value, where  $\text{df} = \text{degrees of freedom}$ ). Means not sharing the same letter are statistically significantly different ( $P < 0.05$ ).

545 bp downstream of the predicted *miR395* target site in the *NtaSULTR2* mRNA, so the product of the first round PCR should have a length of about 589 bp. As shown in Figure 4.9, the first round PCR with transgenic tobacco cDNA indeed generated a clear band of about 600bp.

A second round PCR was then conducted using the first round PCR product as template to confirm that it was the adapter-linked 3' end cleavage *NtaSULTR2* mRNA. A new set of primers were used in the second round PCR. Forward NASP (Nest Aadapter Specific Primer) is localized on the adapter from 14 bp to 44 bp, and reverse NGSP (Nest Gene Specific Primer) is localized 463 bp downstream of the predicted *miR395* target site in the *NtaSULTR2* mRNA, so the product of the second round PCR should be about 493 bp. As shown in Figure 4.9, the second round PCR with transgenic tobacco first round PCR product generated a clear main band of about 500 bp. PCR product cloning and sequencing further confirm the predicted cleavage site (data not shown).

## DISCUSSION

Previous studies on *Arabidopsis miR395* indicated its involvement in sulfate starvation response by repressing the expression of genes in sulfate transportation and assimilation pathways. Under -S condition, the accumulation of *AthmiR395* will be enhanced under low internal sulfate levels, and it's also correlate to GSH pool, indicating that the regulation of *AthmiR395* is mediated by internal sulfate level and redox signaling in *Arabidopsis* (Matthewman et al., 2012; Jagadeeswaran et al., 2014). The increased

*AthmiR395* then represses the expression of *AthATPS1*, *AthATPS3*, *AthATPS4* and *AthSULTR2;1* (Kawashima et al., 2009; Jagadeeswaran et al., 2014).

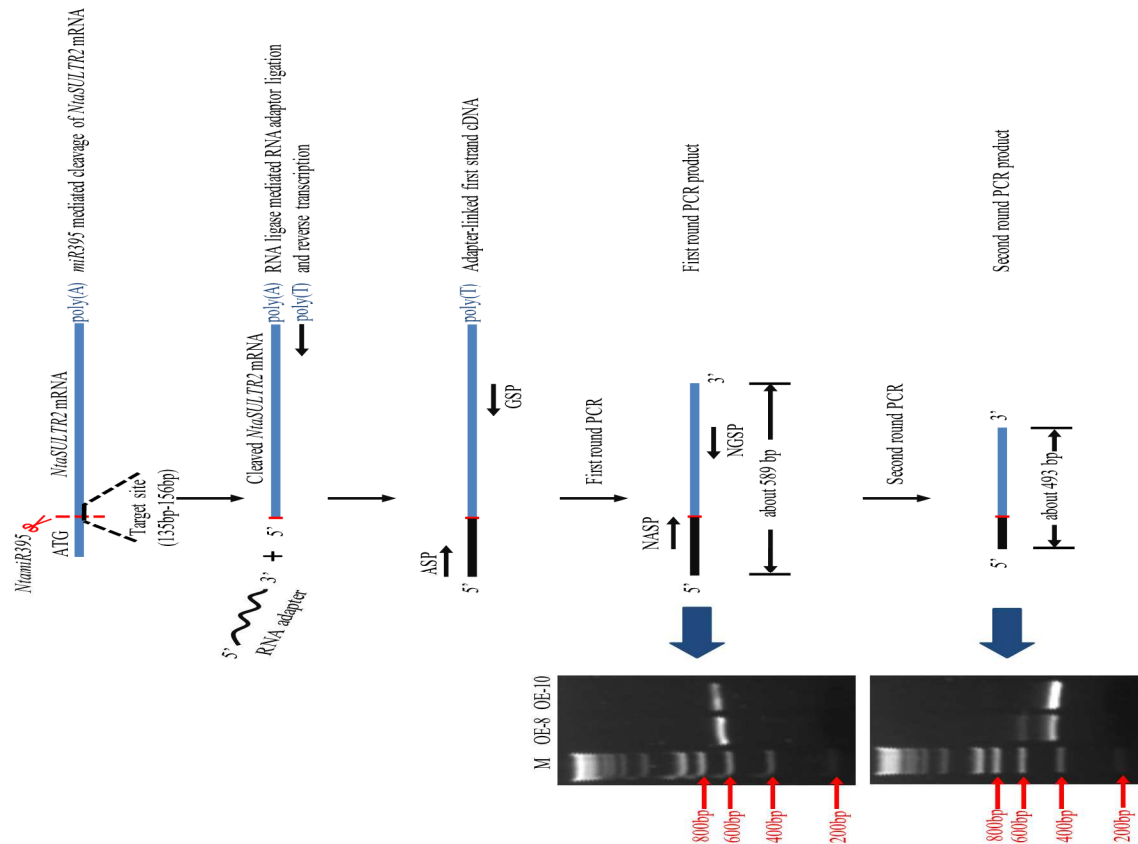


**Figure 3.9. Confirmation of *miR395* mediated cleavage of *NtSULTR2* mRNA.** RLM-RACE (T4-RNA ligase mediated amplification of 5' cDNA ends) was conducted to confirm the cleavage of *NtSULTR2* mRNA. Total RNA samples were isolated from two-week-old transgenic tobacco. 44 bp RNA adapter was ligated to the purified RNA by using T4 RNA ligase. Adapter-linked RNA was then used to synthesize first strand cDNA, followed by amplification of 5' ends using forward primer ASP and reverse primer GSP. The 589 bp product from the first round PCR was then used as template for the second round PCR using forward nest primer NASP and reverse nest primer NGSP, producing a 493 bp second round PCR product. M: DNA molecular weight marker. OE: overexpression line. Red lines indicate *miR395* cutting site.

Further study in *Arabidopsis* revealed a whole picture of how *AthmiR395* is involved in plant response to sulfate starvation. When sulfate supply is limited, the induced *AthmiR395* mediates the degradation of *ATPS* mRNA leading to the accumulation of sulfate in leaf tissues as a result of decelerated sulfate assimilation (Liang et al., 2010). At the same time, the cleavage of *AthSULTR2;1* mRNA in shoots by *AthmiR395* results in blocked sulfate transport into new leaves from old ones (Liang et al., 2010). Furthermore, the impaired sulfate homeostasis and reduced sulfate assimilation impact seed germination under ABA-treated condition (Kim et al., 2010).

*MiR395* is highly conserved across species, which strongly suggests that its function in regulating plant response to nutrition, particularly sulfate supply could also be conserved during evolution. Our results in rice indicate that indeed, the transcript of mature *OsamiR395* increases under –S condition, and this change in expression might be regulated at the transcription level (Figure 3.1). Computational prediction led to the identification of four putative target genes of *OsamiR395* in rice. We confirmed that *OsaSULTR2;1* and *OsaSULTR2* are regulated by *OsamiR395* in roots suggesting that they may be the *OsamiR395* target genes.

Knowledge about the functions of rice sulfate transporters is limited. Phylogenetic analysis grouped the fourteen rice sulfate transporters together with their *Arabidopsis* counterparts<sup>11</sup>, suggesting that they may share similar function. *OsaSULTR2;1* and *OsaSULTR2* may be responsible for the root-to-shoot sulfate transportation and distribution of sulfate between leaves of different ages. Our results (Figure 2 b-d) showed that the expression patterns of rice sulfate transporter genes were different from their

*Arabidopsis* homologs, both *OsaSULTR2;1* and *OsaSULTR2* were reduced in leaves with the increasing sulfate concentrations. We speculate that the two sulfate transporter genes and *miR395* may be differentially expressed in different leaf tissues and thus, *OsaSULTR2;1* and *OsaSULTR2* may not be subjected to *miR395* regulation. Instead, other regulatory machineries may participate in the control of their expression in response to sulfate levels. It is likely that when rice plants are subjected to sulfate starvation, there is a need for the two sulfate transporters to be active, driving the transportation of sulfate from old leaves to younger ones to ensure plant growth and development. However, with abundant sulfate supply in the environment, there is no need for sulfate distribution to young leaves, and therefore the expression of both *OsaSULTR2;1* and *OsaSULTR2* declines.

The miRNA-mediated gene regulation mechanism emerged about 425 million years ago, which is at a very early stage of plant phylogeny prior to the divergence of monocot and dicot plants (Zhang et al., 2006b). This suggests that monocot and dicot plants should have a similar miRNA-mediated gene regulation mechanism, and some highly conserved miRNA families regulating the same biological process have evolved from the same gene ancestors. Indeed, research data in the past twenty years indicate that 21 miRNA families, such as miR156 and miR399, are conserved in sequence across monocots and dicots (Cuperus et al., 2011). More specifically, Zhang et al. found that 9 miRNA families are highly conserved (Zhang et al., 2006b), 10 miRNA families are moderately conserved and 16 miRNA families including *miR395* are lowly conserved across plant species. In a later work, *miR395* family was identified in the common ancestor of all embryophytes

(Cuperus et al., 2011). Besides the miRNA sequences, the genes involved in miRNA and siRNA biogenesis pathways are also conserved across species. In plants, Dicer-like (DCL) is a key protein in the miRNA genesis pathway. DCL interacting with HYPONASTIC LEAVES1 (HYL1) and C2H2-zinc finger protein SERRATE (SE) in D-bodies cleaves the pri-miRNA from the base to yield a pre-miRNA with stem-loop structure, and this pre-miRNA is sliced again to yield mature miRNA (Kurihara et al., 2006; Liu et al., 2009; Voinnet, 2009; Axtell et al., 2011). Phylogenetic analysis indicated that divergence of *DCL1* gene associated with miRNA production from other *DCLs* could be traced to the time before the emergence of moss *Physcomitrella patens* (Liu et al., 2009), indicating that *DCLs* may have the same origin and are conserved across vascular plants.

Based on previous findings, we hypothesize that miRNA biogenesis pathway in dicots could accept pri-miRNAs from monocots, and process it into mature miRNA with function. To verify our hypothesis, full-length DNA sequence of pri-*OsamiR395h* was cloned from rice genome. The expression cassette of the CaMV35S-controlled rice pri-*OsamiR395h* was then prepared and introduced into tobacco genome. By performing small molecule Northern analysis, we observed high transcript level of *miR395* in transgenic tobacco under normal condition, indicating that rice pri-*OsamiR395h* could be successfully expressed and processed into mature *miR395h* in tobacco (Figure 3.4). At the same time, we also observed low level of endogenous mature *miR395* in WT tobacco, confirming that tobacco mature *miR395* is highly conserved with its rice homolog. All of the three transgenic tobacco lines exhibited impaired sulfate homeostasis and distribution (Figure

3.5). Furthermore, transgenic plant had retarded growth phenotype (Fig. 6). All the facts suggest that mature *OsamiR395* functions in transgenic tobacco.

Data obtained from this research revealed that the sulfate-S contents in transgenic tobacco are higher in leaf tissue, but lower in root tissue than those in WT controls. An even more significant difference in total sulfur content was observed between WT controls and *OsamiR395h* overexpression plants (Figure 3.5 a and 5 b). Besides, we also observed that sulfate distribution between leaves of different ages is impaired in transgenic tobacco plants (Figure 3.5 c).

To reveal the molecular mechanism underlying *miR395*-mediated plant sulfate metabolism, we studied genes impacted by excessive dose of *miR395* in transgenic tobacco, and identified a novel sulfate transporter gene *NtaSULTR2* belonging to the second group of sulfate transporter genes (Figure 3.7). Based on the results of real-time PCR and RML-RACE, we verified that *NtaSULTR2* is the target gene of *miR395* (Figure 3. 8 and 3.9). We believe that the repression of *NtaSULTR2* gene in transgenic tobacco plants partially impaired the sulfate homeostasis. In *Arabidopsis* shoot tissue, sulfate transporter *AthSULTR2;1* is localized in both xylem and phloem, particularly in phloem parenchyma cells surrounding sieve and companion cells, and involved in distribution of sulfur between leaves of different ages (Takahashi et al., 2000; Takahashi, 2010). We conjecture that in tobacco shoot tissue, *NtaSULTR2*, likes its homologs in *Arabidopsis*, retrieves sulfate from mesophyll cells to xylem and phloem cells, and sulfate is transported from old leaves to young leaves. But in transgenic plants, the delivery of sulfate from old



leaves to young leaves is impaired because of significantly repressed *NtaSULTR2* gene (Figure 3.5 c).

Although no *ATPS* gene have been identified and cloned in tobacco, we believe that there must be one or more *ATPS* gene(s) repressed in transgenic tobacco, causing interrupted sulfate assimilation. The interruption of the sulfate assimilation pathway would cause a shortage in cysteine and other sulfate metabolic products, resulting in retarded plant growth and triggering plant sulfate starvation signaling, which would promote sulfate absorption and transport into leaf tissue, and consequently a much more sulfur accumulation in leaves of transgenics than in that of WT controls (Figure 3.5 a and b).

## **MATERIALS AND METHODS**

### **Plant materials and growth conditions**

To investigate the expression levels of *OsamiR395* and its targets in rice under different sulfate concentrations, rice seeds were surface sterilized and grown in N6 medium under 16 h-light/8 h-dark at 28 °C (Chu, 1975). Sulfate salts of the N6 medium were replaced with chloride salts and supplemented with 0, 20, 1500 or 2000  $\mu\text{M}$   $(\text{NH}_4^+)_2\text{SO}_4$ . Rice seeds were also grown in regular N6 medium (+S) and N6 medium without  $\text{SO}_4^{+}$  (-S) under 16 h-light/8-h dark at 28 °C. Two-week-old plants were harvested for RNA isolation.

To investigate the expression patterns of *OsamiR395* and its targets in different developmental stages and tissues of rice, rice seeds were grown in soil in a greenhouse. Root and leaf samples were collected two, four and eight weeks after germination.

To investigate the expression levels of pri-*OsamiR395h*, mature *miR395* and *NtaSULTR2* in tobacco, tobacco seeds were surface sterilized and grown in MS medium under 16 h light/8 h dark at 22 °C (Murashige and Skoog, 1962). To prepare MS mediums with different sulfate concentrations, sulfate salts of the MS medium were replaced with chloride salts and supplemented with 0, 20, 1500 or 2000  $\mu\text{M}$   $(\text{NH}_4^+)_2\text{SO}_4$ . Two-week-old and four-week-old plants were harvested for RNA isolation.

To measure total sulfate content and sulfate-S concentration in tobacco, and to determine the growth rate of tobacco, tobacco were grown in soil in a greenhouse. Four-week-old and 12-week-old plants were collected for analysis.

### **Genomic DNA and Total RNA Isolation, and cDNA Synthesis**

Plant genomic DNA was isolated following previously described method (Zhou et al., 2013).

Total RNA was isolated from 100 mg plant samples with Trizol reagent (Ambion, USA), and the genomic DNA is removed by using RNase-free DNase I (Invitrogen, USA). 2  $\mu\text{g}$  total RNA was used to synthesize first strand cDNA with SuperScript III Reverse Transcriptase (Invitrogen, USA) according to manufacturer's instructions. The first strand cDNA was used for semi quantitative RT-PCR and regular real-time PCR.

To determine the transcript level of mature *miR395*, the first-strand cDNA used for stem-loop real-time PCR was synthesized following the regular SuperScript III Reverse Transcriptase (Invitrogen, USA) mediated method, except that the oligo  $(\text{dT})_{20}$  was

replaced with *miR395* specific reverse transcription primer. Primers were all listed in Appendix Table B-1.

### **Semi-quantitative RT-PCR, stem-loop and regular real-time PCR**

To conduct semi-quantitative RT-PCR, first-strand cDNA samples were diluted to 0.25 times based on the concentration of the first-strand cDNA samples. The loading volume of the cDNA samples was adjusted basing on the transcript level of a reference gene.

To conduct stem-loop and regular real-time PCR, first-strand cDNA samples were diluted to 0.025 to 0.005 times based on the concentration of the first-strand cDNA samples. Both stem-loop and regular real-time PCR were performed using SYBR Green Supermix (Bio-Rad, USA) following manufacturer's instructions, and iQ5 real-time detection system (Bio-Rad USA) was used to detect and analyze the real-time PCR result.

Stem-loop and regular real-time PCR results were determined by using  $\Delta\Delta Ct$  method.  $\Delta Ct$  was defined as  $Ct_{test} - Ct_{0h}$ , in which  $Ct_{test}$  stands for threshold cycle of one gene after treatment, and  $Ct_{0h}$  stands for threshold cycle of one gene before treatment.  $\Delta\Delta Ct$  was defined as  $\Delta Ct_{reference} - \Delta Ct_{target}$ , in which  $\Delta Ct_{reference}$  stands for  $\Delta Ct$  of the endogenous gene used as a reference, and  $\Delta Ct_{target}$  stands for  $\Delta Ct$  of target gene. Finally, related expression ratio was calculated as  $2^{-\Delta\Delta Ct}$ .

Primers used for semi-quantitative RT-PCR, stem-loop real-time PCR and regular real-time PCR were all listed in Appendix Table B-1.

### **Small molecule Northern analysis**

Small molecule Northern analysis was performed following the method previously described with minor modification (Tran, 2009). 10 µg total RNA denatured at 95 °C was separated in 12.5% urea-polyacrylamide gel and transferred to Hybond-N+ nylon membrane (Amersham, USA) in a Trans-Blot SD Semi-Dry Transfer Cell (Bio-Rad, USA). To prepare radiolabeled probe for detecting mature *miR395*, DNA oligonucleotide GAGTTCCCCAAACTTCAC was synthesized (<http://www.idtdna.com/site>) and labeled with  $\gamma$ -[<sup>32</sup>P]-ATP by using T4 polynucleotide kinase. RNA membrane was then hybridized with radiolabeled probe and detected on a phosphorimaging screen.

### **Plasmid construction, bacterial strains and plant transformation**

The predicted pri-*OsamiR395h* was amplified from rice genomic DNA and cloned at downstream of CaMV35S (Cauliflower Mosaic Virus 35S) promoter of binary vector pZH01, resulting in CaMV35S/*OsamiR395h*-CaMV35S/*hygromycin* (Xiao et al., 2003). This chimeric gene expression construct was then mobilized into *Agrobacterium tumefaciens* strain LBA4404 by electroporation for tobacco transformation. The *Escherichia coli* strain used in this experiment was DH5 $\alpha$ .

The primers used for plasmid construction were all listed in Appendix Table B-1.

### **Determination of total sulfur content and sulfate-sulfur concentration**

For determination of total sulfur, plant samples were collected and dried for 48 h at 80 °C. Total sulfur contents in dry samples were determined as previously described (Plank, 1992).

Sulfate-S concentration was determined following a previous method with minor modification (Tabatabai and Bremner, 1970). 10 mg dry plant sample or 200 mg fresh plant sample was immersed in 1 ml 0.1 M HCl for 2 h at room temperature, followed by 20 min centrifugation at 12000 g. Clear supernatant liquid was then transferred to a 50 ml Erlenmeyer flask and made to 20 ml by water. One ml of barium chloride-gelatin reagent was added to the liquid. After 40 min (no more than 120 min), absorbance of the resulting cloudy liquid was determined at 454 nm by using a spectrometer.

### **Rapid amplification of cDNA ends**

To obtain 5' cDNA end and 3' cDNA end of *NtaSULTR2*, total RNA was extracted from 100 mg two-week-old WT tobacco with Trizol reagent (Ambion, USA) and treated with RNase-free DNase I (Invitrogen, USA) to remove genomic DNA. 1 µg total RNA was then used to amplify 5' end and 3' end cDNA of *NtaSULTR2* with SMARTer RACE 5'/3' commercial kit (Clontech, USA) following the manufacture's instruction. Then, the 5' end and 3' end cDNA fragments were sequenced. Sequence information was used to design primers for cloning of full-length *NtaSULTR2* cDNA.

The primers used for RACE and for cloning of full length *NtaSULTR2* cDNA were all listed in Appendix Table B-1.

### **T4-RNA ligase mediated amplification of 5' cDNA ends**

To verify *miR395* cleavage site within *NtaSULTR2*, T4-RNA ligase mediated amplification of 5' cDNA ends was conducted following a previously described method (Llave et al., 2011). Briefly, total RNA was isolated from 100 mg plant sample using Trizol reagent (Ambion, USA), followed by purification of RNA with RNeasy mini kit (Qiagen, Germany). RNA adapter was ligated to the purified RNA by using T4 RNA ligase (New England Biolabs, USA). Based on the fact that miRNAs mediated mRNA cleavage will generate 5'-monophosphate ends on the 3' end cleavage product of target mRNAs, it is possible to ligate RNA oligonucleotide adapter to the 5' terminus of 3' end cleavage product by using T4 RNA ligase, while such RNA oligonucleotide adapter would not be ligated to mRNAs with conventional 5' cap (Llave et al., 2011). Adapter-linked RNA was then used to synthesize first strand cDNA with SuperScript II Reverse Transcriptase (Invitrogen, USA), followed by amplification of 5' ends using forward primer ASP and reverse primer GSP. The product from the first round PCR was then used as template for the second round PCR using forward nest primer NASP and reverse NEST primer NGSP. PCR product was cloned for sequencing.

The primers used for RML-RACE were all listed in Appendix Table B-1.

### **Phylogenetic analysis of sulfate transporters**

Phylogenetic tree of *NtaSULTR2* and other sulfate transporter genes in rice and *Arabidopsis* inferred using the Neighbor-Joining method (Saitou and Nei, 1987). The optimal tree with the sum of branch length = 3.89795523 is shown. The tree is drawn to

scale, with branch lengths in the same units as those of the evolutionary distances used to infer the phylogenetic tree. The evolutionary distances were computed using the Poisson correction method and are in the units of the number of amino acid substitutions per site (Zuckermandl and Pauling, 1965). The analysis involved 17 amino acid sequences. All positions containing gaps and missing data were eliminated. There was a total of 347 positions in the final dataset. Evolutionary analyses were conducted in MEGA6 (Tamura et al., 2013). WT: wild type plant. OE: overexpression line.

### **Statistical analysis**

Student's t test was used to test the difference between the means from two groups.  $P < 0.05$  was considered to be statistically significant and marked as \*.  $P < 0.01$  was considered to be statistically highly significant and marked as \*\*.

One-way ANOVA ( $F(df_{\text{between}}, df_{\text{within}}) = F$  ration,  $p = p$ -value, where  $df$  = degrees of freedom) with post hoc comparisons using the Tukey HSD test was used to determine the statistically significant difference between the means from three or more groups. Means not sharing the same letter are statistically significantly different ( $P < 0.05$ ).

### **Accession number**

Sequence data from this article can be found in the *Arabidopsis* Genome Initiative database and European Molecular Biology Laboratory under the following accession numbers:

*AthSULTR2;1*: NM\_121056.2, *AthATPS1*: NM\_113189.4, *AthATPS3*: U06275.1,  
*AthATPS4*: AT5G43780, *OsaSULTR2;1*: NM\_001055792, *OsaSULTR2*:  
NM\_001055793, *OsaSULTR3;4*: Os06g0143700, *OsaATPS*: NM\_001057769, *OsaSiz1*:  
Os05g0125000, *NtaL25*: L18908, *NtaSULTR2*: KT373983.



## REFERENCES

- Adai, A., Johnson, C., Mlotshwa, S., Archer-Evans, S., Manocha, V., Vance, V., and Sundaresan, V.** (2005). Computational prediction of miRNAs in *Arabidopsis thaliana*. *Genome research* **15**, 78-91.
- Axtell, M.J., Westholm, J.O., and Lai, E.C.** (2011). Vive la difference: biogenesis and evolution of microRNAs in plants and animals. *Genome Biol* **12**, 221.
- Bartel, D.P.** (2004). MicroRNAs: genomics, biogenesis, mechanism, and function. *Cell* **116**, 281-297.
- Bonnet, E., Wuyts, J., Rouze, P., and Van de Peer, Y.** (2004). Detection of 91 potential conserved plant microRNAs in *Arabidopsis thaliana* and *Oryza sativa* identifies important target genes. *Proc Natl Acad Sci USA* **101**, 11511-11516.
- Chu, C.-C.** (1975). Establishment of an efficient medium for anther culture of rice through comparative experiments on the nitrogen sources. *Scientia sinica* **18**, 659-668.
- Cuperus, J.T., Fahlgren, N., and Carrington, J.C.** (2011). Evolution and functional diversification of MIRNA genes. *Plant Cell* **23**, 431-442.
- Frazier, T.P., Xie, F.L., Freistaedter, A., Burklew, C.E., and Zhang, B.H.** (2010). Identification and characterization of microRNAs and their target genes in tobacco (*Nicotiana tabacum*). *Planta* **232**, 1289-1308.
- Godwin, R.M., Rae, A.L., Carroll, B.J., and Smith, F.W.** (2003). Cloning and characterization of two genes encoding sulfate transporters from rice (*Oryza sativa* L.)\*. *Plant and soil* **257**, 113-123.
- Guddeti, S., Zhang, D.C., Li, A.L., Leseberg, C.H., Kang, H., Li, X.G., Zhai, W.X., Johns, M.A., and Mao, L.** (2005). Molecular evolution of the rice miR395 gene family. *Cell Res* **15**, 631-638.
- Hawkesford, M.J.** (2000). Plant responses to sulphur deficiency and the genetic manipulation of sulphate transporters to improve S-utilization efficiency. *J Exp Bot* **51**, 131-138.
- Jagadeeswaran, G., Li, Y.F., and Sunkar, R.** (2014). Redox signaling mediates the expression of a sulfate-deprivation-inducible microRNA395 in *Arabidopsis*. *Plant J* **77**, 85-96.
- Jeong, D.H., Park, S., Zhai, J., Gurazada, S.G., De Paoli, E., Meyers, B.C., and Green, P.J.** (2011). Massive analysis of rice small RNAs: mechanistic implications of

- regulated microRNAs and variants for differential target RNA cleavage. *Plant Cell* **23**, 4185-4207.
- Jones-Rhoades, M.W., and Bartel, D.P.** (2004). Computational identification of plant microRNAs and their targets, including a stress-induced miRNA. *Mol Cell* **14**, 787-799.
- Jones-Rhoades, M.W., Bartel, D.P., and Bartel, B.** (2006). MicroRNAs and their regulatory roles in plants. *Annual Review of Plant Biology* **57**, 19-53.
- Kataoka, T., Hayashi, N., Yamaya, T., and Takahashi, H.** (2004a). Root-to-shoot transport of sulfate in Arabidopsis. Evidence for the role of SULTR3;5 as a component of low-affinity sulfate transport system in the root vasculature. *Plant Physiology* **136**, 4198-4204.
- Kataoka, T., Watanabe-Takahashi, A., Hayashi, N., Ohnishi, M., Mimura, T., Buchner, P., Hawkesford, M.J., Yamaya, T., and Takahashi, H.** (2004b). Vacuolar sulfate transporters are essential determinants controlling internal distribution of sulfate in Arabidopsis. *Plant Cell* **16**, 2693-2704.
- Kawashima, C.G., Yoshimoto, N., Maruyama-Nakashita, A., Tsuchiya, Y.N., Saito, K., Takahashi, H., and Dalmay, T.** (2009). Sulphur starvation induces the expression of microRNA-395 and one of its target genes but in different cell types. *Plant J* **57**, 313-321.
- Kim, J.Y., Lee, H.J., Jung, H.J., Maruyama, K., Suzuki, N., and Kang, H.** (2010). Overexpression of microRNA395c or 395e affects differently the seed germination of Arabidopsis thaliana under stress conditions. *Planta* **232**, 1447-1454.
- Klonus, D., Hofgen, R., Willmitzer, L., and Riesmeier, J.W.** (1994). Isolation and characterization of two cDNA clones encoding ATP-sulfurylases from potato by complementation of a yeast mutant. *Plant J* **6**, 105-112.
- Kopriva, S.** (2006). Regulation of sulfate assimilation in Arabidopsis and beyond. *Ann Bot* **97**, 479-495.
- Kumar, S., Asif, M.H., Chakrabarty, D., Tripathi, R.D., and Trivedi, P.K.** (2011). Differential expression and alternative splicing of rice sulphate transporter family members regulate sulphur status during plant growth, development and stress conditions. *Functional & Integrative Genomics* **11**, 259-273.
- Kurihara, Y., Takashi, Y., and Watanabe, Y.** (2006). The interaction between DCL1 and HYL1 is important for efficient and precise processing of pri-miRNA in plant microRNA biogenesis. *RNA* **12**, 206-212.

- Liang, G., Yang, F., and Yu, D.** (2010). MicroRNA395 mediates regulation of sulfate accumulation and allocation in *Arabidopsis thaliana*. *Plant J* **62**, 1046-1057.
- Liu, Q., Feng, Y., and Zhu, Z.** (2009). Dicer-like (DCL) proteins in plants. *Functional & Integrative Genomics* **9**, 277-286.
- Llave, C., Franco-Zorrilla, J.M., Solano, R., and Barajas, D.** (2011). Target validation of plant microRNAs. *Methods in Molecular Biology* **732**, 187-208.
- Lunn, J.E., Droux, M., Martin, J., and Douce, R.** (1990). Localization of ATP sulfurylase and O-acetylserine (thiol) lyase in spinach leaves. *Plant Physiology* **94**, 1345-1352.
- Matthewman, C.A., Kawashima, C.G., Huska, D., Csorba, T., Dalmay, T., and Kopriva, S.** (2012). miR395 is a general component of the sulfate assimilation regulatory network in *Arabidopsis*. *FEBS Letters* **586**, 3242-3248.
- Murashige, T., and Skoog, F.** (1962). A revised medium for rapid growth and bio assays with tobacco tissue cultures. *Physiologia Plantarum* **15**, 473-497.
- Patron, N.J., Durnford, D.G., and Kopriva, S.** (2008). Sulfate assimilation in eukaryotes: fusions, relocations and lateral transfers. *BMC Evol Biol* **8**, 39.
- Plank, C.O.** (1992). Plant analysis reference procedures for the southern region of the United States. Southern Cooperative Series Bulletin (USA).
- Rotte, C., and Leustek, T.** (2000). Differential subcellular localization and expression of ATP sulfurylase and 5'-adenylylsulfate reductase during ontogenesis of *Arabidopsis* leaves indicates that cytosolic and plastid forms of ATP sulfurylase may have specialized functions. *Plant Physiology* **124**, 715-724.
- Saitou, N., and Nei, M.** (1987). The neighbor-joining method: a new method for reconstructing phylogenetic trees. *Molecular Biology and Evolution* **4**, 406-425.
- Shibagaki, N., Rose, A., McDermott, J.P., Fujiwara, T., Hayashi, H., Yoneyama, T., and Davies, J.P.** (2002). Selenate-resistant mutants of *Arabidopsis thaliana* identify Sultr1;2, a sulfate transporter required for efficient transport of sulfate into roots. *Plant J* **29**, 475-486.
- Smith, F.W., Ealing, P.M., Hawkesford, M.J., and Clarkson, D.T.** (1995). Plant members of a family of sulfate transporters reveal functional subtypes. *Proc Natl Acad Sci USA* **92**, 9373-9377.

- Tabatabai, M., and Bremner, J.** (1970). A simple turbidimetric method of determining total sulfur in plant materials. *Agronomy Journal* **62**, 805-806.
- Takahashi, H.** (2010). Regulation of sulfate transport and assimilation in plants. *International Review of Cell And Molecular biology* **281**, 129-159.
- Takahashi, H., Kopriva, S., Giordano, M., Saito, K., and Hell, R.** (2011). Sulfur assimilation in photosynthetic organisms: molecular functions and regulations of transporters and assimilatory enzymes. *Annual Review of Plant Biology* **62**, 157-184.
- Takahashi, H., Watanabe-Takahashi, A., Smith, F.W., Blake-Kalff, M., Hawkesford, M.J., and Saito, K.** (2000). The roles of three functional sulphate transporters involved in uptake and translocation of sulphate in *Arabidopsis thaliana*. *Plant J* **23**, 171-182.
- Takahashi, H., Yamazaki, M., Sasakura, N., Watanabe, A., Leustek, T., Engler, J.A., Engler, G., Van Montagu, M., and Saito, K.** (1997). Regulation of sulfur assimilation in higher plants: a sulfate transporter induced in sulfate-starved roots plays a central role in *Arabidopsis thaliana*. *Proc Natl Acad Sci USA* **94**, 11102-11107.
- Tamura, K., Stecher, G., Peterson, D., Filipski, A., and Kumar, S.** (2013). MEGA6: Molecular Evolutionary Genetics Analysis version 6.0. *Molecular Biology and Evolution* **30**, 2725-2729.
- Tran, N.** (2009). Fast and Simple micro-RNA Northern Blots. *Biochemistry Insights* **2**, 1-3.
- Voinnet, O.** (2009). Origin, biogenesis, and activity of plant microRNAs. *Cell* **136**, 669-687.
- Wolfe, K.H., Gouy, M., Yang, Y.W., Sharp, P.M., and Li, W.H.** (1989). Date of the monocot-dicot divergence estimated from chloroplast DNA sequence data. *Proc Natl Acad Sci USA* **86**, 6201-6205.
- Xiao, H., Wang, Y., Liu, D., Wang, W., Li, X., Zhao, X., Xu, J., Zhai, W., and Zhu, L.** (2003). Functional analysis of the rice AP3 homologue OsMADS16 by RNA interference. *Plant Molecular Biology* **52**, 957-966.
- Zhang, B., Pan, X., Cobb, G.P., and Anderson, T.A.** (2006a). Plant microRNA: a small regulatory molecule with big impact. *Dev Biol* **289**, 3-16.

- Zhang, B., Pan, X., Cannon, C.H., Cobb, G.P., and Anderson, T.A.** (2006b). Conservation and divergence of plant microRNA genes. *Plant J* **46**, 243-259.
- Zhou, M., Li, D., Li, Z., Hu, Q., Yang, C., Zhu, L., and Luo, H.** (2013). Constitutive expression of a miR319 gene alters plant development and enhances salt and drought tolerance in transgenic creeping bentgrass (*Agrostis stolonifera* L.). *Plant Physiology* **161**, 1375-1391
- Zuckerlandl, E., and Pauling, L.** (1965). Evolutionary divergence and convergence in proteins. *Evolving Genes and Proteins* **97**, 97-166.

## CHAPTER FOUR

*SRF3* PROMOTER, A STRONG NOVEL REGULATORY ELEMENT DRIVES  
CONSTITUTIVE AND TISSUE SPECIFIC GENE EXPRESSION IN DIVERSE  
PLANT SPECIES

## ABSTRACT

Promoter is a critical element in initiating the transcription of downstream coding or noncoding genes in gene expression cassettes. We have identified a new *Arabidopsis* leaf specific promoter, Srf3abc and studied its potential for use in driving tissue-specific expression of foreign genes in various plant species. To evaluate promoter activity and investigate the regulatory pattern of this promoter, we constructed a series of GUS reporter systems, in which GUS gene is under the control of either CaMV 35S, maize *Ubi-1*, full-length or different truncated versions of Srf3abc promoters. GUS staining and activity assay in stable transgenic *Arabidopsis* show that Srf3abc is a strong promoter in *Arabidopsis*, and also functions in driving tissue specific gene expression in other dicot and monocot species. Analysis of different truncated versions of Srf3 promoter also suggest that the *cis* regulatory element resides in the middle part of the Srf3abc promoter, comprising of 3' end of the region a, and 5' end of the region b. Srf3c is the 5' end deletion version of the Srf3abc promoter, which is only 383 bp in size but has strong activity in almost the whole *Arabidopsis* plant except in seeds and most floral organs. When Srf3c was used to drive an herbicide resistant gene *bar*, only transgenic *Arabidopsis* harboring Srf3c-*bar* survived under herbicide treatment. Srf3c can also function in tobacco and creeping bentgrass. Our study not only reveals the *cis* regulatory region in the strong leaf specific promoter, Srf3abc, but also demonstrates the great potential of the small-sized promoter, Srf3abc for use in driving gene expression in various plant species, serving as important tool for agriculture biotechnology.

Key words: promoter, leaf-specific, gene expression, truncation, *Arabidopsis*

## INTRODUCTION

Promoter, which contains *cis* regulatory sequences for RNA polymerases and transcription factors to bind, is a required element in initiating the transcription of downstream coding or noncoding genes in gene expression cassettes. They can be classified into three main groups based on their activity patterns, constitutive, inducible and tissue specific promoters, respectively. In order to efficiently express foreign genes in genetically modified organisms (GMOs), a large number of constitutive promoters that exhibit strong activities in different species and under various conditions have been identified and utilized in transgenic research and product development.

CaMV 35S (Cauliflower Mosaic Virus 35S) promoter is one of the most popular and general-purpose constitutive promoters used in GMOs and biological research (Benfey and Chua, 1990; Odell et al., 1985). It is 343 bp in length, in which the TATA box (TATATAA) is localized between -32 bp to -26 bp. Robert Kay and his colleagues created a stronger artificial CaMV 35S promoter by duplicating its transcription activating sequence (Kay et al., 1987). Though CaMV 35S promoter shows strong activity in dicots, it is not as strong in monocots because of the difference in gene regulation and transcription factors between the two classes (Schledzewski and Mendel, 1994). Later, another strong constitutive promoter, maize *Ubi-1* that controls the expression of a maize ubiquitin gene was isolated from maize genome. The 1.98kb maize *Ubi-1* promoter contains three regions, including the promoter region, the first exon and the first intron (Toki et al., 1992). Ubiquitin proteins' involvement in protein modification and degradation is highly conserved not only across plant kingdom but also among all eukaryotes, so it is reasoned



to utilize the regulatory sequence of ubiquitin to drive gene expression in GMOs efficiently (Christensen and Quail, 1996). The maize *Ubi-1* promoter exhibits very strong activity in most tissues of monocots, and therefore has been widely utilized to drive foreign gene expression in monocot plants (Castillo et al., 1994; Cornejo et al., 1993; Miki et al., 2005; Rooke et al., 2000). Besides CaMV 35S and maize *Ubi-1* promoters, some other constitutive promoters are also broadly used in transgenic plants, such as promoters derived from the *NOS* (Nopaline Synthase) and *OCS* (Octopine Synthase) genes of *Agrobacterium tumefaciens* that have strong activity in dicots (De Block et al., 1984; Ebert et al., 1987; Velten et al., 1984), and rice *actin1* promoter which works very well in monocots (McElroy et al., 1990).

However, constitutive promoters are not always the best option for driving foreign gene expression in transgenic plants. Massive accumulation of heterologous proteins or final metabolites may interrupt the metabolic homeostasis of transgenic plants, which may repress their growth and development, or even cause death. Furthermore, plants have evolved a defense mechanism which monitors and represses expression of a foreign gene to minimize the adverse effect brought by its excess transcripts, leading to a phenomenon called transgene silencing or co-suppression (Dietz-Pfeilstetter, 2010; Kooter et al., 1999; Kumpatla et al., 1998). To avoid the adversity brought by the use of constitutive promoters in transgenic plants, scientists have exploited the potential of many inducible and tissue specific promoters, such as rice original light inducible promoter *rbcS* which is specifically expressed in leaf and stem, heat inducible promoter *Gmhsp17* cloned from soybean, light inducible and green tissue specific rice promoter *Cab1R*, root and seedling specific

promoter *Pyk10* cloned from *Arabidopsis*, fruit specific promoter *E-8* cloned from tomato, and seed specific promoter *napin* cloned from *Brassica napus* (Ellerstrom et al., 1996; Krasnyanski et al., 2001; Luan and Bogorad, 1992; Nitz et al., 2001; Nomura et al., 2000; Schoffl et al., 1989). The advantage of the inducible and tissue specific promoters is that they are only active under certain conditions or in specific tissues, thus reducing the accumulation of heterologous proteins or final metabolites in transgenic plants. However, the activities of most of the inducible and tissue specific promoters are not always as strong as constitutive promoters.

Leaf specific promoter is one of the most useful tissue specific promoters in agriculture industry, because it can reduce accumulation of heterologous proteins or final metabolites in the fruits or seeds of GMOs. So far only one promoter, *Gh-rbcS* identified in cotton has been reported to show predominant leaf specificity (Song et al., 2000). Here we report a newly identified *Arabidopsis* promoter *Srf3abc*. *Srf3abc* is a leaf specific promoter and has activity stronger than CaMV 35S promoter in the leaves of *Arabidopsis*. Truncation in *Srf3abc* abolish its leaf specificity. Some truncated promoters exhibit strong constitutive activity in *Arabidopsis*. The *cis* regulatory region responsible for its leaf specificity is identified. Furthermore, *Srf3abc* and truncated promoters can function in different plant species, including dicots and monocots.

## **RESULT**

### **Identification and cloning of Srf3 promoters**

In search for tissue-specific promoters, we cloned an *Arabidopsis* gene, *SRF3* belonging to a newly identified LRR-RLK (Leucine-rich-repeat Receptor Like Protein Kinase) kinase family, SRF (Stress Responsive Factor) (Figure 2.3). *SRF3* encodes a classic LRR-RLK and specifically expressed in *Arabidopsis* leaf tissue (Figure 4.1). To confirm the leaf specificity of the *SRF3* promoter, the 1534 bp upstream region of the *SRF3* gene was cloned and fused with *GUS* reporter gene for use in plant transformation. The leaf specificity of the *SRF3* gene also prompted us to investigate its upstream *cis* regulatory sequences to dissect the promoter function. To this end, we first conducted bioinformatics analysis using online database PlantCARE to predict the *cis* acting regulatory elements of the *SRF3* promoter (Lescot et al., 2002). We found that *SRF3* promoter comprises not only universal *cis* acting elements such as CAAT-box and TATA-box, but also many specific *cis*-regulatory elements required for stress response and tissue differentiation, such as TC-rich repeats and HD-ZIP1/2 (Appendix Table C-1). Interestingly, no *cis*-regulatory element involved in leaf specific or predominant regulation was predicted.

To identify *cis* regulatory element responsible for its leaf specificity, the *SRF3* promoter was arbitrarily divided into three regions, including Srf3a (-1536 bp - -1035 bp), Srf3b (-1034 bp - -396 bp) and Srf3c (-395 bp – -13 bp). Individual regions (Srf3a, Srf3b, Srf3c) and their pair-wise combinations (Srf3ab, Srf3ac, Srf3bc) were all fused with *GUS* gene and introduced into *Arabidopsis thaliana* (Col-0) for GUS activity investigation (Figure 4.2). We also generated CaMV35S/*GUS* and maize *Ubi-1*/*GUS* transgenic *Arabidopsis* lines as positive controls (Figure 4.2).

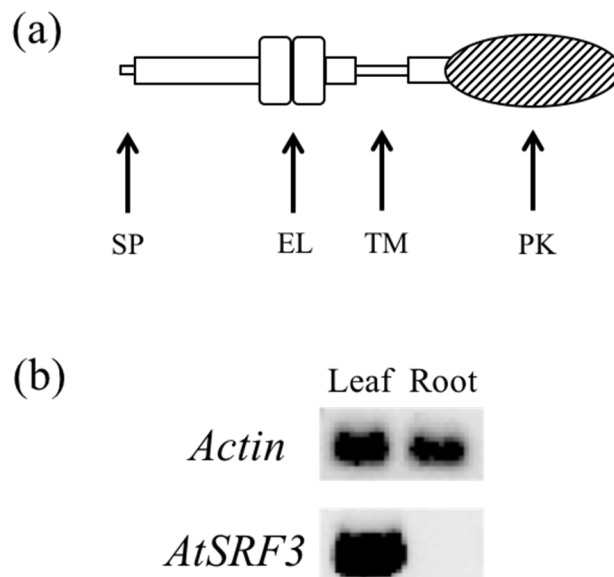


**Figure 4.1. Structure of SRF3 protein and its expression pattern in three-week-old *Arabidopsis*.** (a) SRF3 is a classic Leucine-Rich-Repeat Receptor Like Protein Kinase with a length of 884 amino acid residues, which contains an N-terminal signal peptide (SP), an extracellular domain (EL) with 2 LRRs, a transmembrane domain (TM), and a cytoplasmic protein kinase domain (PK). (b) Tissue-specific expression of *SRF3* in three-week-old *Arabidopsis thaliana*. Roots and leaves collected from three-week-old *Arabidopsis* grown in hydroponic system were used for RT-PCR analysis. *Actin* was used as a reference gene. Experiment was repeated three times.

---

#### Activity of the *Srf3* promoters in *Arabidopsis*

Histochemical localization of GUS in stable transgenic *Arabidopsis* plants was determined using GUS staining assay. In two-week-old *Arabidopsis* plants harboring CaMV35S/GUS and *Ubi-1*/GUS constructs, blue staining indicating GUS activity was observed in both leaves and roots, whereas no blue staining was detected in WT *Arabidopsis* (Figure 4.3 a). Different from the two positive controls, strong GUS staining was only detected in the leaves of the *Srf3abc*/GUS transgenic plants (Figure 4.3 b). However, both leaves and roots of the transgenic *Arabidopsis* lines harboring the six

truncated promoter/GUS constructs were stained blue, indicating that the critical *cis*-regulatory region which is responsible for the leaf specificity of Srf3abc was either deleted or incomplete in the truncated promoters (Figure 4.3 b).

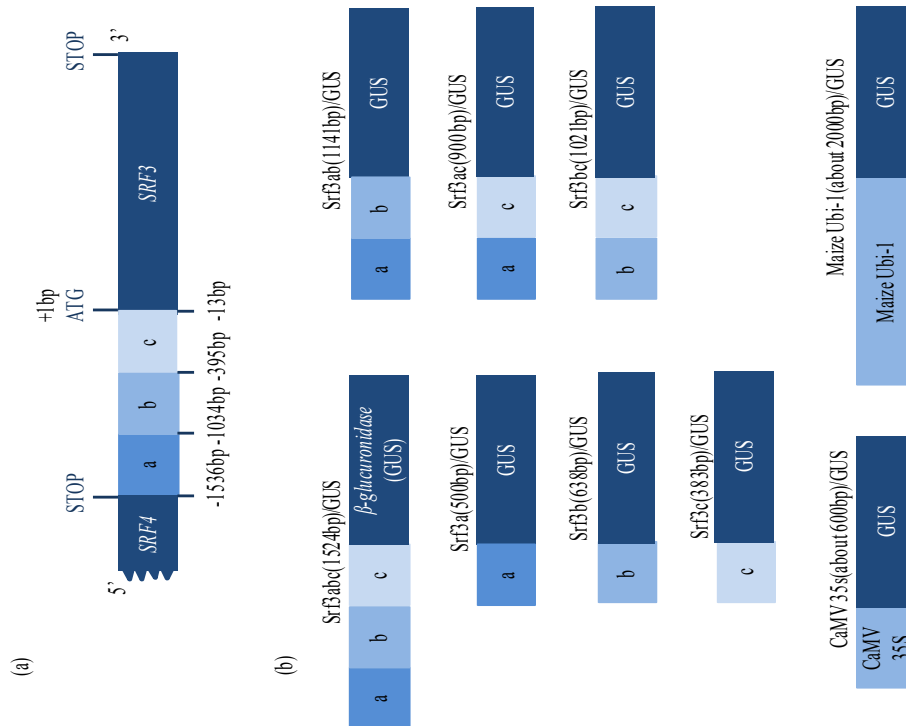


**Figure 4.2. Schematic diagrams of the GUS reporter gene constructs.** (a) 1524 bp upstream promoter regions of *SRF3* gene is arbitrarily divided into three regions, including region a from -1536 bp to -1033 bp (503 bp), region b from -1034 bp to -396 bp (638 bp), and region c from -395 bp to -13 bp (383 bp). STOP: stop codon. (b) Region a, region b, region c, and their combinations were constructed in the upstream of *GUS* gene for analysis of their activities. CaMV 35S and maize *Ubi-1* promoters fused with *GUS* gene were used as positive controls. These constructs were introduced into wild type *Arabidopsis thaliana* (Col-0) using floral dip method. In addition, Srf3abc-GUS was introduced into tobacco and rice. Srf3c-GUS was introduced into tobacco and creeping bentgrass.

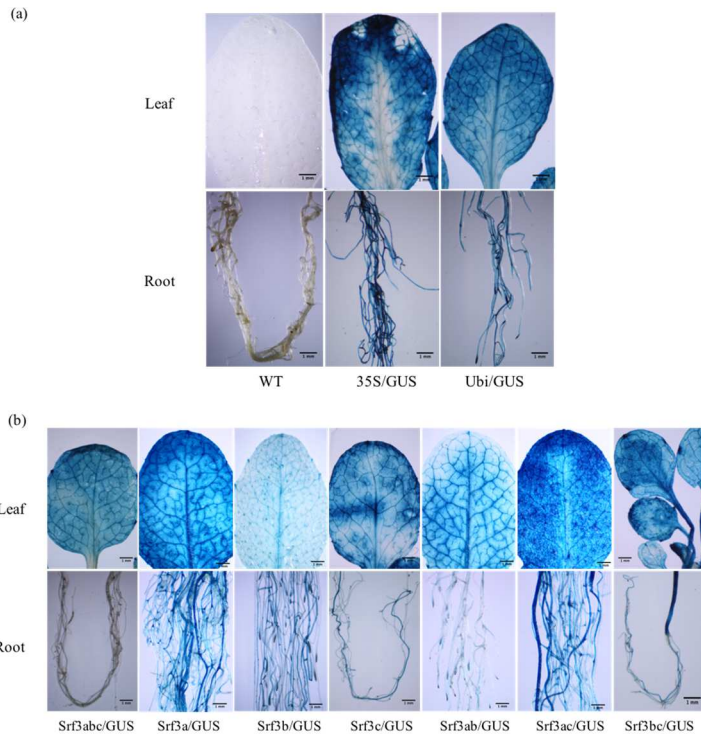


**Figure 4.3. Histochemical GUS staining of the two-week-old *Arabidopsis*.** Wild type, transgenic plants harboring CaMV 35S/GUS or *Ubi-1*/GUS (a), and transgenic lines harboring truncated Srf3 promoter-GUS constructs were histochemically stained for GUS activity. Leaves and roots were detached from the GUS stained *Arabidopsis* and photographed under optical microscope. At least three plants from three independent *Arabidopsis* lines were used for analysis. One representative was exhibited. WT: wild type plant. 35S: CaMV 35S promoter. Ubi: Maize *Ubi-1* promoter. Scale bar: 1 mm.

It is noteworthy that very weak GUS staining was detected in both leaves and roots of Srf3ab/GUS *Arabidopsis* and in the leaves of Srf3b-GUS *Arabidopsis*. Additionally, Srf3ac/GUS *Arabidopsis* gained strong GUS staining in the roots when region b is deleted from Srf3abc (Figure 4.3 b). These observations indicate that region b may play an important role in determining the activity of the Srf3 promoter.

Similar results were obtained in four-week-old flowering *Arabidopsis* plants (Figure 4.4). In 35S/GUS transgenic plants, GUS staining was observed in leaves, roots, siliques and all floral organs including sepals, petals, filaments, anthers, style and stigma. GUS gene was also expressed in most of the tissues except anthers and siliques in Ubi/GUS transgenic plants (Figure 4.4 a). In Srf3abc/GUS *Arabidopsis*, blue staining was limited to leaves and sepals with slightly or no blue staining observed in roots (Figure 4.4 b), which

provides another piece of evidence indicating that Srf3abc is a leaf specific promoter in *Arabidopsis*. In roots, all transgenic *Arabidopsis* harboring promoters comprising the region b (Srf3abc, Srf3b, Srf3ab and Srf3bc) exhibited much weaker GUS staining than transgenic *Arabidopsis* harboring promoters without region b (Srf3ac, Srf3a, Srf3c) (Figure 4.4 b). Additionally, Srf3b/GUS and Srf3ab/GUS *Arabidopsis* have very weak GUS staining in their leaves and sepals, and no blue staining was observed in any other tissues of both transgenic lines (Figure 4.4 b). These results point to the important regulatory function of the region b.

To quantitatively measure the GUS activity in four-week-old transgenic *Arabidopsis*, GUS activity assay was conducted. In roots, all of the three Srf3 promoters comprising no region b (Srf3ac, Srf3a, Srf3c) exhibited stronger activities than the two constitutive promoters (CaMV 35S and maize *Ubi-1*), while Srf3abc, Srf3b, Srf3ab and Srf3bc have similar or lower activities compared to the two positive controls (Figure 4.5 a). In leaves, Srf3abc exhibited the strongest activity while Srf3ab did not show any activity (Figure 4.5 b). In stem tissues, the GUS activities of the three promoters comprising the region c (Srf3c, Srf3ac and Srf3bc) are similar or higher than CaMV 35S and maize *Ubi-1* promoters (Figure 4.5 c). However, promoters without the regions c (Srf3b, Srf3ab, Srf3a) and Srf3abc promoter has no or very weak activity in the stem tissues (Figure 4.5 c). In *Arabidopsis* seeds, none of these seven Srf3 promoters was active (Figure 4.5 d), which is consistent with the histochemical GUS staining results.

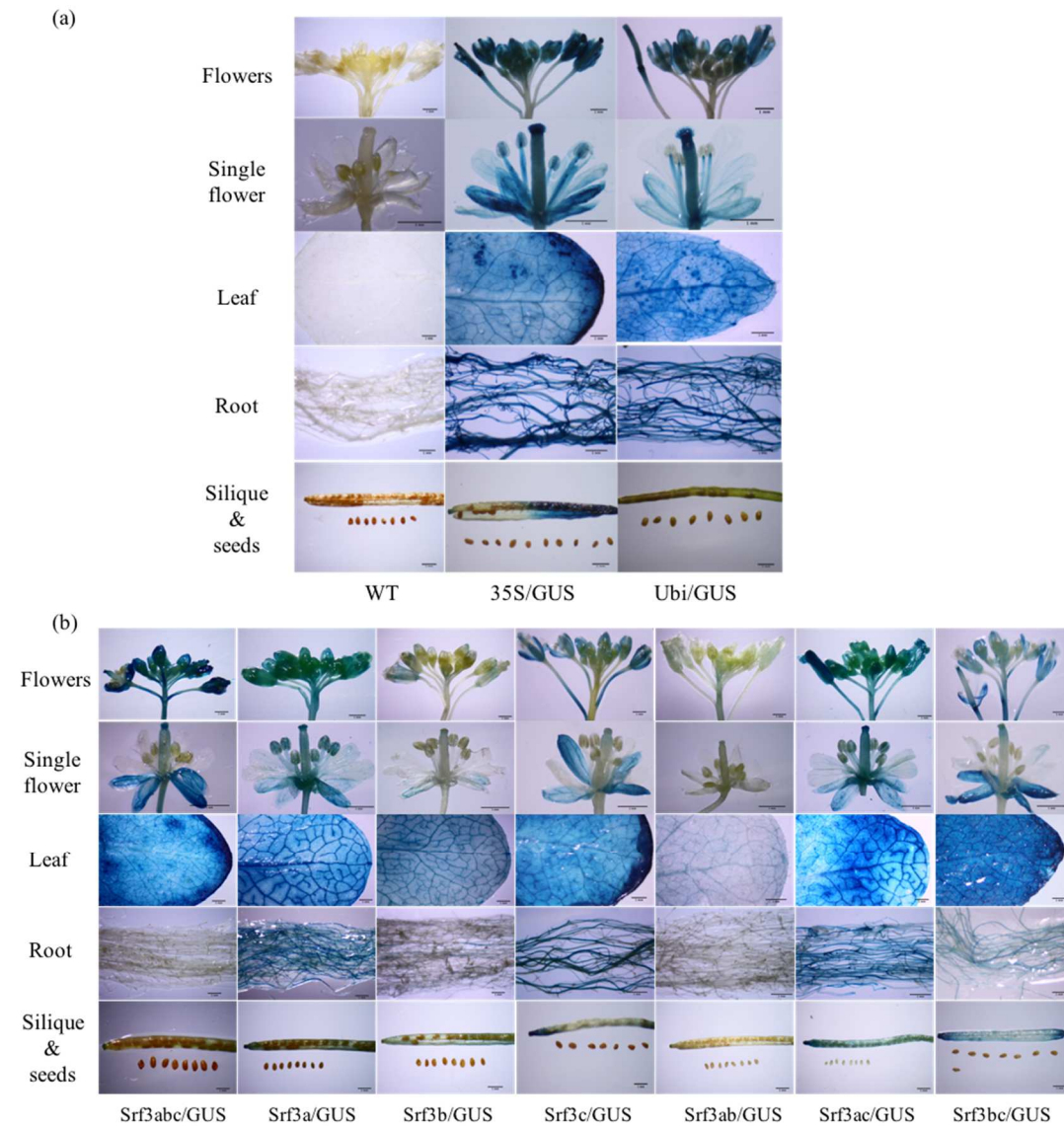


**Figure 4.4. Histochemical GUS staining of the four-week-old *Arabidopsis*.** (a) Wild type, CaMV 35S/GUS transgenic, maize *Ubi-1*/GUS transgenic *Arabidopsis*, and (b) transgenic plants harboring different versions of the truncated Srf3 promoter/GUS constructs were histochemically stained for GUS activity. Rosette leaves, roots, flowers, siliques and seeds were detached from the GUS stained *Arabidopsis* and photographed under optical microscope. At least three plants from three independent *Arabidopsis* lines were used for analysis. One representative was exhibited. WT: wild type plant. 35S: CaMV 35S promoter. Ubi: Maize *Ubi-1* promoter. Scale bar: 1 mm.



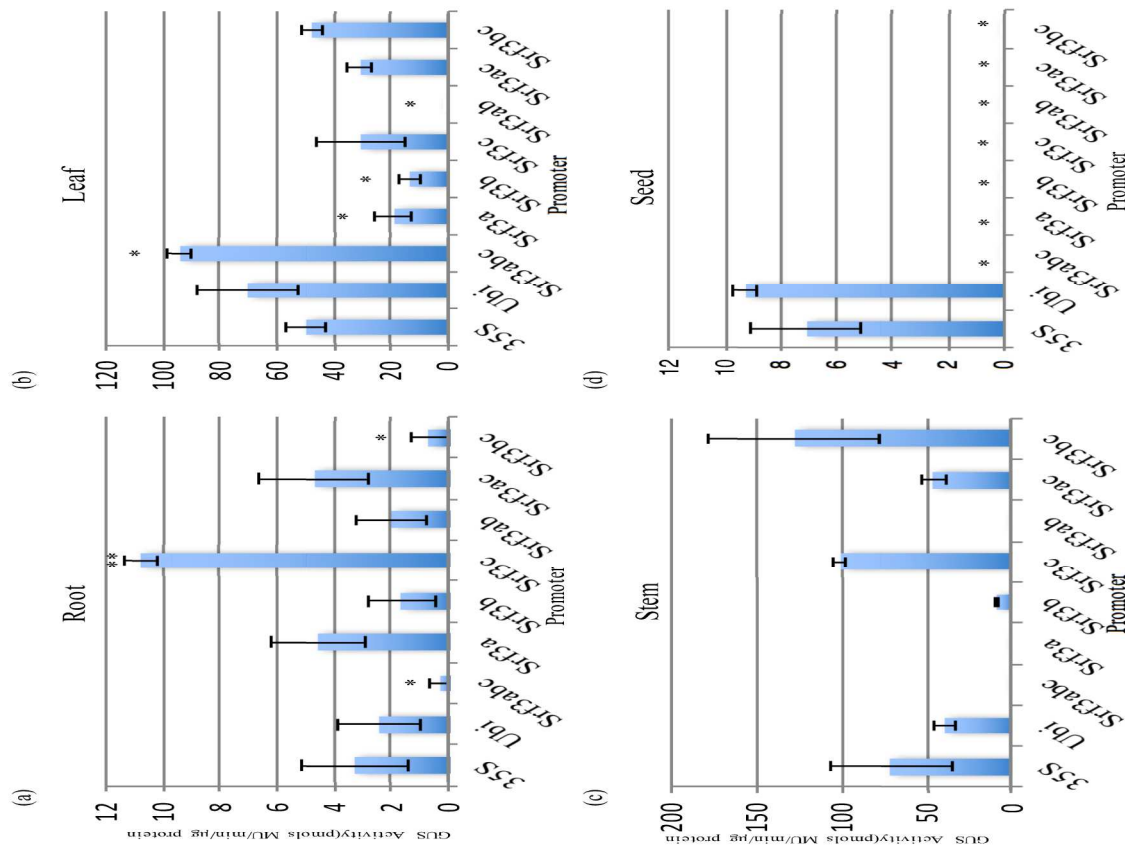


**Figure 4.5. Quantitative measurement of GUS activities in transgenic *Arabidopsis*.** (a) Promoter strength (measured as GUS activity) in *Arabidopsis* roots. Plant roots were harvested from four-week-old transgenic *Arabidopsis*. For each transgenic *Arabidopsis* line, data are presented as means of three technical replicates and three biological replicates of two independent events, error bar represents SD (n=18). Promoter strength (measured as GUS activity) in transgenic *Arabidopsis* leaves (b), stem (c) and seeds (d). For each transgenic line, samples were harvested from pooled plant tissues taken from at least seven independent events. Data are presented as means of three technical replicates and three biological replicates, error bar represents SD (n=9). Asterisks indicate the significant difference between CaMV 35S and other promoters. P<0.05 was considered to be statistically significant and marked as \*. P<0.01 was considered to be statistically highly significant and marked as \*\*. 35S: CaMV 35S promoter. Ubi: Maize *Ubi-1* promoter.

### Srf3c actively drives a Selectable Marker Gene (SMG) in transgenic *Arabidopsis*

To assess the feasibility of Srf3c for use in driving foreign gene expression in plants, we prepared a construct in which Srf3c was fused with *bar* gene, which is a broadly

used SMG conferring herbicide resistance (Figure 4.6 A). This construct was introduced into *Arabidopsis* using floral dip method. Seeds were then collected and sowed in soil. Two weeks later, *Arabidopsis* seedlings were sprayed with PPT (phosphinothricin). Figure 4.6 b shows that transgenic *Arabidopsis* plants harboring Srf3c/*bar* expression cassette survived, indicating that Srf3c could be used as an effective promoter to drive SMG or other genes of interest for developing GMO products.

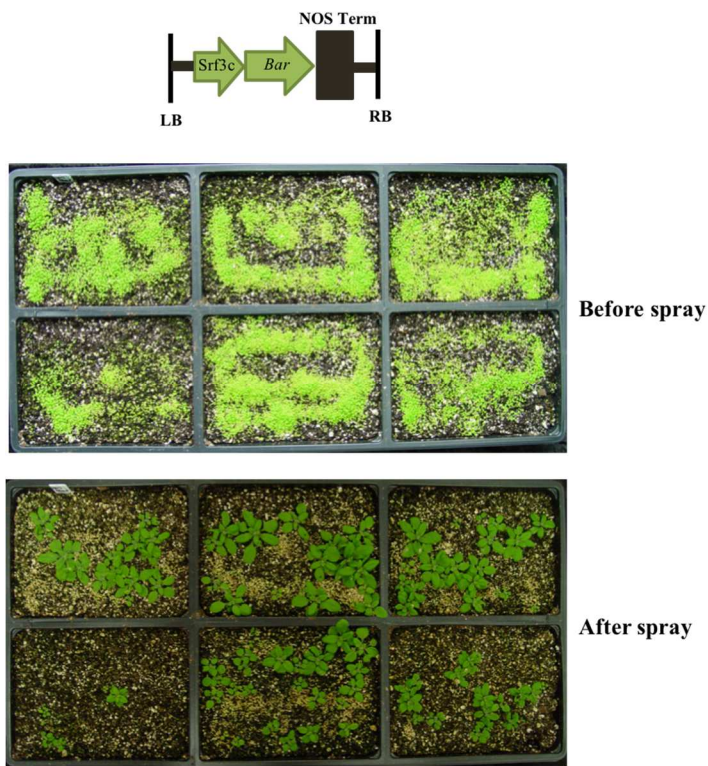


**Figure 4.6. Srf3c promoter drives foreign gene expression in transgenic *Arabidopsis*.**

(a) Schematic diagram of the Srf3c/*bar* construct. Srf3c promoter was inserted in the upstream of *bar* gene. LB: Left border. RB: right border. *bar*: phosphinothricin N-acetyltransferase. NOS term: nos terminator. (b) Srf3c/*bar* was introduced into wild type *Arabidopsis thaliana* (Col-0) using floral dip method. Seeds were then harvested and germinated in soil. After two weeks of growth, *Arabidopsis* seedling were sprayed with 0.5% PPT. Pictures were taken before and after herbicide spraying.

---

### Activity of the Srf3 promoters in other plant species

To test whether Srf3 promoter is active across species, Srf3abc/GUS and Srf3c-GUS were introduced into another dicot plant species, tobacco (*Nicotiana tabacum*) and their activities were assessed. As shown in Figure 4.7, constitutive promoter CaMV 35S

exhibited strong and universal activity in all of the tobacco developmental stages, while the activity of maize *Ubi-1* was very weak in young plants (Figure 4.7 a and b). Unlike CaMV 35S, Srf3abc was active exclusively in tobacco leaves, and its activity was much stronger than maize *Ubi-1* promoter, suggesting that Srf3abc can function as a strong leaf specific promoter in tobacco (Figure 4.7 a and c). Though Srf3c was only active in the leaves of young plants (Figure 4.7 a and b), it functioned as a strong universal promoter in flowering plants (Figure 4.7 c).

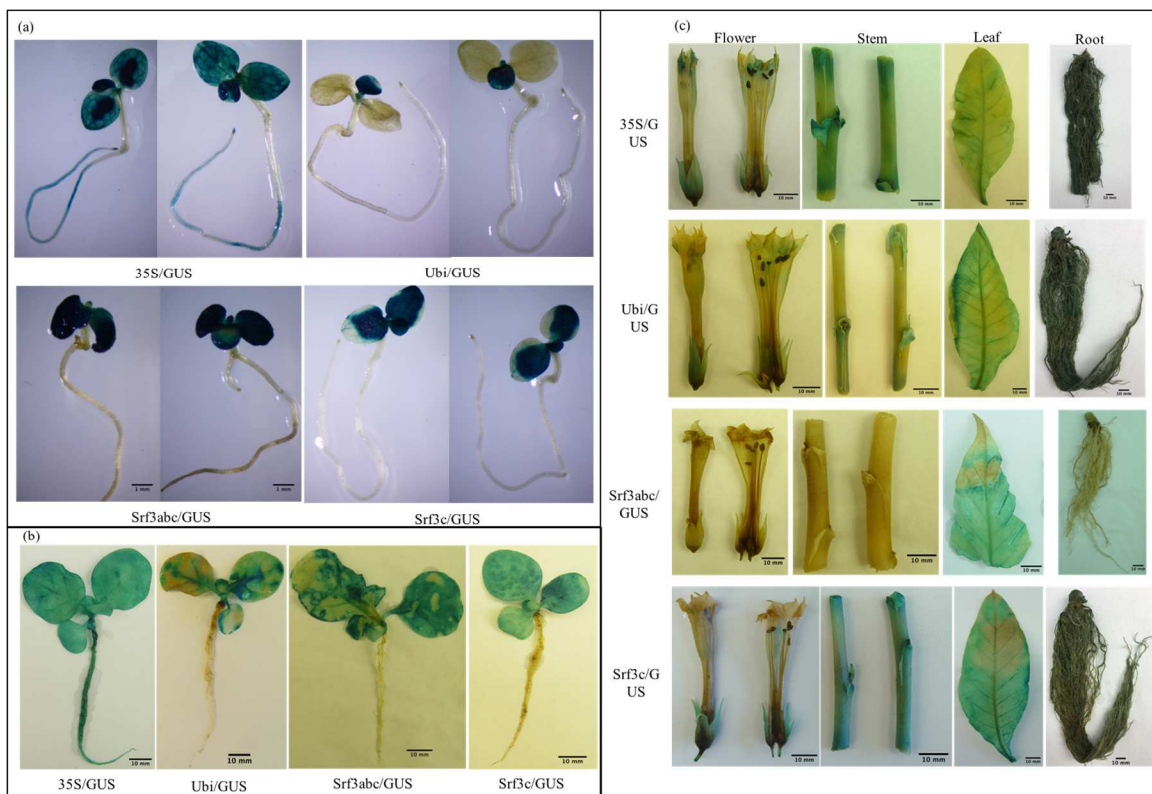


**Figure 4.7. Histochemical GUS staining of transgenic tobacco.** (a) Seven-day-old, (b) three-week-old, and (c) flowering transgenic tobacco (*Nicotiana tabacum*) harboring CaMV 35S/GUS, maize *Ubi-1*/GUS, Srf3abc-GUS or Srf3c-GUS were used for histochemical GUS staining. For seven days and three-week-old tobacco, whole plants were GUS stained and photographed. For flowering tobacco, flowers, stem, leaves and roots were detached for GUS staining. At least three plants from three independent

(Figure 4.7. continued) transgenic lines were used for analysis. One representative was exhibited. 35S: CaMV 35S promoter. Ubi: Maize *Ubi-1* promoter. Scale bar: 10 mm.

---

We also tested the activity of Srf3abc in rice (*Oryza sativa*) and the activity of Srf3c in creeping bentgrass (*Agrostis stolonifera*). In the Srf3abc/GUS transgenic rice, GUS staining was very weak in the leaves, nodes and husk, while no GUS staining was observed in the seeds and roots (Figure 4.8 a). Surprisingly, Srf3c exhibited strong and universal activity in creeping bentgrass (Figure 4.8 b), suggesting its potential for use driving gene expression in monocot plants.

## DISCUSSION

Our results demonstrate that Srf3abc is a leaf specific promoter (Figure 4.3 b and 4.4 b), suggesting its potential as a valuable molecular tool used to drive gene expression in GMOs. However, Srf3abc (1524 bp) is relative large compared to CaMV 35S promoter (~600 bp). In order to identify *cis*-regulatory elements in Srf3abc promoter that confers leaf specificity and reduce its size for future application, a series of truncated versions of the Srf3abc promoter were constructed and their activities were tested in *Arabidopsis*. Based on our histochemical GUS staining and quantitative GUS activity results, Srf3 promoters without region b, including Srf3a, Srf3c and Srf3ac, have strong activities in leaves, roots, stems, flowers, and siliques in four-week-old *Arabidopsis* (Figure 4.4 b and Figure 4.5). This result indicates that the region b may have important regulatory function in Srf3abc promoter.

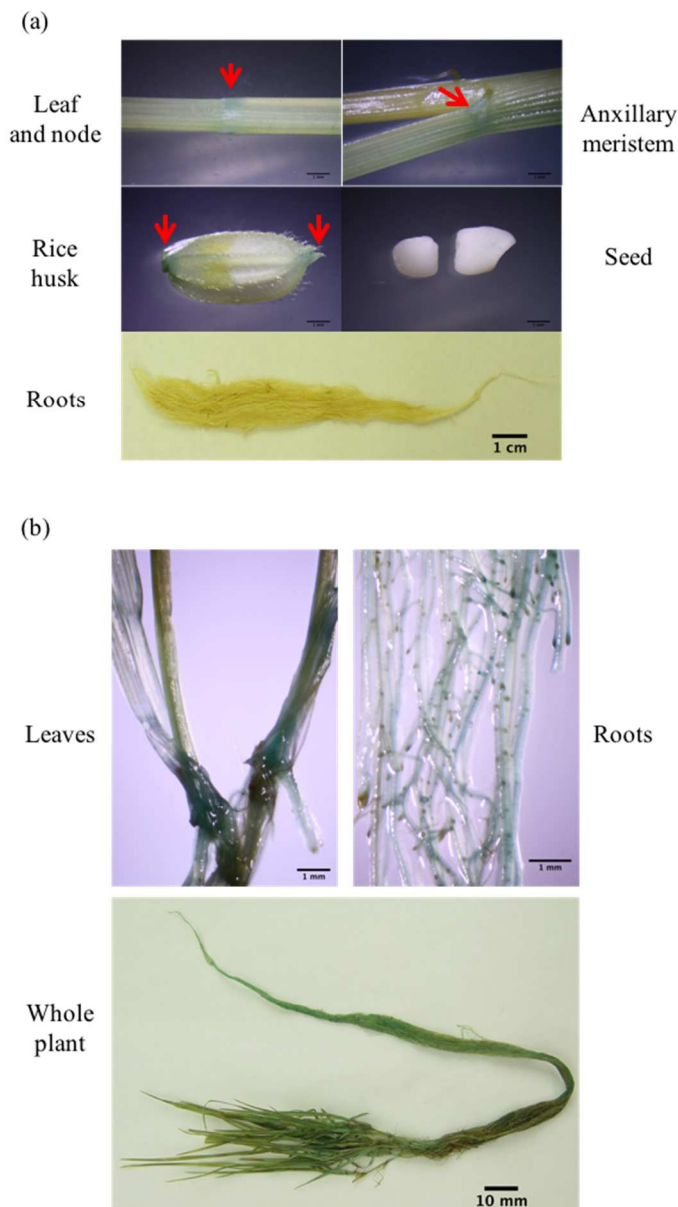


**Figure 4.8. Histochemical GUS staining of the transgenic rice and creeping bentgrass.** (a) Flowering transgenic rice (*Oryza sativa*) harboring Srf3abc-GUS was histochemically stained for GUS activity. Leaves, roots and seeds were first detached from plants and then GUS stained. Plants from three transgenic events were analyzed. One representative was exhibited. (b) Transgenic creeping bentgrass (*Agrostis stolonifera*) harboring Srf3c-GUS was histochemically stained for GUS staining. Plants from three transgenic events were analyzed. One representative was exhibited.

---

In Srf3bc/GUS transgenic *Arabidopsis*, GUS staining was observed in leaves, roots, stems, sepals and siliques, which is as strong as observed in Srf3c/GUS transgenic *Arabidopsis* except in roots. However, in Srf3abc/GUS transgenic *Arabidopsis*, GUS staining can only be detected in leaves and sepals (Figure 4.4 b and Figure 4.5). These

results indicate that the region b alone is not sufficient to repress the constitutive activity of the region c and part of the region a may work together with the region b to perform a function in repressing gene expression.

Srf3b has weak activity in leaves, roots, stems, sepals and siliques. When it is fused with the region a to form Srf3ab promoter, GUS staining becomes weaker and could only be observed in leaves (Figure 4.4 b and Figure 4.5). These results are another piece of evidence suggesting that the *cis*-regulatory element which restricts Srf3abc promoter to function specifically in leaves also comprises part of the region a.

Based on these results, we proposed a model here regarding the regulatory pattern of Srf3abc promoter. As shown in Figure 4.9, Srf3abc comprises three functional regions. The first region is localized in the 5' end of the region a, and functions as a strong constitutive promoter. The second region is comprised of 3' end of the region a, and 5' end of the region b, which is the *cis*-regulatory region and responsible for the leaf specificity of Srf3abc promoter. The *cis* regulatory region can repress the activity of the first constitutive promoter completely. There is another strong constitutive promoter including the 3' end of the region b and the whole region c. Its function can be partially repressed by the middle *cis* regulatory region.

#### ***Potential applications of Srf3 promoters***

In this study, we showed that Srf3c has very strong activities in almost the whole *Arabidopsis* plant except in seeds and most floral organs. Furthermore, Srf3c was successfully used to drive *bar* gene in *Arabidopsis* (Figure 4.6).

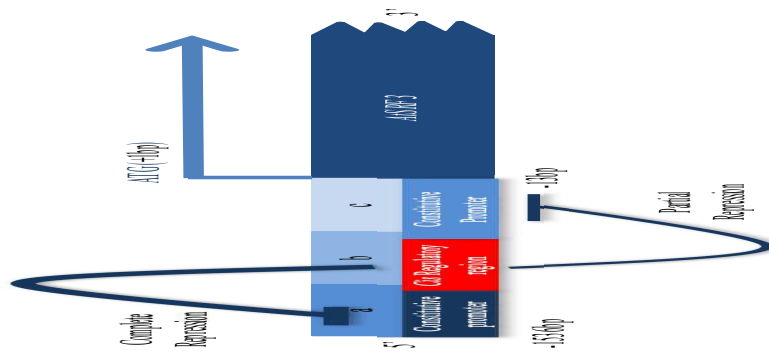


**Figure 4.9. Putative structure of the Srf3abc promoter.** Based on the GUS staining and activity results, we speculate that the Srf3abc promoter comprises three functional regions, including two constitutive promoter regions and one *cis* regulatory region. The first constitutive promoter region is localized in the 5' end of the region a, which functions in whole *Arabidopsis* plant except stem and seeds. The *cis* regulatory region is localized in the 3' end of the region a, and 5' end of the region b. The second constitutive promoter region resides in the 3' end of the region b, and across the whole region c, which functions in whole *Arabidopsis* plant except in seeds and floral organs. The *cis*-regulatory region can completely repress the activity of the first constitutive promoter region, but it can only partially repress the activity of the second constitutive promoter region, making Srf3abc a leaf specific promoter.

Constitutive promoters, such as CaMV 35S, are usually used to drive SMGs (Selectable Marker Genes) in transgenic plants, because high expression levels of selectable markers could avoid regeneration of false positive transgenic plants during plant transformation process. Though there is no evidence showing that foreign proteins encoded by SMGs such as PAT (Phosphinothricin Acetyl Transferase) and HPTII (Hygromycin Phosphotransferase II) and SMGs themselves in GMOs will bring any harmful consequence, the public are still concerned about the safety of GMOs (Fuchs et al., 1993; Herouet et al., 2005). A couple of methods including co-transformation and recombinase-mediated excision have been developed and adopted to generate maker-free GMOs, but these methods require complicated breeding process, causing the deletion of SMGs in

GMOs time-consuming and low efficient (Jia et al., 2006; Komari et al., 1996; Mizutani et al., 2012). Using tissue specific promoters to drive SMGs is a more convenient method since it can confine the expression of SMGs in certain tissues to eliminate or reduce the accumulation of foreign proteins in fruits, seeds or other edible tissues of GMOs, making the deletion of SMGs from GMOs unnecessary. Because of its short length (383 bp) and strong activity in certain tissues, Srf3c is an ideal candidate promoter, which can be used in GMOs for edible seeds.

In this study, we also showed that Srf3c could function in dicot plant, tobacco and monocot plant, creeping bentgrass (Figure 4.7 and Figure 4.8 b). With a length of only 383 bp, Srf3c is an ideal constitutive promoter that can function across both dicot and monocot species, making it very useful in developing GMOs and basic research.

In addition to Srf3c, Srf3abc has very strong activity in *Arabidopsis* leaves, and it can also function in tobacco (Figure 4.7 and Figure 4.8 a). These results suggest that Srf3abc could be used as a strong leaf specific promoter in dicot plants.

In the future, we first need to identify the exact region of the *cis* regulatory element responsible for the leaf specificity of Srf3abc promoter. Once this region is identified and cloned, it could be fused with constitutive promoters such as CaMV 35S and maize *Ubi-1*, making them become strong leaf specific promoters. Second, we need to further verify that Srf3 promoters are universal promoters functioning across various species. We will introduce them to other plant species including both dicot plants and monocot plants to test their activities.



## **MATERIALS AND METHODS**

### **Plant materials and growth conditions**

*Arabidopsis thaliana* (Col-0) was grown on half Murashige and Skoog plates or in soil under a 16 h-day/8 h-night photoperiod at 22 °C-day/20 °C-night in growth chamber.

For RT-PCR experiment, *Arabidopsis thaliana* was grown in hydroponic system under a 16 h-day/8 h-night photoperiod at 22 °C-day/20 °C-night in growth chamber (Huttner and Bar-Zvi, 2003).

Rice, tobacco and creeping bentgrass were grown in soil in greenhouse under a 12 h-light/12 h-dark photoperiod at 27 °C.

### **DNA and RNA isolation, RT-PCR analysis**

Plant genomic DNA used for promoter cloning was isolated from wild type *Arabidopsis* Col-0 following previously described cetyltrimethylammonium bromide method (Luo et al., 2005).

Total RNA were extracted from 100 mg leaf or root tissues with Trizol reagent (Ambion, USA). 2 µg RNA was then treated with RNase-free DNase I (Invitrogen, USA) to remove genomic DNA and used for synthesis of the first strand cDNA with reverse transcriptase (Invitrogen USA). Synthesized cDNA were then diluted for RT-PCR analysis.

Primers used for RT-PCR analysis were listed in Appendix Table C-2.

### **Binary vector construction and plant transformation**

1524 bp upstream promoter regions of *SRF3* gene was amplified from *Arabidopsis* genomic DNA using iProof high-fidelity DNA polymerase (Bio-Rad, USA) and subcloned into pGEM®-T Easy Vector (Promega, USA). This T-easy vector was transformed into *E.coli* DH5-alpha for propagation, followed by extraction and digestion with HindIII and XhoI. The Srf3abc fragment with 5' XhoI sticky end and 3' HindIII sticky end was then purified by using QIAquick Gel Extraction Kit (Qiagen, Germany) and inserted into the XhoI and HindIII digested binary vector pSBbar#5-GUS-nos in the upstream of *GUS* gene using T4 ligase (NEB, USA), resulting in *Srf3abc/GUS/nos*.

Similar strategy was performed to generate binary vectors harboring *Srf3/GUS/nos*, *Srf3b/GUS/nos*, *Srf3c/GUS/nos*, *Srf3ab/GUS/nos* and *Srf3bc/GUS/nos*.

Overlapping PCR was performed to generate *Srf3ac-GUS-nos*. Specifically, reverse primer used to clone region a was designed to have a 5' overhang complementary to 5' end of the forward primer used to clone region c. In the first round of PCR amplification, region a and region c were amplified separately. In the second round of PCR amplification, the two PCR products were mixed and PCR was carried out using the forward primer for region a and reverse primer for region c. *Srf3ac* fragment was then inserted into the pSBbar#5-GUS-nos to generate *Srf3ac-GUS-nos* following the same strategy described above.

All the primers used for plasmid construction were listed in Appendix Table C-2.

CaMV 35S fragment with BamHI overhangs at both ends was ligated to the BamHI digested sites of pSBbar#5-GUS-nos to fuse with *GUS* gene.

Binary vectors were then transformed into *Agrobacterium tumefaciens* strain LBA4404 by electroporation for plant transformation. *Arabidopsis thaliana* transformation, tobacco transformation, rice transformation and creeping bentgrass transformation were performed as previously described methods (Clough and Bent, 1998; Horsch et al., 1985; Luo et al., 2004; Toki, 1997).

### **Histochemical GUS staining**

GUS activity was assayed by histochemical staining with X-Gluc (Biosynth AG, Switzerland). Generally, plant samples immersed in 100 µl to 10 mL reaction buffer (50 mM NaPO<sub>4</sub> pH 7.0, 0.2% Triton X, 2 mM Potassium Ferrocyanide, 2 mM Potassium Ferricyanide, 1 mM X-Gluc) were vacuum infiltrated for 10 min twice, followed by incubation at 37 °C overnight. Prior to photography, plant samples were destained in 70% ethanol (Jefferson et al., 1987).

### **Quantitative measurement of GUS activity**

GUS activity was determined according to the previously described method with minor modification (Francis and Spiker, 2005; Jefferson et al., 1987).

Generally, 100 mg plant sample was grinded in extraction buffer (50 mM NaHPO<sub>4</sub> pH 7.0, 10 mM Na<sub>2</sub>EDTA, 10 mM β-mercaptoethanol, 0.1% Triton X-100, 0.1% sarcosyl, 140 µM PMSF) on ice followed by centrifugation for 15 min at 13000 rpm at 8 °C. 400 µl supernatant was transferred to a clean 1.5 ml microcentrifuge tube. 10 µl supernatant was then transferred to a new tube with 130 µl assay buffer (extraction buffer with 2 mM 4-

methylumbelliferyl  $\beta$ -D-glucuronide (4-MUG) as substrate) and incubated in 37 °C under dark condition for 25 min. 10  $\mu$ l reaction solution was transferred to a 96-well microtiter plate with 190  $\mu$ l stop buffer (0.2 M Sodium Carbonate, anhydrous) to quench the reaction. Fluorescence intensity of the reaction product 4-methylumbelliferyl (4-MU) was measured in a microplate reader at an emission wavelength of 480 nm and an excitation wavelength of 360 nm. Protein concentration was determined following Bradford's method (Bradford, 1976). GUS activity was finally expressed in pmol 4-MU/min/ $\mu$ g protein unit.

#### **Accession numbers**

Sequence data from this article can be found in the *Arabidopsis* Genome Initiative database under the following accession numbers: *SRF3* (AT1G51805), *Actin2* (AT3G18780)

## REFERENCES

- Benfey, P.N. and Chua, N.H.** (1990). The Cauliflower Mosaic Virus 35S Promoter: Combinatorial Regulation of Transcription in Plants. *Science* **250**, 959-966.
- Bradford, M.M.** (1976). A rapid and sensitive method for the quantitation of microgram quantities of protein utilizing the principle of protein-dye binding. *Anal Biochem* **72**, 248-254.
- Castillo, A.M., Vasil, V. and Vasil, I.K.** (1994). Rapid Production of Fertile Transgenic Plants of Rye (*Secale-Cereale* L). *Bio-Technol* **12**, 1366-1371.
- Christensen, A.H. and Quail, P.H.** (1996). Ubiquitin promoter-based vectors for high-level expression of selectable and/or screenable marker genes in monocotyledonous plants. *Transgenic Research* **5**, 213-218.
- Clough, S.J. and Bent, A.F.** (1998). Floral dip: a simplified method for *Agrobacterium*-mediated transformation of *Arabidopsis thaliana*. *Plant J* **16**, 735-743.
- Cornejo, M.J., Luth, D., Blankenship, K.M., Anderson, O.D. and Blechl, A.E.** (1993). Activity of a maize ubiquitin promoter in transgenic rice. *Plant Molecular Biology* **23**, 567-581.
- De Block, M., Herrera-Estrella, L., Van Montagu, M., Schell, J. and Zambryski, P.** (1984). Expression of foreign genes in regenerated plants and in their progeny. *EMBO J* **3**, 1681.
- Dietz-Pfeilstetter, A.** (2010). Stability of transgene expression as a challenge for genetic engineering. *Plant Science* **179**, 164-167.
- Ebert, P.R., Ha, S.B. and An, G.** (1987). Identification of an essential upstream element in the nopaline synthase promoter by stable and transient assays. *Proc Natl Acad Sci USA* **84**, 5745-5749.
- Ellerstrom, M., Stalberg, K., Ezcurra, I. and Rask, L.** (1996). Functional dissection of a napin gene promoter: identification of promoter elements required for embryo and endosperm-specific transcription. *Plant Molecular Biology* **32**, 1019-1027.
- Francis, K.E. and Spiker, S.** (2005). Identification of *Arabidopsis thaliana* transformants without selection reveals a high occurrence of silenced T-DNA integrations. *Plant J* **41**, 464-477.

- Fuchs, R.L., Ream, J.E., Hammond, B.G., Naylor, M.W., Leimgruber, R.M. and Berberich, S.A.** (1993). Safety Assessment of the Neomycin Phosphotransferase-II (NptII) Protein. *Bio-Technol* **11**, 1543-1547.
- Herouet, C., Esdaile, D.J., Mallyon, B.A., Debruyne, E., Schulz, A., Currier, T., Hendrickx, D., van der Klis, R.J. and Rouan, D.** (2005). Safety evaluation of the phosphinothricin acetyltransferase proteins encoded by the pat and bar sequences that confer tolerance to glufosinate-ammonium herbicide in transgenic plants. *Regul Toxicol Pharm* **41**, 134-149.
- Horsch, R., Fry, J., Hoffmann, N., Eichholtz, D., Rogers, S.a. and Fraley, R.** (1985). A simple and general method for transferring genes into plants. *Science* **227**, 1229-1231.
- Huttner, D. and Bar-Zvi, D.** (2003). An improved, simple, hydroponic method for growing *Arabidopsis thaliana*. *Plant Molecular Biology Reporter* **21**, 59-63.
- Jefferson, R.A., Kavanagh, T.A. and Bevan, M.W.** (1987). GUS fusions: beta-glucuronidase as a sensitive and versatile gene fusion marker in higher plants. *Embo J* **6**, 3901-3907.
- Jia, H.G., Pang, Y.Q., Chen, X.Y. and Fang, R.X.** (2006). Removal of the selectable marker gene from transgenic tobacco plants by expression of cre recombinase from a tobacco mosaic virus vector through agroinfection. *Transgenic Research* **15**, 375-384.
- Kay, R., Chan, A., Daly, M. and McPherson, J.** (1987). Duplication of CaMV 35S Promoter Sequences Creates a Strong Enhancer for Plant Genes. *Science* **236**, 1299-1302.
- Komari, T., Hiei, Y., Saito, Y., Murai, N. and Kumashiro, T.** (1996). Vectors carrying two separate T-DNAs for co-transformation of higher plants mediated by *Agrobacterium tumefaciens* and segregation of transformants free from selection markers. *Plant J* **10**, 165-174.
- Kooter, J.M., Matzke, M.A. and Meyer, P.** (1999). Listening to the silent genes: transgene silencing, gene regulation and pathogen control. *Trends Plant Sci* **4**, 340-347.
- Krasnyanski, S.F., Sandhu, J., Domier, L.L., Buetow, D.E. and Korban, S.S.** (2001). Effect of an enhanced CaMV 35S promoter and a fruit-specific promoter on UDA gene expression in transgenic tomato plants. *In Vitro Cell Dev-Pl* **37**, 427-433.

- Kumapatla, S.P., Chandrasekharan, M.B., Iyer, L.M., Guofu, L. and Hall, T.C.** (1998). Genome intruder scanning and modulation systems and transgene silencing. *Trends in Plant Science* **3**, 97-104.
- Lescot, M., Dehais, P., Thijs, G., Marchal, K., Moreau, Y., Van de Peer, Y., Rouze, P. and Rombauts, S.** (2002). PlantCARE, a database of plant cis-acting regulatory elements and a portal to tools for in silico analysis of promoter sequences. *Nucleic Acids Res* **30**, 325-327.
- Luan, S. and Bogorad, L.** (1992). A rice cab gene promoter contains separate cis-acting elements that regulate expression in dicot and monocot plants. *Plant Cell* **4**, 971-981.
- Luo, H., Hu, Q., Nelson, K., Longo, C., Kausch, A.P., Chandlee, J.M., Wipff, J.K. and Fricker, C.R.** (2004). Agrobacterium tumefaciens-mediated creeping bentgrass (*Agrostis stolonifera* L.) transformation using phosphinothricin selection results in a high frequency of single-copy transgene integration. *Plant Cell Rep* **22**, 645-652.
- Luo, H., Kausch, A.P., Hu, Q., Nelson, K., Wipff, J.K., Fricker, C.C., Owen, T.P., Moreno, M.A., Lee, J.-Y. and Hodges, T.K.** (2005). Controlling transgene escape in GM creeping bentgrass. *Molecular Breeding* **16**, 185-188.
- McElroy, D., Zhang, W., Cao, J. and Wu, R.** (1990). Isolation of an efficient actin promoter for use in rice transformation. *The Plant Cell Online* **2**, 163-171.
- Miki, D., Itoh, R. and Shimamoto, K.** (2005). RNA silencing of single and multiple members in a gene family of rice. *Plant Physiology* **138**, 1903-1913.
- Mizutani, O., Masaki, K., Gomi, K. and Iefuji, H.** (2012). Modified Cre-loxP Recombination in *Aspergillus oryzae* by Direct Introduction of Cre Recombinase for Marker Gene Rescue. *Appl Environ Microb* **78**, 4126-4133.
- Nitz, I., Berkefeld, H., Puzio, P.S. and Grundler, F.M.W.** (2001). Pyk10, a seedling and root specific gene and promoter from *Arabidopsis thaliana*. *Plant Science* **161**, 337-346.
- Nomura, M., Katayama, K., Nishimura, A., Ishida, Y., Ohta, S., Komari, T., Miyao-Tokutomi, M., Tajima, S. and Matsuoka, M.** (2000). The promoter of rbcS in a C3 plant (rice) directs organ-specific, light-dependent expression in a C4 plant (maize), but does not confer bundle sheath cell-specific expression. *Plant Molecular Biology* **44**, 99-106.
- Odell, J.T., Nagy, F. and Chua, N.H.** (1985). Identification of DNA sequences required for activity of the cauliflower mosaic virus 35S promoter. *Nature* **313**, 810-812.

- Rooke, L., Byrne, D. and Salgueiro, S.** (2000). Marker gene expression driven by the maize ubiquitin promoter in transgenic wheat. *Ann Appl Biol* **136**, 167-172.
- Schledzewski, K. and Mendel, R.R.** (1994). Quantitative transient gene expression: Comparison of the promoters for maize polyubiquitin1, rice actin1, maize-derived Emu and CaMV 35S in cells of barley, maize and tobacco. *Transgenic Research* **3**, 249-255.
- Schoffl, F., Rieping, M., Baumann, G., Bevan, M. and Angermuller, S.** (1989). The function of plant heat shock promoter elements in the regulated expression of chimaeric genes in transgenic tobacco. *Molecular & General Genetics : MGG* **217**, 246-253.
- Song, P., Heinen, J.L., Burns, T.H. and Allen, R.D.** (2000). Expression of two tissue-specific promoters in transgenic cotton plants. *The Journal of Cotton Science* **4**, 217-223.
- Toki, S.** (1997). Rapid and efficient Agrobacterium-mediated transformation in rice. *Plant Molecular Biology Reporter* **15**, 16-21.
- Toki, S., Takamatsu, S., Nojiri, C., Ooba, S., Anzai, H., Iwata, M., Christensen, A.H., Quail, P.H. and Uchimiya, H.** (1992). Expression of a Maize Ubiquitin Gene Promoter-bar Chimeric Gene in Transgenic Rice Plants. *Plant Physiology* **100**, 1503-1507.
- Velten, J., Velten, L., Hain, R. and Schell, J.** (1984). Isolation of a dual plant promoter fragment from the Ti plasmid of *Agrobacterium tumefaciens*. *Embo J* **3**, 2723-2730.



## CHAPTER FIVE

### CONCLUSIONS AND FUTURE PERSPECTIVES

Abiotic stress, biotic stress, rapidly increasing world population and limited arable land exert huge pressure on global agriculture production. To meet the challenge of environment and population, it is essential to develop crops with desired traits that are flexible and adaptable to extreme environment. Besides successful traditional breeding method, biotechnology employing recombinant DNA and transgenic technologies has been demonstrated to be an effective approach for use in trait modification, creating new crops with significantly improved performance. The foundation of biotechnology approach for enhancing plant stress tolerance is to understand how plant senses and resists adverse conditions. To this end, my work focused on deciphering the signaling pathway in plant response to both abiotic and biotic stresses. We identified a new *A. thaliana* protein kinase family, SRF comprising four family members (SRF1-4), which function as receptors on the plasma membrane of plant cells. The evidence from my work indicates that SRF2, one of the SRF kinase protein family members, plays a critical role in the pathogen resistance pathway. SRF2 functions as a PRR, sensing the presence of pathogen and interacting with co-receptor BAK1 to transmit the signal to cytoplasm and activate downstream defense-related genes and basal immunities through MAPK cascade. Our work also shows that SRF1 and SRF2 may negatively regulate the salt resistance of *A. thaliana*. To further reveal SRF protein family-mediated signaling pathway, a number of questions remain to be answered in the future. What is the PAMP recognized by SRF2? How does the SRF2 interact with BAK1 to activate downstream MAPKs? How does the MAPK cascade triggers the basal immunities? How are the SRF1 and SRF2 involved in the signaling pathway of *A. thaliana* salt resistance?

In addition to the genes involved in osmotic stress and biotic stress, we also investigated the role of one of the microRNAs, *miR395*, in rice plant responses to sulfate deficiency. Our work suggests that rice *OsmiR395*, like its *Arabidopsis* counterpart, *AthmiR395*, is intensively upregulated under sulfate starvation condition. We further confirmed that two sulfate transporter genes, *OsSULTR2* and *OsSULTR2;1*, are the targets of *OsmiR395* in rice root. To better understand the function of *OsmiR395*, we overexpressed this gene in tobacco. The data obtained show that overexpression of rice *miR395* interrupts the sulfate homeostasis in transgenic tobacco and represses its growth. Additionally, we identified a *miR395* target gene, sulfate transporter gene *NtaSULTR2*, in tobacco. We confirmed that *NtaSULTR2* mRNAs are indeed cleaved by *miR395* at the predicted cutting site. Taken together, our research suggests that rice *miR395* has essential function to sulfate starvation response in both rice and tobacco. To reveal how *miR395*-mediated target gene modification regulates the sulfate homeostasis under sulfate starvation condition in tobacco, more *miR395* target genes, especially ATPS genes, which mediate sulfate assimilation, need to be identified.

Availability of various molecular tools is critical for the success of biotechnology approach in crop improvement. In this work, we identified a strong leaf specific promoter from *A. thaliana* for use in controlling foreign gene expression in transgenic plants. Our data indicate that *Srf3abc* is highly and specifically active in the leaves of *A. thaliana*, exhibiting stronger activity than the commonly used CaMV 35S promoter. Truncations in *Srf3abc* impair its leaf specificity, and one truncated version of the promoter, *Srf3c*, exhibits strong, constitutive activity in *Arabidopsis* and other plant species such as tobacco,

rice and creeping bentgrass, implying their potential wide applications in agriculture biotechnology. Our future work will focus on identification of the *cis*-regulatory element in Srf3abc that determines leaf specificity of the promoter. This *cis*-regulatory element could then be used to develop synthetic or chimeric new promoters for use in controlled target gene expression in transgenic plants.

## APPENDICES

APPENDIX A

SUPPORTING MATERIAL FOR CHAPTER TWO

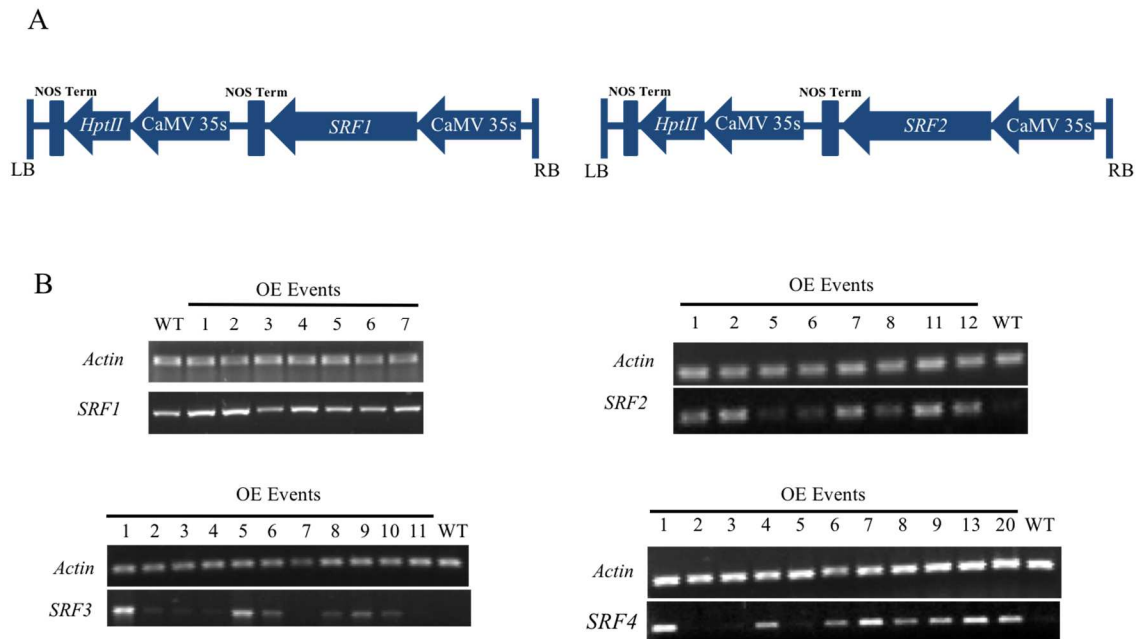
**TABLE A-1: Primers for Northern analysis, gene cloning and RT-PCR analyses**

Primers for RT-PCR and qPCR analyses			
Gene		Primer sequence	Note
SRF1	F	CAAGGGGAGGAGCGATTCC	
	R	CTGAATTCTTCATGTA AAAAGTCGACC	
SRF2	F	TAGCCATGAGTTGTCTCAATCC	
	R	TCCACGTTACATATGGCGAAA	
SRF3	F	GTTCTGTGTGGAAAGCTGTTG	
	R	AGGTGGCCTATAAGAGAGATACT	
SRF4	F	ATATACATCAGATGCCGATTTAGTAGCT	
	R	GTAAAGAGTTGGATCTGGTCACAAGGATT	
Actin	F	TCCATTCTTGCTTCCCTCAG	
	R	TCCATTCATAAAAACCCAGC	
Primers for cloning of promoter regions			
Promoter		Primer sequence	Note
SRF1pro	F	ACCTAGGCTAGGCTCGGCTTTGATACCACG	A+AvrII tagged
	R	AGGATCCGGTTCCTGACTGTCCACATGAGAG	A+BamHI tagged
SRF2pro	F	ACCTAGGATTTGAGAAATTCTTTATGTGATTTATGGG	A+AvrII tagged
	R	ACTCAGATGTTCTCCTTACTGTCCACAGG	A+XhoI tagged
SRF3pro	F	ACCTAGGCTCGGTAGAGGTCTGATTATATTTTC	A+AvrII tagged
	R	ACTCGAGTTACTATGCAAAGAAGGGATCTGT	A+XhoI tagged
SRF4pro	F	ACCTAGGTTTACATGAAGAATTCAGCTTCTTTTTTG	A+AvrII tagged
	R	ACTCGAGTATTCTTCTTACTGTCCAAAAGAAAGA	A+XhoI tagged
Primers for rapid amplification of cDNA ends			
Gene		Primer sequence	Note
SRF1	3' RACE	CCGCGACGCCGCTAAATGCTAATGC	
	5' RACE	GAAGTGAGAGAGGCACCGATCCAGTGAG	
SRF2	3' RACE	GCTGATTCATGTGTGAAAAAAGGAGAGG	
	5' RACE	TTAATAAGACATACCGTAGTCCACAAATTCGG	
Primers for cloning of full length cDNA			
Gene		Primer sequence	Note
SRF1	F	ATCTAGAATGTGGACAGTCAGGAGAACCATGGAGAGACATTGTGTG	A+XbaI tagged
	R	AGTCGACATGCCGAGCCAATGGGGTCACTTCGG	A+Sall tagged
SRF2	F	ATCTAGAATCTTAAAAAAAAGCTCTCCTGTGGACAG	A+XbaI tagged
	R	AGTCGACTAAATAAAAATCCACGTTACATATGGCG	A+Sall tagged

**TABLE A-1 (continued)**

Primers for subcellular localization analyses			
Gene		Primer sequence	Note
SRF1	F	AGGATCCATGGAGAGACATTGTGTGTTTCGTTACC	A+BamHI tagged
	R	AGGATCCCCTTATACGACGACTTGAATTGCTA	A+BamHI tagged
SRF2	F	ACCCGGGATCTTAAAAAAAAGCTCTCCTGTGGACAG	A+SmaI tagged
	R	ACCCGGGTCCGAGCCGTTGGGCTCAGTTC	A+SmaI tagged
SRF3	F	ATACGTACAGATCCCTTCTTTGCATAGTAAGG	A+SnaBI tagged
	R	ATACGTATCCTAGCCATTGGGCTCACATCAGTATC	A+SnaBI tagged
SRF4	F	ACCCGGGATGGAGAGACATTTTGTGTTTATTGCCACC	A+SmaI tagged
	R	ACCCGGGTTCGAGCGTTTGGGCTCACTTCAGTACCAAAC	A+SmaI tagged
Primers for analyses of T-DNA positions in T-DNA insertion mutants			
Gene		Primer sequence	Note
T-DNA	T-DNA LBb1.3	ATTTTGCCGATTTCGGAAC	on the left border of T-DNA
SRF1	LP1	TGGAGACGCTGAAATCAACTC	on the flanking genomic DNA
	RP1	TCGACGCTTGACATATGCTG	
SRF2	LP2	CACATTGAATCCCTTGCATC	on the flanking genomic DNA
	RP2	GCTCAGGATCAAATTGGTACG	
SRF3	LP3	TCATGTAAGAATTCTAAAGCACACG	on the flanking genomic DNA
	RP3	CAAAAATTTGGCTTGGTCAG	
SRF4	LP4	TTTTAGGGGGTGTTATTGGTTG	on the flanking genomic DNA
	RP4	TTGAACATTCTTGATCCCAGC	
Primers for construction of RNAi <i>Arabidopsis</i> line			
Gene		Primer sequence	Note
SRF1	F	ACTGCAGGGATCCACGAATCAAAGAACACCATGG	A+PstI+BamHI tagged A+KpnI+HindIII tagged
	R	AGGTACCAAGCTTGGGGTACTTACAAATATCAACCA	
Primers for Northern blot probe synthesis			
Gene		Primer sequence	Note
FRK1	F	AACCGGCTTCTACTGTCATGAGC	
	R	CAAGGGCGTTAATGATCGGTGGA	
WKRY53	F	CCGAGAAGTGAAGAGTTTGCCGA	
	R	CTCTGGTGTCTTGTCGCTTCTCC	
Ath rRNA18	F	GGTCTGTGATGCCCTTAGATG	
	R	CCTTGTTACGACTTCTCCTTCC	
Primers for BiFC analyses			
Gene		Primer sequence	Note
SRF2	F	ATCTAGAATGGAGAGACATTGTGTGTTAGTTG	A+XbaI tagged A+XhoI tagged
	R	ACTCGAGCCGAGCCGTTGGGCTCAGTTCGGTA	
BAK1	F	ATCTAGAATGGAACGAAGATTAATGATCCCTTGC	A+XbaI tagged A+XhoI tagged
	R	ACTCGAGTCTTGACCCGAGGGGTATTCGTTTTCG	
CERK1	F	ATCTAGAATGAAGCTAAAGATTTCTCTAATCGC	A+XbaI tagged A+KpnI tagged
	R	AGGTACCCGGCCGACATAAGACTGACTAAATC	

**FIGURE A-1: Overexpression of *SRF* genes in *Arabidopsis thaliana***

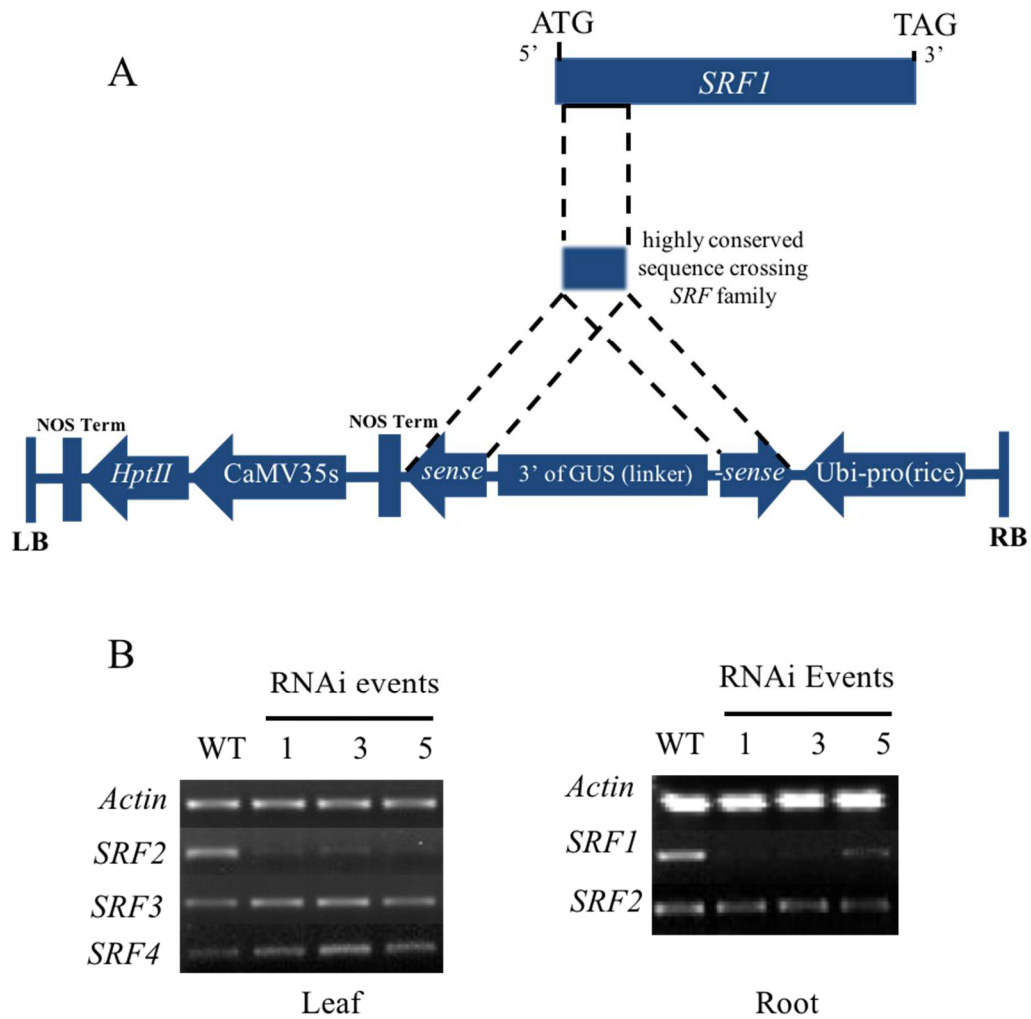


(A) The Schematic diagram of *SRF* overexpression constructs. The full length cDNA of *SRF* gene was under the control of CaMV 35s promoter. CaMV 35s driving *HptII* was used as selectable marker gene in transgenic plants. LB: left border of T-DNA. RB: right border of T-DNA.

(B) RT-PCR analysis of *SRF1*, *SRF2*, *SRF3*, or *SRF4* gene in their over-expression plants. Root tissue of two-week-old *SRF1* transgenic plants, and leaf tissues of two-week-old *SRF2*, *SRF3*, and *SRF4* transgenic plants were collected and used for RT-PCR analysis. *Actin2* was used as reference gene.



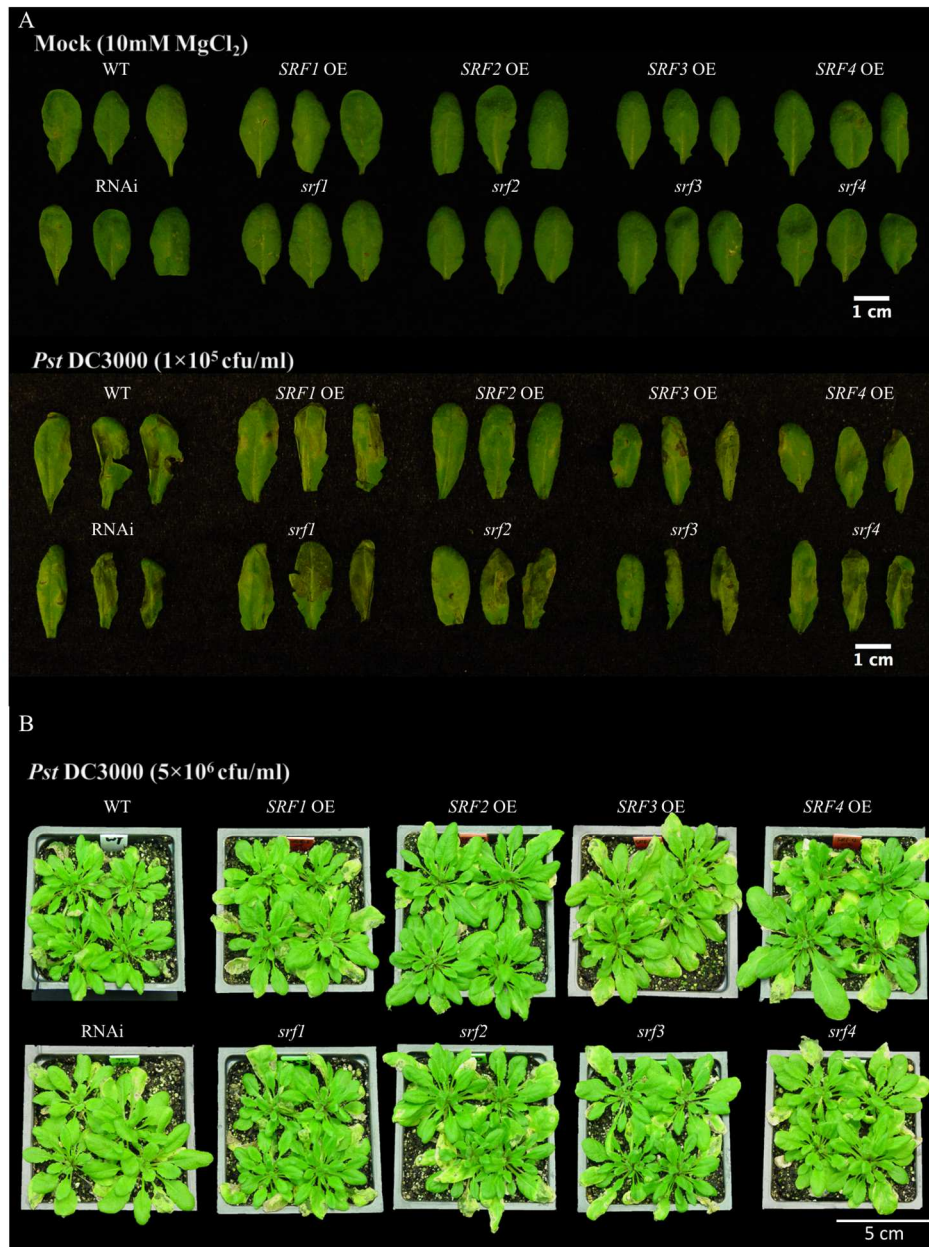
**FIGURE A-2: Construction of RNAi line**



(A) The schematic diagram of RNA interference construct.

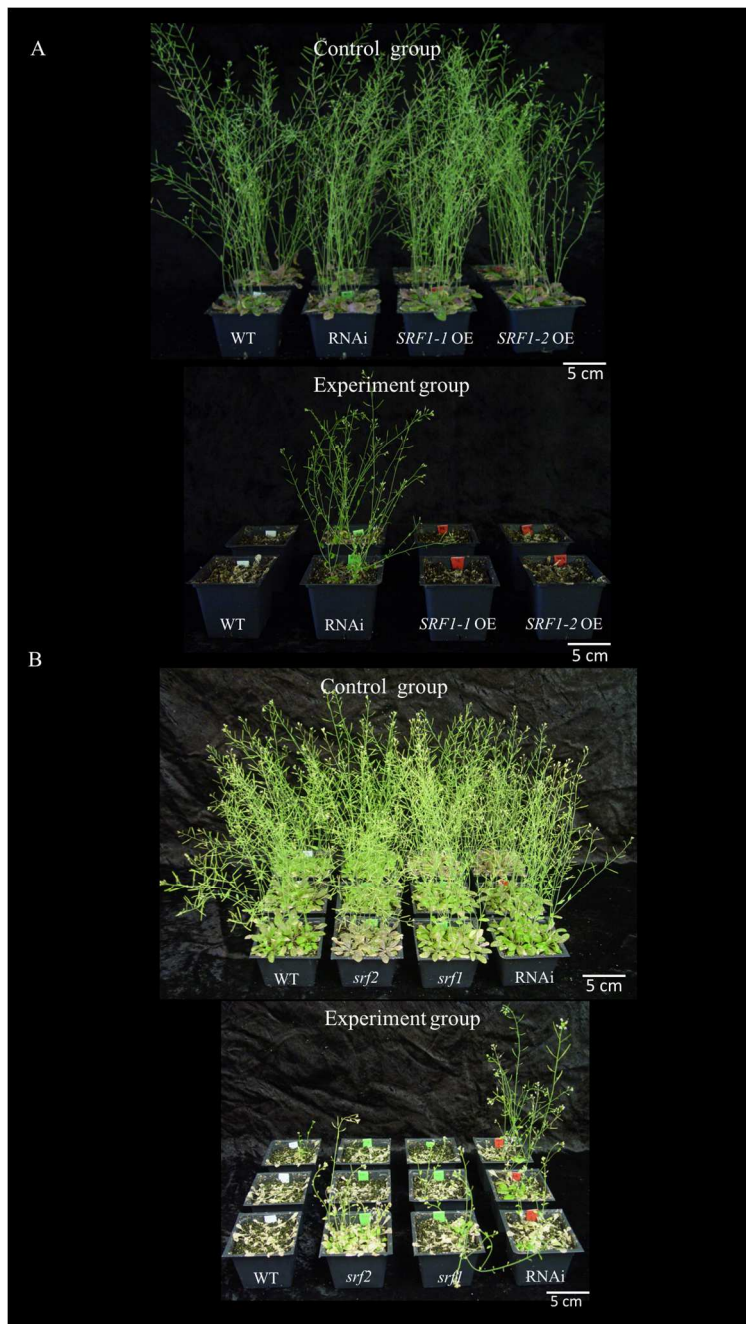
(B) RT-PCR analysis of the expression of *SRF1*, *SRF2*, *SRF3*, and *SRF4* in different tissues of transgenic *Arabidopsis* harboring the RNAi construct. Two-week-old plants were used for the RT-PCR analysis. *Actin2* was used as reference gene.

**FIGURE A-3: Phenotype analysis of different *Arabidopsis* lines under pathogen infection**



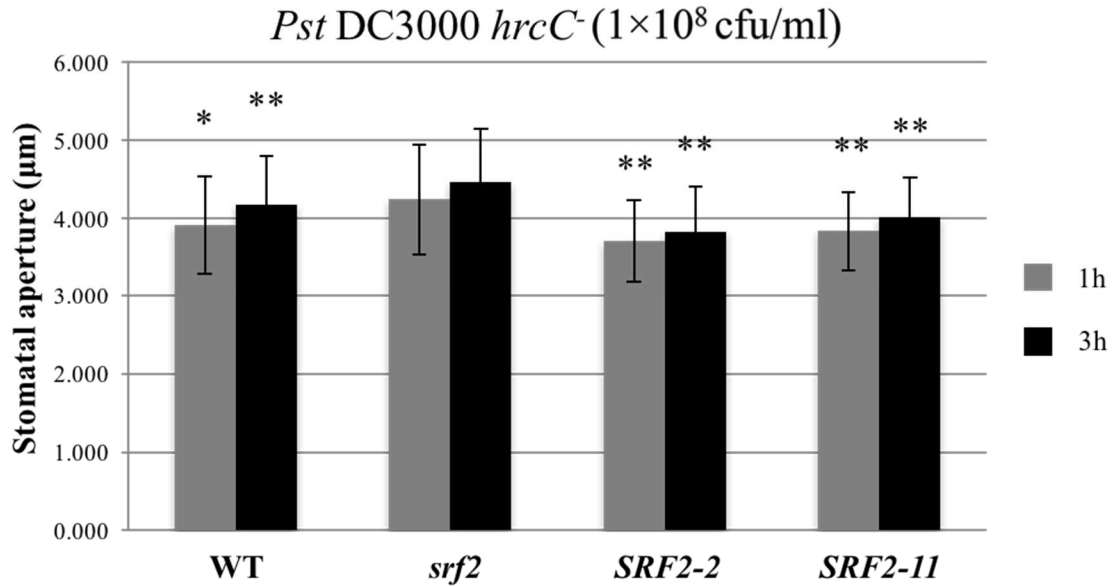
(A) The leaves of four-week-old plants grown under short day condition (8 h/16 h day/night) in soil were infiltrated with  $\text{MgCl}_2$  and pathogen *Pst* DC3000 in indicated concentration. At three days after inoculation, infiltrate leaves were photographed.  
 (B) The leaves of four-week-old plants grown under short day condition (8 h/16 h day/night) in soil were spray-inoculated with pathogen *Pst* DC3000 in indicated concentration. At three days after inoculation, inoculated plants were photographed.

**FIGURE A-4: Phenotype analysis of different *Arabidopsis* lines under salt treatment**



Two-week-old *Arabidopsis* plants grown under long day condition (16 h/8 h day/night) were (A) treated with 200 mM of NaCl for five days and then recovered with water for three weeks or (B) treated with 175 mM of NaCl for three days and then recovered with water for 10 days.

**FIGURE A-5: Stomatal apertures of *Arabidopsis* leaves under *Pst* DC3000 *hrcC*<sup>-</sup> treatment**



The leaves of five-week-old *Arabidopsis* plants were immersed in *Pst* DC3000 *hrcC*<sup>-</sup> ( $1 \times 10^8$  cfu/ml). At 1.5 and 3.5 hours later, stomata from random regions in leaf epidermal of four fully expanded leaves from four plants (four leaves in total) were photographed under optical microscope.

The width of the stomatal aperture was measured using the measure function of ImageJ. Data shown are an average of four independent biological replicates each consisting of 15 stomatal apertures. Error represents S.D. (n=60). Asterisks indicate the significant differences between *srf1* and other *Arabidopsis* lines. P < 0.05 was marked as \*. P < 0.01 was marked as \*\*.

APPENDIX B

SUPPORTING MATERIAL FOR CHAPTER THREE

**TABLE B-1: Primers for Northern analysis, gene cloning and RT-PCR analyses**

Primers for RT-PCR analysis			
Gene		Primer sequence	Note
Mature miRNA395	395_stemloop_RT	GTCGTATCCAGTGCAGGGTCCGAGGTATTTCGCACTGGA TACGACGAGTTC	
	Osa395_stemloop_F	TCGCTGTGAAGTGTTTGGGG	
	Nta395_stemloop_F	TCGCTCTGAAGTGTTTGGGG	
	Universal_stemloop_R	GCAGTGGAAGGGGCATGCA	
Pri-OsmiRNA395h	F	ACAGATCTCTCGGTTGGTGG	
	R	CTTGTTGGCACCGAGAGTTC	
Rice <i>SIZ1</i>	F	GTGATTTGGAAGTGGTTGCG	
	R	ATCTCCAGCAATCCTCATTC	
Rice <i>SULTR2;1</i>	F	TTGGAGGCACCGATAACATTG	
	R	TCTGCAAAAGCTGTCCCTATG	
Rice <i>SULTR2</i>	F	TCTTCACCGTCACCTTCCTC	
	R	CTGCCATGAACCCAACGATC	
Rice <i>ATPS</i>	F	AATCTTCCCCTCTCCAATGC	
	R	ACAGGTCCCTCTTTTCAGTTG	
Rice <i>SULTR3;4</i>	F	GGCTGTTAATTTGTTTCGCGTG	
	R	GAGATCAGCACCCGGAGTTA	
Tobacco <i>L25</i>	F	CCTCGTATTAGTGCACCTGGA	
	R	CAGCCTTGATGTCCACAATGA	
Tobacco <i>SULTR2</i>	F	CAACTCTTCCAAC TTTGGTTG	
	R	TCAGGTTGGAAAACAGGCCTG	
Primers for cloning of pri-OsmiRNA395			
Gene		Primer sequence	Note
pri-OsmiR395	F	<b>TCTAGAG</b> CAGGTCATCCTCTTCAAGT	<b>XbaI</b> tagged
	R	<b>GTCGACC</b> ATCAAACGTGGCATATGA	<b>Sall</b> tagged
Primers for cloning of full length <i>NtaSULTR2</i> cDNA			
Gene		Primer sequence	Note
NtaSULTR2	Ntasultr2_5'GSP	GGCAGCTTGAAAAGTACCCGCGAAGAA	
	Ntasultr2_5'NSP	CAGGCCTGGTGGTTCCGGCACATTTAG	
	Ntasultr2_3'GSP	TCAGAGCATTGGCTACGCGACTCTTG	
	Ntasultr2_cDNA_F	GATGGGGGAAGATGTGCTTTTGAAC	
	Ntasultr2_cDNA_R	GAGAGAATTAGTTTGCATTTAAACCTTC	

**TABLE B-1 (continued)**

Primers for RML-RACE			
Gene		Primer sequence	Note
NtaSULTR2	RML_RACE_RNAadaptor	CGACUGGAGCACGAGGACACUGACAU	RNA adaptor
	RML_RACE_ASPF	GGACUGAAGGAGUAGAAA	Forward primer
	RML_RACE_NASPF	CGACTGGAGCACGAGGACACTGA	Forward nest primer
	NtaSULTR2_GSPR	GGACACTGACATGGACTGAAGGAGTA	Reverse primer
	NtaSULTR2_NGSPR	AGCACGAGTTTTGTATATGCAGCT	Reverse nest primer
		CAGCAACTGGTCCAATTGCTAT	
Probe for small RNA Northern blot			
Gene		sequence	Note
Mature miR395	Osami395_probe21	GAGTTCCCCCAAACACTTCAC	

## APPENDIX C

### SUPPORTING MATERIAL FOR CHAPTER FOUR

**TABLE C-1: Bioinformatic analysis of Srf3abc promoter**

For CPU reasons Srf3abc was truncated to 1500nt from the 3'end

Site Name	Organism	Position	Strand	Matrix score	Sequence	Function
5'UTR Pyrich stretch	<i>Lycopersicon esculentum</i>	318	-	9	TTTCTTCTCT	cis-acting element conferring high transcription levels
5'UTR Pyrich stretch	<i>Lycopersicon esculentum</i>	1175	-	9	TTTCTTCTCT	cis-acting element conferring high transcription levels
A-box	<i>Petroselinum crispum</i>	961	-	6	CCGTCC	cis-acting regulatory element
AAGAA-motif	<i>Avena sativa</i>	1212	-	7	GAAAGAA	
AE-box	<i>Arabidopsis thaliana</i>	186	-	8	AGAAACAT	part of a module for light response
AE-box	<i>Arabidopsis thaliana</i>	972	+	8	AGAAACAA	part of a module for light response
ARE	<i>Zea mays</i>	391	+	6	TGGTTT	cis-acting regulatory element essential for the anaerobic induction
ARE	<i>Zea mays</i>	656	+	6	TGGTTT	cis-acting regulatory element essential for the anaerobic induction
ARE	<i>Zea mays</i>	605	-	6	TGGTTT	cis-acting regulatory element essential for the anaerobic induction
ARE	<i>Zea mays</i>	830	-	6	TGGTTT	cis-acting regulatory element essential for the anaerobic induction
AT-rich sequence	<i>Pisum sativum</i>	593	-	9	TAAAATACT	element for maximal elicitor-mediated activation (2copies)
Box 4	<i>Petroselinum crispum</i>	214	+	6	ATTAAT	part of a conserved DNA module involved in light responsiveness
Box 4	<i>Petroselinum crispum</i>	1106	-	6	ATTAAT	part of a conserved DNA module involved in light responsiveness
Box 4	<i>Petroselinum crispum</i>	575	+	6	ATTAAT	part of a conserved DNA module involved in light responsiveness
Box 4	<i>Petroselinum crispum</i>	1376	-	6	ATTAAT	part of a conserved DNA module involved in light responsiveness
Box I	<i>Pisum sativum</i>	365	+	7	TTTCAA	light responsive element
Box III	<i>Pisum sativum</i>	798	+	9	CATTTACT	protein binding site
CAAT-box	<i>Hordeum vulgare</i>	5	-	4	CAAT	common cis-acting element in promoter and enhancer regions

**TABLE C-1 (continued)**

CAAT-box	Glycine max	70	+	5	CAATT	common cis-acting element in promoter and enhancer regions
CAAT-box	Hordeum vulgare	89	+	4	CAAT	common cis-acting element in promoter and enhancer regions
CAAT-box	Hordeum vulgare	106	+	4	CAAT	common cis-acting element in promoter and enhancer regions
CAAT-box	Brassica rapa	229	-	5	CAAAT	common cis-acting element in promoter and enhancer regions
CAAT-box	Hordeum vulgare	335	+	4	CAAT	common cis-acting element in promoter and enhancer regions
CAAT-box	Brassica rapa	368	+	5	CAAAT	common cis-acting element in promoter and enhancer regions
CAAT-box	Glycine max	378	-	5	CAATT	common cis-acting element in promoter and enhancer regions
CAAT-box	Hordeum vulgare	379	-	4	CAAT	common cis-acting element in promoter and enhancer regions
CAAT-box	Brassica rapa	388	-	5	CAAAT	common cis-acting element in promoter and enhancer regions
CAAT-box	Arabidopsis thaliana	410	-	5	CCAAT	common cis-acting element in promoter and enhancer regions
CAAT-box	Brassica rapa	417	+	5	CAAAT	common cis-acting element in promoter and enhancer regions
CAAT-box	Arabidopsis thaliana	443	-	5	CCAAT	common cis-acting element in promoter and enhancer regions
CAAT-box	Glycine max	472	+	5	CAATT	common cis-acting element in promoter and enhancer regions
CAAT-box	Hordeum vulgare	490	-	4	CAAT	common cis-acting element in promoter and enhancer regions
CAAT-box	Hordeum vulgare	532	+	4	CAAT	common cis-acting element in promoter and enhancer regions
CAAT-box	Brassica rapa	567	+	5	CAAAT	common cis-acting element in promoter and enhancer regions
CAAT-box	Glycine max	585	-	5	CAATT	common cis-acting element in promoter and enhancer regions
CAAT-box	Arabidopsis thaliana	586	-	5	CCAAT	common cis-acting element in promoter and enhancer regions
CAAT-box	Arabidopsis thaliana	608	+	5	CCAAT	common cis-acting element in promoter and enhancer regions
CAAT-box	Hordeum vulgare	609	+	4	CAAT	common cis-acting element in promoter and enhancer regions
CAAT-box	Hordeum vulgare	614	-	4	CAAT	common cis-acting element in promoter and enhancer regions



**TABLE C-1 (continued)**

CAAT-box	<i>Arabidopsis thaliana</i>	719	-	5	CCAAT	common cis-acting element in promoter and enhancer regions
CAAT-box	<i>Hordeum vulgare</i>	843	-	4	CAAT	common cis-acting element in promoter and enhancer regions
CAAT-box	<i>Arabidopsis thaliana</i>	856	-	5	CCAAT	common cis-acting element in promoter and enhancer regions
CAAT-box	<i>Brassica rapa</i>	870	+	5	CAAAT	common cis-acting element in promoter and enhancer regions
CAAT-box	<i>Brassica rapa</i>	904	-	5	CAAAT	common cis-acting element in promoter and enhancer regions
CAAT-box	<i>Arabidopsis thaliana</i>	958	-	5	CCAAT	common cis-acting element in promoter and enhancer regions
CAAT-box	<i>Brassica rapa</i>	1008	+	5	CAAAT	common cis-acting element in promoter and enhancer regions
CAAT-box	<i>Glycine max</i>	1010	-	5	CAATT	common cis-acting element in promoter and enhancer regions
CAAT-box	<i>Hordeum vulgare</i>	1011	-	4	CAAT	common cis-acting element in promoter and enhancer regions
CAAT-box	<i>Hordeum vulgare</i>	1073	-	4	CAAT	common cis-acting element in promoter and enhancer regions
CAAT-box	<i>Hordeum vulgare</i>	1100	-	4	CAAT	common cis-acting element in promoter and enhancer regions
CAAT-box	<i>Hordeum vulgare</i>	1166	+	4	CAAT	common cis-acting element in promoter and enhancer regions
CAAT-box	<i>Hordeum vulgare</i>	1170	-	4	CAAT	common cis-acting element in promoter and enhancer regions
CAAT-box	<i>Hordeum vulgare</i>	1208	-	4	CAAT	common cis-acting element in promoter and enhancer regions
CAAT-box	<i>Brassica rapa</i>	1313	+	5	CAAAT	common cis-acting element in promoter and enhancer regions
CAAT-box	<i>Glycine max</i>	1362	+	5	CAATT	common cis-acting element in promoter and enhancer regions
CAAT-box	<i>Brassica rapa</i>	1367	-	5	CAAAT	common cis-acting element in promoter and enhancer regions
CAAT-box	<i>Brassica rapa</i>	1397	-	5	CAAAT	common cis-acting element in promoter and enhancer regions
CCAAT-box	<i>Hordeum vulgare</i>	504	+	6	CAACGG	MYBHv1 binding site
CCAAT-box	<i>Hordeum vulgare</i>	1232	+	6	CAACGG	MYBHv1 binding site
CCAAT-box	<i>Hordeum vulgare</i>	746	-	6	CAACGG	MYBHv1 binding site
CCGTCC-box	<i>Arabidopsis thaliana</i>	961	-	6	CCGTCC	cis-acting regulatory element related to meristem specific activation

**TABLE C-1 (continued)**

CGTCA-motif	<i>Hordeum vulgare</i>	285	+	5	CGTCA	cis-acting regulatory element involved in the MeJA-responsiveness
GARE-motif	<i>Brassica oleracea</i>	316	+	7	AAACAGA	gibberellin-responsive element
GARE-motif	<i>Brassica oleracea</i>	1476	+	7	AAACAGA	gibberellin-responsive element
GCN4 motif	<i>Oryza sativa</i>	850	+	7	CAAGCCA	cis-regulatory element involved in endosperm expression
HD-Zip 1	<i>Arabidopsis thaliana</i>	609	+	8	CAAT(A/T)ATTG	element involved in differentiation of the palisade mesophyll cells
HD-Zip 2	<i>Arabidopsis thaliana</i>	609	+	8.5	CAAT(G/C)ATTG	element involved in the control of leaf morphology development
HSE	<i>Brassica oleracea</i>	700	-	9	AAAAAATTC	cis-acting element involved in heat stress responsiveness
HSE	<i>Brassica oleracea</i>	1180	+	9	AGAAAATTCG	cis-acting element involved in heat stress responsiveness
I-box	<i>Triticum aestivum</i>	1174	+	9	aAGATAAGA	part of a light responsive element
MBS	<i>Arabidopsis thaliana</i>	623	+	6	CAACTG	MYB binding site involved in drought-inducibility
MBS	<i>Arabidopsis thaliana</i>	809	+	6	TAACTG	MYB binding site involved in drought-inducibility
P-box	<i>Oryza sativa</i>	694	+	7	CCTTTTG	gibberellin-responsive element
P-box	<i>Oryza sativa</i>	889	-	7	CCTTTTG	gibberellin-responsive element
Skn-1 motif	<i>Oryza sativa</i>	237	-	5	GTCAT	cis-acting regulatory element required for endosperm expression
Skn-1 motif	<i>Oryza sativa</i>	1297	+	5	GTCAT	cis-acting regulatory element required for endosperm expression
Skn-1 motif	<i>Oryza sativa</i>	1097	+	5	GTCAT	cis-acting regulatory element required for endosperm expression
Skn-1 motif	<i>Oryza sativa</i>	619	-	5	GTCAT	cis-acting regulatory element required for endosperm expression
Skn-1 motif	<i>Oryza sativa</i>	1103	+	5	GTCAT	cis-acting regulatory element required for endosperm expression
Sp1	<i>Zea mays</i>	174	-	5.5	CC(G/A)CCC	light responsive element
TATA-box	<i>Lycopersicon esculentum</i>	26	+	5	TTTTA	core promoter element around -30 of transcription start
TATA-box	<i>Arabidopsis thaliana</i>	34	+	4	TATA	core promoter element around -30 of transcription start
TATA-box	<i>Brassica napus</i>	35	+	6	ATATAT	core promoter element around -30 of transcription start
TATA-box	<i>Arabidopsis thaliana</i>	36	+	4	TATA	core promoter element around -30 of transcription start

**TABLE C-1 (continued)**

TATA-box	Lycopersicon esculentum	73	+	5	TTTTA	core promoter element around -30 of transcription start
TATA-box	Oryza sativa	80	-	7	TACAAAA	core promoter element around -30 of transcription start
TATA-box	Lycopersicon esculentum	193	+	5	TTTTA	core promoter element around -30 of transcription start
TATA-box	Glycine max	216	+	5	TAATA	core promoter element around -30 of transcription start
TATA-box	Arabidopsis thaliana	223	+	4	TATA	core promoter element around -30 of transcription start
TATA-box	Arabidopsis thaliana	268	-	9	taTATAAAgg	core promoter element around -30 of transcription start
TATA-box	Helianthus annuus	272	-	6	TATACA	core promoter element around -30 of transcription start
TATA-box	Arabidopsis thaliana	274	+	4	TATA	core promoter element around -30 of transcription start
TATA-box	Brassica oleracea	275	+	6	ATATAA	core promoter element around -30 of transcription start
TATA-box	Arabidopsis thaliana	276	+	4	TATA	core promoter element around -30 of transcription start
TATA-box	Lycopersicon esculentum	338	-	5	TTTTA	core promoter element around -30 of transcription start
TATA-box	Oryza sativa	373	+	7	TACAAAA	core promoter element around -30 of transcription start
TATA-box	Arabidopsis thaliana	394	-	6	TATAAA	core promoter element around -30 of transcription start
TATA-box	Arabidopsis thaliana	395	-	5	TATAA	core promoter element around -30 of transcription start
TATA-box	Arabidopsis thaliana	396	+	4	TATA	core promoter element around -30 of transcription start
TATA-box	Brassica napus	534	+	6	ATATAT	core promoter element around -30 of transcription start
TATA-box	Arabidopsis thaliana	535	+	4	TATA	core promoter element around -30 of transcription start
TATA-box	Brassica oleracea	552	+	6	ATATAA	core promoter element around -30 of transcription start
TATA-box	Arabidopsis thaliana	553	+	4	TATA	core promoter element around -30 of transcription start
TATA-box	Glycine max	571	-	5	TAATA	core promoter element around -30 of transcription start
TATA-box	Glycine max	574	-	5	TAATA	core promoter element around -30 of transcription start

**TABLE C-1 (continued)**

TATA-box	<i>Glycine max</i>	577	+	5	TAATA	core promoter element around -30 of transcription start
TATA-box	<i>Lycopersicon esculentum</i>	597	+	5	TTTTA	core promoter element around -30 of transcription start
TATA-box	<i>Lycopersicon esculentum</i>	715	+	5	TTTTA	core promoter element around -30 of transcription start
TATA-box	<i>Lycopersicon esculentum</i>	731	+	5	TTTTA	core promoter element around -30 of transcription start
TATA-box	<i>Zea mays</i>	778	-	8	TTTAAAAA	core promoter element around -30 of transcription start
TATA-box	<i>Lycopersicon esculentum</i>	779	+	5	TTTTA	core promoter element around -30 of transcription start
TATA-box	<i>Lycopersicon esculentum</i>	782	-	5	TTTTA	core promoter element around -30 of transcription start
TATA-box	<i>Arabidopsis thaliana</i>	807	-	4	TATA	core promoter element around -30 of transcription start
TATA-box	<i>Lycopersicon esculentum</i>	825	+	5	TTTTA	core promoter element around -30 of transcription start
TATA-box	<i>Lycopersicon esculentum</i>	828	-	5	TTTTA	core promoter element around -30 of transcription start
TATA-box	<i>Lycopersicon esculentum</i>	836	-	5	TTTTA	core promoter element around -30 of transcription start
TATA-box	<i>Brassica oleracea</i>	863	+	7	ATATAAT	core promoter element around -30 of transcription start
TATA-box	<i>Arabidopsis thaliana</i>	864	-	4	TATA	core promoter element around -30 of transcription start
TATA-box	<i>Arabidopsis thaliana</i>	872	-	9	tcTATATAtt	core promoter element around -30 of transcription start
TATA-box	<i>Brassica napus</i>	873	-	6	ATATAT	core promoter element around -30 of transcription start
TATA-box	<i>Arabidopsis thaliana</i>	874	-	8	TATATATA	core promoter element around -30 of transcription start
TATA-box	<i>Brassica napus</i>	875	-	6	ATATAT	core promoter element around -30 of transcription start
TATA-box	<i>Arabidopsis thaliana</i>	876	-	4	TATA	core promoter element around -30 of transcription start
TATA-box	<i>Arabidopsis thaliana</i>	878	-	4	TATA	core promoter element around -30 of transcription start
TATA-box	<i>Oryza sativa</i>	896	+	8	TACATAAA	core promoter element around -30 of transcription start
TATA-box	<i>Lycopersicon esculentum</i>	900	-	5	TTTTA	core promoter element around -30 of transcription start

**TABLE C-1 (continued)**

TATA-box	Glycine max	1044	+	5	TAATA	core promoter element around -30 of transcription start
TATA-box	Arabidopsis thaliana	1052	-	4	TATA	core promoter element around -30 of transcription start
TATA-box	Glycine max	1140	+	5	TAATA	core promoter element around -30 of transcription start
TATA-box	Arabidopsis thaliana	1143	-	4	TATA	core promoter element around -30 of transcription start
TATA-box	Lycopersicon esculentum	1320	+	5	TTTTA	core promoter element around -30 of transcription start
TATA-box	Glycine max	1336	+	5	TAATA	core promoter element around -30 of transcription start
TATA-box	Arabidopsis thaliana	1389	-	5	TATAA	core promoter element around -30 of transcription start
TATA-box	Arabidopsis thaliana	1390	-	4	TATA	core promoter element around -30 of transcription start
TATA-box	Arabidopsis thaliana	1427	-	4	TATA	core promoter element around -30 of transcription start
TATA-box	Arabidopsis thaliana	1444	-	5	TATAA	core promoter element around -30 of transcription start
TATA-box	Arabidopsis thaliana	1445	-	4	TATA	core promoter element around -30 of transcription start
TC-rich repeats	Nicotiana tabacum	401	+	9	ATTTCTTCA	cis-acting element involved in defense and stress responsiveness
TCA-element	Brassica oleracea	949	+	9	GAGAAGAATA	cis-acting element involved in salicylic acid responsiveness
TCA-element	Brassica oleracea	980	+	9	GAGAAGAATA	cis-acting element involved in salicylic acid responsiveness
TGACG-motif	Hordeum vulgare	285	-	5	TGACG	cis-acting regulatory element involved in the MeJA-responsiveness
circadian	Lycopersicon esculentum	1309	+	6	CAANNNATC	cis-acting regulatory element involved in circadian control

**Reference:** Lescot, M., Déhais, P., Moreau, Y., De Moor, B., Rouzé, P., and Rombauts, S. (2002) *Nucleic Acids Res.*, PlantCARE: a database of plant cis-acting regulatory elements and a portal to tools for in silico analysis of promoter sequences. *Database Issue*, **30(1)**, 325-327.

**TABLE C-2: Primers for gene cloning and RT-PCR analyses**

Primers for RT-PCR analysis of gene expression			
Gene		Primer sequence	Note
SRF3	F	GTTCTGTGTGGAAAGCTGTTG	
	R	AGGTGGCCTATAAGAGAGATACT	
Actin	F	TTCCATTCTTGCTTCCCTCAG	
	R	TCCCATTCATAAAACCCCAGC	
Primers for cloning of promoters			
promoter		Primer sequence	Note
Srf3abc	F	ACCTAGGCTCGGTAGAGGTCCTGATTATATTTTC	A+AvrII tagged
	R	ACTCGAGTTACTATGCAAAGAAGGGATCTGT	A+XhoI tagged
Srf3a	F	ACCTAGGCTCGGTAGAGGTCCTGATTATATTTTC	A+AvrII tagged
	R	ACTCGAGAAAATTGTCCCGTTCTATTCCATG	A+XhoI tagged
Srf3b	F	ACCTAGGGGAAATAACAG ATT GAG AGC	A+AvrII tagged
	R	ACTCGAGGTGGACATAAGTAATCATCTG	A+XhoI tagged
Srf3c	F	ACCTAGG CAGATGATTACTTATGTCCAC	A+AvrII tagged
	R	ACTCGAGTTACTATGCAAAGAAGGGATCTGT	A+XhoI tagged
Srf3ab	F	ACCTAGGCTCGGTAGAGGTCCTGATTATATTTTC	A+AvrII tagged
	R	ACTCGAGGTGGACATAAGTAATCATCTG	A+XhoI tagged
Srf3bc	F	ACCTAGGGGAAATAACAGATTGAGAGC	A+AvrII tagged
	R	ACTCGAGTTACTATGCAAAGAAGGGATCTGT	A+XhoI tagged
Primers for cloning of promoter Srf3ac			
region a	F	ACCTAGGCTCGGTAGAGGTCCTGATTATATTTTC	A+AvrII tagged
	R	GACATAAGTAATCATCTGAAAATTGTCCCGTTCT	
region c	F	AGAACGGGACAATTTTCAGATGATTACTTATGTC	
	R	ACTCGAGTTACTATGCAAAGAAGGGATCTGT	A+XhoI tagged

# SCIENTIFIC REPORTS

OPEN

## Heterologous expression of a rice *miR395* gene in *Nicotiana tabacum* impairs sulfate homeostasis

Ning Yuan, Shuangrong Yuan, Zhigang Li, Dayong Li, Qian Hu &amp; Hong Luo

Received: 27 April 2016  
Accepted: 10 June 2016  
Published: 28 June 2016

Sulfur participates in many important mechanisms and pathways of plant development. The most common source of sulfur in soil  $-\text{SO}_4^{2-}$  is absorbed into root tissue and distributed into aerial part through vasculature system, where it is reduced into sulfite and finally sulfide within the subcellular organs such as chloroplasts and mitochondria and used for cysteine and methionine biosynthesis. MicroRNAs are involved in many regulation pathways by repressing the expression of their target genes. *MiR395* family in *Arabidopsis thaliana* has been reported to be an important regulator involved in sulfate transport and assimilation, and a high-affinity sulphate transporter and three ATP sulfurylases (ATPS) were the target genes of *AthmiR395* (*Arabidopsis thaliana miR395*). We have cloned a *miR395* gene from rice (*Oryza sativa*) and studied its function in plant nutritional response. Our results indicated that in rice, transcript level of *OsamiR395* (*Oryza sativa miR395*) increased under sulfate deficiency conditions, and the two predicted target genes of *miR395* were down-regulated under the same conditions. Overexpression of *OsamiR395h* in tobacco impaired its sulfate homeostasis, and sulfate distribution was also slightly impacted among leaves of different ages. One sulfate transporter (SULTR) gene *NtaSULTR2* was identified to be the target of *miR395* in *Nicotiana tabacum*, which belongs to low affinity sulfate transporter group. Both *miR395* and *NtaSULTR2* respond to sulfate starvation in tobacco.

As a rudimental and essential element, sulfur is one of the six macronutrients required for plant growth and participates in many important physiological and biochemical processes. In nature, sulfur exists in both inorganic and organic forms, and sulfate ( $\text{SO}_4^{2-}$ ) is the most common inorganic source of sulfur plants acquire from soil.

The sulfate absorption and assimilation pathway in plants is a complex system. In the very beginning, sulfate is absorbed into root tissue. Except for a small amount of sulfate stored in vacuole of root cells, the majority of them are distributed into aerial part through vasculature system. Upon transfer into subcellular organs such as chloroplasts and mitochondria in cells of aerial part, the sulfate is reduced into sulfite, then sulfide used for the synthesis of cysteine and methionine, two amino acids that play a pivotal role in sulfate assimilation pathway<sup>1</sup>, and essential for supporting many important redox reactions in plants. The reduced form of the cysteine could function as an electron donor and its oxidized form could act as an electron acceptor.

Given the important role sulfur plays in plant growth and development, its deficiency ( $-\text{S}$ ) would cause severe problems to plants, resulting in decreased plant yields and quality<sup>2</sup>. To genetically improve plant sulfate uptake and utilization under  $-\text{S}$  conditions, it is essential to fully understand the functions of the genes encoding sulfate transporters and other important components involved in sulfate assimilation pathways<sup>2</sup>.

Over the course of the past 20 years, essential genes involved in sulfate uptake, distribution and assimilation pathways have been identified and well-studied in different plant species. *Shst 1*, *Shst 2* and *Shst 3* were the first sulfate transporter genes cloned from *Stylosanthes hamate* responsible for initial sulfate uptake and internal transport<sup>3</sup>. In *Arabidopsis*, since the cloning of the first sulfate transporters, AST56 and AST68 two decades ago<sup>4</sup>, at least 12 *Arabidopsis* sulfate transporters belonging to five different groups have been identified<sup>5</sup>. These include two high-affinity sulfate transporters SULTR1;1 and SULTR1;2 responsible for uptake of sulfate from soil<sup>6,7</sup> low-affinity sulfate transporters SULTR2;1 and SULTR2;2 responsible for internal transport of sulfate from root to shoot<sup>7</sup>, SULTR3;5, the function partner of the SULTR2;1 that facilitates the influx of sulfate<sup>8</sup>, and SULTR4;1 and SULTR4;2 involved in distribution of sulfate between *Arabidopsis* vacuoles and symplastic<sup>9</sup>. The *ORYsa:Sultr1;1*

Department of Genetics and Biochemistry, Clemson University, 105 Collings street, 110 Biosystems Research Complex, Clemson, South Carolina, 29634-0318, USA. Correspondence and requests for materials should be addressed to H.L. (email: hluo@clemson.edu)

and *ORYSa;Sultr4;1* are the first two sulfate transporters cloned from rice in early 2000s<sup>10</sup>, followed by the identification of additional 12 sulfate transporters<sup>11</sup>.

ATP sulfurylase (ATPS) catalyzes the synthesis of the essential metabolic intermediate, adenosine 5'-phosphosulfate (APS), and this step is the branch point of the sulfate assimilation pathway followed by the synthesis subpathways of either cysteine or other sulfated compounds. ATPS has been extensively studied for the past decade because of its important role in the sulfate assimilation pathway<sup>12–15</sup>. *SULTR* or *ATPS* gene families would be the ideal targets for genetic modification to increase the efficiency of plant sulfate uptake and assimilation under  $-S$  conditions. It is therefore important to understand how they are regulated in plants.

MicroRNAs (miRNAs) are short non-coding RNAs with only 20–24 nt, regulating many metabolisms in the post-transcriptional level by repressing translation of their target genes. In plants, with the help of RISC (RNA inducing silence complex), mature miRNA could form near-perfect pairs with its complementary sequences of the mRNA target, followed by cleavage of the base-pairing region and degradation of the transcripts<sup>16</sup>. Among thousands of identified miRNAs, *miR395* family in *Arabidopsis* has previously been reported to be an important regulator involved in sulfate transport and assimilation<sup>17–19</sup>. The targets of *AthmiR395* (*Arabidopsis thaliana miR395*) are sulfate transporter genes and ATPS, such as high-affinity sulfate transporter gene, *AthSULTR2;1* and ATP sulfurylase genes, *AthATPS1*, 3, and 4<sup>19–22</sup>.

The divergence of monocot and dicot plants occurred at 200 million years ago<sup>23</sup>, but the miRNA-mediated gene regulation mechanism has an even longer history, which is more than 425 million years<sup>24</sup>. These facts suggest that monocot and dicot plants should have a similar miRNA-mediated gene regulation mechanism and conserved miRNA families sharing the same gene ancestors and regulating the same biological events. Research for the past two decades has led to the identification of 21 miRNA families including many well-studied ones such as miR156 and miR399 that seem to be highly conserved between monocots and dicots<sup>25</sup>. *MiR395* is also on the list, but experimental support is still lacking.

Sequences of mature *miR395* are highly conserved between model plant, *Arabidopsis* and crop species. Understanding the role *miR395* plays in important food crops would allow development of novel biotechnology approaches to genetically engineer these plants for ameliorated nutrient uptake and utilization, improving plant growth, yield and agricultural productivity. We have cloned *pri-OsamiR395h* (*Oryza sativa miR395*) from rice (*Oryza sativa*) and studied its function in plant nutritional response. Our results showed that transcript level of *OsamiR395* increased under  $-S$  condition accompanied with down regulation of its two predicted target genes. Overexpression of *pri-OsamiR395h* in tobacco (*Nicotiana tabacum*) impaired its sulfate homeostasis. Sulfate distribution was also slightly impacted between leaves of different ages in transgenic plants. One potential target gene of *miR395* named *NtaSULTR2* was identified in tobacco (*Nicotiana tabacum*), which encodes a sulfate transporter. The expression of both endogenous *NtamiR395* (*Nicotiana tabacum miR395*) and *NtaSULTR2* was significantly induced under low sulfate conditions in tobacco leaf tissues, but the expression level of *NtaSULTR2* was inversely correlated to that of *NtamiR395* under different sulfate conditions in root tissues. These results indicate that *OsamiR395* responds to  $-S$  by inducing degradation of two target genes, and *pri-OsamiR395h* can function in dicot plant tobacco and impact its sulfate transportation and distribution. As the first target gene of *miR395* identified in tobacco, *NtaSULTR2* encodes a sulfate transporter belonging to the low-affinity group.

## Results

**Sulfate regulates the expression of *OsamiR395* and its target genes.** According to previous research and miRNA database (<http://mirbase.org>), 24 family members belonging to four clusters comprise *OsamiR395* family<sup>26</sup>. The sequence of mature *OsamiR395* is highly conserved while the pre-microRNA sequences are divergent. It has previously been demonstrated in *Arabidopsis* that mature *AthmiR395* transcript accumulates under sulfur-limited conditions<sup>18,19,27</sup>. To investigate whether *OsamiR395* also responds to low sulfate conditions as its counterpart in *Arabidopsis*, transcript level of *OsamiR395* in two weeks old rice plants grown in N6 solid medium supplemented with different concentrations of sulfate was analyzed. Both northern blotting and stem-loop RT-PCR results showed that the transcripts of mature *OsamiR395* accumulated under low sulfate conditions (0 and 20  $\mu\text{M SO}_4^{2-}$ ), but declined significantly under sulfate-adequate conditions (1500 and 2000  $\mu\text{M SO}_4^{2-}$ , Fig. 1a,b).

In plant nucleus, *miRNA* gene is first transcribed into a long *pri-miRNA*, which is then processed into *pre-miRNA* and finally mature *miRNA* that is later translocated by HASTY into cytoplasm and induces the degradation of its target gene(s). To further understand whether *OsamiR395* is regulated at the transcription level or post-transcription level, real-time PCR experiment was conducted to investigate the transcript level of *pri-OsamiR395h* in two weeks old rice plants grown in N6 solid medium supplemented with 0, 20, 1500 or 2000  $\mu\text{M SO}_4^{2-}$ . Real-time PCR results showed that excess sulfate could repress the accumulation of *pri-OsamiR395h* transcript (Fig. 1c). Conversely, the transcription level of *pri-OsamiR395h* increased significantly under sulfate deficient conditions (0 and 20  $\mu\text{M SO}_4^{2-}$ , Fig. 1c). Transcript levels of *pri-* and mature *OsamiR395* exhibit the same trend under sulfate starvation stress, indicating that *OsamiR395* expression is transcriptionally regulated by sulfate. Sulfate starvation stress induces the expression of *pri-OsamiR395h*, leading to the production of more mature *OsamiR395* transcripts.

Computational analysis of the rice genome sequences leads to the identification of four putative targets of *OsamiR395*, including one ATPS and three sulfate transporter genes, *OsaSULTR2;1*, *OsaSULTR2* and *OsaSULTR3;4* (Fig. 2a)<sup>17,27</sup>. RT-PCR results indicated that *OsaATPS* did not exhibit any responses in both roots and leaves under  $-S$  stress. *OsaSULTR3;4* did not respond to sulfate treatment in leaves either, but was down-regulated in roots with the increasing sulfate concentrations, exhibiting similar expression pattern as *OsamiR395* (Fig. 2b). *OsaSULTR2;1* and *OsaSULTR2* genes were both down-regulated in leaves with the increasing sulfate concentrations (Fig. 2b), similar to the expression pattern of *OsamiR395* in response to sulfate treatment (Fig. 1). On the contrary, they were both up-regulated in roots in response to increasing sulfate concentrations



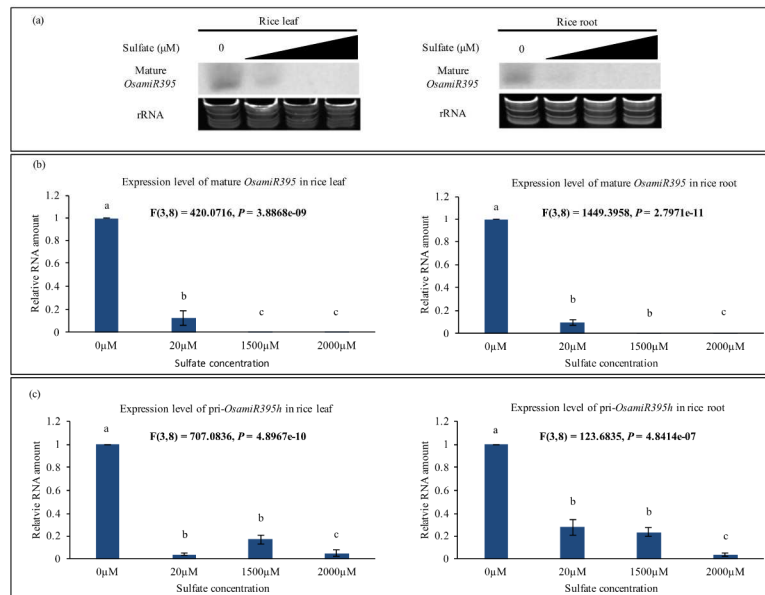


**Figure 1. Sulfate deficiency induces accumulation of *OsamiR395* in rice.** (a) Small RNA northern blotting analysis of mature *OsamiR395* under different sulfate concentrations. Total RNA samples were prepared from leaf and root tissues of two weeks old rice grown in N6 medium with 0, 20, 1500 or 2000  $\mu\text{M}$   $(\text{NH}_4^+)_2\text{SO}_4$  and used for small RNA northern blotting analysis. Antisense oligonucleotides of *OsamiR395* was labeled with  $\gamma$ - $^{32}\text{P}$ ATP and used as probe to detect the transcript level of mature *OsamiR395*. rRNA was used as a loading control. (b) Stem-loop real-time PCR analysis of mature *OsamiR395* under different sulfate concentrations. Total RNA samples were prepared as in (a) and used for stem-loop real-time PCR analysis. *OsaSIZ1* was used as a reference gene. Data are presented as means of three technique replicates, error bars represent SD ( $n = 3$ ). (c) Real-time PCR analysis of rice pri-*OsamiR395h* under different sulfate concentrations. Total RNA samples were prepared as in (a) and used for real-time PCR analysis. *OsaSIZ1* was used as a reference gene. Data are presented as means of three technique replicates, error bars represent SD ( $n = 3$ ). The statistically significant difference between groups was determined by one-way ANOVA ( $F(df_{\text{between}}, df_{\text{within}}) = F$  ration,  $p = p$ -value, where  $df = \text{degrees of freedom}$ ). Means not sharing the same letter are statistically significantly different ( $P < 0.05$ ).

(Fig. 2b). It should be noted that *OsaSULTR2* exhibited the highest induction under 20  $\mu\text{M}$  sulfate, suggesting that other regulation machineries may also participate in the regulation of the *OsaSULTR2* gene under this particular condition. These results support the hypothesis that *OsaSULTR2;1* and *OsaSULTR2* are the putative target genes of, and regulated by *OsamiR395* in rice roots. In rice leaves, however, *OsamiR395*-mediated transcript cleavage of the *OsaSULTR2;1* and *OsaSULTR2* genes may not be able to take place due to their non-overlapping tissue-specific expression. Instead, there may exist some other mechanisms regulating the expression of *OsaSULTR2;1* and *OsaSULTR2*. This is also likely the case for *OsaSULTR3;4* in roots. Similar phenomena have previously been observed in *Arabidopsis*<sup>18,19</sup>. It should be noted that there are multiple mismatches in the *OsamiR395* target sequence of the *OsaSULTR3;4* (Fig. 2a). This raises the question of whether or not *OsaSULTR3;4* is indeed the true target of *OsamiR395*.

To confirm the results of semi-quantitative RT-PCR, real-time RT-PCR was conducted to determine the expression levels of *OsamiR395* and its putative targets in rice under  $-S$  condition (N6 medium without sulfate) and  $+S$  condition (regular N6 medium). Real-time PCR results were consistent with that of the semi-quantitative RT-PCR. In both leaves and roots, pri- and mature *OsamiR395* were up-regulated under  $-S$  condition (Fig. 2c). Among the four putative target genes, only *OsaSULTR2;1* and *OsaSULTR2* were significantly down-regulated in rice roots under  $-S$  condition, exhibiting opposite trend of expression to *OsamiR395* (Fig. 2d), in agreement with the results obtained by semi-quantitative RT-PCR and supporting the notion that *OsaSULTR2;1* and *OsaSULTR2* are the putative targets of *OsamiR395* in rice roots.

**Expression of the *OsamiR395* and its target genes is spatiotemporally regulated.** Besides the response of *OsamiR395* and its targets to sulfate starvation stress, we also investigated the expression patterns of

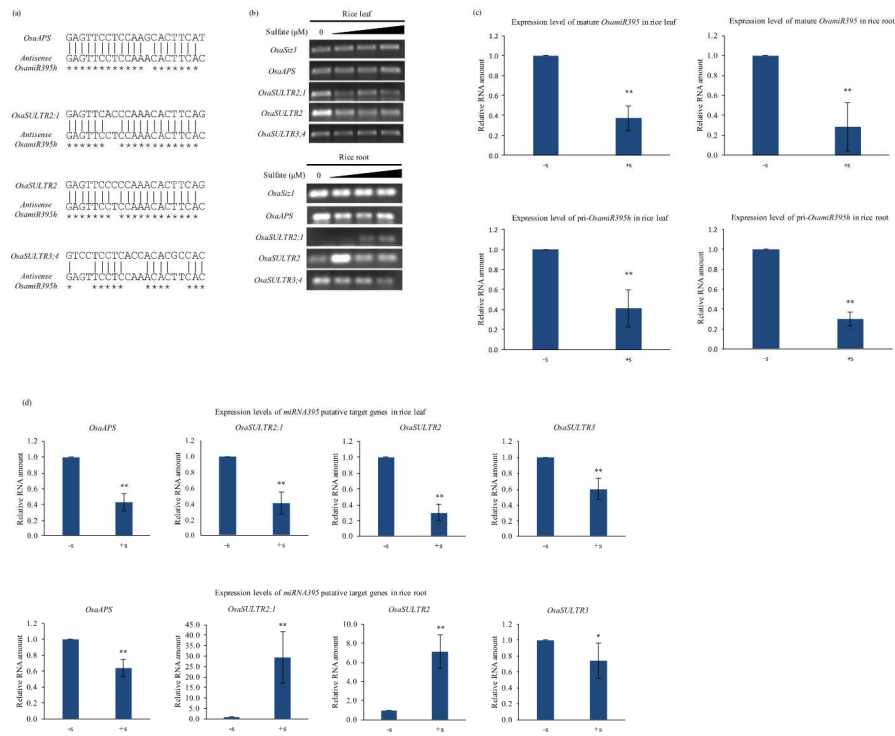


**Figure 2. Predicted target *OsaSULTR1* and *OsaSULTR2* exhibit opposite expression patterns to that of the *OsmiR395* in rice root.** (a) Target sites of the four putative *OsmiR395* target genes in rice. The target sites were compared with the complementary sequence of mature *OsmiR395h*. Asterisks indicate the identical sequences. (b) RT-PCR analysis of expression levels of the *OsmiR395* putative targets. Total RNA samples used for RT-PCR were extracted from leaf and root tissues of two weeks old rice grown in N6 medium with 0, 20, 1500 or 2000  $\mu\text{M}$   $(\text{NH}_4^+)_2\text{SO}_4$  and used for RT-PCR analysis. *OsaSIZ1* was used as a reference gene. Experiment was repeated three times. (c) Stem-loop real-time RT-PCR analysis of mature *OsmiR395* and real-time RT-PCR analysis of *pri-OsmiR395h*. Total RNA samples were prepared from leaf and root tissues of two weeks old rice grown in regular N6 medium (+S) or N6 medium without  $\text{SO}_4^{2-}$  (-S) and used for RT-PCR analysis. *OsaSIZ1* was used as a reference gene. (d) Real-time RT-PCR analysis was also conducted to determine the expression levels of the *OsmiR395* putative targets in rice leaves and roots. Total RNA samples were prepared as in (c) and used for real-time RT-PCR analysis. *OsaSIZ1* was used as a reference gene. For (c,d), data are presented as means of two independent biological replicates and three technical replicates, error bars represent SD (n = 6). Asterisks indicate the significant differences between expression levels under -S and +S conditions.  $P < 0.05$  is marked as \*,  $P < 0.01$  is marked as\*\*.

*OsmiR395* and its target genes in different developmental stages and tissues. To this end, we particularly focused on the primary miRNA level for one of the rice *OsmiR395* genes, *OsmiR395h* and the expression of its putative target genes in both roots and leaves at different developmental stages under normal growth conditions. The RT-PCR results showed that the expression of *pri-OsmiR395h* was strongly induced only in the roots of the four weeks old plants, but otherwise remained very low in both roots and leaves in any other developmental stages (Fig. 3).

The expression of the *ATPS* again was quite stable in both tissues throughout the rice development, but an elevated expression level in roots was observed compared to that in leaves (Fig. 3). The expression levels of the three sulfate transporter genes were variable, but none of them was inversely correlated with that of the *OsmiR395h* (Fig. 3).

**Heterologous expression of *pri-OsmiR395h* in *Nicotiana tabacum*.** To further study the role *OsmiR395* plays in sulfate transportation and distribution, we generated a chimeric DNA construct containing

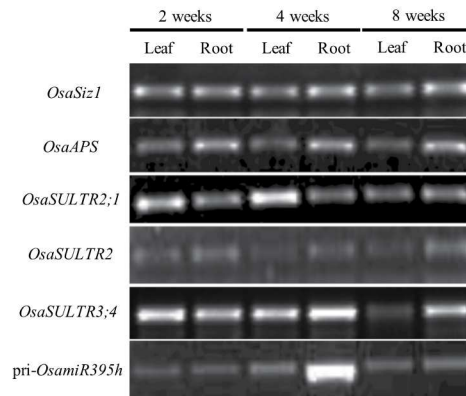


**Figure 3.** Expression level of *pri-OsamiR395h* and its target genes in rice leaf and root tissues at different developmental stages. Total RNA samples were prepared from leaf and root tissues of rice harvested at indicated time points and used for RT-PCR analysis. *OsaSIZ1* was used as a reference gene. Experiment was repeated three times.

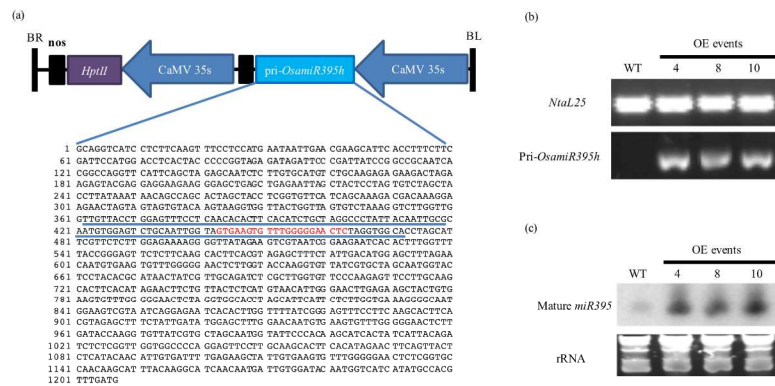


**Figure 4.** Heterologous expression of *pri-OsamiR395h* in *Nicotiana tabacum*. (a) The Schematic diagram of rice *pri-OsamiR395h* overexpression construct. Rice *pri-OsamiR395h* sequence containing stem-loop structure of *OsamiR395h* was cloned from rice genomic DNA and put under the control of the CaMV35S promoter. The *hptII* gene driven by CaMV35S promoter was used as selectable maker. The pre-*OsamiR395h* sequence was underlined. Sequence emphasized with red color indicates the mature *miR395h*. LB, Left border; RB, right border. (b) RT-PCR analysis of *pri-OsamiR395h* expression in wild type and three transgenic tobacco lines. Total RNA samples were prepared from two weeks old wild type and transgenic tobacco plants grown in MS medium. *NtAtL25* was used as reference gene. (c) Small RNA northern blotting analysis of mature *miR395* transcripts in wild type and three transgenic tobacco lines. Total RNA samples were prepared from two weeks old wild type and transgenic tobacco plants grown in MS medium. *rRNA* was used as loading control. WT: wild type plant. OE: overexpression line.

the *pri-OsamiR395h* sequence driven by the CaMV35S promoter (Fig. 4a). This construct was then introduced into tobacco (*Nicotiana tabacum*) to produce a total of 10 independent transgenic events. RT-PCR analysis suggested rice *pri-OsamiR395h* was successfully expressed in tobacco (Fig. 4b), and small RNA northern blotting result suggested rice *pri-OsamiR395h* was successfully processed into mature *miR395* (Fig. 4c). The detection of tobacco endogenous mature *NtamiR395* in northern blotting indicated that mature *NtamiR395* shares a highly conserved sequence with its rice homolog. Three independent transgenic events were selected for further analysis.

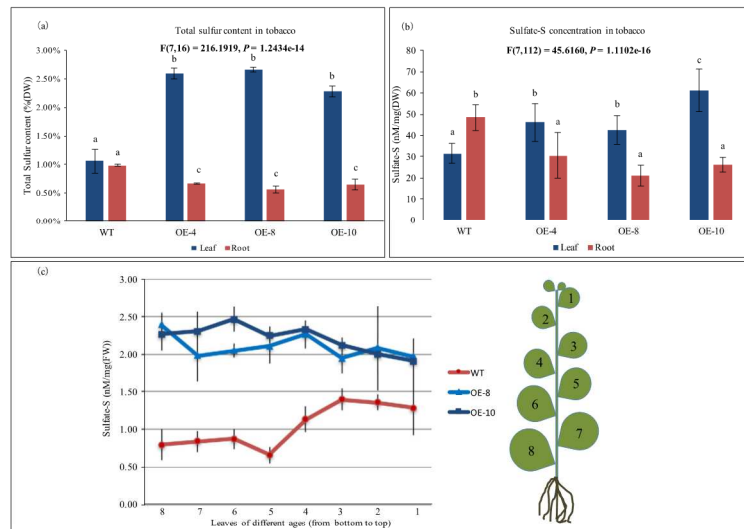


**Figure 5. Overexpression of *pri-OsamiR395h* impacts tobacco sulfate transportation and distribution.** (a) Statistical analysis of total sulfur in leaf and root tissues. Samples were harvested from four weeks old wild type and three transgenic tobacco lines. Data are presented as means of three biological replicates contains mixed samples from five biological replications, error bars represent SD (n = 3). (b) Statistical analysis of sulfate-S concentrations in leaf and root tissues. Samples were harvested from four weeks old wild type plants and three transgenic tobacco lines. Data are presented as means of fifteen biological replicates, error bars represent SD (n = 15). The statistically significant difference between groups was determined by one-way ANOVA ( $F(df_{\text{between}}, df_{\text{within}}) = F \text{ ratio}, p = p\text{-value}$ , where  $df = \text{degrees of freedom}$ ). Means not sharing the same letter are statistically significantly different ( $P < 0.05$ ). (c) Statistical analysis of sulfate concentration in tobacco leaves of different ages. Leaves of 12 weeks old wild type and three transgenic tobacco lines were harvested in the positions as indicated in the figure. Data shown are an average of three biological replicates, error bars represent SD (n = 3). DW: dry weight. FW: fresh weight. WT: wild type.

#### Overexpression of the rice *pri-OsamiR395h* impairs sulfate homeostasis and leads to retarded plant growth in transgenic tobacco.

It has previously been shown that overexpression of *AthmiR395* in *Arabidopsis* impairs its sulfate distribution and assimilation<sup>19</sup>. To evaluate the impact of the *OsamiR395* in tobacco sulfate metabolism and plant development, we first measured the total sulfur contents in transgenic tobacco plants and wild type (WT) controls. Not surprisingly, the total leaf sulfur content of all the transgenic lines was 2.16 to 2.50 times higher than that in WT controls. On the contrary, the root sulfur content in transgenic lines was 32% to 42% less than that in WT controls (Fig. 5a).

Next, we determined the sulfate-S (sulfate-sulfur) concentration in WT and transgenic plants. Again, the difference in sulfate-S concentrations between transgenics and WT controls was similar to that of the total sulfur contents. In transgenic leaf tissues, the sulfate-S concentration was 1.35 to 1.96 times higher than that in WT leaves, whereas in roots, transgenics had 38% to 57% less sulfate than WT controls (Fig. 5b). This result indicated that the high-level of *miR395* accumulation in transgenic plants impacts the uptake and transportation of sulfur and sulfate.

Similar to a previous report in *Arabidopsis* that overexpression of *AthmiR395* represses the expression of sulfate transporter gene *AthSULTR2;1* and causes impaired sulfate distributions between leaves of different ages<sup>19</sup>, we also observed that leaf sulfate distribution patterns are different between transgenic tobacco plants and WT controls (Fig. 5c). Because sulfate or sulfur compounds could be transported from old to young leaves under normal or sulfate-adequate conditions<sup>28</sup>, sulfate accumulation in young leaves should be higher than that in old ones as observed in WT control plants (Fig. 5c). Contrary to this, transgenic tobacco plants accumulate fewer sulfates in younger leaves than in older ones (Fig. 5c), indicating that sulfate delivery pathway is impaired in transgenics, which is most likely one of the consequences caused by repressed expression of sulfate transporter genes. Furthermore, compared with WT controls, transgenic tobacco exhibited retarded growth (Fig. 6a,d). As shown in Fig. 6b,c, one-month-old transgenic plants displayed shorter root and less fresh weight than wild type controls, a similar phenotype observed in transgenic *Arabidopsis* overexpressing *AthmiR395*<sup>19</sup>. The slow-growth phenotype of transgenic plants suggests that the expression of *ATPS* may also have been strongly repressed in transgenics,

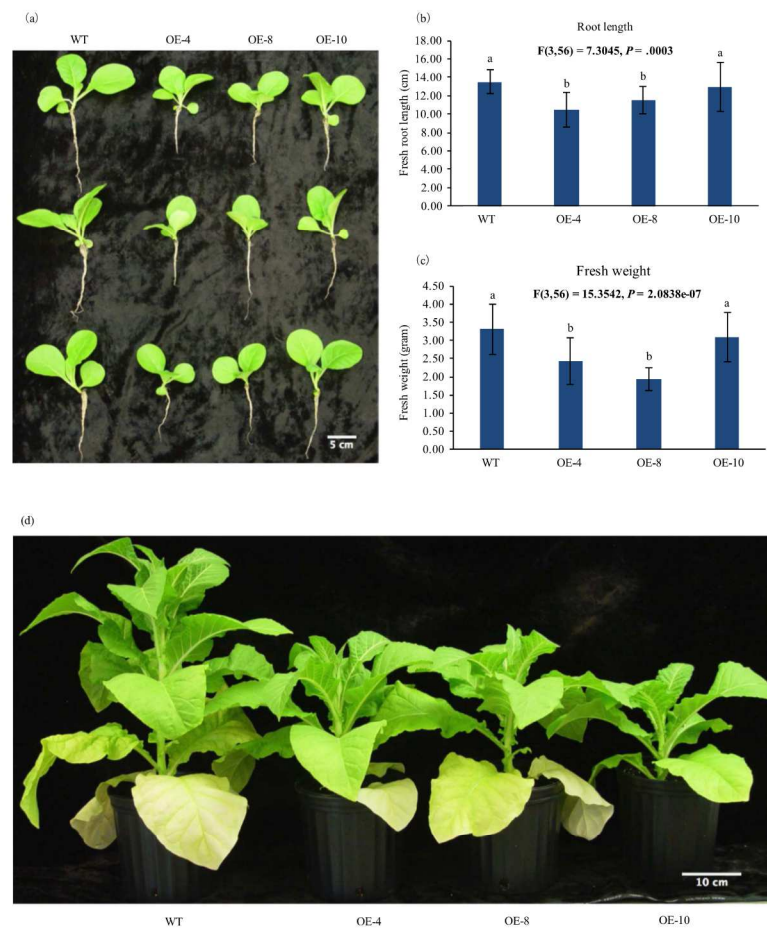


**Figure 6. Overexpression of pri-*OsamiR395h* leads to retarded growth of transgenic tobacco.** Wild type and transgenic tobacco were grown in soil under 16 h light/8 h dark in greenhouse. Photos were taken (a) four weeks and (d) seven weeks after seed germination. Representative plants were shown. (b) Root length and (c) fresh weight of wild type and transgenic tobacco were measured. Data are presented as means of fifteen biological replicates, error bars represent SD ( $n = 15$ ). The statistically significant difference between groups was determined by one-way ANOVA ( $F(df_{\text{between}}, df_{\text{within}}) = F$  ration,  $p = p$ -value, where  $df =$  degrees of freedom). Means not sharing the same letter are statistically significantly different ( $P < 0.05$ ). WT: wild type plant. OE: overexpression line.

resulting in interrupted sulfate assimilation pathway and consequently retardation in plant growth because of the shortage of cysteine and other sulfate metabolic products.

**Identification of *miR395* target gene in tobacco.** To understand how the excess *miR395* impacts tobacco sulfate homeostasis at the molecular level, we sought to identify putative new target genes of *miR395* using two approaches<sup>29</sup>. We first used the DNA sequences of the *Arabidopsis* *SULTR2;1* and *ATPS* genes to blast against the *Nicotiana tabacum* EST sequences. All the DNA sequences with high similarity (identity of more than 70%) were used to do alignment with complementary sequence of the mature *OsamiR395h*. The following criteria were used to determine the predicted target sequences with minor modifications: (1) No more than four mismatches between *OsamiR395h* and its predicted target genes; (2) No more than two constitutive mismatches

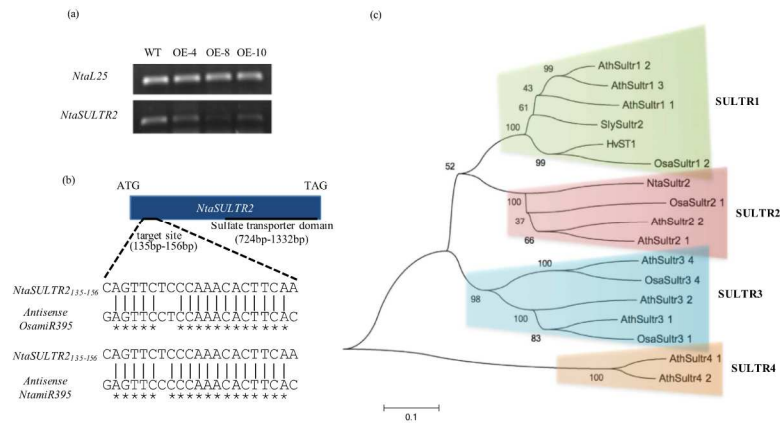


**Figure 7.** Identification of a sulfate transporter gene, *NtaSULTR2*, the target of *miR395* in tobacco. (a) RT-PCR analysis of *NtaSULTR2* expression in tobacco. Total RNA samples were prepared from two weeks old wild type and transgenic tobacco and used for RT-PCR analysis. *NtaL25* was used as a reference gene. Experiment was repeated three times. (b) General structure of tobacco gene *NtaSULTR2*. *NtaSULTR2* with a length of 1335 bp contains a sulfate transporter domain between 724 bp to 1332 bp, and a *miR395* target site between 135 bp to 156 bp. The target site was compared with the complementary sequence of mature *OsamiR395* and *NtamiR395*. Asterisks indicate the identical sequences. (c) phylogenetic analysis of *NtaSULTR2* protein. Protein sequences of *NtaSULTR2* and 16 sulfate transporters of rice and *Arabidopsis* were used to establish phylogenetic tree with MEGA6. In this phylogenetic tree, *NtaSULTR2* protein is classified into the second group of sulfate transporter subfamily together with *AthSULTR2;1*, *AthSULTR2;2* and *OsaSULTR2;1*.

between *OsamiR395h* and its predicted target genes; (3) No mismatches between position 10 and 11; (4) No gaps between *OsamiR395h* and its predicted target genes<sup>29</sup>. Besides, we also designed primers based on the *AthmiR395* target genes (*AthSULTR2;1* and *AthATPS1*, 3, 4) to amplify and identify the putative homologous genes in tobacco.

Using these approaches, we identified a novel gene named *NtaSULTR2* to be a putative target of *OsamiR395h* (Fig. 7). Semi-quantitative RT-PCR analysis revealed that *NtaSULTR2* was significantly down-regulated in transgenic tobacco (Fig. 7a). We cloned the full-length cDNA sequence of *NtaSULTR2* using RACE (Rapid Amplification of cDNA Ends) method, and identified the target site of *miR395* that is located between 135 bp and 156 bp of its coding region. There are four mismatches and three mismatches between *NtaSULTR2* target sequence and mature *OsamiR395* and *NtamiR395*, separately (Fig. 7b), indicating that *NtaSULTR2* should be efficiently regulated by *miR395* because of their near perfect complementary sequence.

We further characterized *NtaSULTR2* by generating a phylogenetic tree using protein sequence of *NtaSULTR2* and other sixteen well-studied sulfate transporters from rice and *Arabidopsis* using MEGA6. In this phylogenetic tree, *NtaSULTR2* protein is classified into the second group of sulfate transporter subfamily together with *AthSULTR2;1*, *AthSULTR2;2* and *OsaSULTR2;1* proteins (Fig. 7c). The three sulfate transporters from *Arabidopsis* and rice are low-affinity sulfate transporters and involved in the inter-organ delivery of sulfate in vascular to transport sulfate from root to leaf, and distribution of sulfate between leaves<sup>4,7,8</sup>.

Taken together, our results indicate that overexpression of *OsamiR395h* in tobacco represses sulfate transporter *NtaSULTR2*, which may play an important role in sulfate transportation and distribution, thus interrupting sulfate homeostasis and distribution in transgenics.

**Sulfate regulates tobacco *NtamiR395* and *NtaSULTR2*.** To confirm that *NtaSULTR2* is the target of *miR395* in tobacco, we investigated the expression level of both *NtaSULTR2* and mature *NtamiR395* under different sulfate concentrations.

In leaf tissues, the transcription of the mature *NtamiR395* was gradually up-regulated, contrary to the gradually reduced sulfate concentration. However, *NtaSULTR2* did not exhibit an opposite, but a similar expression pattern to *NtamiR395* with its lowest transcript level being under 1500  $\mu\text{M}$ , but not 2000  $\mu\text{M}$   $(\text{NH}^+)_2\text{SO}_4$  (Fig. 8a).

In root tissues, the situation was different. The transcript level of the mature *NtamiR395* increased in response to sulfate depletion, similar to that observed in leaves, whereas *NtaSULTR2* exhibited a roughly opposite, but more complex expression pattern (Fig. 8b). Compared to sulfate depletion conditions with 0  $\mu\text{M}$   $(\text{NH}^+)_2\text{SO}_4$  supply, *NtaSULTR2* was up-regulated under both 20  $\mu\text{M}$  and 2000  $\mu\text{M}$   $(\text{NH}^+)_2\text{SO}_4$ , but down-regulated under 1500  $\mu\text{M}$   $(\text{NH}^+)_2\text{SO}_4$ . The results indicate that *NtaSULTR2* might be regulated by *NtamiR395* in roots but not in leaf tissues. These results correspond to the previous studies in *Arabidopsis* and rice showing that the expression level of *AthSULTR2* is opposite to that of *AthmiR395* in some, but not all plant tissues most likely due to the fact

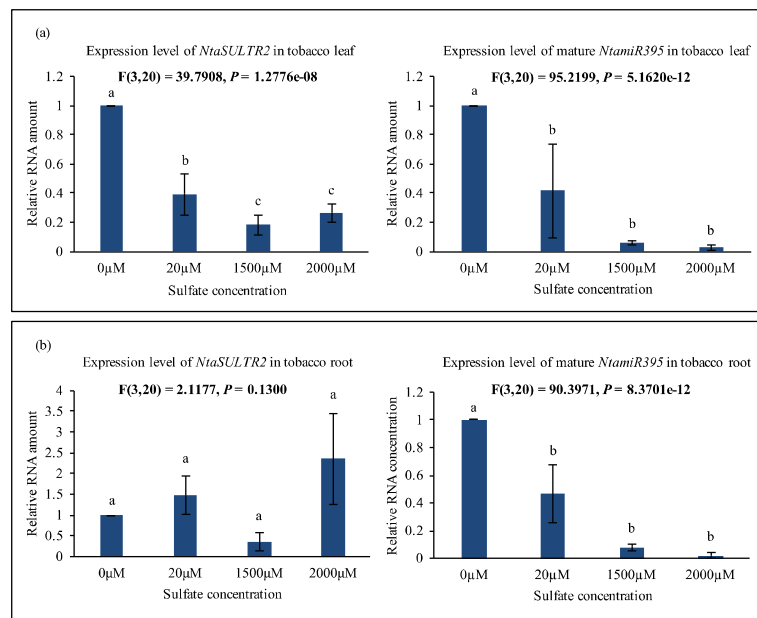


**Figure 8. *NtamiR395* and *NtaSULTR2* exhibit opposite expression patterns in tobacco roots.** Real-time PCR analysis of expressions of *NtaSULTR2* and mature *NtamiR395* under different sulfate concentrations. Total RNA samples were prepared from (a) leaf tissue and (b) root tissue of four weeks old tobacco grown in MS medium with 0, 20, 1500 or 2000  $\mu\text{M}$   $(\text{NH}_4^+)_2\text{SO}_4$ . *NtaL25* was used as a reference gene. Data are presented as means of three technical replicates and two biological replicates, error bars represent SD ( $n = 6$ ). The statistically significant difference between groups was determined by one-way ANOVA ( $F(df_{\text{between}}, df_{\text{within}}) = F$  ratio,  $p = p$ -value, where  $df =$  degrees of freedom). Means not sharing the same letter are statistically significantly different ( $P < 0.05$ ).

that the spatial expression pattern of *AthmiR395* does not overlap with that of *AthSULTR2;1*<sup>18,19,30</sup>, which could probably also explain the similar observation in tobacco from this study.

***MiR395* mediates the cleavage of *NtaSULTR2* mRNA.** To further confirm that *NtaSULTR2* is the true target of *miR395*, we conducted RLM-RACE (T4 RNA Ligase Mediated Rapid Amplification of cDNA Ends) to verify that *NtaSULTR2* transcripts are cleaved by *miR395*. We used RNA from the *miR395*-overexpressing transgenic tobacco plants to facilitate the detection of cleaved *NtaSULTR2* mRNA.

We used the forward primer ASP (Adapter Specific Primer) and the reverse primer GSP (Gene Specific Primer) to conduct the first round PCR after the adapter-linked first strand cDNA ends were generated. The RNA adapter has a length of 44 bp, and the reverse GSP is localized 545 bp downstream of the predicted *miR395* target site in the *NtaSULTR2* mRNA, so the product of the first round PCR should have a length of about 589 bp. As shown in Fig. 9, the first round PCR with transgenic tobacco cDNA indeed generated a clear band of about 600 bp.

A second round PCR was then conducted using the first round PCR product as template and a new set of primers to confirm the authenticity of the PCR product. The forward primer NASP (Nest Adapter Specific Primer) is localized on the adapter from 14 bp to 44 bp, and the reverse primer NGSP (Nest Gene Specific Primer) is localized 463 bp downstream of the predicted *miR395* target site in the *NtaSULTR2* mRNA, so the product of the second round PCR should be about 493 bp. As shown in Fig. 9, the second round PCR indeed generated a clear main band of about 500 bp as expected. Cloning and sequencing of the PCR product further confirmed the predicted *miR395* cleavage site in the *NtaSULTR2* mRNA.

## Discussion

Previous studies on *Arabidopsis miR395* have indicated its involvement in sulfate starvation response by repressing the expression of genes in sulfate transportation and assimilation pathways.

Under  $-S$  condition, the accumulation of *AthmiR395* is enhanced under low internal sulfate level, and correlated to GSH pool, indicating that the regulation of *AthmiR395* is mediated by internal sulfate level and redox

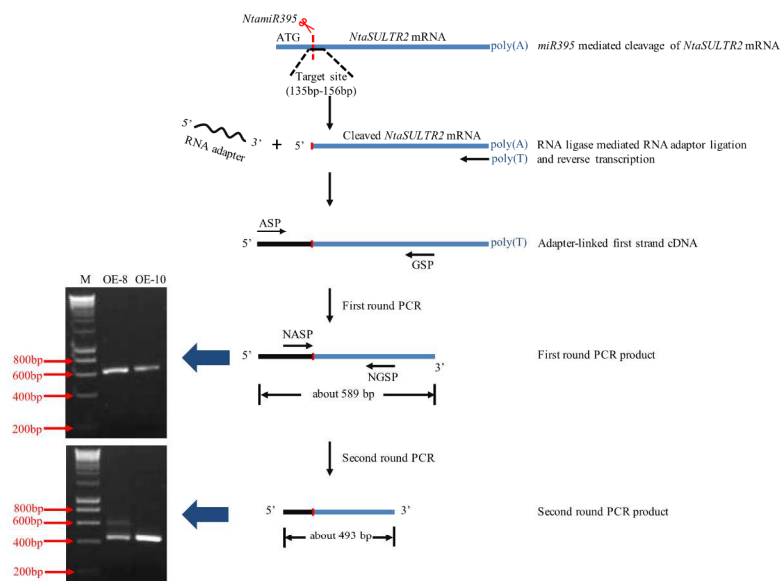


**Figure 9.** Confirmation of *miR395*-mediated cleavage of *NtSULTR2* mRNA. RLM-RACE (T4-RNA ligase mediated amplification of 5' cDNA ends) was conducted to confirm the cleavage of *NtSULTR2* mRNA. Total RNA samples were isolated from two weeks old transgenic tobacco. 44 bp RNA adapter was ligated to the purified RNA by using T4 RNA ligase. Adapter-linked RNA was then used to synthesize first strand cDNA, followed by amplification of 5' ends using the forward primer ASP and the reverse primer GSP. The 589 bp product from the first round PCR was then used as template for the second round PCR using the forward nest primer NASP and the reverse nest primer NGSP, producing a 493 bp second round PCR product. M: DNA molecular weight marker. OE: overexpression line. Red lines indicate *miR395* cutting site.

signaling in *Arabidopsis*<sup>22,31</sup>. The increased *AthmiR395* then represses the expression of *AthATPS1*, *AthATPS3*, *AthATPS4* and *AthSULTR2;1*<sup>18,22</sup>. Further study in *Arabidopsis* revealed a whole picture of how *AthmiR395* is involved in plant response to sulfate starvation. When sulfate supply is limited, the induced *AthmiR395* mediates the degradation of *ATPS* mRNA leading to the accumulation of sulfate in leaf tissues as a result of decelerated sulfate assimilation<sup>19</sup>. At the same time, the cleavage of *AthSULTR2;1* mRNA in shoots by *AthmiR395* results in blocked sulfate transport into new leaves from old ones<sup>19</sup>. Furthermore, the impaired sulfate homeostasis and reduced sulfate assimilation impact seed germination under ABA-treated condition<sup>32</sup>.

*MiR395* is highly conserved across species, which strongly suggests that its function in regulating plant response to nutrition, particularly sulfate supply could also be conserved during evolution. Our results in rice indicate that indeed, the transcript of mature *OsamiR395* increases under -S condition, and this change in expression might be regulated at the transcription level (Fig. 1). Computational prediction led to the identification of four putative target genes of *OsamiR395* in rice. We confirmed that *OsaSULTR2;1* and *OsaSULTR2* are regulated by *OsamiR395* in roots suggesting that they may be the *OsamiR395* target genes.

Knowledge about the functions of rice sulfate transporters is limited. Phylogenetic analysis grouped the fourteen rice sulfate transporters together with their *Arabidopsis* counterparts<sup>11</sup>, suggesting that they may share similar function. *OsaSULTR2;1* and *OsaSULTR2* may be responsible for the root-to-shoot sulfate transportation and distribution of sulfate between leaves of different ages. Our results (Fig. 2b–d) showed that the expression patterns of rice sulfate transporter genes were different from their *Arabidopsis* homologs, both *OsaSULTR2;1* and *OsaSULTR2* were reduced in leaves with the increasing sulfate concentrations. We speculate that the two sulfate transporter genes and *miR395* may be differentially expressed in different leaf tissues and thus, *OsaSULTR2;1* and *OsaSULTR2* may not be subjected to *miR395* regulation. Instead, other regulatory machineries may participate in the control of their expression in response to sulfate levels. It is likely that when rice plants are subjected to sulfate starvation, there is a need for the two sulfate transporters to be active, driving the transportation of sulfate from old leaves to younger ones to ensure plant growth and development. However, with abundant sulfate supply in the environment, there is no need for sulfate distribution to young leaves, and therefore the expression of both *OsaSULTR2;1* and *OsaSULTR2* declines.

The miRNA-mediated gene regulation mechanism emerged about 425 million years ago, which is at a very early stage of plant phylogeny prior to the divergence of monocot and dicot plants<sup>33</sup>. This suggests that monocot



and dicot plants should have a similar miRNA-mediated gene regulation mechanism, and some highly conserved miRNA families regulating the same biological process have evolved from the same gene ancestors. Indeed, research data in the past twenty years indicate that 21 miRNA families, such as miR156 and miR399, are conserved in sequence across monocots and dicots<sup>25</sup>. More specifically, Zhang *et al.* found that 9 miRNA families are highly conserved<sup>33</sup>, 10 miRNA families are moderately conserved and 16 miRNA families including *miR395* are lowly conserved across plant species. In a later work, *miR395* family was identified in the common ancestor of all embryophytes<sup>25</sup>. Besides the miRNA sequences, the genes involved in miRNA and siRNA biogenesis pathways are also conserved across species. In plants, Dicer-like (DCL) is a key protein in the miRNA genesis pathway. DCL interacting with HYPONASTIC LEAVES1 (HYL1) and C2H2-zinc finger protein SERRATE (SE) in D-bodies cleaves the pri-miRNA from the base to yield a pre-miRNA with stem-loop structure, and this pre-miRNA is sliced again to yield mature miRNA<sup>34–37</sup>. Phylogenetic analysis indicated that divergence of *DCL1* gene associated with miRNA production from other *DCLs* could be traced to the time before the emergence of moss *Physcomitrella patens*<sup>36</sup>, indicating that *DCLs* may have the same origin and are conserved across vascular plants.

Based on previous findings, we hypothesize that miRNA biogenesis pathway in dicots could accept pri-miRNAs from monocots, and process it into mature miRNA with function. To verify our hypothesis, the full-length DNA sequence of pri-*OsamiR395h* was cloned from rice genome. The expression cassette of the CaMV35S-controlled rice pri-*OsamiR395h* was then prepared and introduced into tobacco genome. By performing small molecule northern blotting, we observed high transcript level of *miR395* in transgenic tobacco under normal condition, indicating that rice pri-*OsamiR395h* could be successfully expressed and processed into mature *miR395h* in tobacco (Fig. 4). At the same time, we also observed low level of endogenous mature *miR395* in WT tobacco, confirming that tobacco mature *miR395* is highly conserved with its rice homolog. All of the three transgenic tobacco lines exhibited impaired sulfate homeostasis and distribution (Fig. 5). Furthermore, transgenic plant had retarded growth phenotype (Fig. 6). All the facts suggest that mature *OsamiR395* functions in transgenic tobacco.

Data obtained from this research revealed that the sulfate-S contents in transgenic tobacco are higher in leaf tissue, but lower in root tissue than those in WT controls. An even more significant difference in total sulfur content was observed between WT controls and *OsamiR395h* overexpression plants (Fig. 5a,b). Besides, we also observed that sulfate distribution between leaves of different ages is impaired in transgenic tobacco plants (Fig. 5c).

To reveal the molecular mechanism underlying *miR395*-mediated plant sulfate metabolism, we studied genes impacted by excessive dose of *miR395* in transgenic tobacco, and identified a novel sulfate transporter gene *NtaSULTR2* belonging to the second group of sulfate transporter genes (Fig. 7). Based on the results of real-time PCR and RML-RACE, we verified that *NtaSULTR2* is the target gene of *miR395* (Figs 8 and 9). We believe that the repression of *NtaSULTR2* gene in transgenic tobacco plants partially impaired the sulfate homeostasis. In *Arabidopsis* shoot tissue, sulfate transporter *AthSULTR2;1* is localized in both xylem and phloem, particularly in phloem parenchyma cells surrounding sieve and companion cells, and involved in distribution of sulfur between leaves of different ages<sup>7,28</sup>. We conjecture that in tobacco shoot tissue, *NtaSULTR2*, like its homologs in *Arabidopsis*, retrieves sulfate from mesophyll cells to xylem and phloem cells, and sulfate is transported from old leaves to young leaves. But in transgenic plants, the delivery of sulfate from old leaves to young leaves is impaired because of significantly repressed *NtaSULTR2* gene (Fig. 5c).

Although no *ATPS* gene have been identified and cloned in tobacco, we believe that there must be one or more *ATPS* gene(s) repressed in transgenic tobacco, causing interrupted sulfate assimilation. The interruption of the sulfate assimilation pathway would cause a shortage in cysteine and other sulfate metabolic products, resulting in retarded plant growth and triggering plant sulfate starvation signaling, which would promote sulfate absorption and transport into leaf tissue, and consequently a much more sulfur accumulation in leaves of transgenics than in that of WT controls (Fig. 5a,b).

## Materials and Methods

**Plant materials and growth conditions.** To investigate the expression levels of *OsamiR395* and its targets in rice under different sulfate concentrations, rice seeds were surface sterilized and grown in N6 medium under 16h light/8h dark at 28 °C<sup>38</sup>. Sulfate salts of the N6 medium were replaced with chloride salts and supplemented with 0, 20, 1500 or 2000 μM (NH<sup>+</sup>)<sub>2</sub>SO<sub>4</sub>. Sterilized rice seeds were also grown in regular N6 medium (+S) and N6 medium without SO<sub>4</sub><sup>2-</sup> (–S) under 16h light/8h dark at 28 °C. Two weeks old plants were harvested for RNA isolation.

To investigate the expression patterns of *OsamiR395* and its targets in different developmental stages and tissues of rice, rice seeds were grown in soil in a greenhouse. Root and leaf samples were collected two, four and eight weeks after germination.

To investigate the expression levels of pri-*OsamiR395h*, mature *miR395* and *NtaSULTR2* in tobacco, tobacco seeds were surface sterilized and grown in MS medium under 16h light/8h dark at 22 °C<sup>39</sup>. To prepare MS mediums with different sulfate concentrations, sulfate salts of the MS medium were replaced with chloride salts and supplemented with 0, 20, 1500 or 2000 μM (NH<sup>+</sup>)<sub>2</sub>SO<sub>4</sub>. Two weeks old and four weeks old plants were harvested for RNA isolation.

To measure total sulfate content and sulfate-S concentration in tobacco, and to determine the growth rate of tobacco, tobacco were grown in soil in a greenhouse. Four weeks old and 12 weeks old plants were collected for analysis.

**Genomic DNA and total RNA isolation, and cDNA synthesis.** Plant genomic DNA was isolated following previously described method<sup>40</sup>.

Total RNA was isolated from 100 mg plant samples with Trizol reagent (Ambion, USA), and the genomic DNA is removed by using RNase-free DNase I (Invitrogen, USA). 2  $\mu$ g total RNA was used to synthesize first strand cDNA with SuperScript III Reverse Transcriptase (Invitrogen, USA) according to manufacturer's instructions. The first strand cDNA was used for semi quantitative RT-PCR and regular real-time PCR.

To determine the transcript level of mature *miR395*, the first-strand cDNA used for stem-loop real-time PCR was synthesized following the regular SuperScript III Reverse Transcriptase (Invitrogen, USA) mediated method, except that the oligo (dT)<sub>20</sub> was replaced with *miR395* specific reverse transcription primer. Primers were all listed in Supplementary Table S1.

**Semi-quantitative RT-PCR, stem-loop and regular real-time PCR.** To conduct semi-quantitative RT-PCR, first-strand cDNA samples were diluted to 0.25 times based on the concentration of the first-strand cDNA samples. The loading volume of the cDNA samples was adjusted basing on the transcript level of a reference gene.

To conduct stem-loop and regular real-time PCR, first-strand cDNA samples were diluted to 0.025 to 0.005 times based on the concentration of the first-strand cDNA samples. Both stem-loop and regular real-time PCR were performed using SYBR Green Supermix (Bio-Rad, USA) following manufacturer's instructions, and iQ5 real-time detection system (Bio-Rad USA) was used to detect and analyze the real-time PCR result.

Stem-loop and regular real-time PCR results were determined by using  $\Delta\Delta C_t$  method.  $\Delta C_t$  was defined as  $C_{t_{\text{test}}} - C_{t_{\text{ref}}}$ , in which  $C_{t_{\text{test}}}$  stands for threshold cycle of one gene after treatment, and  $C_{t_{\text{ref}}}$  stands for threshold cycle of one gene before treatment.  $\Delta\Delta C_t$  was defined as  $\Delta C_{t_{\text{reference}}} - \Delta C_{t_{\text{target}}}$ , in which  $\Delta C_{t_{\text{reference}}}$  stands for  $\Delta C_t$  of the endogenous gene used as a reference, and  $\Delta C_{t_{\text{target}}}$  stands for  $\Delta C_t$  of target gene. Finally, related expression ratio was calculated as  $2^{-\Delta\Delta C_t}$ .

Primers used for semi-quantitative RT-PCR, stem-loop real-time PCR and regular real-time PCR were all listed in Supplementary Table 1.

**Small molecule Northern blotting.** Small molecule northern blotting was performed following the method previously described with minor modification<sup>41</sup>. 10  $\mu$ g total RNA denatured at 95 °C was separated in 12.5% urea-polyacrylamide gel and transferred to Hybond-N+ nylon membrane (Amersham, USA) in a Trans-Blot SD Semi-Dry Transfer Cell (Bio-Rad, USA). To prepare radiolabeled probe for detecting mature *miR395*, DNA oligonucleotide GAGTTCGCCCAACACTTCAC was synthesized (<http://www.idtdna.com/site>) and labeled with  $\gamma$ -[<sup>32</sup>P]-ATP by using T4 polynucleotide kinase. RNA membrane was then hybridized with radiolabeled probe and detected on a phosphorimaging screen.

**Plasmid construction, bacterial strains and plant transformation.** The predicted pri-*OsamiR395h* was amplified from rice genomic DNA and cloned at downstream of CaMV35S (Cauliflower Mosaic Virus 35S) promoter of binary vector pZH01, resulting in CaMV35S/*OsamiR395h*-CaMV35S/*hygromycin*<sup>42</sup>. This chimeric gene expression construct was then mobilized into *Agrobacterium tumefaciens* strain LBA4404 by electroporation for tobacco transformation. The *Escherichia coli* strain used in this experiment was DH5 $\alpha$ .

The primers used for plasmid construction were all listed in Supplementary Table 1.

**Determination of total sulfur content and sulfate-sulfur concentration.** For determination of total sulfur, plant samples were collected and dried for 48 h at 80 °C. Total sulfur contents in dry samples were determined as previously described<sup>43</sup> sulfate-S concentration was determined following a previous method with minor modification<sup>44</sup>. 10 mg dry plant sample or 200 mg fresh plant sample was immersed in 1 ml 0.1 M HCl for 2 h at room temperature, followed by 20 min centrifugation at 12000 g. Clear supernatant liquid was then transferred to a 50 ml Erlenmeyer flask and made to 20 ml by water. One ml of barium chloride-gelatin reagent was added to the liquid. After 40 min (no more than 120 min), absorbance of the resulting cloudy liquid was determined at 454 nm by using a spectrometer.

**Rapid amplification of cDNA ends.** To obtain 5' cDNA end and 3' cDNA end of *NtaSULTR2*, total RNA was extracted from 100 mg two weeks old WT tobacco with Trizol reagent (Ambion, USA) and treated with RNase-free DNase I (Invitrogen, USA) to remove genomic DNA. 1  $\mu$ g total RNA was then used to amplify 5' end and 3' end cDNA of *NtaSULTR2* with SMARTer RACE 5'/3' commercial kit (Clontech, USA) following the manufacturer's instruction. Then, the 5' end and 3' end cDNA fragments were sequenced. Sequence information was used to design primers for cloning of full-length *NtaSULTR2* cDNA.

The primers used for RACE and for cloning of full length *NtaSULTR2* cDNA were all listed in Supplementary Table S1.

**T4-RNA ligase mediated amplification of 5' cDNA ends.** To verify *miR395* cleavage site within *NtaSULTR2*, T4-RNA ligase mediated amplification of 5' cDNA ends was conducted following a previously described method<sup>45</sup>. Briefly, total RNA was isolated from 100 mg plant sample using Trizol reagent (Ambion, USA), followed by purification of RNA with RNeasy mini kit (Qiagen, Germany). RNA adapter was ligated to the purified RNA by using T4 RNA ligase (New England Biolabs, USA). Based on the fact that miRNA-mediated mRNA cleavage will generate 5'-monophosphate ends on the 3' end cleavage product of the target mRNAs, it is possible to ligate RNA oligonucleotide adapter to the 5' terminus of the 3' end cleavage product by using T4 RNA ligase, whereas such RNA oligonucleotide adapter would not be ligated to mRNAs with conventional 5' cap<sup>45</sup>. Adapter-linked RNA was then used to synthesize first strand cDNA with SuperScript II Reverse Transcriptase (Invitrogen, USA), followed by amplification of 5' ends using the forward primer ASP and the reverse primer GSP. The product from the first round PCR was then used as template for the second round PCR with the forward nest primer NASP and the reverse nest primer NGSP. PCR product was cloned for sequencing.

The primer sequences used for RML-RACE were all listed in Supplementary Table 1.

**Phylogenetic analysis of sulfate transporters.** Phylogenetic tree of *NtaSULTR2* and other sulfate transporter genes in rice and *Arabidopsis* inferred using the Neighbor-Joining method<sup>46</sup>. The optimal tree with the sum of branch length = 3.89795523 is shown. The tree is drawn to scale, with branch lengths in the same units as those of the evolutionary distances used to infer the phylogenetic tree. The evolutionary distances were computed using the Poisson correction method<sup>47</sup> and are in the units of the number of amino acid substitutions per site. The analysis involved 17 amino acid sequences. All positions containing gaps and missing data were eliminated. There was a total of 347 positions in the final dataset. Evolutionary analyses were conducted in MEGA6<sup>48</sup>. WT: wild type plant. OE: overexpression line.

**Statistical analysis.** Student's t test was used to test the difference between the means from two groups.  $P < 0.05$  was considered to be statistically significant and marked as \* $P < 0.01$  was considered to be statistically highly significant and marked as\*\*.

One-way ANOVA ( $F(df_{\text{between}}, df_{\text{within}}) = F$  ration,  $p = p$ -value, where  $df =$  degrees of freedom) with post hoc comparisons using the Tukey HSD test was used to determine the statistically significant difference between the means from three or more groups. Means not sharing the same letter are statistically significantly different ( $P < 0.05$ ).

## References

1. Takahashi, H., Kopriva, S., Giordano, M., Saito, K. & Hell, R. Sulfur assimilation in photosynthetic organisms: molecular functions and regulations of transporters and assimilatory enzymes. *Annu Rev Plant Biol* **62**, 157–184, doi: 10.1146/annurev-arplant-042110-103921 (2011).
2. Hawkesford, M. J. Plant responses to sulphur deficiency and the genetic manipulation of sulphate transporters to improve S-utilization efficiency. *J Exp Bot* **51**, 131–138 (2000).
3. Smith, F. W., Ealing, P. M., Hawkesford, M. J. & Clarkson, D. T. Plant members of a family of sulfate transporters reveal functional subtypes. *Proc Natl Acad Sci USA* **92**, 9373–9377 (1995).
4. Takahashi, H. *et al.* Regulation of sulfur assimilation in higher plants: a sulfate transporter induced in sulfate-starved roots plays a central role in *Arabidopsis thaliana*. *Proc Natl Acad Sci USA* **94**, 11102–11107 (1997).
5. Kopriva, S. Regulation of sulfate assimilation in Arabidopsis and beyond. *Ann Bot* **97**, 479–495, doi: 10.1093/aob/mc006 (2006).
6. Shibagaki, N. *et al.* Selenate-resistant mutants of *Arabidopsis thaliana* identify Sultr1;2, a sulfate transporter required for efficient transport of sulfate into roots. *Plant J* **29**, 475–486 (2002).
7. Takahashi, H. *et al.* The roles of three functional sulphate transporters involved in uptake and translocation of sulphate in *Arabidopsis thaliana*. *Plant J* **23**, 171–182 (2000).
8. Kataoka, T., Hayashi, N., Yamaya, T. & Takahashi, H. Root-to-shoot transport of sulfate in Arabidopsis. Evidence for the role of SULTR3;5 as a component of low-affinity sulfate transport system in the root vasculature. *Plant Physiology* **136**, 4198–4204, doi: 10.1104/pp.104.045625 (2004).
9. Kataoka, T. *et al.* Vacuolar sulfate transporters are essential determinants controlling internal distribution of sulfate in Arabidopsis. *Plant Cell* **16**, 2693–2704, doi: 10.1105/tpc.104.023960 (2004).
10. Godwin, R. M., Rae, A. L., Carroll, B. J. & Smith, F. W. Cloning and characterization of two genes encoding sulfate transporters from rice (*Oryza sativa* L.). *Plant and soil* **257**, 113–123 (2003).
11. Kumar, S., Asif, M. H., Chakrabarty, D., Tripathi, R. D. & Trivedi, P. K. Differential expression and alternative splicing of rice sulphate transporter family members regulate sulphur status during plant growth, development and stress conditions. *Functional & integrative genomics* **11**, 259–273, doi: 10.1007/s10142-010-0207-y (2011).
12. Klonus, D., Hofgen, R., Willmitzer, L. & Riesmeier, J. W. Isolation and characterization of two cDNA clones encoding ATP-sulphyrylases from potato by complementation of a yeast mutant. *Plant J* **6**, 105–112 (1994).
13. Lunn, J. E., Droux, M., Martin, J. & Douce, R. Localization of ATP sulphyrylase and O-acetylserine (thiol) lyase in spinach leaves. *Plant Physiology* **94**, 1345–1352 (1990).
14. Patron, N. J., Durnford, D. G. & Kopriva, S. Sulfate assimilation in eukaryotes: fusions, relocations and lateral transfers. *BMC Evol Biol* **8**, 39, doi: 10.1186/1471-2148-8-39 (2008).
15. Rotte, C. & Leustek, T. Differential subcellular localization and expression of ATP sulphyrylase and 5'-adenylylsulfate reductase during ontogenesis of arabidopsis leaves indicates that cytosolic and plastid forms of ATP sulphyrylase may have specialized functions. *Plant Physiology* **124**, 715–724, doi: 10.1104/PP.124.2.715 (2000).
16. Bartel, D. P. MicroRNAs: genomics, biogenesis, mechanism, and function. *Cell* **116**, 281–297 (2004).
17. Jones-Rhoades, M. W., Bartel, D. P. & Bartel, B. MicroRNAs and their regulatory roles in plants. *Annu Rev Plant Biol* **57**, 19–53, doi: 10.1146/Annurev.Arplant.57.032905.105218 (2006).
18. Kawashima, C. G. *et al.* Sulphur starvation induces the expression of microRNA-395 and one of its target genes but in different cell types. *Plant J* **57**, 313–321, doi: 10.1111/j.1365-313X.2008.03690.x (2009).
19. Liang, G., Yang, F. & Yu, D. MicroRNA395 mediates regulation of sulfate accumulation and allocation in *Arabidopsis thaliana*. *The Plant journal: for cell and molecular biology* **62**, 1046–1057, doi: 10.1111/j.1365-313X.2010.04216.x (2010).
20. Adai, A. *et al.* Computational prediction of miRNAs in *Arabidopsis thaliana*. *Genome research* **15**, 78–91, doi: 10.1101/gr.2908205 (2005).
21. Bonnet, E., Wuyts, J., Rouze, P. & Van de Peer, Y. Detection of 91 potential conserved plant microRNAs in *Arabidopsis thaliana* and *Oryza sativa* identifies important target genes. *Proc Natl Acad Sci USA* **101**, 11511–11516, doi: 10.1073/pnas.0404025101 (2004).
22. Jagadeeswaran, G., Li, Y. F. & Sunkar, R. Redox signaling mediates the expression of a sulfate-deprivation-inducible microRNA395 in Arabidopsis. *The Plant Journal* (2014).
23. Wolfe, K. H., Gouy, M., Yang, Y. W., Sharp, P. M. & Li, W. H. Date of the monocot-dicot divergence estimated from chloroplast DNA sequence data. *Proc Natl Acad Sci USA* **86**, 6201–6205 (1989).
24. Zhang, B., Pan, X., Cobb, G. P. & Anderson, T. A. Plant microRNA: a small regulatory molecule with big impact. *Dev Biol* **289**, 3–16, doi: 10.1016/j.ydbio.2005.10.036 (2006).
25. Cuperus, J. T., Fahlgren, N. & Carrington, J. C. Evolution and functional diversification of MIRNA genes. *Plant Cell* **23**, 431–442, doi: 10.1105/tpc.110.082784 (2011).
26. Guddeti, S. *et al.* Molecular evolution of the rice miR395 gene family. *Cell Res* **15**, 631–638, doi: 10.1038/sj.cr.7290333 (2005).
27. Jones-Rhoades, M. W. & Bartel, D. P. Computational identification of plant microRNAs and their targets, including a stress-induced miRNA. *Mol Cell* **14**, 787–799 (2004).
28. Takahashi, H. Regulation of sulfate transport and assimilation in plants. *International review of cell and molecular biology* **281**, 129–159, doi: 10.1016/S1937-6448(10)81004-4 (2010).
29. Frazier, T. P., Xie, F. L., Freistaedter, A., Burklew, C. E. & Zhang, B. H. Identification and characterization of microRNAs and their target genes in tobacco (*Nicotiana tabacum*). *Planta* **232**, 1289–1308, doi: 10.1007/S00425-010-1255-1 (2010).

30. Jeong, D. H. *et al.* Massive analysis of rice small RNAs: mechanistic implications of regulated microRNAs and variants for differential target RNA cleavage. *Plant Cell* **23**, 4185–4207, doi: 10.1105/tpc.111.089045 (2011).
31. Matthewman, C. A. *et al.* miR395 is a general component of the sulfate assimilation regulatory network in Arabidopsis. *FEBS letters* **586**, 3242–3248, doi: 10.1016/j.febslet.2012.06.044 (2012).
32. Kim, J. Y. *et al.* Overexpression of microRNA395c or 395e affects differently the seed germination of *Arabidopsis thaliana* under stress conditions. *Planta* **232**, 1447–1454, doi: 10.1007/s00425-010-1267-x (2010).
33. Zhang, B., Pan, X., Cannon, C. H., Cobb, G. P. & Anderson, T. A. Conservation and divergence of plant microRNA genes. *Plant J* **46**, 243–259, doi: 10.1111/j.1365-3113X.2006.02697.x (2006).
34. Axtell, M. J., Westholm, J. O. & Lai, E. C. Vive la difference: biogenesis and evolution of microRNAs in plants and animals. *Genome Biol* **12**, 221, doi: 10.1186/gb-2011-12-4-221 (2011).
35. Kurihara, Y., Takashi, Y. & Watanabe, Y. The interaction between DCL1 and HYL1 is important for efficient and precise processing of pri-miRNA in plant microRNA biogenesis. *Rna* **12**, 206–212 (2006).
36. Liu, Q., Feng, Y. & Zhu, Z. Dicer-like (DCL) proteins in plants. *Functional & integrative genomics* **9**, 277–286, doi: 10.1007/s10142-009-0111-5 (2009).
37. Voynet, O. Origin, biogenesis, and activity of plant microRNAs. *Cell* **136**, 669–687, doi: 10.1016/j.cell.2009.01.046 (2009).
38. Chu, C.-C. Establishment of an efficient medium for anther culture of rice through comparative experiments on the nitrogen sources. *Scientia sinica* **18**, 659–668 (1975).
39. Murashige, T. & Skoog, F. A revised medium for rapid growth and bio assays with tobacco tissue cultures. *Physiologia plantarum* **15**, 473–497 (1962).
40. Zhou, M. *et al.* Constitutive expression of a miR319 gene alters plant development and enhances salt and drought tolerance in transgenic creeping bentgrass (*Agrostis stolonifera* L.). *Plant Physiology*, doi: 10.1104/pp.112.208702 (2013).
41. Tran, N. Fast and Simple micro-RNA Northern Blots. *Biochemistry Insights* **2**, 1–3 (2009).
42. Xiao, H. *et al.* Functional analysis of the rice AP3 homologue OsmADS16 by RNA interference. *Plant Mol Biol* **52**, 957–966 (2003).
43. Plank, C. O. Plant analysis reference procedures for the southern region of the United States. *Southern cooperative series bulletin (USA)* (1992).
44. Tabatabai, M. & Bremner, J. A simple turbidimetric method of determining total sulfur in plant materials. *Agronomy Journal* **62**, 805–806 (1970).
45. Llave, C., Franco-Zorrilla, J. M., Solano, R. & Barajas, D. Target validation of plant microRNAs. *Methods in molecular biology* **732**, 187–208, doi: 10.1007/978-1-61779-083-6\_14 (2011).
46. Saitou, N. & Nei, M. The neighbor-joining method: a new method for reconstructing phylogenetic trees. *Molecular biology and evolution* **4**, 406–425 (1987).
47. Zuckerkandl, E. & Pauling, L. Evolutionary divergence and convergence in proteins. *Evolving genes and proteins* **97**, 97–166 (1965).
48. Tamura, K., Stecher, G., Peterson, D., FilipSKI, A. & Kumar, S. MEGA6: Molecular Evolutionary Genetics Analysis version 6.0. *Molecular biology and evolution* **30**, 2725–2729, doi: 10.1093/molbev/mst197 (2013).

#### Acknowledgements

This work was supported by the U.S. Department of Agriculture Cooperative State Research, Education, and Extension Service grant no. SC-1700450. This is Technical Contribution no. 6290 of the Clemson University Experiment Station.

#### Author Contributions

N.Y., Z.L. and H.L. designed the study. N.Y., D.L., S.Y. and Q.H. developed the methodology, performed the analysis, and collected the data. N.Y. and H.L. wrote the manuscript.


#### Additional Information

**Accession codes:** *AthSULTR2;1*: NM\_121056.2, *AthATPS1*: NM\_113189.4, *AthATPS3*: U06275.1, *AthATPS4*: AT5G43780, *OsaSULTR2;1*: NM\_001055792, *OsaSULTR2*: NM\_001055793, *OsaSULTR3;4*: Os06g0143700, *OsaATPS*: NM\_001057769, *OsaSiz1*: Os05g0125000, *NtaL25*: L18908, *NtaSULTR2*: KT373983.

**Supplementary information** accompanies this paper at <http://www.nature.com/srep>

**Competing financial interests:** The authors declare no competing financial interests.

**How to cite this article:** Yuan, N. *et al.* Heterologous expression of a rice *miR395* gene in *Nicotiana tabacum* impairs sulfate homeostasis. *Sci. Rep.* **6**, 28791; doi: 10.1038/srep28791 (2016).

 This work is licensed under a Creative Commons Attribution 4.0 International License. The images or other third party material in this article are included in the article's Creative Commons license, unless indicated otherwise in the credit line; if the material is not included under the Creative Commons license, users will need to obtain permission from the license holder to reproduce the material. To view a copy of this license, visit <http://creativecommons.org/licenses/by/4.0/>

## APPENDIX E

### COPY RIGHT PERMISSION FOR CHAPTER THREE

Creative Commons — Attribution 4.0 International — CC BY 4.0

7/15/16, 2:32 PM



#### Creative Commons Legal Code

Attribution 4.0 International

Official translations of this license are available [in other languages](#).



Creative Commons Corporation (“Creative Commons”) is not a law firm and does not provide legal services or legal advice. Distribution of Creative Commons public licenses does not create a lawyer-client or other relationship. Creative Commons makes its licenses and related information available on an “as-is” basis. Creative Commons gives no warranties regarding its licenses, any material licensed under their terms and conditions, or any related information. Creative Commons disclaims all liability for damages resulting from their use to the fullest extent possible.

#### Using Creative Commons Public Licenses

Creative Commons public licenses provide a standard set of terms and conditions that creators and other rights holders may use to share original works of authorship and other material subject to copyright and certain other rights specified in the public license below. The following considerations are for informational purposes only, are not exhaustive, and do not form part of our licenses.

**Considerations for licensors:** *Our public licenses are intended for use by those authorized to give the public permission to use material in ways otherwise restricted by copyright and certain other rights. Our licenses are irrevocable. Licensors should read and understand the terms and conditions of the license they choose before applying it. Licensors should also secure all rights necessary before applying our licenses so that the public can reuse the material as expected. Licensors should clearly mark any material not subject to the license. This includes other CC-licensed material, or material used under an exception or limitation to copyright. [More considerations for licensors.](#)*

**Considerations for the public:** *By using one of our public licenses, a licensor grants the public permission to use the licensed material under specified terms and conditions. If the licensor’s permission is not necessary for any reason—for example, because of any applicable exception or limitation to copyright—then that use is not regulated by the license. Our licenses grant only permissions under copyright and certain other rights that a licensor has authority to grant. Use of the licensed material may still be restricted for other reasons, including because others have copyright or other rights in the material. A licensor may make special requests, such as asking that all changes be marked or described. Although not required by our licenses, you are encouraged to respect those requests where reasonable. [More considerations for the public.](#)*

#### Creative Commons Attribution 4.0 International Public License

<https://creativecommons.org/licenses/by/4.0/legalcode>

Page 1 of 5

By exercising the Licensed Rights (defined below), You accept and agree to be bound by the terms and conditions of this Creative Commons Attribution 4.0 International Public License ("Public License"). To the extent this Public License may be interpreted as a contract, You are granted the Licensed Rights in consideration of Your acceptance of these terms and conditions, and the Licensor grants You such rights in consideration of benefits the Licensor receives from making the Licensed Material available under these terms and conditions.

### Section 1 – Definitions.

- a. **Adapted Material** means material subject to Copyright and Similar Rights that is derived from or based upon the Licensed Material and in which the Licensed Material is translated, altered, arranged, transformed, or otherwise modified in a manner requiring permission under the Copyright and Similar Rights held by the Licensor. For purposes of this Public License, where the Licensed Material is a musical work, performance, or sound recording, Adapted Material is always produced where the Licensed Material is synched in timed relation with a moving image.
- b. **Adapter's License** means the license You apply to Your Copyright and Similar Rights in Your contributions to Adapted Material in accordance with the terms and conditions of this Public License.
- c. **Copyright and Similar Rights** means copyright and/or similar rights closely related to copyright including, without limitation, performance, broadcast, sound recording, and Sui Generis Database Rights, without regard to how the rights are labeled or categorized. For purposes of this Public License, the rights specified in Section 2(b)(1)-(2) are not Copyright and Similar Rights.
- d. **Effective Technological Measures** means those measures that, in the absence of proper authority, may not be circumvented under laws fulfilling obligations under Article 11 of the WIPO Copyright Treaty adopted on December 20, 1996, and/or similar international agreements.
- e. **Exceptions and Limitations** means fair use, fair dealing, and/or any other exception or limitation to Copyright and Similar Rights that applies to Your use of the Licensed Material.
- f. **Licensed Material** means the artistic or literary work, database, or other material to which the Licensor applied this Public License.
- g. **Licensed Rights** means the rights granted to You subject to the terms and conditions of this Public License, which are limited to all Copyright and Similar Rights that apply to Your use of the Licensed Material and that the Licensor has authority to license.
- h. **Licensor** means the individual(s) or entity(ies) granting rights under this Public License.
- i. **Share** means to provide material to the public by any means or process that requires permission under the Licensed Rights, such as reproduction, public display, public performance, distribution, dissemination, communication, or importation, and to make material available to the public including in ways that members of the public may access the material from a place and at a time individually chosen by them.
- j. **Sui Generis Database Rights** means rights other than copyright resulting from Directive 96/9/EC of the European Parliament and of the Council of 11 March 1996 on the legal protection of databases, as amended and/or succeeded, as well as other essentially equivalent rights anywhere in the world.
- k. **You** means the individual or entity exercising the Licensed Rights under this Public License. **Your** has a corresponding meaning.

### Section 2 – Scope.

- a. **License grant.**
  1. Subject to the terms and conditions of this Public License, the Licensor hereby grants You a worldwide, royalty-free, non-sublicensable, non-exclusive, irrevocable license to exercise the Licensed Rights in the Licensed Material to:
    - A. reproduce and Share the Licensed Material, in whole or in part; and
    - B. produce, reproduce, and Share Adapted Material.
  2. Exceptions and Limitations. For the avoidance of doubt, where Exceptions and Limitations apply to Your use, this Public License does not apply, and You do not need to comply with its terms and conditions.

3. **Term.** The term of this Public License is specified in Section [6\(a\)](#).
4. **Media and formats; technical modifications allowed.** The Licensor authorizes You to exercise the Licensed Rights in all media and formats whether now known or hereafter created, and to make technical modifications necessary to do so. The Licensor waives and/or agrees not to assert any right or authority to forbid You from making technical modifications necessary to exercise the Licensed Rights, including technical modifications necessary to circumvent Effective Technological Measures. For purposes of this Public License, simply making modifications authorized by this Section [2\(a\)\(4\)](#) never produces Adapted Material.
5. **Downstream recipients.**
  - A. **Offer from the Licensor – Licensed Material.** Every recipient of the Licensed Material automatically receives an offer from the Licensor to exercise the Licensed Rights under the terms and conditions of this Public License.
  - B. **No downstream restrictions.** You may not offer or impose any additional or different terms or conditions on, or apply any Effective Technological Measures to, the Licensed Material if doing so restricts exercise of the Licensed Rights by any recipient of the Licensed Material.
6. **No endorsement.** Nothing in this Public License constitutes or may be construed as permission to assert or imply that You are, or that Your use of the Licensed Material is, connected with, or sponsored, endorsed, or granted official status by, the Licensor or others designated to receive attribution as provided in Section [3\(a\)\(1\)\(A\)\(i\)](#).

**b. Other rights.**

1. Moral rights, such as the right of integrity, are not licensed under this Public License, nor are publicity, privacy, and/or other similar personality rights; however, to the extent possible, the Licensor waives and/or agrees not to assert any such rights held by the Licensor to the limited extent necessary to allow You to exercise the Licensed Rights, but not otherwise.
2. Patent and trademark rights are not licensed under this Public License.
3. To the extent possible, the Licensor waives any right to collect royalties from You for the exercise of the Licensed Rights, whether directly or through a collecting society under any voluntary or waivable statutory or compulsory licensing scheme. In all other cases the Licensor expressly reserves any right to collect such royalties.

**Section 3 – License Conditions.**

Your exercise of the Licensed Rights is expressly made subject to the following conditions.

**a. Attribution.**

1. If You Share the Licensed Material (including in modified form), You must:
  - A. retain the following if it is supplied by the Licensor with the Licensed Material:
    - i. identification of the creator(s) of the Licensed Material and any others designated to receive attribution, in any reasonable manner requested by the Licensor (including by pseudonym if designated);
    - ii. a copyright notice;
    - iii. a notice that refers to this Public License;
    - iv. a notice that refers to the disclaimer of warranties;
    - v. a URI or hyperlink to the Licensed Material to the extent reasonably practicable;
  - B. indicate if You modified the Licensed Material and retain an indication of any previous modifications; and
  - C. indicate the Licensed Material is licensed under this Public License, and include the text of, or the URI or hyperlink to, this Public License.
2. You may satisfy the conditions in Section [3\(a\)\(1\)](#) in any reasonable manner based on the

medium, means, and context in which You Share the Licensed Material. For example, it may be reasonable to satisfy the conditions by providing a URI or hyperlink to a resource that includes the required information.

3. If requested by the Licensor, You must remove any of the information required by Section [3\(a\)\(1\)\(A\)](#) to the extent reasonably practicable.
4. If You Share Adapted Material You produce, the Adapter's License You apply must not prevent recipients of the Adapted Material from complying with this Public License.

#### **Section 4 – Sui Generis Database Rights.**

Where the Licensed Rights include Sui Generis Database Rights that apply to Your use of the Licensed Material:

- a. for the avoidance of doubt, Section [2\(a\)\(1\)](#) grants You the right to extract, reuse, reproduce, and Share all or a substantial portion of the contents of the database;
- b. if You include all or a substantial portion of the database contents in a database in which You have Sui Generis Database Rights, then the database in which You have Sui Generis Database Rights (but not its individual contents) is Adapted Material; and
- c. You must comply with the conditions in Section [3\(a\)](#) if You Share all or a substantial portion of the contents of the database.

For the avoidance of doubt, this Section [4](#) supplements and does not replace Your obligations under this Public License where the Licensed Rights include other Copyright and Similar Rights.

#### **Section 5 – Disclaimer of Warranties and Limitation of Liability.**

- a. **Unless otherwise separately undertaken by the Licensor, to the extent possible, the Licensor offers the Licensed Material as-is and as-available, and makes no representations or warranties of any kind concerning the Licensed Material, whether express, implied, statutory, or other. This includes, without limitation, warranties of title, merchantability, fitness for a particular purpose, non-infringement, absence of latent or other defects, accuracy, or the presence or absence of errors, whether or not known or discoverable. Where disclaimers of warranties are not allowed in full or in part, this disclaimer may not apply to You.**
- b. **To the extent possible, in no event will the Licensor be liable to You on any legal theory (including, without limitation, negligence) or otherwise for any direct, special, indirect, incidental, consequential, punitive, exemplary, or other losses, costs, expenses, or damages arising out of this Public License or use of the Licensed Material, even if the Licensor has been advised of the possibility of such losses, costs, expenses, or damages. Where a limitation of liability is not allowed in full or in part, this limitation may not apply to You.**
- c. The disclaimer of warranties and limitation of liability provided above shall be interpreted in a manner that, to the extent possible, most closely approximates an absolute disclaimer and waiver of all liability.

#### **Section 6 – Term and Termination.**

- a. This Public License applies for the term of the Copyright and Similar Rights licensed here. However, if You fail to comply with this Public License, then Your rights under this Public License terminate automatically.
- b. Where Your right to use the Licensed Material has terminated under Section [6\(a\)](#), it reinstates:
  1. automatically as of the date the violation is cured, provided it is cured within 30 days of Your discovery of the violation; or
  2. upon express reinstatement by the Licensor.



For the avoidance of doubt, this Section 6(b) does not affect any right the Licensor may have to seek remedies for Your violations of this Public License.

- c. For the avoidance of doubt, the Licensor may also offer the Licensed Material under separate terms or conditions or stop distributing the Licensed Material at any time; however, doing so will not terminate this Public License.
- d. Sections 1, 5, 6, 7, and 8 survive termination of this Public License.

#### **Section 7 – Other Terms and Conditions.**

- a. The Licensor shall not be bound by any additional or different terms or conditions communicated by You unless expressly agreed.
- b. Any arrangements, understandings, or agreements regarding the Licensed Material not stated herein are separate from and independent of the terms and conditions of this Public License.

#### **Section 8 – Interpretation.**

- a. For the avoidance of doubt, this Public License does not, and shall not be interpreted to, reduce, limit, restrict, or impose conditions on any use of the Licensed Material that could lawfully be made without permission under this Public License.
- b. To the extent possible, if any provision of this Public License is deemed unenforceable, it shall be automatically reformed to the minimum extent necessary to make it enforceable. If the provision cannot be reformed, it shall be severed from this Public License without affecting the enforceability of the remaining terms and conditions.
- c. No term or condition of this Public License will be waived and no failure to comply consented to unless expressly agreed to by the Licensor.
- d. Nothing in this Public License constitutes or may be interpreted as a limitation upon, or waiver of, any privileges and immunities that apply to the Licensor or You, including from the legal processes of any jurisdiction or authority.

Creative Commons is not a party to its public licenses. Notwithstanding, Creative Commons may elect to apply one of its public licenses to material it publishes and in those instances will be considered the “Licensor.” The text of the Creative Commons public licenses is dedicated to the public domain under the [CC0 Public Domain Dedication](#). Except for the limited purpose of indicating that material is shared under a Creative Commons public license or as otherwise permitted by the Creative Commons policies published at [creativecommons.org/policies](#), Creative Commons does not authorize the use of the trademark “Creative Commons” or any other trademark or logo of Creative Commons without its prior written consent including, without limitation, in connection with any unauthorized modifications to any of its public licenses or any other arrangements, understandings, or agreements concerning use of licensed material. For the avoidance of doubt, this paragraph does not form part of the public licenses.

Creative Commons may be contacted at [creativecommons.org](#).

Additional languages available: [Bahasa Indonesia](#), [Nederlands](#), [norsk](#), [suomeksi](#), [te reo Māori](#), [українська](#), [日本語](#). Please read the [FAQ](#) for more information about official translations.